A Probabilistic Based Application Design Guide for the use of Tubular Conductors in the Design of High Voltage Substations

By

Abraham Johannes Smit Groenewald

Dissertation

submitted in *partial* fulfilment for the requirements of the degree

Master of Science in **Engineering (Electrical)**

Faculty of Engineering

University of KwaZulu-Natal

March 2008

Supervisor (Industrial): **W.C. Van Der Merwe**

Supervisor (Academic): **Prof. N.M. Ijumba**

ACKNOWLEDGEMENTS

My sincere thanks to my two co-ordinators, Mr Chris W. van der Merwe (Industrial) and Prof Nelson M. Ijumba (Academic) for the time they set aside, despite their pressurised commitments, to provide me with guidance during the writing and compiling of this dissetation.

To the Eskom Megawatt Park library staff, particularly Ms Reetsang Setou, a big thankyou for the prompt and courteous service in obtaining various specifications and papers for me necessary for reference purposes.

To my wife and two children for sacrificing many hours of family time over the past few years, you will be rewarded with my total commitment from now on.

ABSTRACT

The requirement for new and existing outdoor air insulated substations to support larger blocks of power in restricted spaces requires an investigation into new bus conductor systems. This study has considered the use of supported, as opposed to suspended, round tubular conductors that have high current capacity necessary for this purpose. The advantages are associated with the fact that smaller clearances are attainable as a result of the restriction of horizontal deflection under fault conditions, and vertical deflection under own weight (sag) due to the rigidity of the tubular conductors as long as the bus tube is correctly sized for the application. Since the tubes are sized for mechanical strength, they are generally oversized electrically, allowing greater flexibility in busbar configuration.

Forces due to gravity, wind vibration, fault current and tubular conductor thermal expansion, as well as the restrictions on electromagnetic fields have been considered. The design criteria for conductor and insulator strength calculations also formed part of the study.

The study was carried out in a step-by-step analysis of the above considerations. An Excel based programme was developed to analyse the sensitivity of conductor and insulator strength calculations, due to errors in the estimation of various parameters that are required for these calculations. The tolerances in manufacturing and deviations in experimental data were determined and used to evaluate the results obtained and provide a level of confidence that any errors that may arrise could be mitigated against by choosing the correct components.

The result of the study is a design guide that allows substation designers to develop tubular busbar systems that will operate successfully in the conditions they were designed for. The guide provides an integrated design approach with methods for calculating the forces to which rigid bus structures are subjected.

CONTENTS

LIST OF FIGURES

LIST OF TABLES

SUMMARY OF SYMBOLS USED

Symbol	Unit	Description
A	mm^2	Conductor Cross-sectional area
A_e	m^2	Projected surface area
A_i	m^2/m	Projected area on bus tubing with ice coating
α	-	Rigid conductor, boundary condition factor
α_n	-	Ratio of the negative switching impulse component to the sum of both components (negative and positive) of a phase-to-phase overvoltage
α'	Np/m	Attenuation constant measured in the direction of z'
α_{th}	$1/^oC$	Coefficient of linear expansion
B_i	μT	Magnetic flux density for a given conductor height
C_{BCS}	mm	Minimum air clearance for conductor-structure gap (co-ordinated with lightning impulse withstand level)
C_{BRS}	mm	Minimum air clearance for rod-structure gap (co-ordinated with lightning impulse withstand level)
C_c	-	Surface curvature coefficient
C_d	-	Wind drag coefficient
CFO_{alt}	kV	Critical Flashover Voltage at Atltitude
CFO_{ccsl}	kV	Critical Flashover Voltage for a conductor-conductor gap at Sea Level
CFO_{cc90sl}	kV	90% Probability Critical Flashover Voltage for a conductor-conductor gap at Sea Level
CFO_{cc98sl}	kV	98% Probability Critical Flashover Voltage for a conductor-conductor gap at Sea Level
CFO_{cssl}	kV	Critical Flashover Voltage for a conductor-structure gap at Sea Level
CFO_{cs90sl}	kV	90% Probability Critical Flashover Voltage for a conductor-structure gap at Sea Level
CFO_{cs98sl}	kV	98% Probability Critical Flashover Voltage for a conductor-structure gap at Sea Level
CFO_{rssl}	kV	Critical Flashover Voltage for a rod-structure gap at Sea Level

CFO_{rs90sl}	kV	90% Probability Critical Flashover Voltage for a rod-structure gap at Sea Level
CFO_{rs98sl}	kV	98% Probability Critical Flashover Voltage for a rod-structure gap at Sea Level
CFO_{sl}	kV	Critical Flashover Voltage at Sea Level
CFO_{90alt}	kV	90% Probability Critical Flashover Voltage at Atltitude
CFO_{98alt}	kV	98% Probability Critical Flashover Voltage at Atltitude
CFO_{90sl}	kV	90% Probability Critical Flashover Voltage at Sea Level
CFO_{98sl}	kV	98% Probability Critical Flashover Voltage at Sea Level
C_{mi}	mm	Mean circumference on ice
C_p	-	Pressure coefficient for a given surface
C_{peCS}	mm	Minimum phase-to-earth air clearance for rod-structure gap (co-ordinated with switchning impulse withstand level)
C_{peRS}	mm	Minimum phase-to-earth air clearance for rod-structure gap (co-ordinated with lightning impulse withstand level)
C_{wh}	mm	Horizontal working clearance
C_{wv}	mm	Vertical working clearance
d	m	Size of gap in the geometry
d_{bi}	m	Inside diameter of conductor
d_{bn}	mm	Width of the phase conductor bundle
d_{bo}	m	Outside diameter of conductor
d_{bs}	mm	Width of busbar support structure
d_c	mm	Diameter of each of the phase bundle conductors
d_{eq}	mm	Width of the live part of the equipment of the equipment on the Red, White and Blue phases
D_i	m	Relative distances between conductors
d_{io}	mm	Diameter on outer edge of ice in mm
d_{mi}	mm	Mean diameter on ice

DYN	-	Dynamic
δ	-	Relative air density (RAD)
δ_s	-	Skin depth or depth of penetration
E	N/m^2	Modulus of elasticity
E_c	kV/cm	Corona threshold surface field strength
E_e	kV/cm	Maximum value of the surface voltage gradient on bus conductor
E_i	kV/m	Electric field strength for a given conductor height
ε	$C^2/N.m^2$	Dielectric constant for air
f	Hz	Electrical system frequency
f_a	Hz	Maximum Aeolian force frequency
F	N	Mechanical force
$F_{(PI)ST}$	N	Static force on post insulator
$F_{(PI)DYN}$	N	Dynamic force on post insulator without auto-re-closure (ARC)
$F_{(PI)DYN+ARC}$	N	Dynamic force on post insulator (with ARC)
$F_{A(PI)ST}$	N	Static force on post insulator A
$F_{A(PI)DYN}$	N	Dynamic force on post insulator A (without ARC)
$F_{A(PI)DYN+ARC}$	N	Dynamic force on post insulator A (with ARC)
$F_{B(PI)ST}$	N	Static force on post insulator B
$F_{B(PI)DYN}$	N	Dynamic force on post insulator B (without ARC)
$F_{B(PI)DYN+ARC}$	N	Dynamic force on post insulator B (with ARC)
f_c	Hz	Fundamental mechanical frequency
$\frac{f_c}{f}$	-	Frequency ratio
F_m	$N/(K.mm^2)$	Mechanical Force due to bus tube expansion or contraction
F^1_{L1p}	N/m	Electromagnetic peak force on outer phase
F^1_{L2p}	N/m	Electromagnetic peak force on centre phase
F^1_{L3p}	N/m	Electromagnetic peak force on outer phase
F_{12p}	N/m	Electromagnetic peak force phase to phase
$F_{R(PI)}$	N	Resulting force acting on post insulator
$F_{RA(PI)}$	N	Resulting force acting on post insulator A
$F_{RA(PI)max}$	N	Resulting force acting on post insulator A (with SF)

$F_{RB(PI)}$	N	Resulting force acting on post insulator B
$F_{RB(PI)max}$	N	Resulting force acting on post insulator B (with SF)
F^{1}_{REF}	N/m	Reference force per unit length
$F^{1}_{R(\sigma)}$	N/m	Resultant force per unit length
$F_{R(\sigma)}$	N	Total resultant force
$F^{1}_{R(\sigma)DYN}$	N/m	Resultant dynamic force per unit length (no ARC)
$F^{1}_{R(\sigma)DYN+ARC}$	N/m	Resultant dynamic force per unit length (with ARC)
$F^{1}_{R(\sigma)DYN+ARC1,2}$	N/m	Resultant dynamic force per unit length (with ARC) on conductor 1 or 2
$F^{1}_{R(\sigma)DYN+ARCH1,2}$	N/m	Resultant dynamic horizontal force per unit length (with ARC) on conductor 1 or 2
$F^{1}_{R(\sigma)DYN+ARCV1,2}$	N/m	Resultant dynamic vertical force per unit length (with ARC) on conductor 1 or 2
F^{1}_{sc}	N/m	Reference force per unit length
F^{1}_{w}	N/m	Wind loading per unit length on bus tubing without ice
F_{w}	N	Total wind loading on bus tubing without ice
F^{1}_{wi}	N/m	Wind loading per unit length on bus tubing with ice
F_{wi}	N	Total wind loading on bus tubing with ice
γ	Hz	Natural frequency factor
H_a	m	Altitude above sea level
H_{a1}	m	Lower altitude
H_{a2}	m	Upper altitude
h_{ave}	mm	Average height of conductors
h_b	mm (m)	Height of bus conductors above the ground
h_c	mm (m)	Height of equipment inter-connector conductors above the ground
h_{ci}	m	Height of conductor i
h_{et}	mm	Height from the base of the equipment porcelain to the conductor connection terminal
h_i	mm	Height of post insulator
h_s	mm	Height of support structure
H(t)	-	Probability density
I_{mi}	A	Maximum system current

$\mathbf{I_{sc}}$	A	Symmetrical three phase short circuit current, RMS value
J (I)	m^4	Moment of inertia (Second moment of area)
k	-	Static stress factor
$\mathbf{K_a}$	-	Atmospheric correction factor
$\mathbf{K_{cc}}$	-	Gap factor for conducto-conductor geometry
$\mathbf{K_{cs}}$	-	Gap factor for conductor-structure geometry
$\mathbf{K_f}$	-	Busbar support flexibility factor
$\mathbf{K_{+ff}}$	-	Gap factor for fast front impulses of positive polarity
$\mathbf{K_g}$	-	Gap factor taking into account the influence of the gap configuration on the strength
$\mathbf{k_p}$	-	A constant dependent on site altitude
$\mathbf{k_{pn}}$	-	Interpolated constant dependent on site altitude
$\mathbf{k_{p1}}$	-	Lower value of site altitude constant
$\mathbf{k_{p2}}$	-	Upper value of site altitude constant
$\mathbf{K_{rs}}$	-	Gap factor for rod-structure geometry
$\mathbf{k_z}$	-	Wind speed multiplier
$\mathbf{k_{zn}}$	-	Wind speed multiplier - interpolated values for intermediate values of z
$\mathbf{k_{z1}}$	-	Wind speed multiplier – Lower value
$\mathbf{k_{z2}}$	-	Wind speed multiplier – Upper value
$\boldsymbol{\kappa}$	-	Kappa factor for peak short circuit current
$\boldsymbol{\ell}$	m	Length of conductor span between supports
$\boldsymbol{\ell_{½}}$	m	Half the span length of a conductor span between supports
L	H	Inductance per unit length
L1	-	Outer conductor
L2	-	Inner (centre) conductor
L3	-	Outer conductor
$\mathbf{L_{bs}}$	mm	Bus tube span length
$\boldsymbol{\lambda}$	-	Factor for mechanical frequency
m	-	Exponent in atmospheric correction factor formula for external insulation withstand
M	N.m	Bending moment

m_l	kg/m	Mass of conductor per unit length
m^1_b	kg/m	Mass per unit length of bus tubing alone
m^1_c	kg/m	Mass per unit length of damping conductor alone
Max	-	Maximum
m^1_{b+c}	kg/m	Mass per unit length of bus tubing and damping conductor
m_a	-	Exponent in atmospheric correction factor formula for external insulation withstand for phase-to-earth insulation
m_b	-	Exponent in atmospheric correction factor formula for external insulation withstand for Longitudinal insulation
m_c	-	Exponent in atmospheric correction factor formula for external insulation withstand for phase-to-phase insulation
m_{di}	-	Exponent in atmospheric correction factor formula for external insulation withstand for Rod-plane gap (reference gap)
m^1_{b+c+i}	kg/m	Mass per unit length of bus tubing, damping conductor and ice
m_r	-	Factor to allow for surface roughness
$M_{R(PI)}$	kN.m	Bending moment at the base of the post insulator
$M_{RA(PI)}$	kN.m	Bending moment at the base of post insulator A
$M_{RB(PI)}$	kN.m	Bending moment at the base of post insulator B
$M_{R(S)}$	kN.m	Bending moment at the base of the post insulator steelwork support structure
$M_{RA(S)}$	kN.m	Bending moment at the base of post insulator A steelwork support structure
$M_{RB(S)}$	kN.m	Bending moment at the base of post insulator B steelwork support structure
N	-	Number of parallel spans of conductor
N_e	-	Number of 'conductor height-electric field' observations
μ	H/m	Permeability of a material

μ_0	H/m	Permeability of free space
μ_r	-	Relative permeability of a material
p_z	N/m^2	Surface pressure at height z
P^1_{wl}	N/m^2 (Pa)	Maximum wind pressure on projected area per unit length
P_{wl}	N/m^2 (Pa)	Total maximum wind pressure on projected area
Q_i	C	Instantaneous charge on conductor i
r^2	-	"Goodness" of fit
R	Ω	Resistance per unit lenth
R_f	-	Risk of failure
r_{bo}	m	Conductor radius
$R_{p0.2}$	MPa	0,2 % Proof stress
s_{cc}	m	Gap distance for a conductor- conductor geometry
s_{cc90sl}	m	90% Probability Gap distance at sea level for a conductor- conductor geometry
s_{cc98sl}	m	98% Probability Gap distance at sea level for a conductor- conductor geometry
s_{cs}	m	Gap distance for a conductor-structure geometry
s_{cs90sl}	m	90% Probability Gap distance at sea level for a conductor-structure geometry
s_{cs98sl}	m	98% Probability Gap distance at sea level for a conductor-structure geometry
s_e	mm (m)	Equipment phase-to-earth separation
S_e	mm (m)	Clearance between an item of primary plant and a busbar structure
s_p	m	Centre line distance between conductors
S_p	mm (m)	Phase spacing between items of primary plant
s_{rc}	m	Gap distance for a rod-conductor geometry
s_{rc90sl}	m	90% Probability Gap distance at sea level for a rod-conductor geometry
s_{rc98sl}	m	98% Probability Gap distance at sea level for a rod-conductor geometry
ST	-	Static
S_2	-	Statistical maximum surge referred to as the

		statistical switching over-voltage
S_{90alt}	m	90% Probability Gap distance at altitude
S_{98alt}	m	98% Probability Gap distance at altitude
S_{90sl}	m	90% Probability Gap distance at sea level
S_{98sl}	m	98% Probability Gap distance at sea level
σ	Ω^{-1} / m	Conductivity per unit lenth of a material
σ_{pu}	pu	Per unit value of the conventional deviation of an overvoltage distribution
σ_{ST}	N/m^2 (Mpa)	Maximum static bending stress
σ_{DYN}	N/m^2 (Mpa)	Maximum dynamic bending stress (without auto re-closure)
$\sigma_{DYN+ARC}$	N/m2 (Mpa)	Maximum dynamic bending stress (with auto re-closure)
t	-	The function value of the normal distribution curve (or value of the independent variable associated with a given area under a normal distribution curve)
T_f	oC	Final temperature
t_i	mm	Thickness of ice coating
T_i	°C	Initial temperature
t_w	mm	Bus tube wall thickness
τ_f	s	Time constant of decaying dc-component of short circuit current
τ_{PI}	kN.m	Rated maximum allowable torque on the post insulator head
τ_{sc}	kN.m	Torque exerted due to short circuit forces on the bus tubing
2	-	Phase-to-phase short circuit
U_{cw}	kV	Co-ordination withstand voltage of equipment
U_m	kV	Maximum system voltage (related to equipment)
U_n	kV	Nominal system voltage
U_{ppe}	kV	Peak phase-to-earth voltage (1 p.u.)
U_{rB}	kV	Standard lightning impulse withstand voltage
U_{rS}	kV	Standard switching impulse withstand voltage
U_{50RP}	kV	Value of the 50% discharge voltage of a rod-plane

		gap
U_{50}	kV	Value of the 50% discharge voltage of self restoring insulation
μ_o	V.s/A.m	Absolute permeability = $4.\pi .10^{-7}$
V	m/s	Regional basic wind speed
v^1_b	m^3/m	Volume per unit length of bus tubing
v_i	m^3/m	Volume per unit length of ice on bus tubing
V_{mi}	kV	Maximum system voltage
V_p	m/s	The component of the Characteristic wind speed in m/s that is perpendicular to the bus tubing
V_z	m/s	Nominal wind speed at height z above the ground
V_1	kV	Instantaneous phase-to-phase voltage on conductor 1
V_2	kV	Instantaneous phase-to-phase voltage on conductor 2
V_3	kV	Instantaneous phase-to-phase voltage on conductor 3
v_F	-	Dynamic factor (force) for support system
v_σ	-	Dynamic factor (stress) for tubular conductor 3 phase
v_r	-	Dynamic factor (auto-reclosure)
W_b	mm	Equipment bay width
w^1	N/m	Weight per unit length of bus tubing alone
w_b	N	Total weight of bus tubing
w^1_c	N/m	Weight per unit length of damping conductor
w_c	N	Total weight of damping conductor
w^1_i	N/m	Weight of ice per unit length on bus tubing
w_i	N	Total weight of ice on bus tubing
W (Z)	m^3	Section modulus
X	Ω	Reactance
X/R	-	Impedance ratio
y_a	mm	Allowable maximum vertical deflection on bus tube
y_c	m	Vertical deflection of bus tube under own weight
y_{DYN}	mm	Maximum Deflection of a Rigid Bus under Short Circuit Current alone (no ARC)
y_{DYNh}	mm	Maximum Horizontal Deflection of a Rigid Bus under Short Circuit Current alone (no ARC)

$y_{DYN+ARC}$	mm	Maximum Deflection of a Rigid Bus under Dynamic Conditions (wind, fault & ARC)
$y_{DYN+ARCh}$	mm	Maximum Horizontal Deflection of a Rigid Bus under Dynamic Conditions (wind, fault & ARC)
z	m	Height above the ground
z′	mm	Measurement from the surface of a conductor towards its centre

ABBREVIATIONS USED IN THIS DISSERTATION

Abbreviation	Description
ABB	Asea Brown Boveri
AIS	Air insulated systems
ANSI	American National Standard Institute
ARC	Auto Re-close or auto re-closure
ASA	American Standards Association
BIL	Basic insulation level
BS	British Standard
CDEGS	Current Distribution Electromagnetic and Grounding Systems
CERAM	A manufacturer of porcelain insulators, now call PPC
CFO	Critical Flashover Voltage
Cigré	International Council on Large Electrical Systems
DIN VDE	German Standard
EHV	Extra High Voltage
EMF	Electromagnetic Field
Eskom	Electricity Supply Commission (of South Africa)
GIS	Geographic Information System
HV	High Voltage
ICNIRP	International Commission on Non-ionising Radiation Protection
IDZ	Industrial Development Zone
IEC	International Electrotechnical Commission
IEEE	Institute of Electrical and Electronic Engineers
IRPA	International Radiation Protection Association
KZN	KwaZulu Natal
LIWL	Lightning impulse withstand level
MATHCAD	Trade name for desktop software for performing and documenting engineering and scientific calculations
MTBF	Mean time between failures
MIG	Metal Inert Gas (welding)
NRPB	Advisory group on Non-ionising Radiation Power Frequency Electromagnetic Fields

PROKON	Trade name for a civil engineering software package for structural analysis and design
RAD	Relative air density
RSA	Republic of South Africa
SIL	Switching impulse level
SIWL	Switching impulse withstand level
TIG	Tungsten Inert Gas (welding)
UK	United Kingdom

1. INTRODUCTION

The cost of land, the sensitivity of the environment to construction, and a host of other techno-economic and social pressures are requiring new **compact** designs for outdoor air insulated (AIS) substations. They are to become more compact, without introducing additional **operational** risks, and at the same time producing the same or improved reliability of supply. In addition to this, greater demands are being placed on utilities to provide substations with larger busbar capacities to service electrical corridors with higher power densities. Of late, this has become the general trend, where existing Eskom substations are being required to service larger electrical loads due to the absence of suitably sized plots of land and power corridors to costruct additional infrastructure. This new requirement has highlighted the limitations of bundled flexible conductors where many of Eskoms Main Transmission Substations with bundled flexible conductor busbars requiring upgrading to larger numbers of conductors per bundle. In most cases additional support steelwork is required to limit the sag of the conductor phases as a result of the limitations in the strain forces that can be exerted on existing busbar strain portals leading to lower tensions per bundle conductor. In many instances, this is impractical due to the limited time that is available for substation outages. It takes several days to "drop" a busbar and to restring it with a larger number of flexible conductors per phase bundle.

In the past, the standards used by Eskom in the design of busbar systems were based on phase-to-earth and phase-to-phase clearances calculated using a deterministic approach [1], i.e. an approach that assumes that all the factors that may contribute to the conditions that could occur at the time of a fault, all occurred at the same time. Strung flexible conductor busbar systems are particularly problematic in this regard due to the excessive horizontal conductor displacement that takes place as a result of conductor swing under fault conditions. The deterministic approach leads to electrical clearances that are very large which, coupled with the excessive conductor swing, require phase-to-structure and phase-conductor separation distances that may be possible for a particular site. This is of particular concern at the EHV (400kV) and UHV (765kV) voltage levels.

One also needs to consider the "skin effect" influences on the current distribution within an electrical conductor. The outer conductor layers of a stranded conductor, conduct higher currents than the inside ones and consequently the theoretical conductancy of the material is not utilized to its full potential.

The conduction current density is given by [2]:-

$$J_x = \sigma.E_{x0}.e^{-z'\sqrt{\pi.f.\mu.\sigma}} \quad (1.1)$$

Considering the exponential term, an exponential decrease in the conduction current density and electric field intensity with penetration into the conductor occurs. At the surface of the conductor, i.e. $z' = 0$ therefore,

$e^{-z'\sqrt{\pi.f.\mu.\sigma}} = 1$, i.e. the exponential factor is unity. (1.2)

When $z' = \frac{1}{\sqrt{\pi . f . \mu . \sigma}}$ therefore, (1.3)

$e^{-z'.\sqrt{\pi.f.\mu.\sigma}} = e^{-1}$
$= 0,368$, i.e. the exponential factor is unity. (1.4)

This distance is termed the the depth of penetration or skin depth and is denoted by δ_s.

$$\delta_s = \frac{1}{\sqrt{\pi . f . \mu . \sigma}} = \frac{1}{\alpha'} \quad (1.5)$$

and

$$\mu = \mu_r \mu_0 \quad (1.6)$$

where:-

f = system frequency
μ = permeability of material
σ = conductivity per unit lenth in Ω^{-1} / m
α' = attenuation constant in Np/m
μ_0 = permeability of free space ($4\pi.10^{-7}$ H/m)
μ_r = relative permeability of material

Table 1.1: Representative Metallic Electical Parameters [2]

Material	Specific Conductivity [σ] (Ω^{-1} / m)	Relative Permeability μ_r
Aluminium	$3,82.10^7$	1,00000065
Copper	$5,8.10^7$	0,99631

1.1 Considering Some Metallic Conductors

1.1.1 Aluminium Conductors

$$\mu_{Al} = 1{,}00000065.\ 4\pi.10^{-7}$$

$$= 1{,}2566.10^{-6}\ \text{H/m}$$

$$\delta_{sAl} = \frac{1}{\sqrt{\pi.50.1{,}2566.10^{-6}.3{,}82.10^{7}}}$$

$$\delta_{sAl} = 11{,}5\text{mm}$$

1.1.2 Considering Copper Conductors

$$\mu_{Cu} = 0{,}9963\ 4\pi.10^{-7}$$

$$= 1{,}2520.10^{-6}\ \text{H/m}$$

$$\delta_{scu} = \frac{1}{\sqrt{\pi.50.1{,}2520.10^{-6}.5{,}8.10^{7}}}$$

$$= 9{,}4\text{mm}$$

At power frequency (50 Hz) therefore, $\delta_{sAl} = 11{,}5$mm and $\delta_{scu} = 9{,}35$ mm. Power density (W/m^2) [2] carries an exponential term $e^{-2\alpha z}$. The power density is then multiplied by a factor of $0{,}368^2 = 0{,}135$ for every 11,5mm of distance into aluminium and 9,35 mm of distance into the copper, the power density.

Therefore, any current density or electric field intensity established at the surface of a good conductor, decays rapidly as one progresses into the conductor. Electromagnetic energy is not transmitted in the interior of a conductor; it travels in the region surrounding the conductor, while the conductor merely guides the waves. The currents established at the conductor surface propagate into the conductor in a direction perpendicular to the direction of the current density, and they are attenuated by ohmic losses. This power loss is the price exacted by the conductor for acting as a guide. The tubular shape of the conductor makes this profile a very efficient one as far as current distribution in the material is concerned, i.e. as a tube, compared to the diameter, has relatively low wall thickness, the differences in the currents between the material zones located on the inside and outside are small. Tubular conductors are therefore far more efficient transmitters of electrical power at power frequency than stranded flexible conductors.

When considering all the above together with the fact that the "skin" effect phenomenon inherent in a.c. systems contributes to lowered effective use of the "solid" flexible conductors, and, that the volume of concrete and steel necessary to realise the infrastructure required to support the larger numbers of conductors per bundle, increases exponentially making this design philosophy techno-economically inefficient. This has prompted the author to concentrate on the alternative conductor configuration of using tubular conductor and associated support systems that would lead to more efficient use of materials and also make it possible to upgrade

existing strung flexible conductor busbar systems as required by the increasing demand for power in a manner that will result in shorter "outages" being required.

The use of rigid conductors for busbars is widely employed in modern HV and EHV outdoor air insulated substations (AIS) [3]. The "structure" must, however, have enough strength to withstand the significant mechanical stresses that develop due to wind and ice loadings, Aeolian vibration and mechanical forces as a result of the short circuit currents that may occur on, or near the busbar system [4]. These stresses are imposed on the tubular conductors and the supporting structures, composed of insulators and substructures (steelwork supports and support foundations). The mechanical requirements to ensure the strength in the tubular conductors inherently leads to a conductor with a high current carrying capacity. The mechanical stresses on equipment is lower with tubular conductors and with a short-circuit they do not clench together and tear at the armature fittings, as is the case with stranded flexible conductors connected in parallel where bundle collapse occurs. The rigidity of the tubular conductors also offers an opportunity for smaller portal clearances due to smaller conductor deflections under fault conditions and due to its own weight.

The corona and thermal performance of tubular conductors is inherently better than that of bundled flexible conductors due to the larger surface areas that are available, leading to lower voltage gradients and and lower running temperatures respectively.

Experiences gained to date have also resulted in a particularly unlimited longevity of aluminium tubes independent of location or environmental conditions. The tubes require neither anodising nor a coat of paint as their natural oxide film has proven to be a sufficient protection against corrosion.

To sum up the problem, substation designers are constantly under pressure to provide cost effective substation designs that meet both the technical requirements, and have low visual impact on the environment. Within this framework, the rigid tubular conductor bus structure comes into its own right for compactness, low visual profile and cost [1]. Since this dissertation is an application design guide, only the results of a comparative cost profile between overhead strung flexible conductor busbars and a chosen tubular busbar arrangement is given and is essentially summarised in Figure 1.1. For a more indepth treatment of the economics involved in substation design, the following references are provided for further reading:

Bayliss C R, Hardy B J, "Transmission and Distribution Electrical Engineering", Newnes, 3rd Ed., 2007, ISBN 0 750666730

Ilic A J, Galiana F D, Fink L H, "Engineering and Economics", Springer, 1998, ISBN 079 238 1637

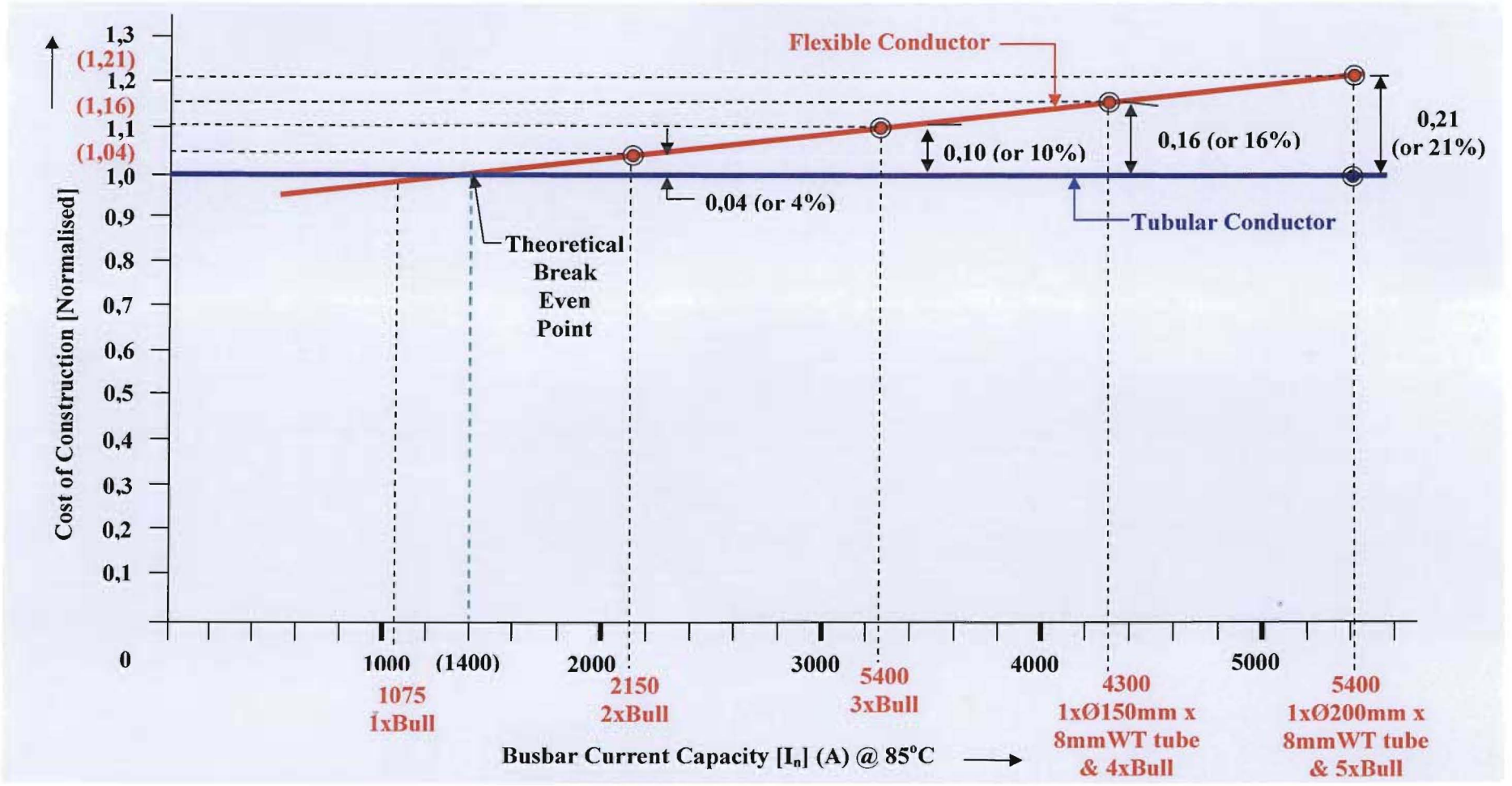

Figure1.1: Cost of Construction [Normalised] vs Busbar Current Capacity (Ampacity) [I_n] (A)

(Cost of the 1xØ200mm x 8mmWT tubular conductor system used as the base value

Several papers ([3] [4] [5] [6] [7] [8] [9]) have been published in recent years on the physics of electromagnetic forces without a holistic practical guideline pertaining to rigid tubular conductors and their performance under steady state and transient conditions. The literature survey embarked upon suggests that the articles discuss the implementation of bus tube systems, by focusing on individual aspects of these systems. It was for this reason that the author has embarked on the study, as an attempt to identify, select and define important parameters, as well as discuss the critical issues relating to clearances, investigate the latest theory and practices. The eventual aim was to produce a Design Application Guide for the use of tubular conductors in the design of substations.

HYPOTHESIS: **"Tubular conductors can provide substantial techno-economic advantages in the design of high voltage substations as compared to conventional overhead suspended bundled flexible conductors."**

2. LITERATURE SURVEY

The preliminary literature servey indicated that a large number of articles relating to air insulation, clearances and the behaviour of conductors under fault conditions are available. However, a detailed step-by-step application guide for the employment of round tubular conductors based on the latest research of statistical methods does not exist.

In qualifying the statements made above for example, a number of papers have been published in recent years on the physics of electromagnetic forces pertaining to rigid tubular conductors and their performance under steady state and transient conditions ([3] [4] [5] [6] [7] [8] [9]). These papers, as their titles suggest, concentrate purely on calculation methods of these forces and the correctness thereof.

Hoseman et al [5] conducted parametric studies with the aid of analytical calculation method and a number of extensive numerical methods. It was found that only a few parameters are of significance, so that even simplified calculation methods may be used with confidence; the dynamic stressing is determined with the aid of factors which are a function of the mechanical fundamental frequency of the conductors.

Cigré Working Group 23 [4] parametric studies determined that there are a number of criteria that influences the dynamic stressing of conductors and insulators. These are as follows:-

- mechanical resonances (see Chapter 11 of this dissertation)
- damping (see Chapter 12 of this dissertation)
- boundary conditions for the ends of the conductors (see Chapter 11 of this dissertation)
- the time patterns of electromagnetic forces, the worst case being the centre phase of a three phase system (see Chapter 10 of this dissertation)

  Centre phase (b)

$$\mathbf{F^{1}_{b}(t)} = \mathbf{F^{1}_{sc.}}\frac{\sqrt{3}}{2}\left[\underbrace{f_0 + f_{2\omega}(\mathbf{t})}_{\textbf{steady state}} + \underbrace{f_{\omega}(\mathbf{t}) + f_{g}(\mathbf{t})}_{\textbf{decaying}}\right]$$

$$= \mathbf{F^{1}_{sc.}} f_{b}(\mathbf{t}) \qquad (2.1)$$

$$= \mathbf{0{,}866.F^{1}_{sc}\kappa^{2}}$$

  Outer phases (a and c)

Where:-

$\mathbf{F^1_b(t)}$ = Force per unit length on the centre phase in N/m

$\mathbf{F^1_{sc}}$ = Reference force per unit length N/m

f_0 = Constant term (arithmetic mean of $f(\mathbf{t})$ in steady state)

$f_{2\omega}(\mathbf{t})$ = Undamped oscillation at double the electrical frequency

$f_{\omega}(\mathbf{t})$ = Oscillation with electrical frequency, decaying with $\tau_f = \frac{\mathbf{L}}{\mathbf{R}}$

$f_g(\mathbf{t})$ = Exponential term decaying with $\frac{\tau_f}{\mathbf{2}}$

κ = Kappa factor

$$\mathbf{F^1_a(t) = F^1_c(t) = F^1_{sc}.\frac{3+2\sqrt{3}}{2}.\left[\underbrace{f_0 + f_{2\omega}(t)}_{\text{steady state}} + \underbrace{f_{\omega}(t) + f_g(t)}_{\text{decaying}}\right]} \text{[4]} \qquad (2.2)$$

$$\mathbf{= 0{,}808.F^1_{sc}\kappa^2}$$

Where:-

$\mathbf{F^1_a(t)}$ = Force per unit length on the outer phase in N/m

$\mathbf{F^1_c(t)}$ = Force per unit length on the outer phase in N/m

- short circuit duration
- supports
- number of conductor spans where the conductor is either supported freely or clamped along the continuous length of conductor (see Chapter 11 of this dissertation)
- unsuccessful auto-reclosure (see Chapter 13 of this dissertation)

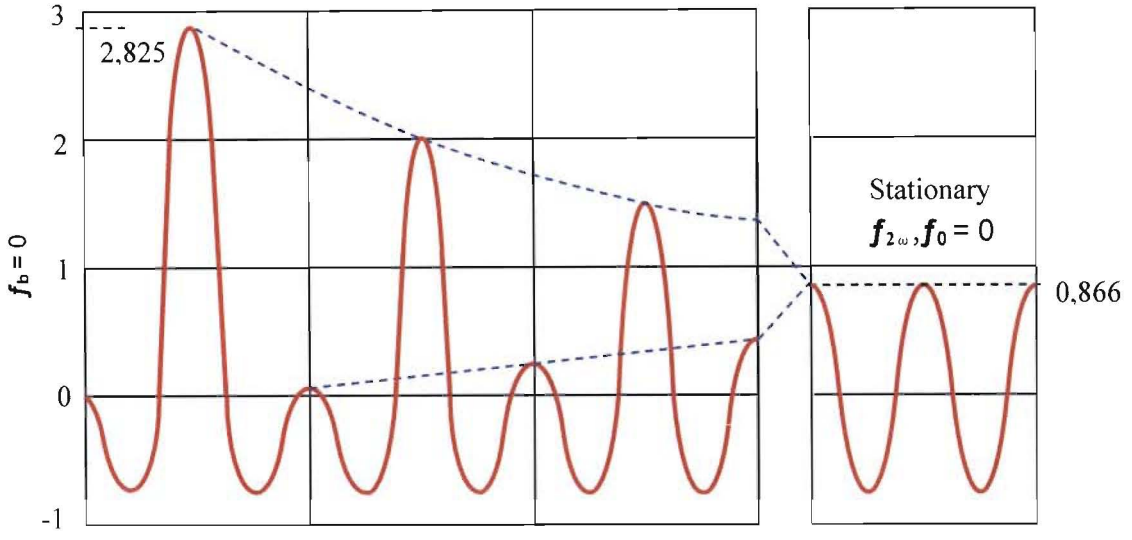

Figure 2.1: Worst Case Curve of Electromagnetic Force on Centre Conductor (b) Related To I_{sc} When X/R = 15 under Three Phase Short Circuit [4]

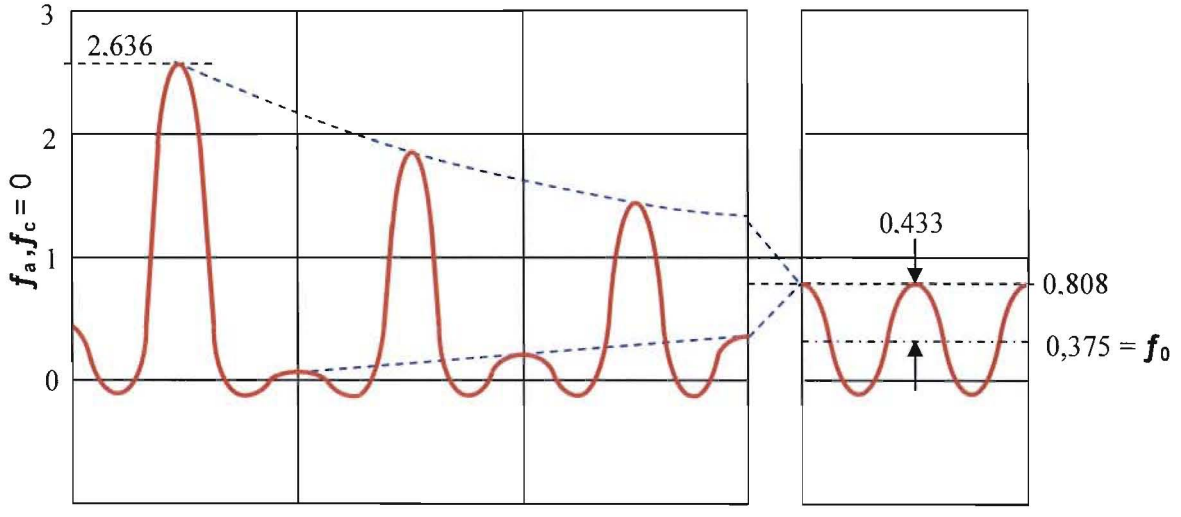

Figure 2.2: Worst Case Curve of Electromagnetic Forces on Outer Conductors (a and c) Related To I_{sc} When X/R = 15 under Three Phase Short Circuit [4]

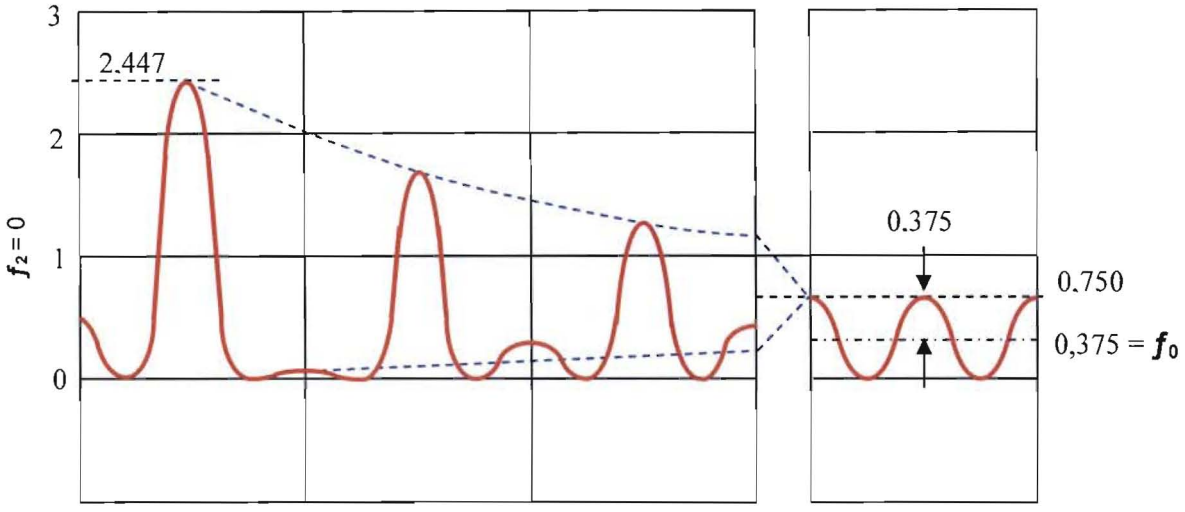

Figure 2.3: Worst Case Curve of Electromagnetic Force on Two Conductors Related To I_{sc} When X/R = 15 under Phase-to-Phase Short Circuit [4]

For further explanation on time patterns of forces, the reader is referred to the two refences provided above, viz. "The Mechanical Effects of Short Circuit Currents in Open Air Substations" [4] and "Dynamic Short-Circuit Stress of Busbars-Structures with Stiff Conductors" [5]

Most of the other papers that have have been published ([3] [6] [7] [8]) are practical or theoretical verifications of the previous work that was done in the past. The following are examples of these:-

- Meintjes et al [3] carried out tests at SABS NETFA as verification that it was indeed possible to design and safely operate tubular bus systems.
- Cigré Study Committee 23 (Working Group 23-02) [6] reported on the calculation methods and comparisons with test results that were published in Electra 30 in 1973.
- Cigré Study Committee 23 (Working Group 23-02) [7] reported on the correctness of a calculation method.
- R J Cakebread and H J Brown [8] produced work on integrated mechanical design loading for open type EHV substation structures and equipment under Working Group 04 of Study Committee No.23

Papers and standards exist for insulation co-ordination discussing lightning and switching impulse levels that lead to the determination of various operational clearances [10] [11] [12] [13] [14].

Zaffanella et al [13] dicuss in great detail the phase-to-earth and phase-to-phase insulation requirements for switching surges on transmission lines and in substations. They provide a graphical means to determine the phase-to-phase critical flash over voltages for given phase separation. They state that the total flashover probability (**P**) for substations needs to be at least $3/2.10^{-4}$ or smaller. Several tables are also provided that enable one to calculate phase-to-phase clearances.

IEC 60-1 [10] and IEC 71-2 [14] are application guides on Insulation Co-ordination. The latter document discusses the insulation optimisation process. This is essentially that amount of insulation required to reduce the probability of a flashover to 2% or conversely, that the insulation will survive 98% of the time. In this regard, tables of phase-to-earth and phase-to-phase clearances are provided for lightning and switching impulses which are essentially translated to system voltage clearances.

DIN VDE 0101 [15] is a standard that provides guidelines of ice loading on conductors.

SABS 0160-1989 with amendments in subsequent years [16] is a civil engineering code of practice that provides valuable information, tablesand methods to determine the characteristic wind speeds in at any given location in South Africa. Characteristic wind speeds can be determined in four diffently categorised terrain types, at different heights above ground level and, to enable engineers to calculate wind pressures on a variety of structures. It lends itself very well to be adapted to substation design

Gujarati [17] was used to provide the mathematical means to perform multi-variable regression and build a model for determining the electric and magnetic field strengths for any given set of parameters within the boundaries of the studies carried out.

Hayt [2] and Edminister [18] provided some of the fundamentals of electromagnetic theory in the "skin" effect considerations. These considerations are taken up in the Introduction in expaining some of the reasons for moving towards round tubular conductors for use in high voltage substations.

The impact of seismic activity is not discussed here due to the complexity of the design criteria. Although individual components such as primary plant are tested for seismic operation 0,3g to 0,5g, the sheer size of whole systems makes it impossible to subject these to the same form of testing. These systems need to be precisely modelled in very complex computer programmes, with computer simulations being run to determine the seismic effects on the whole system. These programmes are extremely costly and generally are proprietory assets.

This dissertaion is an attempt to select the important parameters and develop a logically ordered step-by-step application guideline for the substation designer. It has been presented in such a way that it can be used as applications guide for substation designers, having both academic as well as potential commercial or industrial benefit.

3. METHODOLOGY

Objectives of this Chapter:

- Introduce why considering bus tubing
- Why the design guide?
- What important factors need to be considered?
- Reliability issue and consequences
- Brief summary of the process flow

3.1 Overview

The primary objective of this dissertation is to provide electrical substation designers with an integrated step-by-step guide on the use of round tubular conductors in the design of high voltage tubular busbar substations as well as an understanding of the sensitivity of a number of parameters to material tolerances and error in estimation of parameter values.

As a means for ensuring that the research for the project is kept in line with the primary objective in the most effective manner possible, a "terms of reference" document was set up in the order of the prososed topics to be covered, and then reviewed from time to time to check for continuity and clarity. A discription of the essential components requiring investigation and discussion is provided in paragraph 3.2 below and forms the terms of reference for the whole guide. Reviewing of literature was then approached in the same manner, keeping in mind that there were two essential criteria that had to be met. These are that:

- the proposed busbar system had to withstand the different types of forces that had a high probability of occurring simultaneously, and
- the dielectric strength (electrical insulation) of the air would survive a range of overvoltages in magnitude and type.

The point of departure was to review the differences between the current electrical clearances employed by Eskom and statistical based values as provided by IEC 71-2. The statistical approach to electrical clearances allows smaller clearances, i.e. phases could be brought closer together, by accepting a predetermined an increase in risk of failure. By mitigating against this risk in a more cost effect way, e.g. adding surge arresters in selected positions, one can achieve more compact, low profile substations with high power throughput capability. This aspect is covered in Chapters 5 and 6. In addition, other factors impacting on phase-to-earth and phase-

to-phase clearances needed to be studied. These included the sag of the bus tube under its own weight, and horizontal displacement of the bus tubes under fault conditions with and without unsuccessful auto-reclosing of a circuit breaker. The influence of different support methods such as freely supported and fixed ends, and permutations of these required consideration.

With regard to the strength of the busbar system, it was important to examine all the factors that contribute to placing mechanical stresses on the components of the system and ensure that there was a mathematical means of modelling them. Some of these mathematical representations where provided by the liternature that was reviewed, this having been acknowledged by way of the references enclosed in square brackets, other representations were developed by the author from knowledge of ordinary physics. It was important to determine these relationships so that they could be modelled in an Excel based software programme for study purposes.

Several types of forces and their origin needed to be investigated, these being essentially categorised into static and dynamic forces. The static forces considered being "dead' weight of the bus tube, the additional weight of the damping conductor, ice loading, all of which are gravity enhanced, and lastly wind loading on the bus tube which generally acting perpendicularly to gravity. In order to make the design guide generally applicable to any site in South Africa, it was necessary to obtain metereological information on characteristic regional wind velocities in the Republic and then by mathematical means transform this to a representative wind pressure at a given height above the ground. This could then be converted to a force exerted on the bus tube per unit length. These aspects are covered in Chapters 6 to 8, and then picked up again in Chapter 13 of this dissetation.

The second important force type that needed attention was the dynamic loading on the system, i.e. forces as a result of a symmetrical three phase and assymmetrical phase-to-phase faults with and without unsuccessful auto-reclosing of a circuit breaker. Unsuccessful auto-recosing amplifies the dynamic impact on the bus tube. This is discussed in Chapters 9, 10, 12 and 14 of this dissetation, while Chapter 11 looks at how oscillations set up in the bus tube by laminar wind flow can be damped.

Chapters 15 and 16 of this dissertation considers various mechanical issues such as maximum bending moments and tortion on the substructure (support post insulators and associated steelwork), and ensuring manufacturing limits are not exceeded. In conjunction with this, Chapter 16 provides a means to evaluate the impact of thermal expansion on the bus support system and correct selection of fixings.

The means to evaluate the impact of corona, electric and magnetic fields on the overal design of the busbar system is discussed in detail, having carried out several studies in this regard. This is presented in Chapters 17 and 18 where several graphical representations of the data are provided for clarity.

The theory behind the design process was developed in a logical and orderly manner in order that the parameter sensitivity studies could be embarked upon, and therefore accounts for Chapters 4 to 18 as discussed above. This theory was then transformed into an Excel based programme which was tested against several hand calculations carried out. These hand calculations are recorded in Chapter 20. Chapter 19 is the result of the various sensitivity studies that were performed.

Since it has become a much publicised issue, the associated topics of electric and magnetic fields were also investigated in order to determine the expected exposure levels when personnel access high voltage yards. These calculated values were then compared to the values in the IRPA guidelines. The study was performed using the CDEGS software that enables one to model the proposed bus configuration, and then by providing the programme with all the parameters for a given condition, e.g. maximum expected current, maximum system voltage, phase spacing, bus tube diameter, height of conductors above the ground, etc, will provide a value for either electric or magnetic field strength, whichever is to be determined. **Figure 3.1** is an illustration of an output from CDEGS, resulting in a single item of data, which in this case, is the electric field profile under a 3 phase flat busbar system. Several hundred different parameter permutations were analysed in like manner and Chapter 18 is dedicated to this study. In the end, a relationship between electric and magnetic field strength with with respect to the above given parameters was deteremined using multiple variable regression analysis. In all cases the maximum value of the field strengths were used.

Figure 3.2 is a Spot Plot which provides a visual result of electric field strength at various locations within a 765kV HV yard. One can immediately determine the areas of concerns by visual inspection.

The "RESULTS" arisng out of applying the methodology forms an integral part of the design guide and combined with the discussion within the main text in which the results are analysed and justified.

HIFREQ (Job Id: 765KV SUBSTATION ELECTRIC FIELD EFFECTS 12 METRES 08 JUNE 2005)
Electric Fields/Resultant (Total) Field

09-June-2005 09:53:08 AM

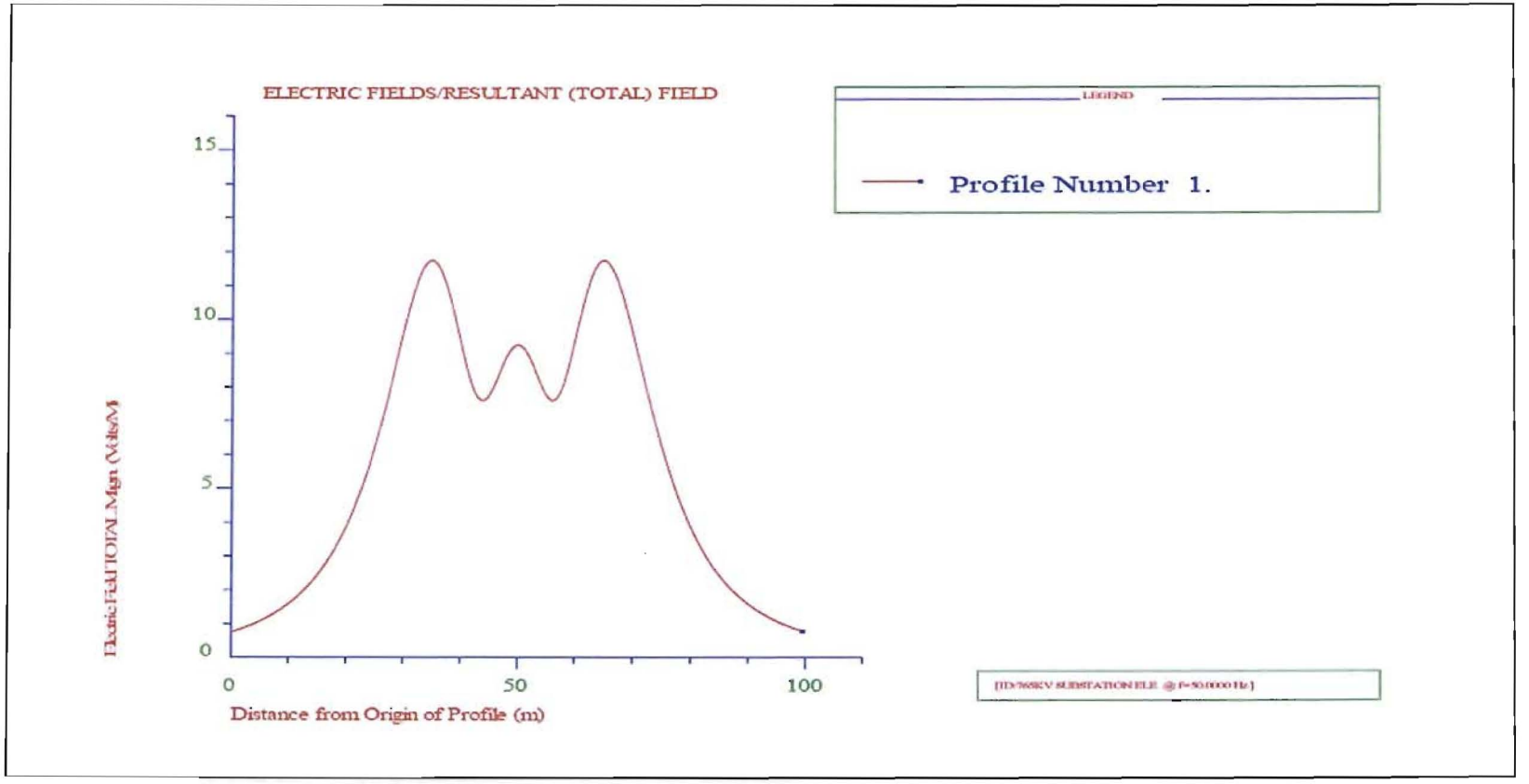

Working Directory: D:\ESKOM\CDEGS\TRANSMISSION STUDIES\SUBSTATIONS\braam 765kv tony

Figure 3.1: A Typical Result from a CDEGS Programme Simulation

Appendix 1: CDEGS Spot Plot for 765kV Mercury Substation.

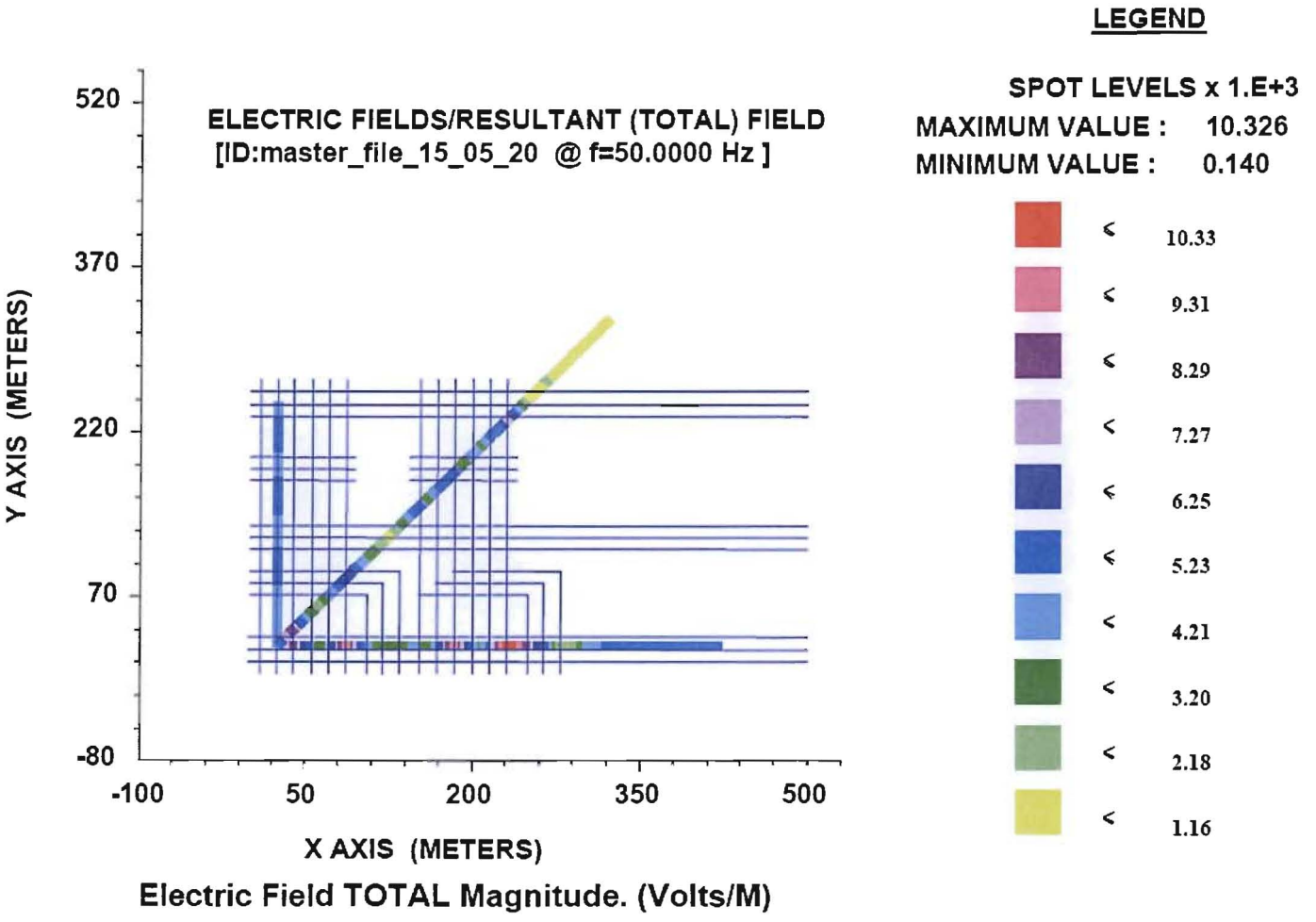

Figure 3.2: A Typical Spot Plot from a CDEGS Programme Simulation

3.2 "Terms of Reference"

. A complete guide for rigid busbar application should at least focus on issues such as:-

- Insulation levels and associated clearances
- Continuous current carrying capability
- Steady state loading, bending moments, stresses and deflections
- Dynamic loading during short circuit conditions
- Resultant loading from a deterministic or probabilistic approach
- Surface electrostatic field strengths and corona inception levels in the limitation of corona
- The limitation of electric and magnetic field strengths to fall in line with the IRPA Guidelines

The aim of this dissertation is to extract the relevant information for calculating the mechanical effects of short circuit current on rigid tubular conductors and their support structures. An attempt has been made to provide a simplified model which yields fast results suitable for everyday design purposes.

Because the consequences of failure within the station, is greater than the consequence of a flashover of a single line, the station reliability criterion must be higher than the line by a factor 10 [5].

Different criteria are usually applied to air- and gas-insulated stations. For example, the mean time between failures (MTBF) of air-insulated stations, vary between 50 and 200 years, whereas for gas-insulated stations, the MTBF has been set as high as 800 years [5]. The basis of this is the consequence of failure in the gas-insulated station that may require significant outage and repair times

The process that is followed for each of the components of the tubular bus system, viz. tubular conductor (maximum stress and maximum deflection) and support insulators can by-enlarge be categorised into the following order:

- Reference calculation
- Static condition
- Dynamic condition
- Dynamic condition with auto-re-close

- Combined static and dynamic forces
- Safety factor
- Test for limits

The behaviour of the tubular busbar system under static and dynamic conditions is dependent upon a number of factors. These factors, one of which is the type of support system employed (boundary condition) will be presented and discussed in turn under different chapters. The order in which these are discussed is an attempt to provide a logical and understandable presentation of the subject concerned. In order to provide the reader with a brief insight into what is to follow, brief descriptions are given:-

3.3 The Length of the Bus Tubing

The length of the bus tubing that is employed is dependent upon:

3.3.1 The boundary conditions of the busbar system employed, i.e. the support system employed at the ends of each bus tube (both ends freely supported, one end freely supported + one end fixed, both ends fixed)

3.3.2 The minimum allowable phase-to-earth and phase-to-phase clearances between items of equipment in a three-phase system

3.3.3 The maximum allowable sag of the bus tubing

3.3.4 Bus tubing outer diameter and wall thickness

3.3.5 The maximum allowable stress in the tube under extreme dynamic conditions - mechanical characteristics of the material (the alloy employed) such as the 0,2% Proof Stress

3.3.6 The maximum horizontal deflection of the bus tubing – required to calculate the phase-to-phase clearance between bus ducting and ensure that minimum values are not infringed.

3.4 Strength of the Support Insulators

3.4.1 The boundary conditions of the busbar system employed, i.e. the support system employed at the ends of each bus tube (both ends freely supported, one end freely supported + one end fixed, both ends fixed)

3.4.2 The minimum allowable phase-to-earth and phase-to-phase clearances between items of equipment in a three-phase system

3.4.3 The maximum allowable sag of the bus tubing

The required strength of the support insulators that are to be employed:

3.4.4 The maximum allowable dynamic force for a given guaranteed static strength

3.4.5 The maximum allowable bending moment at the base of the insulator

3.4.6 The maximum allowable torsion on the head of the insulator

3.5 Conductor Heights

The required conductor heights that are to be employed:

3.5.1 The minimum allowable height of a phase conductor to ensure there is no corona

3.5.2 The minimum allowable height of the three phase conductors to ensure that the electric and magnetic field strengths at 1,8m above ground level do not exceed accepted values in working and public areas

3.6 Summary of Design Process in the Selection of Rigid Tubular Conductors

The rigid bus design process is detailed in ANSI/IEEE Standard 605 "IEEE Guide for Design of Substation Rigid Bus Structures" [9]. The steps in this process are repeated below for reference:

3.6.1 Establish design requirement and bus arrangement

3.6.2 Select bus conductor shape (generally circular) and material (generally aluminium)

3.6.3 Establish minimum bus size based on ampacity and corona

3.6.4 Select trial conductor size

3.6.5 Establish need for damping and select damper type and size

3.6.6 Calculate total gravitational force

3.6.7 Calculate conductor wind force

3.6.8 Calculate conductor short-circuit force

3.6.9 Calculate resultant (total vector sum) force ($\mathbf{F_R}$) on conductor

3.6.10 Location of bus support fittings (i.e. slip, rigid, and expansion fittings)

3.6.11 Calculate maximum span ($\mathbf{L_d}$) based on deflection

3.6.12 Calculate maximum span ($\mathbf{L_s}$) based on material 0,2 % proof stress

3.6.13 Select maximum span equal to ($\mathbf{L_d}$) or ($\mathbf{L_s}$), whichever is the lesser

3.6.14 Calculate total insulator cantilever load

3.6.15 Select insulator strength required based on multiplying the cantilever load multiplied by the appropriate safety factor

3.6.16 Thermal expansion and capacity considerations

3.6.17 Analyse the continuous spans for calculated loading as a final design (with torsion)

3.6.18 Determine locations of welded couplings if these are required to join tubes to make up the full span

3.6.19 Analyse steelwork structures (not in the scope of this dissertation)

3.6.20 Analyse support foundations (not in the scope of this dissertation)

Figure 3.3 is a high level flow diagram produced to illustrate the design process described above. It essentially summarises the process into a much condensed form and was produced by the author and [9] to conform in the order that the subject is presented in this work.

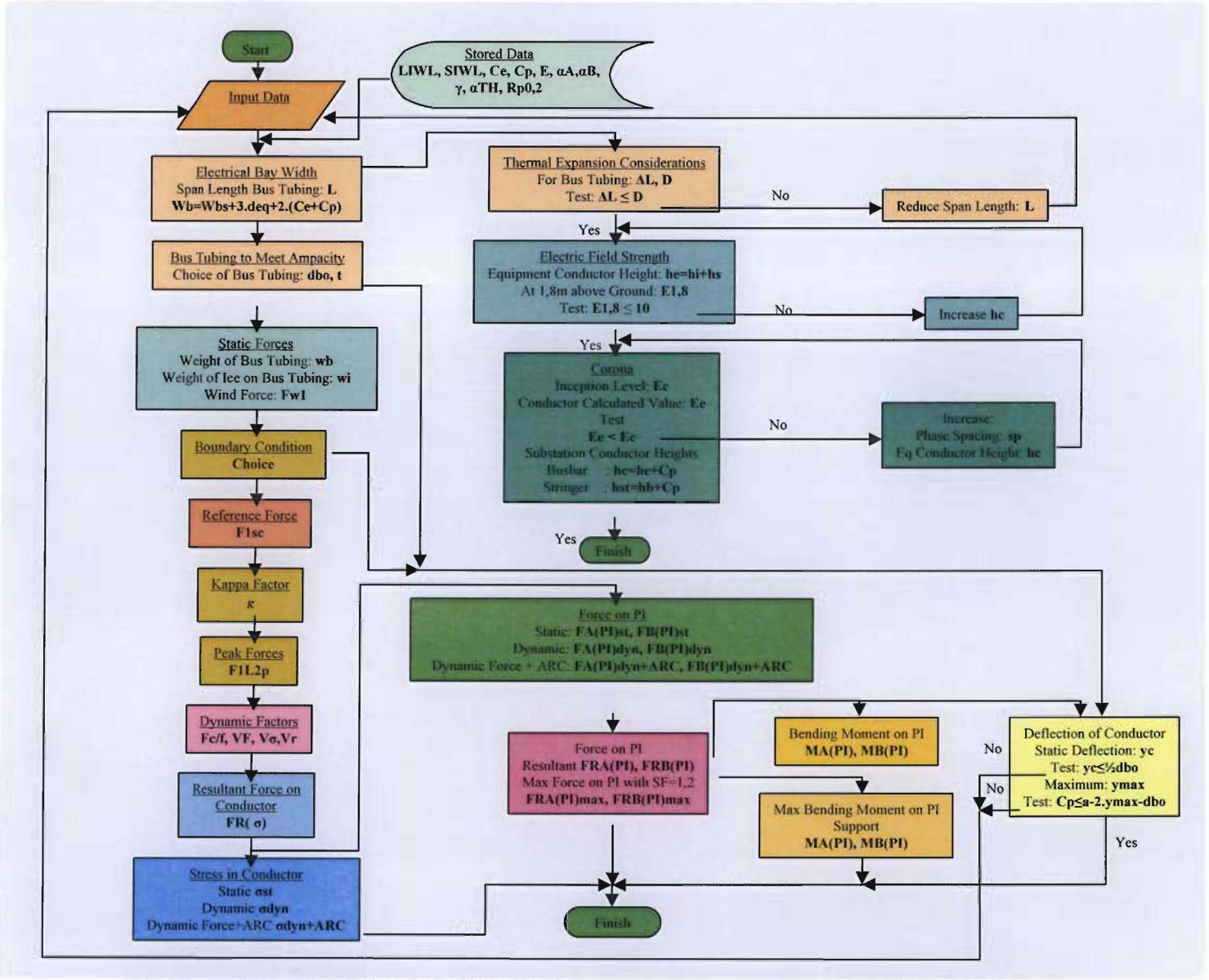

Figure 3.3: High Level Process Flow Diagram forDimensioning Post Insulators and Bus Tubes

3.7 Rigid Bus Design is an Iterative Process

If the calculations indicate that the conductor chosen will not to be suitable, then a number of options are available. By changing the variables one at a time or combinations thereof will eventually provide the best techno-economic solution. The variables are as follows:

- Conductor span length
- Conductor phase spacing
- Conductor size
- Conductor shape
- Conductor material (alloys)
- Conductor height - Although theoretically speaking, the height of the conductor is a design variable in the choice of a tubular conductor, the conductor is normally sized for mechanical strength, i.e. to withstand short circuit, wind and ice loadings on it. This generally results in a bus tube that is oversized for electrical purposes, both in terms of current carrying capacity and corona performance. Although it is necessary to check it, the surface voltage gradient on the tube is in virtually all practical cases, an order of magnitude lower than the corona inception value. This is clearly demonstrated in the example given under paragraph 17.2.2.3.

3.8 Design Criteria and Bus Arrangement

- Bus current carrying capacity (ampacity)
- Maximum expected three phase rms symmetrical short circuit current. This is the ultimate long term value expected at the substation.
- Maximum operating voltage.
- Insulator BIL rating.
- Maximum anticipated wind speed (extreme wind).
- Maximum expected icing condition combined with wind.
- Altitude of the substation (if greater than 900m).
- Basic substation layout (rigid bus arrangement).
- Seismic design conditions if substation is located in an area of seismic activity. Seismic considerations and their impact on the design of substations have not been taken into account in this dissertation due to their complex nature. It would require a dissertation on

its own to deal with all the issues satisfactorily. Suffice it to say that a supported busbar system as is covered in this text needs drastic measures to be taken, and it would be better to suspend tubular conductors.

3.9 Selection of Bus Conductor Shape and Material

For high voltage and extra high voltage substations, seamless, round, aluminium bus tubing should be used. IEC standard tube sizes of various specified grades [1], [19] and [20] (see write-up and test results).

4. ELECTRICAL CLEARANCES BASED ON A STATISTICAL APPROACH

Objectives of this Chapter:

- Choice of Line Voltage $\mathbf{U_n}$
- Choice of BIL based on lightning impulse withstand level (LIWL) or switching impulse withstand level (SIWL) for Line Voltage $\mathbf{U_n}$, whichever is appropriate
- Determine appropriate phase-to-earth clearance ($\mathbf{C_{pe}}$)
- Determine appropriate phase-to-phase clearance ($\mathbf{C_{pp}}$)
- Determine the appropriate safe horizontal working distance ($\mathbf{C_{wh}}$)
- Determine the appropriate safe vertical working distance ($\mathbf{C_{wv}}$)
- Determining the appropriate phase centres ($\mathbf{s_p}$) that are depend on minimum phase-to-earth and phase-to-phase clearances

4.1 Insulation Cordination Procedures

The determination of the co-ordination withstand voltages consists of determining the lowest values of the withstand voltages of the insulation meeting performance criterion when subjected to the representative over-voltages under service conditions.

Two methods for co-ordination to transient over-voltages are in use: **a deterministic method** and **a statistical method**. Many of the applied procedures, however, are a mixture of both methods. For example, some factors used in the deterministic method have been derived from statistical considerations or some statistical variations have been neglected in statistical methods.

4.1.1 Deterministic Method [14]

The deterministic method is normally applied when no statistical information obtained by testing is available on possible failure rates of the equipment to be expected in service.

With the deterministic method:

- when the insulation is characterised by its conventional assumed withstand voltage, i.e. the probability of withstand of self-restoring insulation $\mathbf{P_w}$ = 100%, the withstand value is selected equal to the co-ordination withstand voltage obtained by multiplying the representative over-voltage (an assumed maximum) by a co-ordination factor $\mathbf{K_c}$, accounting for the effect of the uncertainties in the assumptions for the two values (the assumed withstand voltage and the representative over-voltage);

- when, as for external insulation, the insulation is characterised by the statistical withstand voltage (P_w= 90%), K_c should account almost for all differences between this voltage and the assumed withstand voltage

With this method, no reference is made to possible failure rates of the equipment in service.

4.1.2 Statistical Method [13]

For the probability of disruptive discharge of insulation in self-restoring insulation, the ability to withstand dielectric stresses caused by the application of an impulse of given shape can be described in statistical terms. For a given insulation and for impulses of given shape and different peak value **U**, a discharge probability **P** can be associated with every possible value **U**, thus establishing the following relationship:-

$$P = P(U) \tag{4.1}$$

- U_{50} corresponds to the voltage under which the insulation has a 50% probability to flashover or to withstand
- **z** is the conventional deviation which represents the scatter of flashover voltages. It is defined as the difference between the voltages corresponding to flashover probabilities 50% and 16%

$$z = U_{50} - U_{16} \tag{4.2}$$

- U_0 is the truncation voltage, the maximum voltage below which a disruptive discharge is no longer possible

The statistical method is therefore based on the frequency of occurrence of a specific origin, the over-voltage probability distribution belonging to this origin and the discharge probability of the insulation. Alternatively, the risk of failure may be determined by combining over-voltage and discharge probability calculations simultaneously, shot by shot, taking into account the statistical nature of over-voltages and discharge by suitable procedures.

By repeating the calculations for different types of insulations and for different states of the network, the total outage rate of the system due to the insulation failures can be obtained.

Hence the application of the statistical insulation co-ordination gives the possibility to estimate the failure frequency directly as a function of the selected system design factors. In principle, even the optimisation of the insulation could be possible, if outage costs could be related to the different types of faults. In practice, this is very difficult due to the difficulty to evaluate the consequences of even insulation faults in different operation states of the network, and due to the uncertainty of the cost of undelivered energy. Therefore it is better to slightly over-dimension the insulation rather than optimise it. The design of the insulation system is then based on the comparison of the risks corresponding to the different alternative designs.

Once the frequency distribution of the over-voltages and the corresponding breakdown probability distribution are given, the risk of failure of the insulation between phase and earth can be calculated as follows:

$$R_f = \int_0^{\infty} f(U).P(U)dU \qquad (4.3)$$

Where:-

R_f = The risk of failure

$f(U)$ = Probability density of over-voltages (occurrence described by a Gaussian function)

$P(U)$ = Probability of flash-over of the insulation under an impulse value U (described by modified Weibull function)

U_t = truncation value of the over-voltage probability distribution

$U_{50\text{-}4z}$ truncation value of the discharge probability distribution

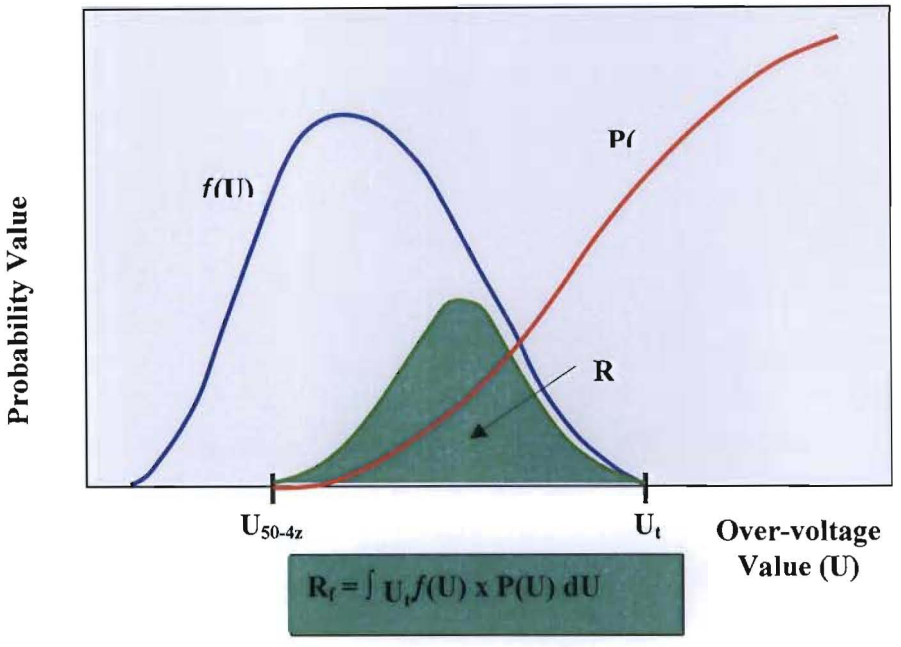

Figure 4.1: Evaluation of the Risk of Failure [14]

4.1.2.1 Relating Overvoltage Stresses to Insulation Strength

For a substation where there could be 10 to 50 locations within the substation to consider regarding possible phase-to-phase flashover, the data given in Figure 4.4, $\alpha_n = 0{,}5$ and Figure 4.5 with standard deviation of the flashover voltage $\sigma_{pu} = 5\%$ should be used [13].

Where:-

α_n = Ratio of the negative switching impulse component to the sum of both components (negative and positive) of a phase-to-phase overvoltage

σ_{pu} = Per unit value of the conventional deviation (S_e) of an overvoltage distribution

Methodology: Minimum phase-to-phase distances in substations are calculated assuming:-

- A total flashover probability $\mathbf{p = \frac{3}{2}.10^{-4}}$ **[13]** (4.4)
- The CFO values for one phase-to-phase insulating element are evaluated for each statistical phase-to-earth voltage first using Figures 4.2 and 4.3 to determine S_2 and σ_s below

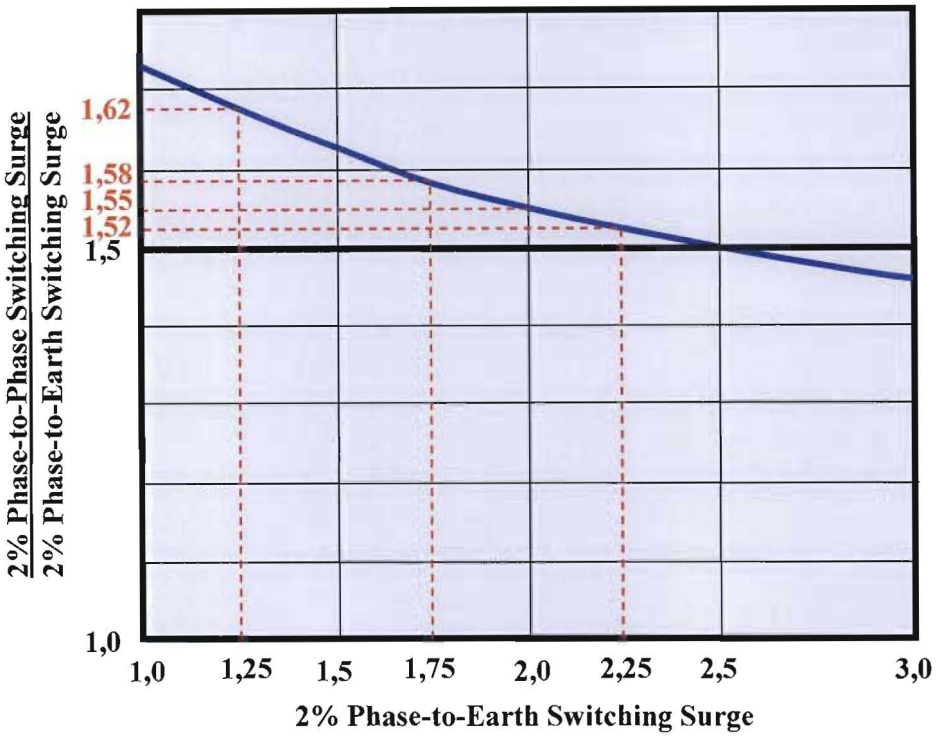

Figure 4.2: Approximate Relation between Phase-to-Phase and Phase-to-Earth Switching-Surge Values [13]

Table 4.1: Determining the Max (2% Value) Phase-to-Phase Surge (p.u.) from Figure 4.2 13]

Max (2% Value) Phase-to-Earth Surge (p.u.)	Ratio Max (2% Value) Phase-to-Phase Surge to Phase-to-Earth Surge	Max (2% Value) Phase-to-Phase Surge (p.u.)	
1,50	1,62	1,50.1.62	2,43
1,75	1.58	1.75.1.58	2,77
2,00	1.55	2,00.1,55	3,10
2,25	1,52	2,25.1,52	3,42

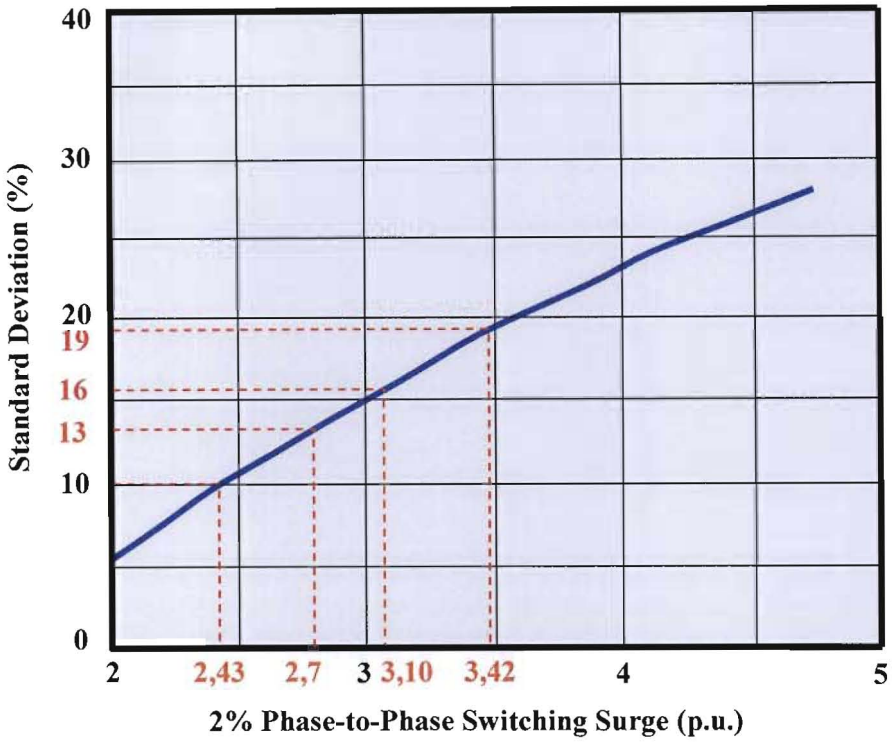

Figure 4.3 Standard Deviation of the Crest Values of Phase-to-Phase Over-voltages vs the Statistical Maximum (2% Value) Phase-to-Phase Over-voltages [13]

Table 4.2: Determining the Standard Deviation of the Crest Values of Phase-to-Phase Over-voltages from Figure 4.3 [13]

Max (2% Value) Phase-to-Phase Surge (p.u.)	Standard Deviation of the Crest Values of Phase-to-Phase Over-voltages [σ_s] (%)
2,43	10
2,77	13
3,10	16
3,42	19

- $\sigma_{pu} = 5\%$
- **N**= 30 (Number of parallel spans)

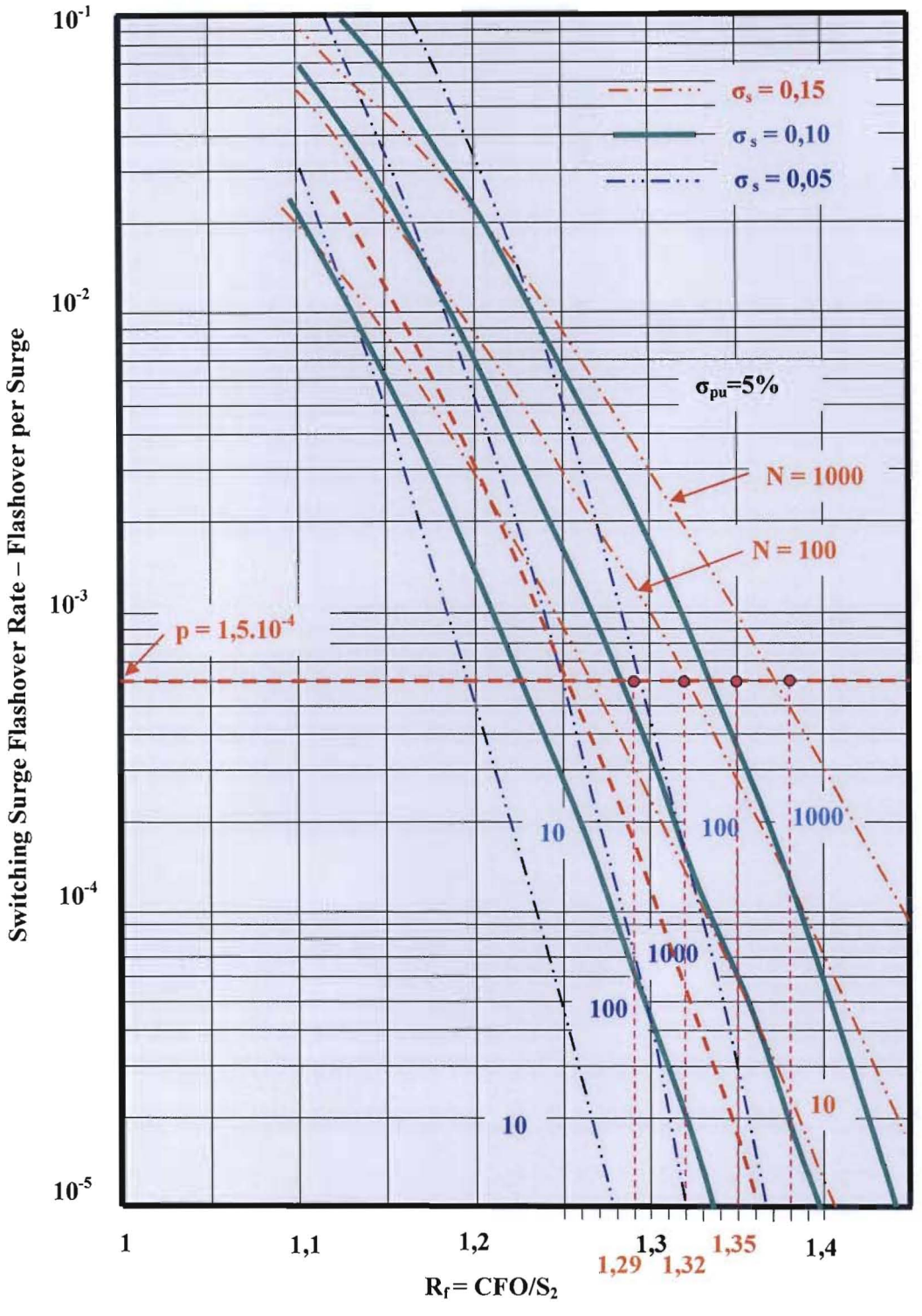

Figure 4.4: Flashover Rate verses Strength/Stress Ratio for Different Values of N and σ_s, σ_{pu}= 5% of CFO [13]

4.1.2.1a) Phase-to-Phase Flashover Probability

Phase-to-phase flashover probability of the parallel three phase conductors is a function of the ratio:-

- $R_f = \frac{CFO}{S_2}$ (4.5)

Where:-

S_2 = Statistical maximum surge referred to as the statistical switching over-voltage

- Use Figure 4.5 to determine R_f. Results shown in Table 4.3.

$$CFO = R_f.S_2 \quad (4.6)$$

The R_f and **CFO** values are provided in Table 4.3 below.

Table 4.3: Determining the Statistical maximum surge referred to as the statistical switching over-voltage from Figure 4.4 [13]

Standard Deviation of the Crest Values of Phase-to-Phase Over-voltages [σ_s] (%)	Phase-to-Phase Flash-Over Probability [R_f]	Max (2% Value) Phase-to-Phase Surge [S_2] (p.u.)	Critical Flashover Voltage [CFO] (pu)	
10	1,29	2,43	1,29.2,43	3,13
13	1,32	2,77	1,32.2,77	3,66
16	1,35	3,10	1,35.3,10	4,18
19	1,38	3,42	1,38.3,42	4,72

4.1.2.2 Determining the Phase-to-Earth and Phase-to-Phase Critical Flashover Voltages

By definition, the 1 p.u. representative peak overvoltage in the transient domain is given by $U_{ppe} = \frac{U_m.\sqrt{2}}{\sqrt{3}}(kV)$. The maximum 2% phase-to-earth surge values in Table 4.4 are expressed in p.u. with reference to this value.

$$CFO\ (kV) = U_m.CFO_{pu} \quad (4.7)$$

Table 4.4: Determining the Phase-to-Earth and Phase-to-Phase CFO [13]

Maximum System Voltage (kV)	Max (2% Value) Phase-to-Earth Surge (p.u.)	Phase-to-Earth CFO (kV)		Max (2% Value) Phase-to-Phase Surge (p.u.)	Phase-to-Phase CFO (kV)	
362	1,75	362. 1,75	634	3,66	362. 3,66	1325
	2,00	362. 2,00	724	4,18	362. 4,18	1514
	2,25	362. 2,25	815	4,72	362. 4,72	1709
550	1,75	550. 1,75	963	3,66	550. 3,66	2013
	2,00	550. 2,00	1100	4,18	550. 4,18	2299
800	1,75	800. 1,75	1600	3,66	800. 3,66	2928
	2,00	800. 2,00	1800	4,18	800. 4,18	3344
1200	1,50	1200. 1,50	1800	3,13	1200. 3,13	3756
	1,75	1200. 1,75	2100	3,66	1200. 3,66	4392
	2,00	1200. 2,00	2400	4,18	1200. 4,18	5016
1500	1,50	1500.1,50	2250	3,13	1500.3,13	4695
	1,75	1500.1,75	2625	3,66	1500. 3,66	5490

4.1.2.3 Determining the Phase-to-Earth and Phase-to-Phase Distances [13]

For a given gap spacing, the lowest phase-to-phase voltage is obtained when a positive voltage is applied to one conductor with the other grounded, and that the highest voltage is obtained when a negative voltage is applied to one conductor with the other grounded.

α_n is defined as the ratio of value of the negative voltage to total voltage, i.e.

$$\alpha_n = \frac{V_{neg}}{V_{neg} + V_{pos}} \tag{4.8}$$

All the crest voltages are negative while positive voltage is zero:

$$\alpha_n = \frac{V_{neg}}{V_{neg} + V_{pos}} = 1 \quad (\text{for } V_{pos} = 0) \tag{4.9}$$

The negative crest voltage equals the positive crest voltage:

$$\alpha_n = \frac{V_{neg}}{V_{neg} + V_{pos}} = 0{,}5 \quad (\text{for } V_{neg} = V_{pos}) \tag{4.10}$$

The positive crest voltage is twice the negative crest voltage:

$$\alpha_n = \frac{V_{neg}}{V_{neg} + 2.V_{neg}} = 0{,}33 \quad (\text{for } V_{neg} = V_{pos}) \tag{4.11}$$

The negative crest voltage is zero:

$$\alpha_n = \frac{V_{neg}}{V_{neg} + V_{pos}} = 0 \quad (\text{for } V_{neg} = 0)$$

The phase-to-phase distances required to withstand switching surges in substations are determined using Figure 4.5 for $\alpha_n = 0{,}5$; and are shown in Table 4.7.

- **CFO** curves of Figure 4.5 with $\alpha_n = 0{,}5$

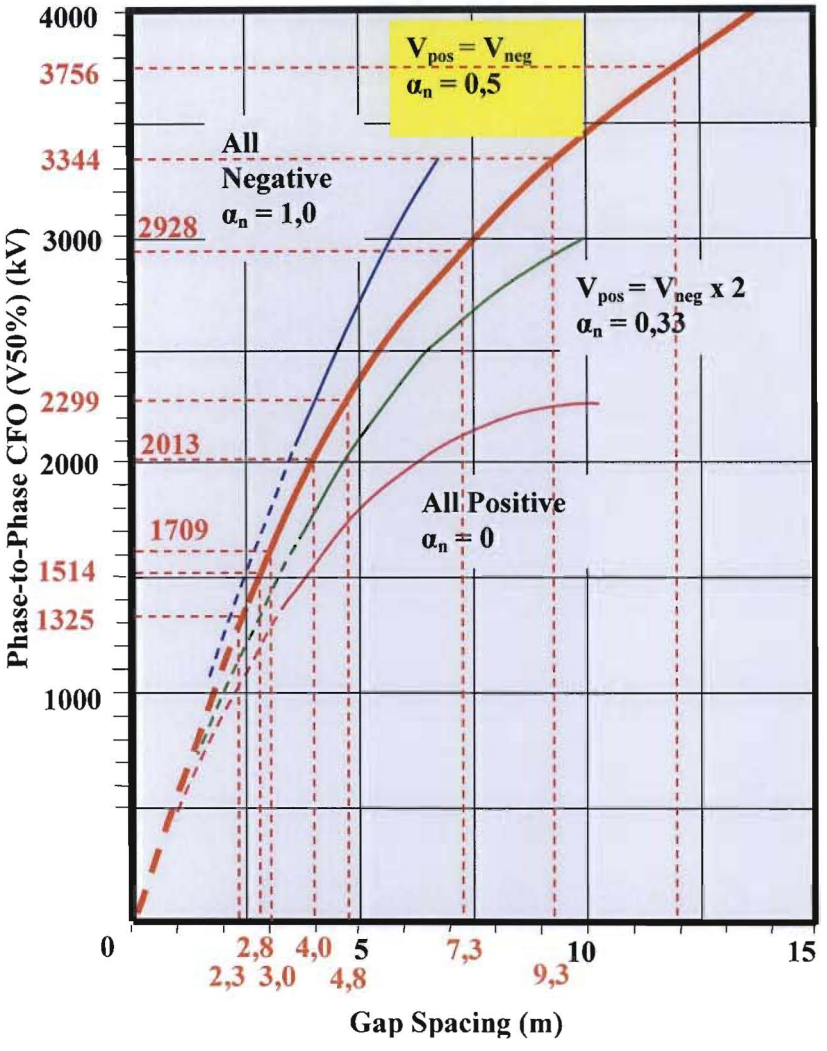

Figure 4.5: Phase-to-Phase CFO of 12m Conductor Sections for Different Phase-to-Earth Voltage Combinations. Time to Crest of Positive Impulse 350μs [13]

Table 4.5: Minimum Phase-to-Phase Distances in Substations to Withstand Switching Surges [13]

Phase-to-Phase CFO (kV)	Phase-to-Phase Distance (m)	Value Used in Existing (m)
1325	2,3	4 - 6
1514	2,8	
1709	3,0	
2013	4,0	7 - 10
2299	4,8	
2928	5,1	10 - 13
3344	6,3	
3756	7,7	-
4392	10,8	
5016	14,8	
4695	12,6	-
5490	18,0	

It is apparent from the table that existing substations have a very conservative design with respect to phase-to-phase switching surges

4.2 Gap Factors

Table 4.6: Gap factors for typical phase-to-phase geometries [14]

Gap type	Parameters	Typical range	Reference values
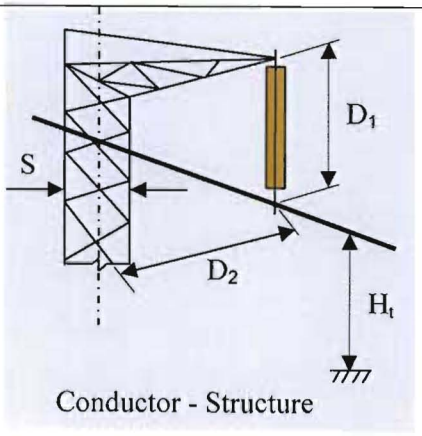	K_g	1,36 – 1,58	1,45
	D_2/D_1	1 – 2	1,5
	H_t/D_1	3,34 – 10	6
	S/D_1	0,67 – 0,2	0,2

Table 4.6: Gap factors for typical phase-to-phase geometries (continued) [14]

Gap type	Parameters	Typical range	Reference values	
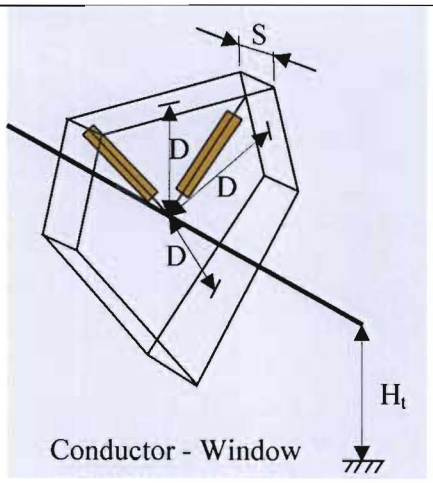	K_g	1,22 – 1,32	1,25	
	H_t/D	8 – 6,7	6	
	S/D	0,4 – 0,1	0,2	
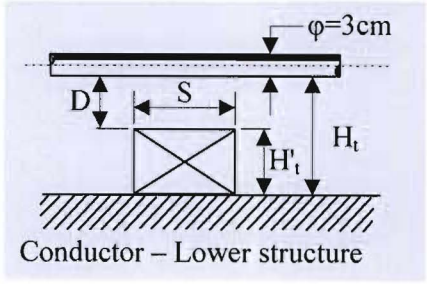	K_g	1,18 – 1,35	1,15 Cond-Plane	1,47 Cond-Rod
	H'_t/H_t	0,75 – 0,75	0	0,909
	H'_t/D	3 - 3	0	10
	S/D	1,4 – 0,05	-	0
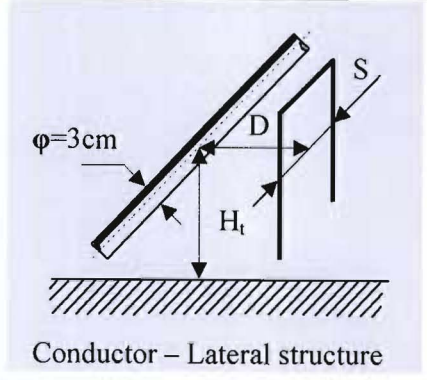	K	1,28 – 1,63	1,45	
	H_t/D	2 - 10	6	
	S/D	1 – 0,1	0,2	
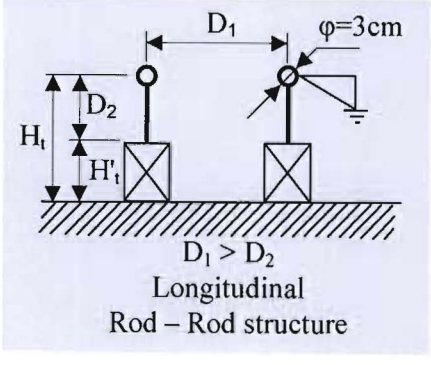	K_g	1,03 – 1,66	1,35	
	H'_t/H_t	0,2 – 0,9	0	
	D/H_t	0,1 – 0,8	0,5	

Table 4.7: Gap factors for typical phase-to-phase geometries [14]

Configuration	K_g	
	$\alpha_n = 0,5$	$\alpha_n = 0,33$
Ring – ring or large smooth electrodes	1,80	1,70
Crossed conductors	1,65	1,53
Rod – rod or conductor – conductor (along the span)	1,62	1,52
Supported busbars (fittings)	1,50	1,40
Asymmetrical geometries	1,45	1,36
NOTE – According to [1] and [4]		

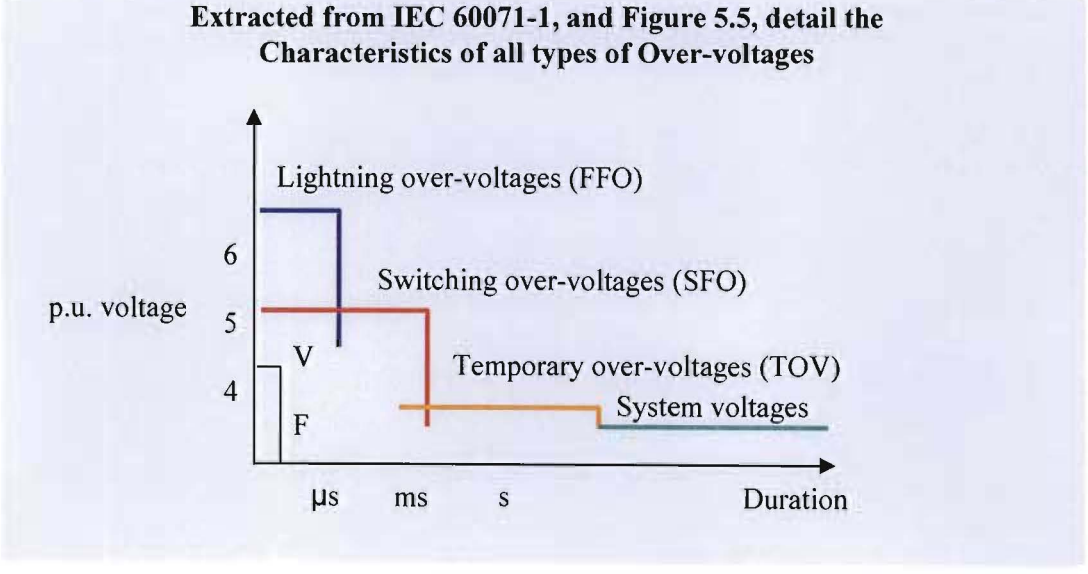

Figure 4.6: Types of Over-voltages (except Very-fast-front Over-voltages) [14]

Table 4.8: Classes and Shapes of Overvoltages – Standard Voltage Shapes and Standard Withstand Tests [10] [19]

Class	Low Frequency		Transient		
	Continuous	Temporary	Slow-front	Fast-front	Very-fast-front
Voltage or Overvoltage Shapes	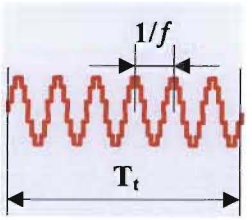	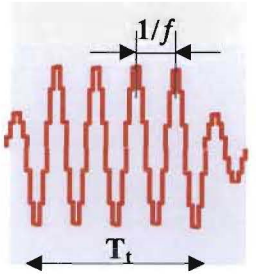	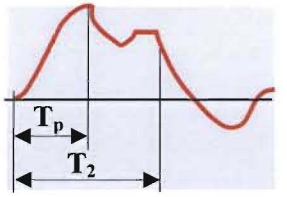	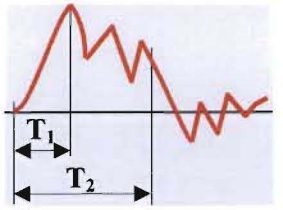	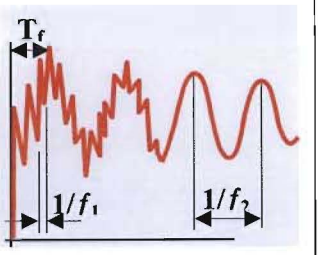
Range of Voltage or Overvoltage Shapes	Or 60Hz $T_t \geq 3\ 600s$	$10Hz < f < 500Hz$ $0,03s \leq T_t \leq 3\ 600s$	$20\mu s < T_p \leq 5000\ \mu s$ $T_2 \leq 20ms$	$0,1\mu s < T_1 \leq 20\ \mu s$ $T_2 \leq 300ms$	$3ns \leq T_f \leq 100ns$ $0,3MHz < f_1 < 100MHz$ $30kHz < f_2 < 300kHz$

Table 4.8 (continued): Classes and Shapes of Overvoltages – Standard Voltage Shapes and Standard Withstand Tests [10] [19]

Standard Voltage Shapes	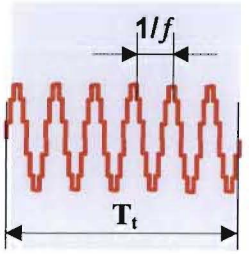	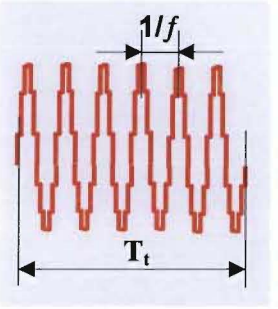	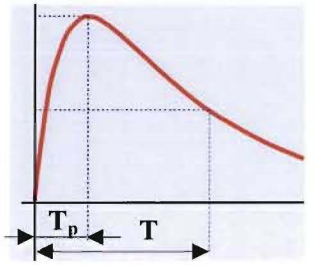	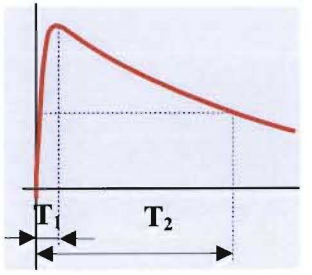	[1]
	f = 50Hz or 60Hz T_t [1]	450Hz ≤ f ≤ 62Hz T_t = 60s	T_p = 250µs T_2 = 2 500µs	T_1 = 1,2µs T = 50µs	
Standard Withstand Test	[1]	**Short Duration Power Frequency Test**	**Switching Impulse Withstand**	**Lightning Impulse Withstand**	[1]

[1] **To be specified by the relevant apparatus committees**

4.3 Minimum Phase-to-Earth and Phase-to-Phase Clearances

In complete installations such as substations which cannot be tested as a whole, it is necessary to ensure that the dielectric strength is adequate.

The switching and lightning impulse withstand voltages in air at standard atmospheric conditions must be equal to, or greater than the standard switching and lightning impulse withstand voltages. Minimum clearances have been determined for different electrode configurations following a conservative approach which takes into account practical experience, economy and size of practical equipment [14].

The minimum phase-to-earth and phase-to-phase clearances are dependant upon the breakdown characteristics of air. The breakdown characteristics of air depend on:-

- Configuration of the live and earth electrodes [14]
- Point-to-plane (worst case used in the deterministic approach throughout the substation making overall dimensions large)
- Conductor-to-structure
- Conductor-to-conductor

Applying these selectively, dimensions can be vastly reduced.

- RAD – altitude
- Pollution levels: marine, industrial
- Over-voltages that the live parts experience (lightning [lightning impulse withstand level], switching [switching impulse withstand level], load rejection [power frequency level], etc.). How to minimise these – station class and line surge arresters surge arresters – do not use arcing horns on transformer bushings due to high frequency harmonics generated back into the transformer – puncture insulation

These clearances may be lower if it has been proven by tests on actual or similar configurations that the standard impulse-withstand voltages are met taking into account all relevant environmental conditions which can create irregularities on the surface of the electrodes, for example rain, pollution [14]. The distances are therefore not applicable to equipment which has an impulse type test included in the specification, since mandatory clearance might hamper the design of equipment, increase its cost, and impede progress.

The **clearances may also be lower**, where it has been confirmed by **operating experience that the over-voltages are lower than those expected in the selection of the standard withstand**

voltages or that the gap **configuration is more favourable** than that assumes for the recommended clearances [14].

The clearances of live parts of a system from one another and from earthed parts must at least comply with Table 4.9. This table lists the minimum air clearances from the Standard Lightning Impulse Withstand Voltages from 20kV $\leq \mathbf{U}_{rB} \leq$ 2100kV. Further on in the text, these withstand voltages are correlated with nominal ($\mathbf{U}_n$) and maximum ($\mathbf{U}_m$) standard equipment voltages. These are in turn correlated with the minimum phase-to-earth and phase-to-phase clearances.

These minimum clearances have been determined in a laboratory under standard atmospheric conditions as defined by IEC 60-1. These standard conditions are:

- temperature : 20°C
- pressure : 101,3kPa (1013mbar)
- absolute humidity : 11g/m^3

Table 4.9: Correlation between Standard Lightning Impulse Withstand Voltages and Minimum Air Clearances [14] [19]

Standard Lightning Impulse Withstand Voltage [U_{rB}] (kV)	Minimum clearance (mm)	
	Rod-Structure [C_{BRS}] (mm)	Conductor-Structure [C_{SCS}] (mm)
20	60	-
40	60	-
60	90	-
75	120	-
95	160	-
125	220	-
145	270	-
170	320	-
250	480	-
325	630	-
450	900	-
550	1100	-
650	1300	-
750	1500	-
850	1700	1600

Table 4.9: Correlation between Standard Lightning Impulse Withstand Voltages and Minimum Air Clearances (Continued) [14] [19]

Standard Lightning Impulse Withstand Voltage [U_{rB}] (kV)	Minimum Clearance (mm)	
	Conductor-Structure [C_{SCS}] (mm)	Rod-Structure [C_{BRS}] (mm)
950	1700	1900
1050	1900	2100
1175	2200	2350
1300	2400	2600
1425	2600	2850
1550	2900	3100
1675	3100	3350
1800	3300	3600
1950	3600	3900
2100	3900	4200

NOTE: The standard lightning impulse is applicable to phase-to-phase and phase-to-earth.

For phase-to-earth, the minimum clearance for conductor-structure and rod-structure is applicable.

For phase-to-phase, the minimum clearance for rod-structure is applicable.

Table 4.10: Correlation between Standard Switching Impulse Withstand Voltages and Minimum Phase-To-Earth Air Clearances (Referred to Standard Atmospheric Conditions as Defined By IEC 60-1) [14] [19]

Standard Switching Impulse Withstand Voltage $[U_{rs}]$ (kV)	Minimum Phase-to-Earth Clearance (mm)	
	Conductor-Structure $[C_{peCS}]$ (mm)	Rod-Structure $[C_{peRS}]$ (mm)
750	1600	1900
850	1800	2400
950	2200	2900
1050	2600	3400
1175	3100	4100
1300	3600	4800
1425	4200	5600
1550	4900	6400

Table 4.11: Correlation between Standard Switching Impulse Withstand Voltages and Minimum Phase-To-Phase Air Clearances (Referred to Standard Atmospheric Conditions as Defined By IEC 60-1) [14] [19]

Standard Switching Impulse Withstand Voltage (kV)			Minimum Phase-to-Phase Clearance (mm)	
Phase-to-Earth	Phase-to-Phase value / Phase-to-Earth value	Phase-to-Phase	Conductor-Conductor Parallel	Rod-Conductor
[U_{rB}] (kV)		[U_{rS}] (kV)	[C_{peCC}] (mm)	[C_{peRC}] (mm)
750	1,5	1125	2300	2600
850	1,5	1275	2600	3100
850	1,6	1360	2900	3400
950	1,5	1425	3100	3600
950	1,7	1615	3700	4300
1050	1,5	1575	3600	4200
1050	1,6	1680	3900	4600
1175	1,5	1763	4200	5000
1300	1,7	2210	6100	7400
1425	1,7	2423	7200	9000
1550	1,6	2480	7600	9400

4.3.1 Extract from IEC 71-2 [14]

4.3.1.1 A.1 Range I

The air clearance phase-to-earth and phase-to-phase is determined from Table 4.9 for the rated lightning impulse-withstand voltage. The standard short-duration power-frequency withstand voltage can be disregarded when the ratio of the standard lightning impulse to the standard short-duration power-frequency withstand voltage is higher than 1,7.

4.3.1.2 A.2 Range II

The phase-to-earth clearance is the higher values of the clearances determined for the rod-structure configuration from Table 4.9 for the standard lightning impulse and from Table 4.10 for the switching impulse withstand voltages respectively

a) **Example:**

$\mathbf{U_{rB}}$ = 1425kV Rod-Structure Clearance ($\mathbf{C_{BRS}}$) = 2850mm (Table 4.9)

$\mathbf{U_{rS}}$ = 950kV Rod-Structure Clearance ($\mathbf{C_{peRS}}$) = 2900mm (Table 4.10)

Minimum phase-to-earth clearance ($\mathbf{C_{pe}}$) = 2900mm

The phase-to-phase clearance is the higher values of the clearances determined for the rod-structure configuration from Table 4.9 for the standard lightning impulse, and from Table 4.11 for the switching impulse withstand voltages respectively

b) **Example:**

$\mathbf{U_{rB}}$ = 1425kV Rod-Structure Clearance ($\mathbf{C_{BRS}}$) = 2850mm (Table 4.9)

$\mathbf{U_{rS}}$ = 950kV Rod-Structure Clearance ($\mathbf{C_{ppRS}}$) = 3600mm (Table 4.11)

Minimum phase-to-phase clearance ($\mathbf{C_{pe}}$) = 3600mm

The values are valid for altitudes which have been taken into account in the determination of the required withstand voltages (see paragraph 4.4)

The clearances necessary to withstand lightning impulse withstand voltage for the longitudinal insulation in Range II can be obtained by adding 0,7 times the maximum operating voltage phase-to-earth peak to the value of the standard lightning impulse voltage and by dividing the sum by 500kV/m.

The clearances necessary for the longitudinal standard switching impulse withstand voltage in range II are smaller than the corresponding phase-to-phase value. Such clearances usually exist only in type tested apparatus and minimum values are therefore given in this guide.

4.4 Ranges for highest voltage for equipment

As discussed earlier, a listing of minimum clearances for the maximum system and apparatus voltages have been correlated with insulation levels for convenience of the designer. The various insulation levels can be selected in accordance with the insulation co-ordination as per this standard.

The standard highest voltages for equipment are divided in to two ranges:

Range I: Above 1kV to 245kV included. This range covers both transmission and distribution systems. The different operational aspects, therefore, shall be taken into account in the selection of the rated insulation level of the equipment. For convenience, Range I is also divided into two tables, for $1kV < \mathbf{U_m} < 52kV$ and $52kV \leq \mathbf{U_m} < 300kV$

Range II: Above 245kV or $\mathbf{U_m} \geq 300kV$. This range covers mainly transmission systems.

Table 4.9 correlates the minimum air clearances with the standard lightning impulse withstand voltage for electrode configurations of the rod-structure type and, in addition for range II, of the conductor-structure type. They are applicable for phase-to-phase clearances as well as for clearances between phases (see note under Table 4.9)

Lower Voltages up to U_n = 220kV (U_m=245kV) co-ordinated for LIWL

Higher Voltages from U_n = 275kV (U_m=300kV) co-ordinated for SIWL

Table 4.12: In the area of 1kV <U_m <52kV [19]

Nominal Voltage [U_n] (kV)	Maximum Voltage for Apparatus [U_m] (kV)	Short Duration Power Frequency Withstand Voltage [U_{pf}] (kV)	Rated Lightning Impulse Withstand Voltage 1,2/50 µs [U_{rS}] (kV)	Minimum Clearance (N) Outdoor Installation Phase-to-Earth and Phase-to- Phase	
				[C_{pe}] (mm)	[C_{pp}] (mm)
3	3,6	10	20	60	120
			40	60	120
6	7,2	20	40	60	120
			60	90	120
10	12	28	60	90	150
			75	120	150
15	17,5	38	75	120	160
			95	150	160
20	24	50	95	160	
			125	220	
30	36	70	145	270	
			170	320	
36	41,5	80	170	320	
			200	360	

Table 4.13: In the area of 52kV < U_m < 300kV [19]

Nominal Voltage $[U_n]$ (kV)	Maximum Voltage for Apparatus $[U_m]$ (kV)	Short Duration Power Frequency Withstand Voltage $[U_{pf}]$ (kV)	Rated Lightning Impulse Withstand Voltage 1,2/50 µs $[U_{rs}]$ (kV)	Minimum Clearance (N) Outdoor Installation Phase-to-Earth and Phase-to- Phase $[C_{pe}],[C_{pp}]$ (mm)
45	52	95	250	480
66	72,5	140	325	630
70	82,5	150	380	750
110	123	185	450	900
		230	550	1100
132	145	185	450	900
		230	550	1100
		275	650	1300
150	170	230	550	1100
		275	650	1300
		325	750	1500
220	245	325	750	1500
		360	850	1700
		395	950	1900
		460	1050	2100

Table 4.14: In the area of U_m > 300kV [19]

Nominal Voltage	Maximum Voltage for Apparatus	Rated Switching Impulse Withstand Voltage 250/2500µs	Minimum Clearance (N)		Rated Switching Impulse Withstand Voltage 250/2500µs	Minimum Clearance (N)	
$[U_n]$ (kV)	$[U_m]$ (kV)	$[U_{rs}]$ (kV)	$[C_{pe}]$ (mm)		$[U_{rs}]$ (kV)	$[C_{pp}]$ (mm)	
		Phase-to-Earth	Conductor/ design	Phase-to-Earth	Phase-to- Phase	Conductor	Bus/ Conductor*
275	300	750	1600	1900	1125	2300	2600
		850	1800	2400	1275	2600	3100
380	420	950	2200	2900	1425	3100	3600
		1050	2600	3400	1575	3600	4200
480	525	1050	2600	3400	1680	3900	4600
		1175	3100	4100	1763	4200	5000
700	765	1425	4200	5600	2423	7200	9000
		1550	4900	6400	2480	7600	9400

* Consequences more serious, hence larger clearance to reduce probability of a flash-over

The introduction of $\mathbf{U_m}$ = 550kV (instead of 525kV), 800kV (instead of 765kV), 1200kV, of a value between 765kV and 1200kV, and of the associated standard withstand voltages, is under consideration.

4.5 Correction of Clearances for Altitude and Atmospheric Conditions [14]

"Breakdown in air is strongly dependent on the gap configuration and on the polarity and wave shape of the applied voltage stress. In addition, relative atmospheric conditions affect the breakdown strength regardless of shape and polarity of applied stress. Relationships for the breakdown strength of air derived from laboratory measurements are referred to standard atmospheric conditions as defined by IEC 60-1, i.e.:

"- temperature : 20°C

"- pressure : 101,3kPa (1013mbar)

"- absolute humidity : 11g/m^3

"For outdoor insulation, the effects of humidity, rain, and surface contamination become very important."

"Wind has an influence on insulation design, especially in the case of selecting gap lengths on the basis of power-frequency and switching impulse strengths."

"Flashover voltages for air gaps depend on the moisture content and density of the air. Insulation strength increases with absolute humidity up to a point where condensation forms on the insulator surface. Insulation strength decreases with decreasing air density (IEC 60-1).

4.5.1 Altitude correction

The correction factor $\mathbf{K_a}$ is based on the dependence of the atmospheric pressure on the altitude as given in IEC 721-2-3. The correction factor can be calculated from

$$\mathbf{K_a = e^{m\left(\frac{Ha}{8150}\right)}\ (dimensionless)\ [14]} \qquad (4.12)$$

Where:-

$\mathbf{H_a}$ = Altitude above sea level in m

$\mathbf{m}$ = 1,0 for co-ordination lightning impulse withstand voltages

= **m** according to Figure 4.7 for co-ordination switching impulse withstand voltages

= 1,0 for short-duration power-frequency withstand voltages of air-clearances and clean insulators

= 0,5 for normal insulators (polluted)

= 0,8 for anti-fog design (polluted)

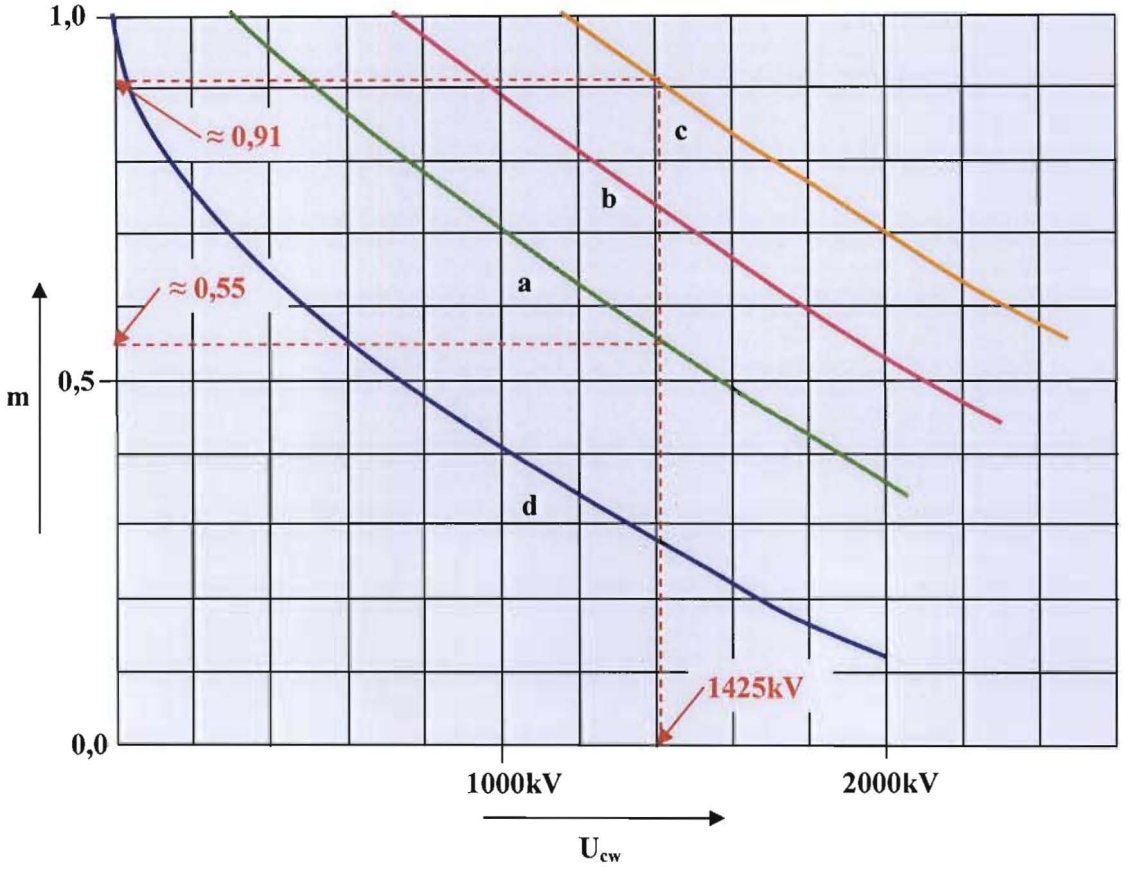

Figure 4.7: Dependence of Exponent 'm' on the Co-ordination Switching Impulse Withstand Voltage [14]

Where:-

a = Phase-to-earth insulation

b = Longitudinal insulation

c = Phase-to-phase insulation

d = Rod-plane gap (reference gap)

The following straight line approximations for functions **a**, **b** and **c** were derived by the author (Appendix A) by applying single variable regression analysis [17].

$$\mathbf{m_a = 1{,}0878 - 3{,}7463.10^{-4}.U_{cw}} \quad \mathbf{r^2 = 0{,}9975} \tag{4.13}$$

$$\mathbf{m_b = 1{,}3094 - 3{,}7745.10^{-4}.U_{cw}} \quad \mathbf{r^2 = 0{,}9988} \tag{4.14}$$

$$\mathbf{m_c = 1{,}3974 - 3{,}4643.10^{-4}.U_{cw}} \quad \mathbf{r^2 = 0{,}9982} \tag{4.15}$$

Function **d** was broken up into 6 sections so that each of the sections would correlate with greater than 95% accuracy (See Appendix A). The accuracies are provided as per unit values. The functions therefore take on the form:

$$\begin{aligned} \mathbf{m} &= \mathbf{e^{\hat{\beta}1}.e^{\beta 2.\ln Ucw}} \\ &= \mathbf{\beta 1.U_{cw}^{\beta 2}} \end{aligned} \tag{4.16}$$

$$\mathbf{m_{d1} = 1.2488.U_{cw}^{-0.0908}} \quad \mathbf{r^2 = 0.9543} \quad \mathbf{0 < U_{cw} < 220kV} \tag{4.17}$$

$$\mathbf{m_{d2} = 2.889.U_{cw}^{-0.2494}} \quad \mathbf{r^2 = 0.9915} \quad \mathbf{220 \leq U_{cw} < 300kV} \tag{4.18}$$

$$\mathbf{m_{d3} = 5.5417.U_{cw}^{-0.3617}} \quad \mathbf{r^2 = 0.9968} \quad \mathbf{300 \leq U_{cw} < 700kV} \tag{4.19}$$

$$\mathbf{m_{d4} = 52.6044.U_{cw}^{-0.7055}} \quad \mathbf{r^2 = 0.9871} \quad \mathbf{700 \leq U_{cw} < 1100kV} \tag{4.20}$$

$$\mathbf{m_{d5} = 4917.U_{cw}^{-1.3519}} \quad \mathbf{r^2 = 0.9799} \quad \mathbf{1100 \leq U_{cw} < 1600kV} \tag{4.21}$$

$$\mathbf{m_{d6} = 818722.U_{cw}^{-2{,}0532}} \quad \mathbf{r^2 = 0.9861} \quad \mathbf{1600 \leq U_{cw} < 2000kV} \tag{4.22}$$

For voltages consists of two components, the voltage value is the sum of the components.

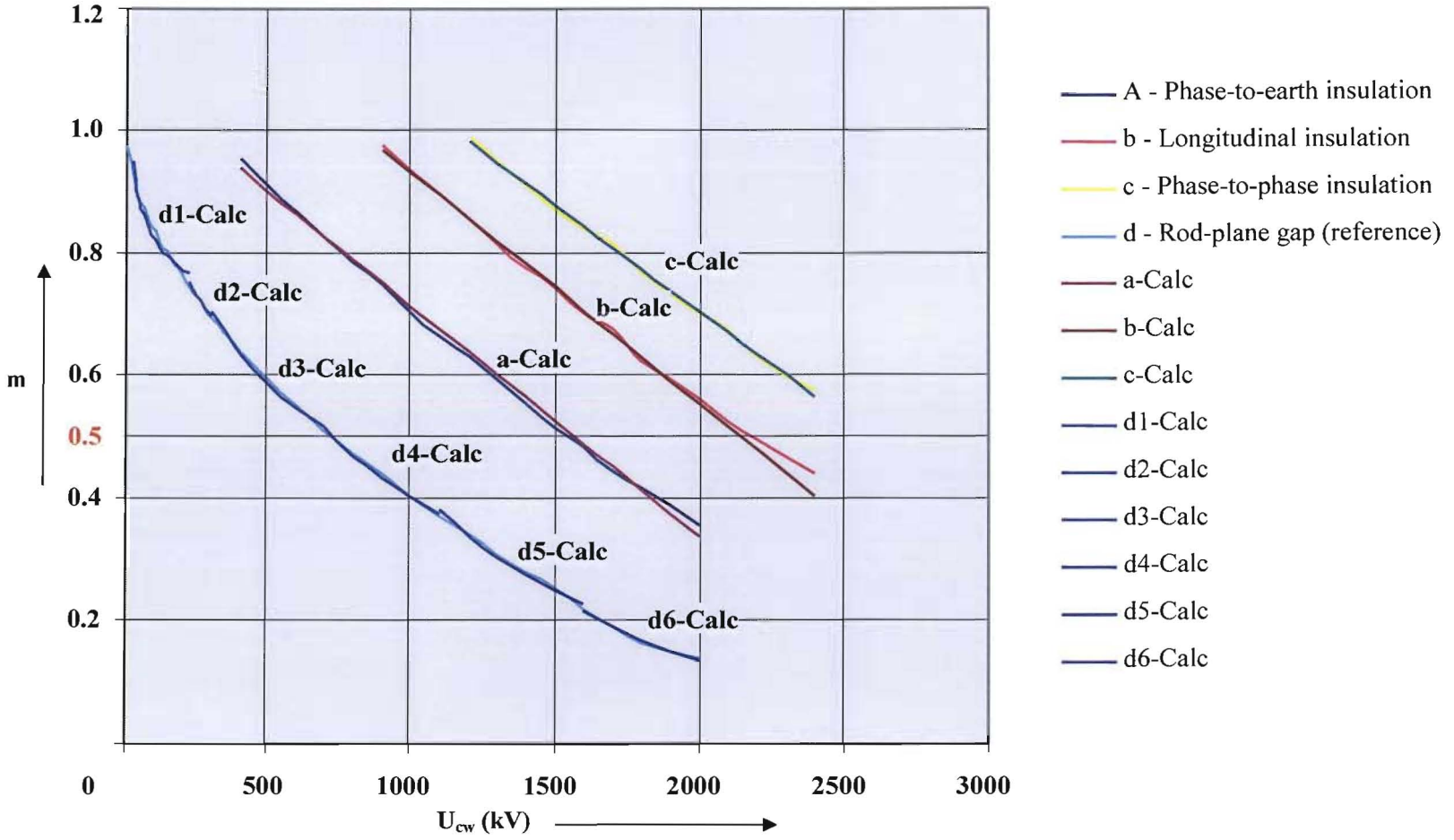

Figure 4.8: The Approximations of the Exponent 'm' on the Co-ordination Switching Impulse withstand Voltage in accordance with the above Functions (See Appendix A)

"When determining the co-ordination with-stand voltage, it should be kept in mind that most adverse conditions from the strength point of view (i.e. low absolute humidity, low air pressure and high temperature) do not usually occur simultaneously. In addition, at a given site, the corrections applicable for humidity and ambient temperature variations cancel each other to all intents and purposes. Therefore, the estimation of the strength can usually be based on the average ambient conditions at the location.

"For insulators, the possible reduction in the withstand voltage due to snow, ice, dew or fog should be taken into account."

2% Chance that Over-voltage will exceed

98% Chance that Over-voltage will not exceed

Critical flash-over (CFO) value (50% value)

Desired total flashover probability $\mathbf{p = \frac{3}{2}.10^{-4}}$ **[13]** (4.23)

Want to convert to 90% value

$$\mathbf{CFO_{sl} = \frac{SIWL}{(1 - t.\sigma_s)}} \quad (4.24)$$

and the probability density function is given by:-

$$\mathbf{H(t) = \frac{1}{2.\pi}\int_0^t e\ (^{-1/2}.^{x^2})dx}\ \textbf{[21]}$$

Where:-

$\mathbf{CFO_{sl}}$	=	Critical Flashover Value in kV (as calculated at sea level)
SIWL	=	Switching Impulse Withstand Level in kV
H(t)	=	Probability density (area under the normal distibution curve)
t	=	The function value of the normal distribution curve (or value of the independent variable associated with a given area under a normal distribution curve)
σ_s	=	Standard Deviation of Voltages in %

The above CFO value is valid at sea level and needs to be corrected for altitude by employing (4.12)

$$\mathbf{CFO_{Alt} = CFO_{sl}.e^{m\left(\frac{Ha}{8150}\right)}(kV)} \tag{4.25}$$

LeRoy/Gallet equation [12] [13]

$$\mathbf{CFO_{sl} = \frac{K_g.3400}{(1+\frac{8}{S_{sl}})}} \tag{4.26}$$

Where:-

s_{sl} = Gap distance (surface-to-surface) in m

$$\mathbf{(1+\frac{8}{S_{sl}}) = \frac{K_g.3400}{CFO_{sl}}}$$

$$\mathbf{\frac{8}{S_{sl}} = \frac{K_g.3400}{CFO_{sl}} - 1}$$

$$\mathbf{\frac{8}{S_{sl}} = \frac{K_g.3400 - CFO_{sl}}{CFO_{sl}}}$$

$$\mathbf{\frac{CFO_{sl}}{K_g.3400 - CFO_{sl}} = \frac{S_{sl}}{8}}$$

$$\mathbf{\frac{8.CFO_{sl}}{K_g.3400 - CFO_{sl}} = S_{sl}}$$

$$\mathbf{S_{sl} = \frac{8.CFO_{sl}}{K_g.3400 - CFO_{sl}}} \tag{4.27}$$

Table 4.15: Area under Normal Distribution Curve vs t [21]

t	0,00	0,01	0,02	0,03	0,04	0,05	0,06	0,07	0,08	0,09
	Probability (Area under a Normal Distibution Curve $\left[\frac{1}{2.\pi}\int_0^t e^{(-\frac{1}{2}\cdot x^2)}dx\right]$)									
0,0	0,50000	0,50399	0,50798	0,51197	0,51595	0,51994	0,52392	0.52790	0,53188	0,53586
0,.1	0,53983	0,54380	0,54776	0,55172	0,55567	0,55962	0,56356	0.56749	0,57142	0,57535
0,2	0,57926	0,58317	0,58706	0,59095	0,59483	0,59871	0,60257	0.60642	0,61026	0,61409
0,3	0,61791	0,62172	0,62552	0,62930	0,63307	0,63683	0,64058	0.64431	0,64803	0,65173
0,4	0,65542	0,65910	0,66276	0,66640	0,67003	0,67364	0,67724	0.68082	0,68439	0,68793
0,5	0,69146	0,69497	0,69847	0,70194	0,70540	0,70884	0,71226	0.71566	0,71904	0,72240
0,6	0,72575	0,72907	0,73237	0,73565	0,73891	0,74215	0,74537	0.74857	0,75175	0,75490
0,7	0,75804	0,76115	0,76424	0,76730	0,77035	0,77337	0,77637	0.77935	0,78230	0,78524
0,8	0,78814	0,79103	0,79389	0,79637	0,79955	0,80234	0,80511	0.80785	0,81057	0,81327
0,9	0,81594	0,81859	0,82121	0,82381	0,82639	0,82894	0,83147	0.83398	0,83646	0,83891
1,0	0,84134	0,84375	0,84614	0,84849	0,85083	0,85314	0,85543	0.85769	0,85993	0,86214
1,1	0,86433	0,86650	0,86864	0,87076	0,87286	0,87493	0,87698	0.87900	0,88100	0,88298
1,2	0,88493	0,88686	0,88877	0,89065	0,89251	0,89435	0,89617	0.89796	0,89973	0,90147
1,3	0,90320	0,90490	0,90658	0,90824	0,90988	0,91149	0,91308	0.91466	0,91621	0,91774
1,4	0,91924	0,92073	0,92220	0,92364	0,92507	0,92647	0,92785	0.92922	0,93056	0,93189
1,5	0,93319	0,93448	0,93574	0,93699	0,93822	0,93943	0,94062	0.94179	0,94295	0,94408

Table 4.15: Area under Normal Distribution Curve vs t [21]

t	0,00	0,01	0,02	0,03	0,04	0,05	0,06	0,07	0,08	0,09
	Probability (Area under a Normal Distibution Curve $\left[\frac{1}{2.\pi}\int_0^t e^{(-\frac{1}{2}\cdot x^2)}dx\right]$)									
1,6	0,9452	0,9463	0,9474	0,9484	0,9495	0,9505	0,9515	0,9525	0,9535	0,9545
1,7	0,9554	0,9564	0,9573	0,9582	0,9591	0,9599	0,9608	0,9616	0,9625	0,9633
1,8	0,9641	0,9649	0,9656	0,9664	0,9671	0,9678	0,9686	0,9693	0,9699	0,9706
1,9	0,9713	0,9719	0,9726	0,9732	0,9738	0,9744	0,9750	0,9756	0,9761	0,9767
2,0	0,9772	0,9778	0,9783	0,9788	0,9793	0,9798	0,9803	0,9808	0,9812	0,9817
2,1	0,9821	0,9826	0,9830	0,9834	0,9838	0,9842	0,9846	0,9850	0,9854	0,9857
2,2	0,9861	0,9864	0,9868	0,9871	0,9875	0,9878	0,9881	0,9884	0,9887	0,9890
2,3	0,98928	0,98956	0,98983	0,99010	0,99036	0,99061	0,99086	0,99111	0,99134	0,99158
2,4	0,99180	0,99202	0,99224	0,99248	0,99266	0,99286	0,99305	0,99324	0,99343	0,99361
2,5	0,99379	0,99396	0,99413	0,99430	0,99446	0,99461	0,99477	0,99492	0,99506	0,9520
2,6	0,99534	0,99547	0,99560	0,99573	0,99585	0,99598	0,99609	0,99621	0,99632	0,9643
2,7	0,99653	0,99664	0,99674	0,99683	0,99693	0,99702	0,99711	0,99720	0,99728	0,99736
2,8	0,99744	0,99752	0,99760	0,99767	0,99774	0,99781	0,99788	0,99795	0,99801	0,99807
2,8	0,99813	0,99819	0,99825	0,99831	0,99836	0,99841	0,99846	0,99851	0,99856	0,99861
3,0	0,99865	0,99869	0,99874	0,99878	0,99882	0,99886	0,99889	0,99893	0,99896	0,99900
3,1	0,99903	0,99906	0,99910	0,99913	0,99916	0,99918	0,99921	0,99924	0,99926	0,99929

Table 4.15: Area under Normal Distribution Curve vs t [21]

t	0,00	0,01	0,02	0,03	0,04	0,05	0,06	0,07	0,08	0,09
	Probability (Area under a Normal Distibution Curve $\left[\frac{1}{2.\pi}\int_0^t e^{(-\frac{1}{2}\cdot x^2)}dx\right]$)									
3,2	0,99931	0,99934	0,99936	0,99938	0,99940	0,99942	0,99944	0,99946	0,99948	0,99950
3,3	0,99952	0,99953	0,99955	0,99957	0,99958	0,99960	0,99961	0,99962	0,99964	0,99965
3,4	0,99966	0,99968	0,99969	0,99970	0,99971	0,99972	0,99973	0,99974	0,99975	0,99976
3,5	0,99977	-	-	-	-	-	-	-	-	-
3,6	0,99984	-	-	-	-	-	-	-	-	-
3,7	0,99989	-	-	-	-	-	-	-	-	-
3,8	0,99993	-	-	-	-	-	-	-	-	-
3,9	0,99995	-	-	-	-	-	-	-	-	-
4,0	0,99997	-	-	-	-	-	-	-	-	-

Example: Given that the Switching Impulse Withstand Level ($SIWL_{pe}$) is 1550kV, to determine the phase-to-earth and phase-to-phase electrical clearances for a number of Gap Factors

SIWL = 1550

For a 90% and 98% withstand probability, i.e. 0,9 and 0,98 require the **t** values that are associated with 0,9 and 0,98 (see table below)

From Table 4.15, the closest to 0,9 is 0,89973 and 0,98 is 0,9798 giving the following **t** values:

$\mathbf{t_{90}}$ = 1,2+0,08 (from Normal Distribution tables)

= 1,28

$\mathbf{t_{98}}$ = 2,0+0,05 (from Normal Distribution tables)

= 2,05

σ_s = 0,06 (6%)

Critical Flashover Voltages

$$\mathbf{CFO_{90sl}} = \frac{1550}{(1-1{,}28.0{,}06)} \qquad \text{(from 4.24)}$$

$\mathbf{CFO_{90sl}}$= 1679kV

$$\mathbf{CFO_{98sl}} = \frac{1550}{(1-2{,}05.0{,}06)} \qquad \text{(from 4.24)}$$

$\mathbf{CFO_{98sl}}$= 1767kV

Correction for Altitude when dealing with Switching Surges

$$\mathbf{K_a} = \mathbf{e}^{\mathbf{m}\left(\frac{\mathbf{Ha}}{8150}\right)}\ \mathbf{(dimensionless)} \qquad \text{(from 4.12)}$$

For Phase-to-earth switching surges

$\mathbf{m_a}$ = $\mathbf{1{,}0878 - 3{,}7463.10^{-4}.U_{cw}}$ $\mathbf{r^2 = 0{,}9975}$ (from 4.13)

= $1{,}0878 - 3{,}7463.10^{-4}.1679$

=0,4588

$$\mathbf{K_a} = \mathbf{e}^{0{,}4588\left(\frac{1800}{8150}\right)} \qquad \text{(from 4.12)}$$

= 1,1066 (dimensionless)

$$\mathbf{CFO_{90Alt}} = \mathbf{K_a}.\mathbf{CFO_{90sl}}$$
$$= 1679.1,1066 \quad \text{(from 4.25)}$$
$$= 1858\text{kV}$$

$$\mathbf{CFO_{98Alt}} = \mathbf{K_a}.\mathbf{CFO_{98sl}}$$
$$= 1767.1,1066 \quad \text{(from 4.25)}$$
$$= 1955\text{kV}$$

$\mathbf{K_g} = 1,3$ (see Tables 4.6 and 4.7)

$$\mathbf{s_{90alt}} = \frac{8.1858}{1,3.3400 - 1858} \quad \text{(from 4.27)}$$

$\mathbf{s_{90alt}} = 5,80\text{m}$ (at altitude of 1800m)

90% probability that gap will survive (conductor-structure)

$$\mathbf{s_{98alt}} = \frac{8.1955}{1,3.3400 - 1955} \quad \text{(from 4.27)}$$

$\mathbf{s_{98alt}} = 6,34\text{m}$ (at altitude of 1800m)

98% probability that gap will survive (conductor-structure)

It is clear from the above that for an additional 140mm, the system insulation has a much greater chance of surviving a 1550kV switching impulse, improving from 90% to 98% for a small increase in clearance.

Calculation [10]

$$\mathbf{SIWL\ (Phase\text{-}phase)} = \mathbf{P\text{-}E.}\frac{\mathbf{SIWL(Phase-to-Phase)}}{\mathbf{SIWL(Phase-to-Earth)}}$$

$\mathbf{SIWL} = 1550.1,6$ (from Table 4.10)

$= 2480\text{kV}$

$$\mathbf{CFO_{90sl}} = \frac{2480}{(1-1,28.0,06)} \quad \text{(from 4.24)}$$

$\mathbf{CFO_{90sl}} = 2686\text{kV}$

$$\mathbf{CFO_{98sl}} = \frac{2480}{(1-2{,}05.0{,}06)} \qquad \text{(from 4.24)}$$

$\mathbf{CFO_{98sl}} = 2828\text{kV}$

Correction for Altitude when dealing with Switching Surges

$\mathbf{m_c} = 0{,}91$ (from Figure 4.7)

$\mathbf{m_c = 1{,}3974 - 3{,}4643.10^{-4}.U_{cw}}$ $\mathbf{r^2 = 0{,}9982}$ (from 4.15)

$\mathbf{m_c} = 1{,}3974 - 3{,}4643.10^{-4}.1550$

$= 0{,}8604$

$$\mathbf{K_a = e^{m\left(\frac{Ha}{8150}\right)}}\ \textbf{(dimensionless)} \qquad \text{(from 4.12)}$$

$$\mathbf{K_a} = e^{0{,}91\left(\frac{1800}{8150}\right)}$$

$= 1{,}2226$ (dimensionless)

$\mathbf{CFO_{90Alt} = K_a.CFO_{90sl}}$

$= 2686.1{,}2226$ (from 4.25)

$= 3283\text{kV}$

$\mathbf{K_g} = 1{,}6$ (see Tables 4.6 and 4.7)

$$\mathbf{s_{90alt}} = \frac{8.3283}{1{,}6.3400 - 3283} \qquad \text{(from 4.27)}$$

$= 12{,}185\text{m}$

$\mathbf{CFO_{98Alt} = K_a.CFO_{98}}$

$= 2828.1{,}2226$ (from 4.25)

$= 3458\text{kV}$

$$\mathbf{s_{98alt}} = \frac{8.3458}{1{,}6.3400 - 3458} \qquad \text{(from 4.27)}$$

$= 13{,}952\text{m}$

In the case of phase-to-phase clearance, an additional 1,77m is required to improve the probability of survival from 90% to 98%. The cost of insulation here is therefore higher than for the phase-to-earth case.

400kV **BIL** = 1425kV, **SIL** = 1050kV

Calculation [12]

Phase-phase = **P-E**.1,6 (see Table 4.11)

Eskom clearances are based on transients, not power frequency

Eskom clearances are based on **BIL**. If recalculated on **SIWL**, the clearances can be reduced significantly. The good surge arresters are an over-kill with such large clearances.

Example: Given that the Switching Impulse Withstand Level (Phase-to-Earth) (SIWL) is 1425kV, to determine the phase-to-earth and phase-to-phase electrical clearances for a number of Gap Factors

From Table 4.15, the closest to 0,9 is 0,89973 giving the following **t** value:

t = 1,2+0,08 (from Normal Distribution tables)

= 1,28

Standard Deviation of Voltages (σ_s) = 0,06

Gap Factor - Rod-to-Structure (K_g) = 1,1

At Sea Level

Critical Flashover Voltage (Phase-to-Earth) (CFO)

$$\mathbf{CFO_{90sl}} = \frac{\mathbf{SIWL}}{\mathbf{(1 - t.\sigma_s)}}$$

$$= \frac{1425}{(1 - 1.28.0.06)} \quad \text{(from 4.24)}$$

$$= 1543{,}54\text{kV}$$

Phase-to-Earth Clearance for Rod-to-Strucutre (s_{rs90sl})

Gap Factor - Rod-to-Structure (K_g) = 1,1 (see Tables 4.6 and 4.7)

$$\mathbf{s_{rs90sl}} = \frac{\mathbf{8.CFO}}{\mathbf{K_g.3400 - CFO}}$$

$$= \frac{8.1543{,}54}{1.1.3400 - 1543{,}54} \quad \text{(from 4.27)}$$

$$= 5{,}623\text{m (at sea level)}$$

Phase-to-Earth Clearance for Conductor-to-Strucutre (s_{cs90sl})

$$S_{cs90sl} = \frac{8.CFO_{cs90sl}}{K_g.3400 - CFO}$$

$$= \frac{8.1543,54}{1.3.3400 - 1543,54} \quad \text{(from 4.27)}$$

$$= 4,293\text{m (at sea level)}$$

Ratio: SIWL (P-P)/SIWL (P-E) = 1,7 (see Table 4.11)

$$SIWL_{pp} = SIWL_{pe}.\ 1,7$$

$$= 1425\ .\ 1,7$$

$$= 2422,5\text{kV}$$

Gap Factor - Rod-to-Conductor (K_g) = 1,46 (see Tables 4.6 and 4.7)

$$S_{rc90sl} = \frac{8.CFO_{rc90sl}}{K_g.3400 - CFO}$$

$$= \frac{8.2422,5}{1.46.3400 - 2422,5} \quad \text{(from 4.27)}$$

$$= 7,625\text{m (at sea level)}$$

Surface-to-Surface Clearance [s_{ss}] = 7,625 (at 1800m above sea level)

Gap Factor - Conductor-to-Conductor (K_{cc}) = 1,6

$$S_{rc} = \frac{8.CFO}{K_g.3400 - CFO}$$

$$= \frac{8.2422,5}{1,6.3400 - 2422,5} \quad \text{(from 4.27)}$$

$$= 6,423\text{m (at sea level)}$$

Surface-to-Surface Clearance [s_{ss}] = 6,423m (at 1800m above sea level)

<u>At Altitude Above Sea Level</u>

At altitude **(H_a)** of 1800m, it is necessary to correct the critical flashover voltage

m_a = 0,55 m (at sea level)

Corrected Critical Flashover Voltage (Phase-to-Earth) [CFO_{Alt}]

$$CFO_{90Alt} = CFO_{90sl}.e^{m\left(\frac{Ha}{8150}\right)}$$

$$= 1543,54_{sl}.e^{0,55\left(\frac{1800}{8150}\right)} \quad \text{(from 4.25)}$$

$$= 1742,91\text{kV}$$

Corrected Phase-to-Earth Clearance for Rod-to-Strucutre ($s_{rs90alt}$)

Gap Factor - Rod-to-Structure (K_{cs}) = 1,3 (see Tables 4.6 and 4.7)

$$S_{rs90alt} = \frac{8.CFO_{rs90alt}}{K_g.3400 - CFO_{rs90alt}}$$

$$= \frac{8.1742,91}{1.1.3400 - 1742,91} \quad \text{(from 4.24)}$$

$$= \underline{\mathbf{6,982m}} \text{ (at 1800m above sea level)}$$

Corrected Phase-to-Earth Clearance for Conductor-to-Strucutre ($s_{cs90alt}$)

$$S_{rs90alt} = \frac{8.CFO_{rs90alt}}{K_g.3400 - CFO_{rs90alt}}$$

$$= \frac{8.1742,91}{1.3.3400 - 1742,91} \quad \text{(from 5.24)}$$

$$= 5,208\text{m (at 1800m above sea level)}$$

Ratio: SIWL (P-P)/SIWL (P-E) = 1,7

$$SIWL_{pp} = SIWL_{pe}.\ 1,7 \quad \text{(see Table 4.11)}$$

$$= 1742,91\ .\ 1,7$$

$$= 2962,95\text{kV}$$

Gap Factor - Rod-to-Conductor (K_{rc}) = 1,46 (see Tables 4.6 and 4.7)

$$S_{rc90slt} \frac{8.CFO_{rc90sl}}{K_g.3400 - CFO_{rc90sl}}$$

$$= \frac{8.2962,95}{1.46.3400 - 2962,95} \quad \text{(from 4.24)}$$

$$= 11,846\text{m (at sea level)}$$

Surface-to-Surface Clearance $[s_{ss}]$ = **11,846m** (at 1800m above sea level)

For parallel conductors, the centre-to-centre distance

Tube Diameter $[d_{bo}]$ = 0,2m

Tube Deflecting under Short Circuit $[y_{max}]$ = 0,2m

Centre-to-Centre distance $[s_{ss}]$ = 11,846 + 0,2 + 0,2.2

= **12,446m** (at 1800m above sea level)

Gap Factor - Conductor-to-Conductor (K_g) = 1,6 (see Tables 4.6 and 4.7)

$$S_{cc90sl} = \frac{8.CFO_{cc90sl}}{K_g.3400 - CFO_{cc90sl}}$$

$$= \frac{8.2962,95}{1,6.3400 - 2962,95} \quad \text{(from 4.24)}$$

$$= 9,569\text{m (at sea level)}$$

Surface-to-Surface Clearance [s_{ss}] = 9,569m (at 1800m above sea level)

For parallel conductors, the centre-to-centre distance

For parallel conductors, the centre-to-centre distance

Tube Diameter [d_{bo}] = 0,2m

Tube Deflecting under Short Circuit [y_{max}] = 0,2m

Centre-to-Centre distance [s_{ss}] = 9,569 + 0,2 + 0,2.2

= **10,169m** (at 1800m above sea level)

Table 4.16: Standard Eskom Electrical and Working Clearances [1]

System Nominal Voltage (kV)	System Highest Voltage (kV)	Minimum Electrical Clearance In mm		Working Clearance In Metres	
		Phase-To-Earth (C_{pe})	Phase-To-Phase(C_{pp})	Vertical (C_{wv})	Horizontal* (C_{wh})
3,3	3,6	80	110	2,5	1,2
6,6	7,2	150	200	2,6	1,2
11	12	200	270	2,7	1,3
15	17,5	230	310	2,7	1,3
22	24	320	430	2,8	1,4
33	36	430	580	2,9	1,5
44	48	540	730	3,0	1,6
66	72	770	1050	3,2	1,8
88	100	840	1150	3,3	1,9
		(1000)	(1350)	(3,5)	(2,1)
132	145	1200	1650	3,7	2,3
220	245	1850	2300	4,3	2,9
275	300	2350	2950	4,8	3,4
330	362	2900	3600	5,4	4,0
400	420	3200	4000	5,7	4,3

Notes: Bracketed figures for 88 kV are for full insulation and are to be used only if the system is not effectively earthed. The figures given for systems of 66 kV and below assume non-effective.

Table 4.16 are dimensions that were calculated in accordance with the electrical properties of gapped type surge arresters and based more deterministic type of criteria. The clearances specified in Tables 4.12, 4.13 and 4.14 are all based on the IEC 71-2, and are determined statistically as previously discussed. The values tend to be somewhat lower than those shown in

Table 4.16, which can facilitate the design of more compact substations as discussed further on in this chapter and document as a whole.

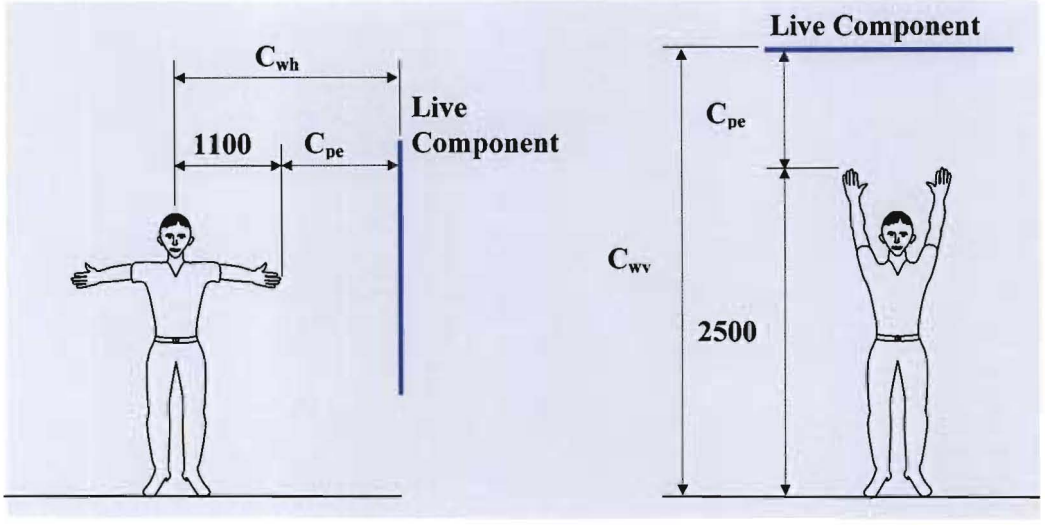

Figure 4.9: Horizontal (C_{wh}) and Vertical (C_{wv}) Working Clearances [1]

Table 4.17: Comparisons between Statistical Phase-to-Earth Clearances and Eskom Current Standards [1] [14]

Max System Voltage (kV)	Standard Switching Impulse Withstand Voltage [U_{rB}] (kV)	CFO at 1800m Above Sea Level (kV)	Gap Factors (K_g)					Standard Eskom Electrical Phase-to-Earth Clearance (m)
			1,80	1,65	1,62	1,50	1,45	
			Ring – ring or large smooth electrodes (m)	Crossed conductors (m)	Rod – rod or conductor – conductor (along the span) (m)	Supported busbars (fittings) (m)	Asymmetrical geometries (m)	
300	750	965,86	1,499	1,611	1,701	1,869	1,949	2,350
	850	1084,87	1,724	1,851	1,962	2,162	2,257	
362	950							2,900
		1201,68	1,955	2,099	2,232	2,466	2,579	
420	1050							3,200
		1316,33	2,192	2,354	2,512	2,783	2,914	
525	1175	1456,62	2,499	2,687	2,876	3,198	3,355	-
	1300	1593,63	2,817	3,340	3,257	3,636	3,821	
800	1425	1727,40	3,146	3,980	3,655	4,097	4,315	-
	1550	1858,00	3,488	3,810	4,072	4,585	4,839	

Table 4.18: Comparisons between Statistical Phase-to-Phase Clearances and Eskom Current Standards (Continued) [1] [14]

Max System Voltage (kV)	Standard Phase-to-Earth Switching Impulse Withstand Voltage U_{rs} (kV)	Ratio P-P/P-E	Standard Phase-to-Phase Switching Impulse Withstand Voltage U_{rs} (kV)	CFO at 1800m Above Sea Level (kV)	Gap Factors (K_g)					Standard Eskom Electrical Phase-to-Earth Clearance (m)
					1,80	1,65	1,62	1,50	1,45	
					Ring – ring or large smooth electrodes (m)	Crossed conductors (m)	Rod – rod or conductor – conductor (along the span) (m)	Supported busbars (fittings) (m)	Asymmetrical geometries (m)	
300	750	1,5	1125	1400,90	2,375	2,552	2,729	3,030	3,176	2,950
	850	1,6	1360	1658,24	2,973	3,207	3,446	3,854	4,055	
362	850	1,5	1275	1566,49	2,752	2,963	3,179	3,547	3,726	3,600
	950	1,7	1615	1924,67	3,670	3,988	4,297	4,849	5,123	
420	950	1,5	1425	1727,40	3,146	3,398	3,655	4,097	4,315	4,000
	1050	1,6	1680	1990,50	3,856	4,201	4,527	5,121	5,417	
525	1175	1,5	1763	2072,86	4,097	4,481	4,827	5,478	5,804	-
	1300	1,7	2210	2496,99	5,514	6,211	6,634	7,674	8,210	
800	1425	1,7	2423	2685,45	6,255	7,195	7,611	8,898	9,571	-
	1550	1,6	2480	2735,06	6,464	7,484	7,891	9,252	9,969	

It is therefore important to know how to interpret the various geometries within a substation in order that the correct gap factor ($\mathbf{K_g}$) can be applied. The more uniform one can make the gap, the smaller the clearances can be made and the better the performance.

4.6 The Width of an Equipment Bay as Defined by Electrical Clearances

The components of an equipment bay depends entirely on the function that bay is to fulfil, e.g. a feeder bay, a transformer bay, a bus coupler bay, etc. The common requirement for all of these is, however, that the installation of equipment is done in 3-phase formation such that the bay offers reliable service with no breakdown of air gaps between live parts, and live parts and earth, even under heavy pollution conditions.

In developing the concept of the width of an equipment bay, an initial basic assumption is made that all components are rigid, i.e. there is no movement whatsoever to infringe on electrical clearances, and that the width of the equipment is initially neglected.

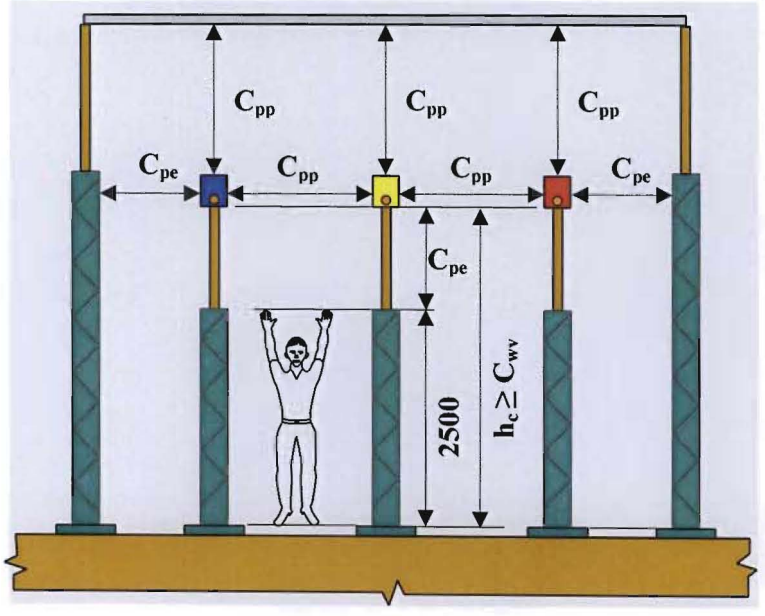

Figure 4.10: Equipment Bay Width

Figure 4.10 provides a starting point from which to develop and refine total bay width. In observing all clearances between all live elements (phase-to-phase) and between elements that are live and earth potential (phase-to-earth), the bay width in its most elementary form is given by:

$$\mathbf{W_b = 2.(C_{pe} + C_{pp})} \tag{4.28}$$

If it is possible to reduce these clearances, then it is possible reduce the bay widths, that in turn reduces the lengths of the busbar conductor. There are, however, practical considerations such as access to equipment for maintenance and replacement that limit the extent to which outdoor air insulated (AIS) equipment bay can be compacted. These clearances are voltage dependant.

4.7 The Height of the Different levels of Conductors in an Equipment Bay as Defined by Electrical Clearances

In this section the determination of the various levels of conductors above the ground are discussed in terms of various electrical clearances. These are generally the only determining factors until very high system currents and Ultra-High system voltages are being considered. Although there is no conclusive evidence that continuous exposure to certain levels of electric and magnetic field strengths are harmful to the human physiology, certain guidelines have been put into place, limiting these field strength values. These values will have a significant impact on the conductor heights. This issue is discussed at length under Chapter 17 of this dissertation.

4.7.1 Equipment Level Conductors

The first conductor level is defined by those conductors that interconnect the items of primary plant that form the equipment bay. This is determined by the minimum statutory height of the metallic bottom of the insulator which needs to be 2500mm as defined in Figures 4.10 and 4.11 [14]. The equipment connecting height is then given by:-

$$\mathbf{h_e = 2500 + C_{pe}}$$

$$\mathbf{= C_{wv}} \qquad (4.29)$$

The above does, however, not take conductor sag into account. In snow free areas, the sag is due to the weight of the conductor alone, whilst in areas where snow is a regular occurrence, the weight of the ice formation around the bus tubular conductors needs to be taken into account. The issues around sag and vertical displacement are discussed in detail under Chapter 13. (4.29) is then simply modified to include the conductor sag.

$$\mathbf{h_e = 2500 + C_{pe} + y_{max}}$$

$$\mathbf{= C_{wv} + y_{max}} \qquad (4.30)$$

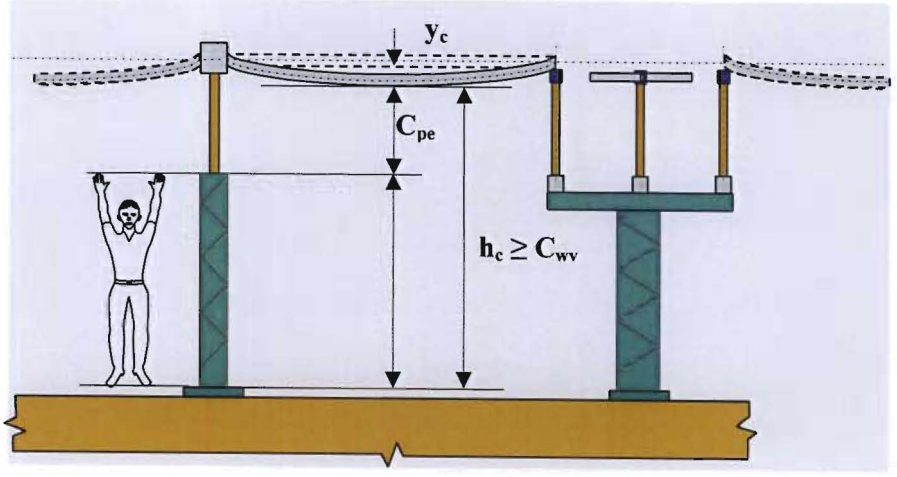

Figure 4.11: Inter-Equipment Conductors

The vertical displacement of inter-equipment conductors is usually negligible due to the rigidity of the bus tubing and short spans between the equipment. Long spans would need attention.

4.7.2 Busbar Level Conductors

The next level of conductor is generally the busbar conductor onto which all the equipment bay circuits are connected via a variety of isolating equipment (conventional and pantograph type isolators). These conductors usually traverse the full length of the substation in the direction normal to the equipment bays. For this reason, the minimum height of the busbar conductor must at least fulfil the phase-to-phase clearance requirement for a given system voltage.

Since the busbar spans are by far longer than the inter-equipment conductors, the vertical displacement or sag needs to be taken into account as is demonstrated in Figure 4.12.

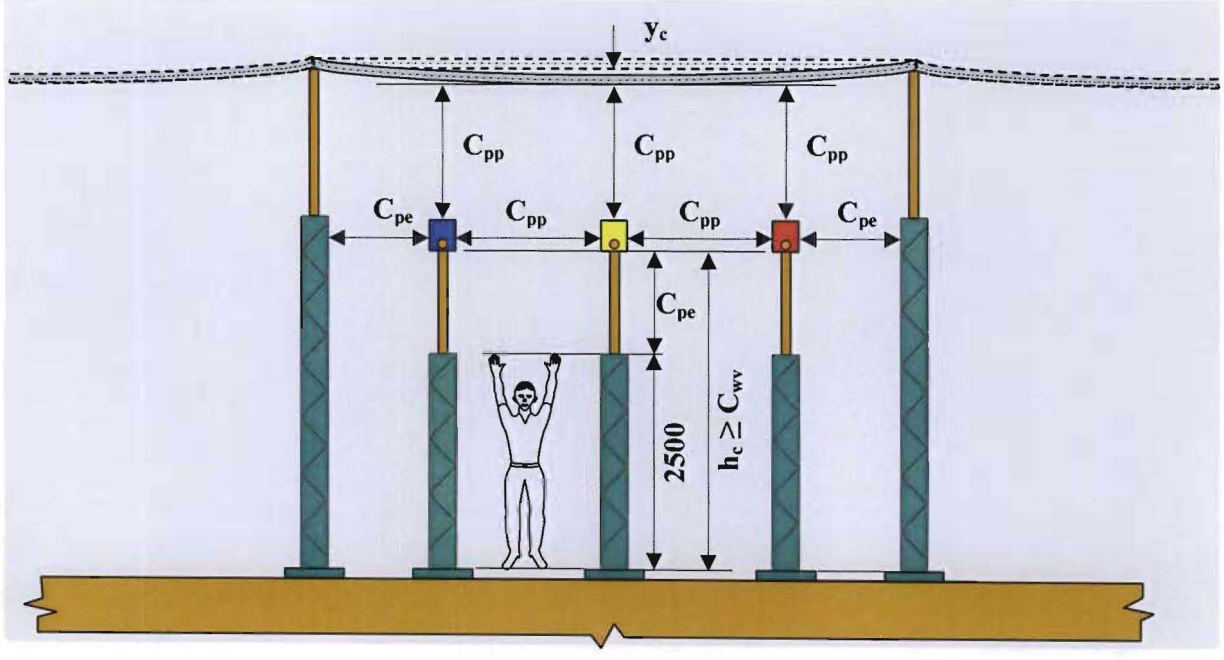

Figure 4.12: Busbar Conductors

$$h_b = 2500 + C_{pe} + C_{pp} + y_c$$

$$= C_{wv} + C_{pp} + y_c \qquad (4.30)$$

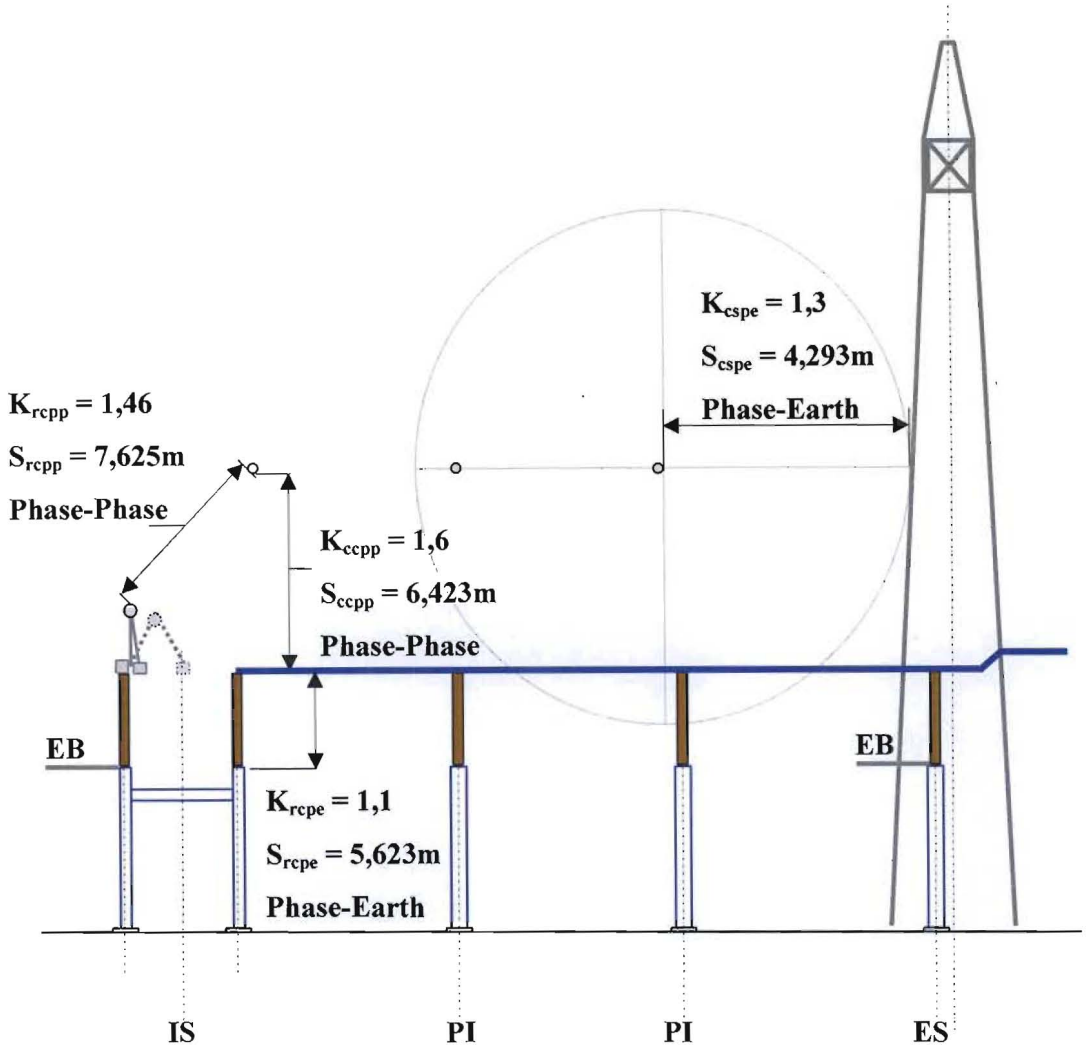

Figure 4.13: Clearances with Different Gap Factors (U_m = 800kV)

The calculations under paragraph 4.5 and illustrated in Figure 4.13 above show very clearly that the air gap that is required is very dependent upon the geometry of the gap. Sharp edges should be avoided as these reduce the insulating properties of the air gap. The more uniform the structures, the better the performance.

5. DETERMINATION OF THE APPROPRIATE SPAN OF BUS TUBING – EQUIPMENT BAY WIDTH

Objectives of this Chapter:

- Determine equipment horizontal phase-phase spacing (s_p) based on the conductor-conductor and rod-to-conductor electrical clearance dependent upon the type of equipment employed
- Determine equipment phase-earth spacing (s_e) based on the conductor-structure and live rod-to-structure electrical clearance dependent upon the type of equipment employed
- Determine the appropriate bay width for the equipment bay and so the appropriate length of bus tubing (W_b)

In most cases, the items of equipment that are close to or under the busbars are the bus selection isolators. For $U_m \leq 145kV$, where single busbars are used in small distribution type substations, the bay width is dictated by a conventional isolator. However, if double busbars are to employed, in-line isolators are a far cheaper alternative to pantograph that are cost effective only above these voltages.

5.1 Bay Width Dictated by Pantograph Type Isolators for Substation System Voltages for $U_m > 145kV$

As a first step in determining the bay width, we make a basic assumption that all components are essentially rigid. The bay width in its most elementary form is then given by:

$$W_b = \tfrac{1}{2}.d_{bs} + C_{pe} + d_{eqB} + C_{pp} + d_{eqW} + C_{pp} + d_{eqR} + C_{pe} + \tfrac{1}{2}.d_{bs}$$

$$= d_{bs} + d_{eqB} + d_{eqW} + d_{eqR} + 2(C_{pe} + C_{pp}) + C_{pp} \qquad (5.1)$$

Where:-

W_b	=	Bay width in mm
d_{bs}	=	Width of the busbar support structure in mm
$d_{eqB,W,R}$	=	Width of the live part of the item of equipment on the blue, white and red phases respectively

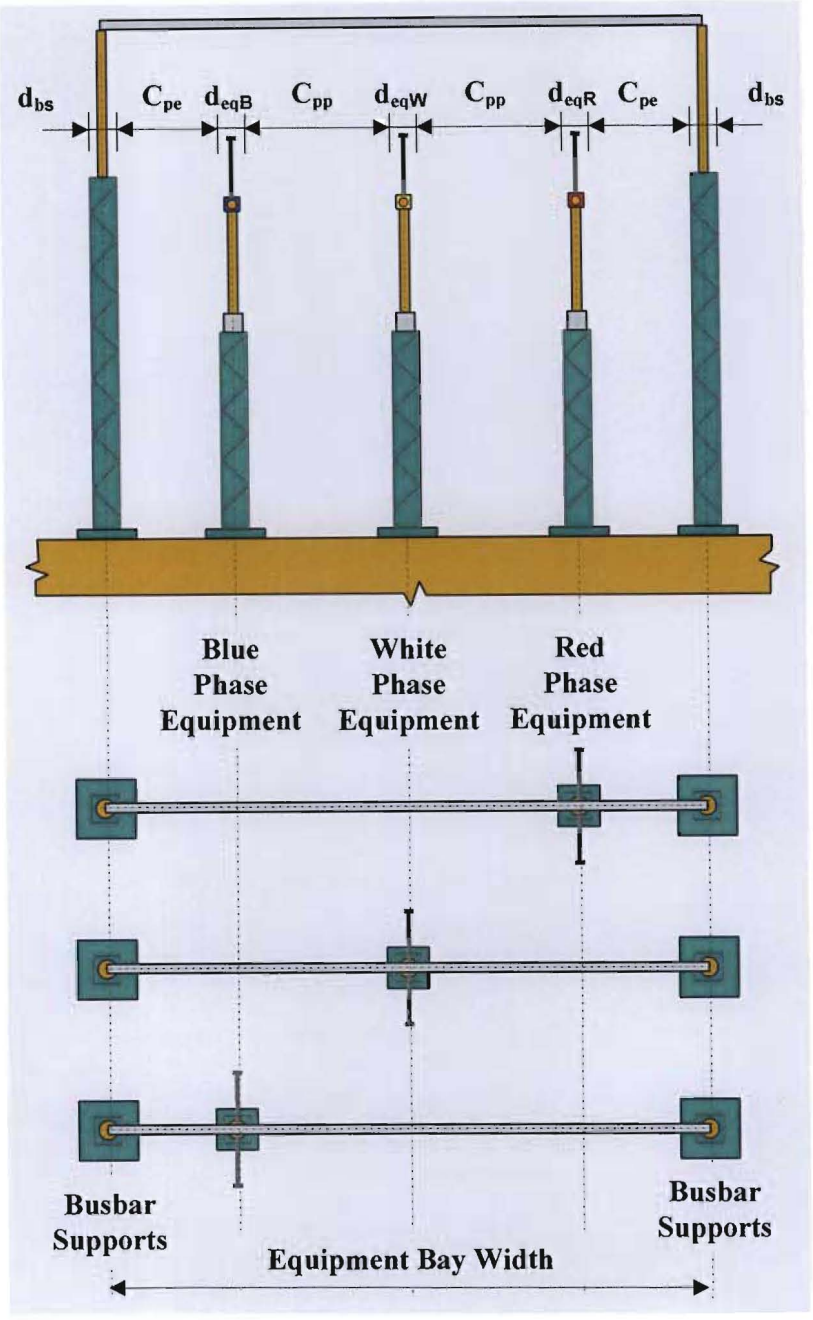

Figure 5.1: Bay Width Dictated by Pantograph Type Isolators for Substation System Voltages for $U_m \leq 145kV$

The equipment on the three phases is usually identical, then:

$$W_b = d_{bs} + 3.d_{eq} + 2.(C_{pe} + C_{pp}) \qquad (5.2)$$

If it is possible to reduce these clearances, then it is possible reduce the bay widths, that in turn reduces the lengths of the busbar conductor.

In the case where items of equipment with moving live parts are located side by side (eg. Isolators) or close to earthed structures (see Figure 5.1 above and 5.2 below), the position of

these live parts relative to one another and earthed parts, need to be taken into account when dimensioning.

5.2 Bay Width Dictated by In-line Type Isolators for Substation System Voltages $U_m \leq$ 145kV

Substation bay widths for system voltages $U_m \leq 145kV$ are generally dictated by In-line type Isolators used for busbar selection. These are a variation on conventional isolators where the isolating unit of each phase is turned through 90°, requiring the bay width to be somewhat larger than normal. In addition, when multi-conductor bundles are used to interconnect items of primary plant, it is necessary to take the bundle dimensions into account as well, i.e. the diameter of the conductors making up the bundle and the width of the bundle.

$$W_b = d_{bs} + 3.d_{eq} + 6.(d_c + d_{bn}) + 2.(C_{pc} + C_{pp}) \qquad (56.3)$$

Where:-

W_b = Bay width in mm

d_c = Diameter of each of the conductors in the bundle in mm

d_{bn} = Width of the conductor bundle in mm

The purpose of this discussion therefore, is to alert the reader to the implications of the positioning of energised air insulated primary equipment. Excessive bay width dimensions could possibly be avoided by repositioning such equipment away from earthed structures.

Once the bay width has been established, this then determines the length of the tubular bus conductor which is effectively also equal to the bay width ($\ell = W_b$)

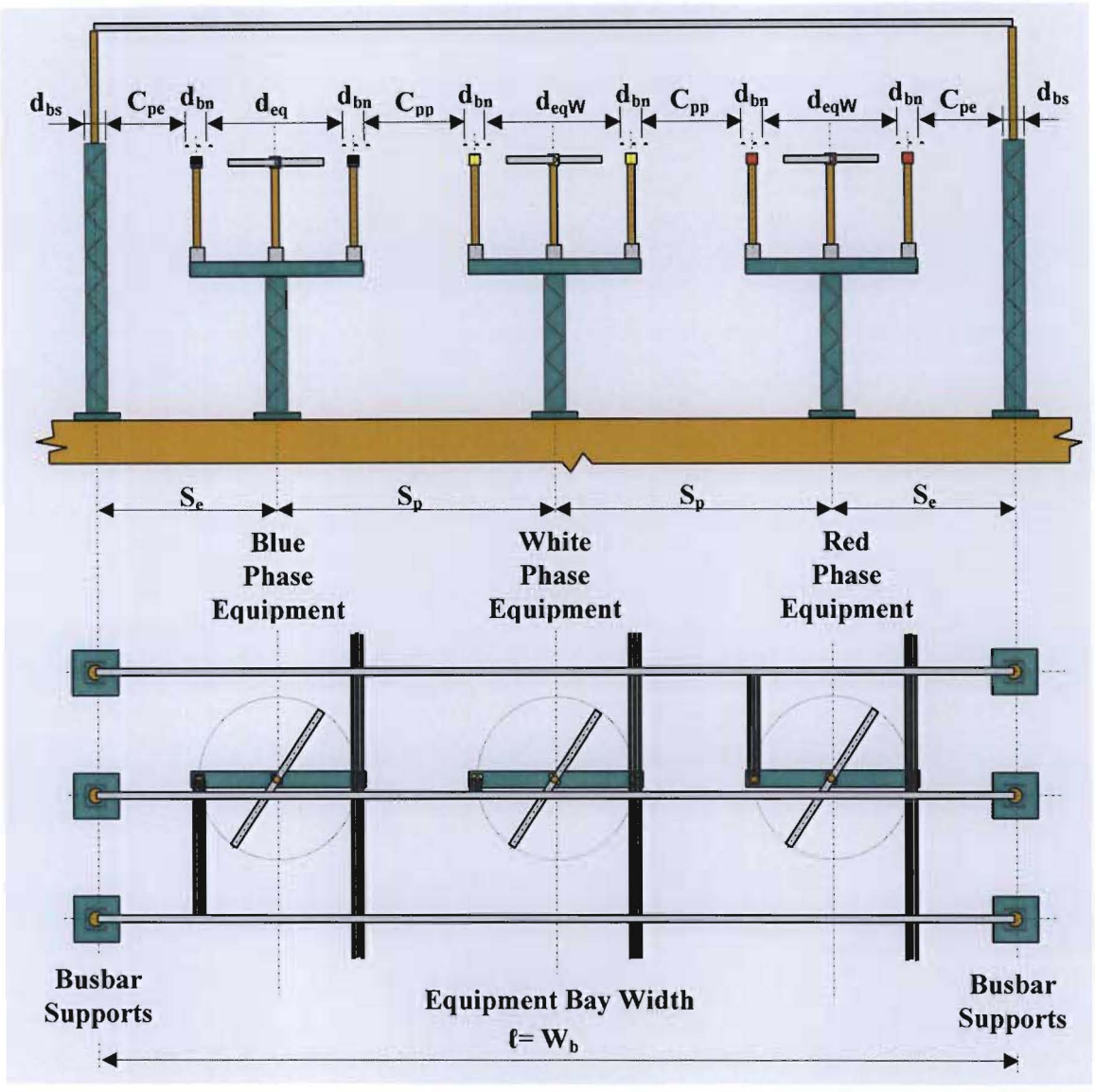

Figure 5.2: Bay Width Dictated by In-line Type Isolators for Substation System Voltages $U_m \leq 145kV$

6. DIMENSIONING OF BUS TUBING BASED ON CURRENT CARRYING CAPACITY (AMPACITY)

Objectives of this Chapter:

- Selection of bus tube size from Manufacturers tables to meet current carrying capacity (ampacity), provides tube outer diameter ($\mathbf{d_{bo}}$) and tube wall thickness ($\mathbf{t_w}$)
- Selection of supporting system to be employed (i.e. choose appropriate boundary condition: both ends supported, one end supported and one end fixed, both ends fixed)

6.1 Dimensioning Of Bus Tubing Based On Current Carrying Capacity (Ampacity) – Tables

Tubular aluminium conductors are provided under various specifications, viz. British Standards (BS), American National Standards, German DIN Standards, South African Bureau of Standards, etc. Table 6.1 is based on the DIN Standards. Table 6.2 provides data on the electrical and mechanical properties of equivalent alloys that are available for this purpose.

Load flow studies are carried out to determine the maximum expected power flow through the bus tubing, taking into account the worst possible contingencies. This maximum power flow is then translated into an equivalent current value at the chosen system voltage. Manufacturers provide tables of electrical and mechanical parameters for of variety of extruded aluminium and copper alloy bus tubes. Table 6.1 is an example of such a table indicating parameters for two such aluminium alloys that are used extensively for this application, E-AlMgSiO,5F22 and E-AlMgSiO,5F25. Bus tubing of the **E-AlMgSiO,5 F25** alloy may be preferred because of its better mechanical properties for only a slightly higher material resistance.

The most important electrical parameter provided in Table 6.1 is the current carrying capacity **(ampacity)** for a given tube size. As a first attempt in selecting the correct tube, a tube with a current rating of at least the expected value must be chosen. This then provides a starting point from which to work. The more familiar one becomes with the process, the better ones feel gets for which tube sizes are better suited for certain span lengths. The tubes are to be selected in accordance with the widest equipment bays, since the same tube size must be used throughout the length of the busbar. The tables then also provide additional parameters that are required in the calculation process, viz. the tube outer diameter ($\mathbf{d_{bo}}$) and tube wall thickness ($\mathbf{t_w}$)

Although a large range of tubular conductor sizes are given, those with the outer diameter sizes shown in bold print, are those that Eskom has standardise on. The related wall thickness sizes in bold print are the IEC preferred sizes.

Table 6.2 provides a comparison of the Electrical and Mechanical Properties of various aluminium alloys used for this application. Bus tubing of the **E-AlMgSiO,5 F25** alloy may be preferred because of its better mechanical properties for only a slightly higher material resistance.

Table 6.1: Aluminium Tubular Conductors [19]

Outer Diameter [d_{bo}] (mm)	Wall Thickness [t_w] (mm)	Cross-Sectional Area (mm^2)	Mass per Metre (kg)	Continuous Current Rating for E-AlMgSiO,5F22		Continuous Current Rating for E-AlMgSiO,5 F 25	
				65 ° (A)	85° (A)	65° (A)	85° (A)
63	4	741	2,00	1150	1530	1110	1480
	5	911	2,46	1280	1700	1240	1640
	6	1074	2,90	1380	1830	1330	1770
	8	1382	3,73	1560	2070	1510	2000
80	4	955	2,58	1400	1860	1350	1800
	5	1178	3,18	1560	2070	1510	2000
	6	1395	3,77	1690	2240	1630	2160
	8	1810	4,89	1920	2550	1850	2460
	10	2199	5,94	2110	2790	2040	2690
100	4	1206	3,26	1690	2240	1630	2160
	5	1492	4,03	1880	2490	1820	2400
	6	1772	4,78	2040	2710	1970	2620
	8	2312	6,24	2320	3070	2240	2960
	10	2827	7,63	2540	3360	2450	3240

Table 6.1: Aluminium Tubular Conductors (continued) [19]

Outer Diameter $[d_{bo}]$ (mm)	Wall Thickness $[t_w]$ (mm)	Cross-Sectional Area (mm^2)	Mass per Metre (kg)	Continuous Current Rating for E-AlMgSiO,5F22		Continuous Current Rating for E-AlMgSiO,5 F 25	
				65 ° (A)	85° (A)	65° (A)	85° (A)
120	4	1458	3,94	1950	2580	1880	2490
	5	1806	4,88	2170	2880	2090	2780
	6	2149	5,80	2370	3140	2290	3030
	8	2815	7,60	2700	3580	2610	3460
	10	3456	9,33	2960	3920	2860	3790
	12	4072	10,99	3130	4150	3020	4010
160	4	1960	5,29	2520	3330	2430	3220
	5	2435	6,57	2790	3700	2690	3570
	6	2903	7,84	3060	4050	2950	3910
	7	3365	9,08	3270	4330	3160	4180
	8	3820	10,31	3490	4630	3370	4470
	10	4712	12,72	3830	5070	3700	4900
	12	5579	15,06	4060	5380	3920	5200

Table 6.1: Aluminium Tubular Conductors (continued) [19]

Outer Diameter $[d_{bo}]$ (mm)	Wall Thickness $[t_w]$ (mm)	Cross-Sectional Area (mm^2)	Mass per Metre (kg)	Continuous Current Rating for E-AlMgSiO,5F22		Continuous Current Rating for E-AlMgSiO,5 F 25	
				65 ° (A)	85° (A)	65° (A)	85° (A)
200	4	2463	6,65	3030	4010	2930	3870
	5	3063	8,27	3410	4520	3290	4360
	6	3657	9,87	3720	4920	3590	4750
	8	4825	13,0	4270	5660	4120	5470
	10	5969	16,1	4680	6200	4520	5990
	12	7087	19,1	4990	6610	4820	6390
250	5	3848	10,4	4140	5490	3900	5300
	6	4599	12,4	4520	5990	4370	5780
	8	6082	16,4	5190	6870	5010	6640
	10	7540	20,4	5700	7560	5500	7300
	12	8972	24,2	6100	8080	5890	7800
	14	10380	28,0	6420	8500	6200	8210
	16	11762	31,8	6640	8800	6410	8500

Table 6.1: Aluminium Tubular Conductors (continued) [19]

Outer Diameter [d_{bo}] (mm)	Wall Thickness [t_w] (mm)	Cross-Sectional Area (mm^2)	Mass per Metre (kg)	Continuous Current Rating for E-AlMgSiO,5F22		Continuous Current Rating for E-AlMgSiO,5 F 25	
				65 ° (A)	85° (A)	65° (A)	85° (A)
300	7	6443	17,4	5810	7700	5610	7440
	8	7339	19,8	6140	8130	5930	7850
	10	9111	24,6	6720	8900	6490	8600
	12	10857	29,3	7180	9510	6930	9190
	14	12579	34,0	7490	9930	7230	9590
	16	14275	38,5	7770	10300	7500	9950
	18	15947	43,0	7920	10500	7650	10140
315	8	7716	20,8	6420	8510	6200	8220
	10	9582	25,9	7060	9360	6820	9040
	12	11423	30,8	7540	9990	7280	9650
	14	13239	35,7	7850	10400	7580	10050
	16	15030	40,6	8150	10800	7870	10430
	18	16795	45,3	8380	11100	8090	10720

Table 6.1: Aluminium Tubular Conductors (continued) [19]

Outer Diameter [d_{bo}] (mm)	Wall Thickness [t_w] (mm)	Cross-Sectional Area (mm^2)	Mass per Metre (kg)	Continuous Current Rating for E-AlMgSiO,5F22		Continuous Current Rating for E-AlMgSiO,5 F 25	
				65 ° (A)	85° (A)	65° (A)	85° (A)
350	8	8595	23,2	7060	9350	6820	9030
	10	10681	28,8	7770	10300	7506	9950
	12	12742	34,4	8230	10900	7950	10530
	14	14778	39,9	8600	11400	8310	11010
	16	16789	45,3	8910	11800	8610	11400
	18	18774	50,7	9130	12100	8820	11670
400	10	12252	33,1	8750	11600	8450	11200
	12	14627	39,5	9360	12400	9040	11980
	14	16977	45,8	9810	13000	9480	12560
	16	19302	52,1	10100	13400	9760	12940
	18	21602	58,3	10300	13700	9950	13230

Table 6.2: Electrical and Mechanical Properties of Various Aluminium Alloys [19]

ALLOY TYPE	HULETT'S S.A.		ASA STANDARD		DIN STANDARD	
	D50STF	**D65STF**	**6063T6**	**6061T6**	**AlMgSi,5F22**	**AlMgSi,5F25**
Electrical resistivity at 20 °C (max.) in Ω mm^2 / m	0,03133	0,037	0,0325	0,0431	0,03333	0,03571
Specific mass kg / m^3	2703	2703	2703	2703	2703	2703
Modules of elasticity E in N / m^2	$65{,}66.10^9$	$69{,}12.10^9$	69.10^9	70.10^9	70.10^9	70.10^9
Thermal co-efficient of expansion per °C	23.10^{-6}	23.10^{-6}	23.10^{-6}	23.10^{-6}	23.10^{-6}	23.10^{-6}
0,2 % Proof stress in MPa Rp0,2	170	240	214	276	160	195

7. BUS CONDUCTOR SUPPORT SYSTEM

Objectives of this Chapter:

Choosing the supporting system to be employed has a major impact on the selection of the tube itself, and upon the strength of the supporting insulators on top of which the tubes are secured. This provides the boundary conditions for the calculation. Three main boundary conditions are defined, viz. both-ends supported, one end supported and one end fixed, both ends fixed.

7.1 Fundamental Busbar Models

The three fundamental busbar models that are usually considered are as follows:

7.1.1 Conductors with Both Ends Freely Supported

The bus support system illustrated in Figure 8.1 is used in the majority of cases where both sides are freely supported. This boundary condition allows lateral movement at both ends of the bus tubing that would otherwise result in a torque on the head of the supporting insulators if they were fixed. The clamps are normally designed in such a manner so as to allow some vertical movement, usually in the region of ±5°.to allow for small deviations in foundation levels and support structure heights.

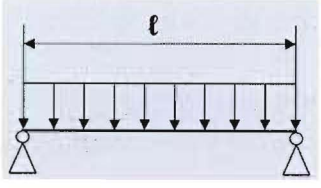

Figure 7.1: Conductors with Both Ends Freely Supported [19]

7.1.2 Conductors with One End Supported and One End Fixed

The bus support system illustrated in Figure 7.2 should only be used in cases where the tube lengths (**ℓ**) are either short so that the torque value, which is a product of half the tube length and resultant force per unit length, does not exceed the insulator rated value (see Chapter 16). Here one end is fixed, while the other end is allowed to move freely to allow for any change in length due to linear expansion. This boundary condition only allows lateral movement at one end. The fixed clamp will not allow for vertical movement, another reason for not applying it in this configuration.

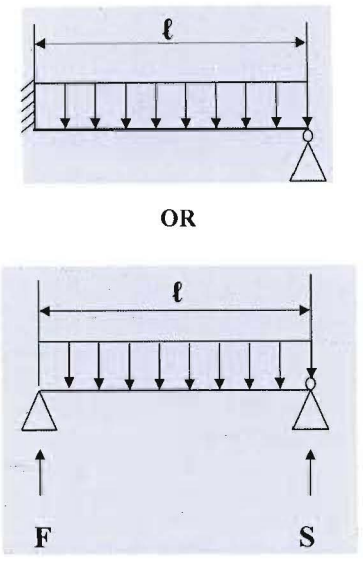

Figure 7.2: Conductor with One End Supported and One End Fixed [19]

7.1.3 Conductor with Both Ends Fixed

Figure 7.3 is, as with the configuration illustrated in Figure 7.2, only employed in the case of short bus tube lengths or where the torsional forces are low and do not exceed the manufacturers rated values. This configuration should in general not be employed in high voltage substations where long tube span lengths are normally required. There may, however, be some application where short interconnecting pieces are required, and the cantilever forces imposed on the post insulators as a result of linear expansion are low. The calculation of these cantilever forces are demonstrated in paragraph 7.4 below.

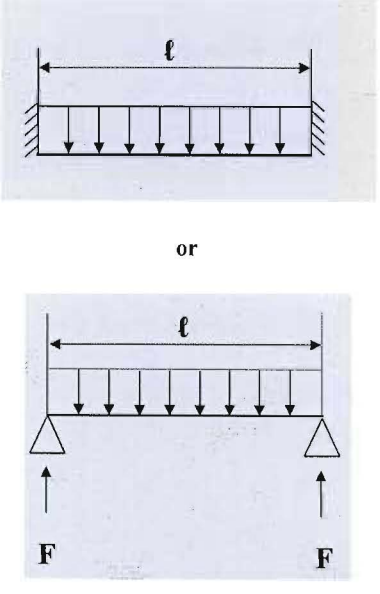

Figure 7.3: Conductor with Both Ends Fixed [19]

7.2 Continuous Beam Busbar Models with a Combination of the Fundamental Models

In reality, however, substations do not consist of a single span of busbars, but rather a series of bays side by side. These busbars may comprise sections made up from single bus tubes of length **ℓ** coupled via an expansion clamp as demonstrated in Chapter 16, or can be continuous beams that are simply supported or fixed as demonstrated below. Continuous beams may result from long lengths of bus tubing that are produced from continuous extrusions or from sections of bus tubing that are welded in a prescribed manner to form long beams. This is briefly discussed under paragraph 7.3.

7.2.1 Two Spans (Simple-Fixed-Simple)

Figure 8.4 illustrates a continuous beam spanning two bays, simply supported at the ends and fixed in the centre. This arrangement is quite acceptable since the torsional forces at the fixed point **F** cancel out. Any linear expansion is allowed for by the simply supported ends **S**.

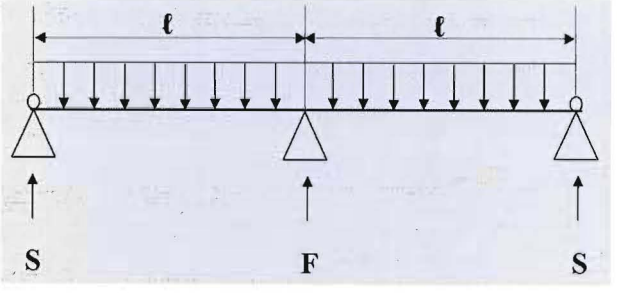

Figure 7.4: Two Spans (Simple-Fixed-Simple) [19]

7.2.2 Three or more spans (simple-fixed-fixed-simple)

This arrangement should only be employed in the case where the two fixed supports (**F**) are short enough so that the cantilever forces imposed on the post insulators as a result of linear expansion are low. The calculation of these forces is given in paragraph 7.4 below.

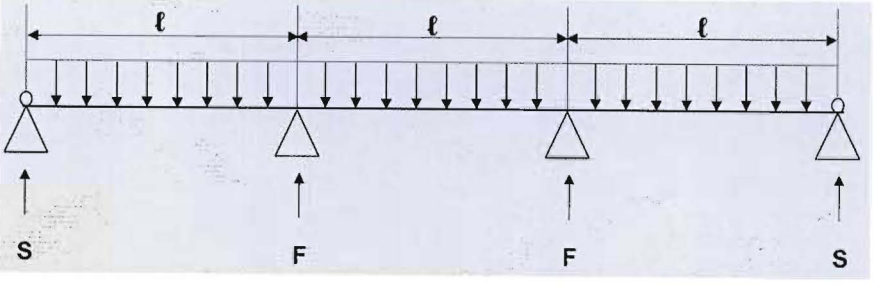

Figure 7.5: Three or More Spans (Simple-Fixed-Fixed-Simple) [19]

7.2.3 Two or More Spans Simple Supports

The arrangement shown in Figure 7.6 is probably the safest of the three arrangements illustrated in this section. There are no restrictions as far as linear expansion and torsional forces are concerned. The sag in the bus tubing is also smaller than in the case of Figure 7.1.1 where the bus system is made up of a series of such arrangements.

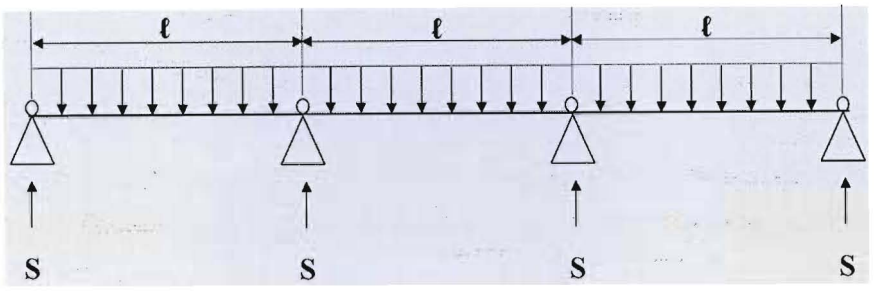

Figure 7.6: Two or More Spans Simple Supports [19]

7.3 Welded Joints and Finish

The large sized aluminium tubes are at times only available in short lengths, but joining of two or more lengths by welding to obtain the required span length has been proved acceptable. A welded joint using a short piece of inner tube as backing plate, gives a joint which is mechanically and electrically acceptable. It is important, however, to follow the tube manufacturer's recommendations with regard to filler rod and weld preparation meticulously. In this regard, the designer is referred to the "Welding Aluminium Manual TIG and MIG" issued by Alcan Booth Sheet Limited.

A build up of weld beads at the joints to the order of 1,0 - 2,0 mm considerably improves the mechanical strength of the joint and will not generate unnecessary corona, provided all sharp edges are removed.

In order to prevent non-required loads of the surrounding area of the welded joint (ca. 50 % weakening due to welding) it is necessary to provide for a minimal bending moment in the joint area or generally to cut the bending moment (see Figure 7.7). When ordering the tubes the resulting tube lengths should be taken into account. Both outside weld joints are placed at the zero passages of the curve of the bending moment. To prevent the individual parts being too short, the third weld joint can be arranged in the middle of field **BC**.

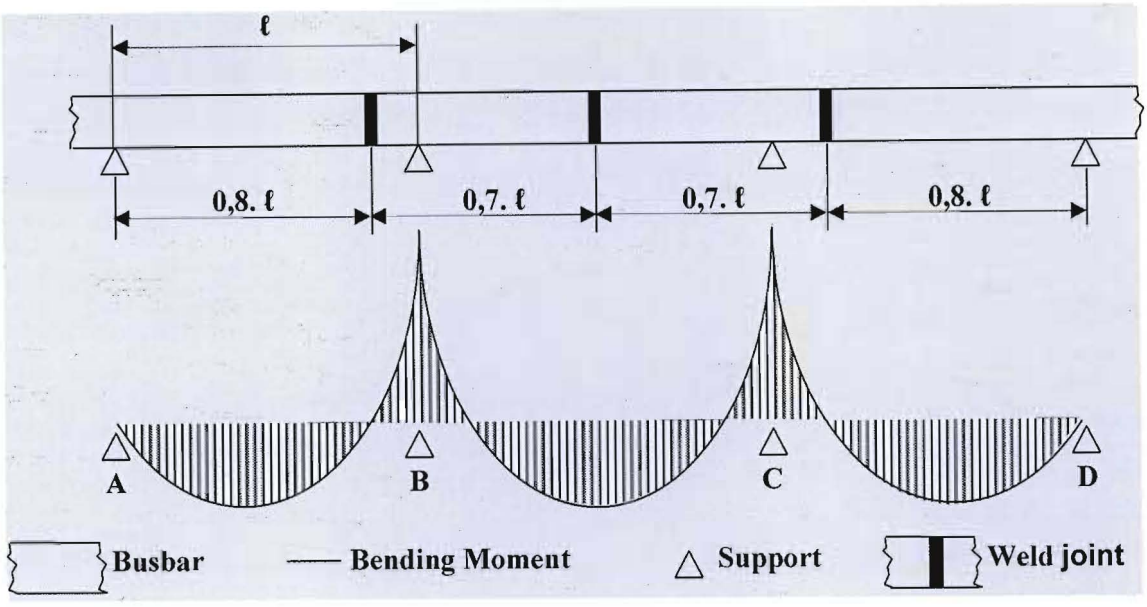

Figure 7.7: Weld Joints [20]

7.4 Longitudinal Expansion of Busbars

Operational temperature variations result in longitudinal expansion or contraction of the busbars. This is calculated from:

$$\ell_t = \ell_0.(1+\alpha_{th}.\Delta\theta_{th}) \qquad (7.1)$$

Where:-

ℓ_t = Length of bus tube at temperature **t** in m

ℓ_0 = Initial length of bus tube in m

α_{th} = Coefficient of linear expansion for material in $^{\circ}C^{-1}$

$\Delta\theta_{th}$ = The difference between the final and initial temperatures in $^{\circ}C$ or $^{\circ}K$

Table 7.1: Materials Coefficients of Linear Expansion [19]

Material	Coefficient of Linear Expansion ($^{\circ}C^{-1}$)
Aluminium	23.10^{-6}
Copper	17.10^{-6}

These temperature induced longitudinal changes may cause significant mechanical stresses on the conductors, on their support insulators and equipment terminal connections if there are no expansion joints. The forces that are generated can be calculated by equating the longitudinal change caused by the change in temperature is assumed to be equal to the longitudinal change that would be caused by a mechanical force $\mathbf{F_m}$.

$$\Delta \ell_t = \ell_0.\alpha_{th}.\Delta\theta_{th} = \frac{F_m.\ell_0}{E.A_c} \quad (7.2)$$

Where:-

F_m = Mechanical Force due to bus tube expansion or contraction in N/(°K.mm)

E = Youngs Modulus of Elasticity in N/m^2

A_c = Cross-sectional are of bus tube in m^2

$$\alpha_{th}.\Delta\theta_{th} = \frac{F_m}{E.A_c} \quad (7.3)$$

$$F_m = \alpha_{th}.E.A_c.\Delta\theta_{th} \quad (7.4)$$

$$F_m = \alpha_{th}.E.\frac{\pi}{4}.[d_{bo}^2 - (d_{bo} - 2.t_w)^2].\Delta\theta_{th}$$

Where:-

d_{bo} = Outer diameter of bus tube in mm

t_w = Bus tube wall thickness in mm

An aluminium bus tube Ø250 x 6WT of length 20m is employed. If we assume that the temperature at installation was 25°C, and the maximum temperature it can reach under operational conditions is 90°C then:

$\Delta \ell_t = 20.23.10^{-6}.(90-25)$

$= 29,9$ mm

$F_m = 0,0299.7.10^{10}.[\frac{\pi}{4}.[0,25^2 - (0,25 - 2.0,006)^2]/20$

$= 243,615$ kN/(K.m^2)

$F_m = 23.10^{-6}.7.10^{10}.[\frac{\pi}{4}.[0,25^2 - (0,25 - 2.0,006)^2].(90-25)$

$= 243,61$ kN/(K.m^2)

$= 0,2436$ N/(K.mm^2)

$= 0,2436.(90-25).2328$

$F_m = 36,86$ kN

From this, it is clear that the insulator will break if the bus tube is fixed at both ends.

8. STATIC FORCES - WEIGHT OF BUS TUBING, DAMPING CONDUCTOR, ICE AND WIND LOADING

Objectives of this Chapter:

- Define the static force
- Determine the mass of bus tubing ($\mathbf{m^1_b}$) alone. This will simply be the mass per unit length of the selected tube obtained from the fourth column of Table 6.1 under the heading **mass per metre** in **kg**, or calculated from first principles.
- Determine the total mass of the tube ($\mathbf{m^1_b}$) inclusive of damping conductor ($\mathbf{m^1_c}$) and excluding ice coating ($\mathbf{m^1_{b+c}}$)
- Determine the total mass of the tube inclusive of damping conductor and ice coating ($\mathbf{m^1_{b+c+i}}$)
- Determine the environmental conditions (IEC requirements on ice coating and wind loading-RSA wind conditions at various heights)
- Wind loading on bus tubing without ice coating (wind force) ($\mathbf{F_w}$)
- Ice loading on bus tubing for additional weight of ice per unit length ($\mathbf{w_i}$)
- Wind loading on bus tubing with ice coating (wind force) ($\mathbf{F_{wi}}$)
- Two cases to be considered, one where the average maximum wind force is applied, the other when a 50 year extreme wind takes place. The consequences of failure need to be weighed up with the cost of over-design for a single occurrence every 50 years

Static forces may be defined those forces that have, at least for a few minutes at a time, a constant magnitude. That is, for all intents and purposes, none time varying. In the context of tubular conductor busbar design these would consist of the weight of the bus tubing itself ($\mathbf{w^1_b}$), the weight of the damping conductor ($\mathbf{w^1_c}$) that is inserted inside the bus tubing, and the weight of ice ($\mathbf{w^1_i}$) that may form around the bus tubing during winter months in areas where this is applicable. These three are directed vertically downward due to gravity. A fourth static component is that due to wind ($\mathbf{F^1_{w1}}$), normally taken as perpendicular to the first three. Figure 8.1 below illustrates how these components act on the bus tubing. The remaining components shown in this drawing will be discussed at a later stage.

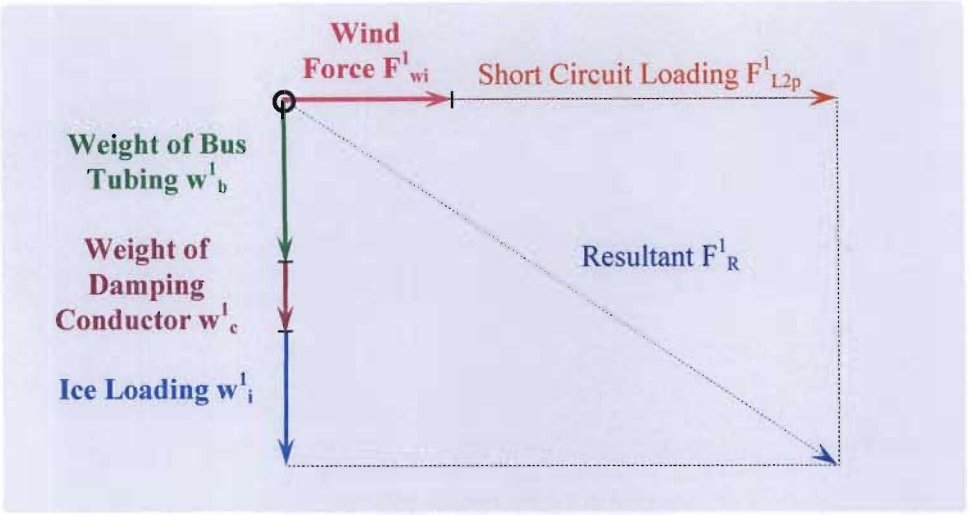

Figure 8.1: Vector Representation of the Per Unit Length Component Forces Exerted on the Tubular Conductors [9]

8.1 Determine the Mass of Bus Tubing (m^1_b) Alone

This will simply be the mass per unit length of the selected tube obtained from the fourth column of Table 6.1.1 under the heading **mass per metre** in **kg**. Alternatively, the mass per unit length can be derived simply by making use of the well known quantity of density.

$$\rho_{al} = \frac{m^1_b}{V_b} \ (kg/m^3) \qquad (8.1)$$

Where:-

ρ_{al} = Density of aluminium in kg/m^3 (Al-Mg-Si = 2700kg/m^3)

m^1_b = Mass per unit length of bus tube in kg/m

v_b = Volume per unit length of bus tube in m^3

The mass per unit length is simply:-

$$m^1_b = \rho_{al}.v_b \ (kg/m) \qquad (8.2)$$

The volume per unit length is not normally a quantity that appears in manufacturers tables so this can be resolved in those parameters that are normally given, viz. outer bus tube diameter and tube wall thickness.

$$v_b = 2{,}5.10^{-7}.\pi\left(d_{bo}^2 - \left[d_{bo} - 2.t_w\right]^2\right) \ (m^3/m) \qquad (8.3)$$

Where:-

d_{bo} = Outer diameter of bus tube in mm

t_w = Bus tube wall thickness in mm

Once the volume ($\mathbf{v_b}$) is calculated, the mass per unit length ($\mathbf{m^1_b}$) is easily arrived at.

8.2 Determine the Total Weight of Bus Tubing

Determine the weight of bus tubing ($\mathbf{w^1_b}$) per unit length + weight of damping conductor ($\mathbf{w^1_c}$) per unit length

8.2.1 Total Conductor Mass per Unit Length.

This will simply be the sum of the mass per unit length of the selected tube and the mass per unit length of the damping conductor. In areas where snow is expected to occur, the mass of the ice that may form around the bus tubing also needs to be taken into account.

8.2.1.1 Bare bus tubing (no ice)

a) Mass of bus tubing and damping conductor

$$\mathbf{m^1_{b+c} = m^1_b + m^1_c\ (kg/m)} \tag{8.4}$$

Where:-

$\mathbf{m^1_{b+c}}$ = Mass of bus tube and damping conductor per unit length in m

$\mathbf{m^1_b}$ = Mass of bus tube per unit length in m

$\mathbf{m^1_c}$ = Mass of damping conductor per unit length in m.

b) Weight of bus tubing and damping conductor [19]

$$\begin{aligned}\mathbf{w^1_{b+c}} &= \mathbf{9.81.m^1_{b+c}} \\ &= \mathbf{9.81.}\left(\mathbf{m^1_b + m^1_c}\right)\mathbf{(N/m)}\end{aligned} \tag{8.5}$$

Where:-

$\mathbf{w^1_{b+c}}$ = Weight of bus tube and damping conductor per unit length in N/m

8.3 Determining the Unit Mass of Ice Forming Around Bus Tubing

According to [15], an ice load equivalent to a layer of ice 15mm, with density of 714 kg/m^3 must be taken into account. [22] on the other hand categorises radial ice thickness as follows:-

Table 8.1: Ice Formation on Tubular Conductors [23]

Loading	Radial Ice Thickness (mm)
Heavy	12,7
Medium	6,4
Light	0

8.3.1 Diameter on outer edge if ice

$$d_{io} = d_{bo} + 2.t_i \quad (mm) \tag{8.6}$$

Where:-

d_{io} = Diameter on outer edge of ice in mm

d_{bo} = Outer diameter of bus tube in mm

t_i = Thickness of ice formed around bus tubing in mm

8.3.2 Mean diameter on the ice

$$d_{mi} = d_{bo} + \frac{(2.t_i)}{2} = d_{bo} + t_i \quad (mm) \tag{8.7}$$

Where:-

d_{mi} = Mean diameter on ice in mm

8.3.3 Volume of ice formed around the bus tubing

8.3.3.1 Circumference on mean diameter of ice

$$C_{mi} = \pi.(d_{bo} + t_i) \ (mm) = \pi.(d_{bo} + t_i).10^{-3} \ (m) \tag{8.8}$$

Where:-

C_{mi} = Mean circumference on ice in mm

8.3.3.2 Projected Area

$$A_i = t_i.10^3 \ (mm^2) = \pi.(d_{bo} + t_i).10^{-3} \ (m^2) \tag{8.9}$$

Where:-

A_i = Projected Area on ice in m^2/m

8.3.3.3 Volume of Ice

$$v^1_i = C_{mi}.A_i$$
$$= \pi.(d_{bo} + t_i).t_i \quad (mm^3/m) \qquad (8.10)$$
$$\pi.(d_{bo} + t_i).t_i.10^{-6} \quad (m^3/m)$$

Where:-

v^1_i = Volume of ice in m^3/m

8.3.3.4 Mass of ice formed around the bus tubing per unit length of bus tubing

$$m^1_i = \rho_i.v_i \quad (kg/m) \qquad (8.11)$$

Where:-

m^1_i = Mass per unit length of ice in kg/m

ρ_i = Density of Ice = $714kg/m^3$ [16]

Normal density of ice = $920kg/m^3$

8.3.3.5 Weight of ice per unit length of bus tubing

$$w^1_i = m_i.9,81$$
$$= \left[\rho_i.v^1_i.10^{-9}\right].9,81 \qquad (8.12)$$
$$= 9,03.10^{-6}.v^1_i \quad (N/m)$$

Where:-

w^1_i = Weight per unit length of ice in N/m

8.4 Wind Force (Loading) per Unit Length.

8.4.1 General

Wind loading on the bus tubing becomes an important component in the determination of the total force per unit length of the bus conductor as the velocity of the air increases. These velocities increase logarithmically with height, and the appropriate velocity at the given height need to be employed in the calculations. A number of additional considerations need to be taken into account, which are given below:

8.4.1.1 Use **nominal wind speed V_z** at height **z** (conductor level, equipment and busbars) above the ground

8.4.1.2 Obtain the nominal wind speed V_z from the appropriate **regional basic wind speed V**, determined in accordance with the geographical location given in Figure 8.5) below. This value is to be adjusted for:-

8.4.1.2a) Mean return period – 50-years [16]

8.4.1.2b) Terrain category – defines the characteristics of those surface irregularities of an area that arise from natural or constructed features and that create a surface roughness affecting the degree of turbulence and the variation of speed with height of the wind passing over the area.

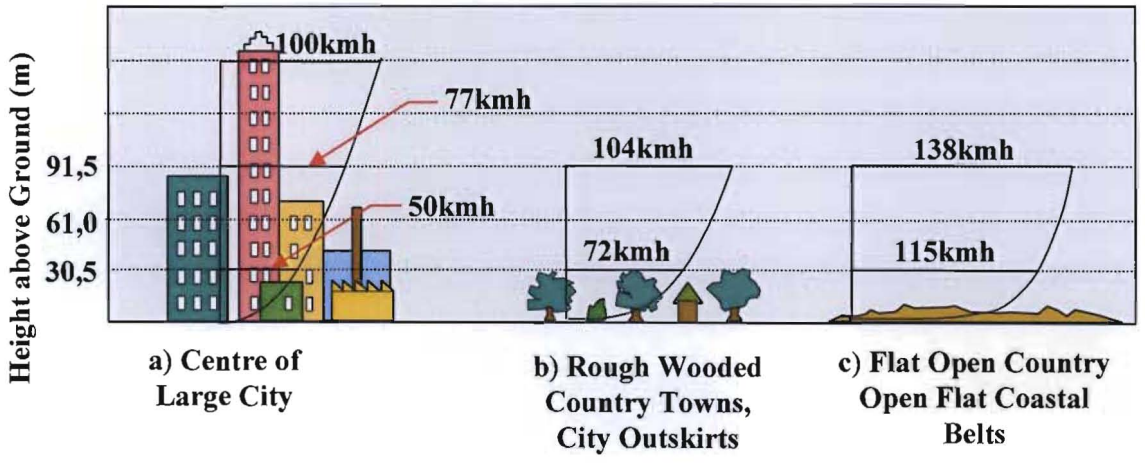

Figure 8.2: An Illustration of Wind Speed Variation with Height Passing Over Different Types of Terrain [16]

On selection of the category, the permanence of a feature that constitutes roughness needs to be taken into account, and the distance (in the direction of upwind of the installation) over which the terrain remains unchanged.

i) Category 1: Exposed smooth terrain with virtually no obstructions and in which the height of any obstruction is less than 1,5m. This category includes open sea coasts, lake shores and flat, treeless plains with little vegetation other than short grass as illustrated by Figure 8.2c).

ii) Category 2: Open terrain with widely spaced obstructions (more than 100m apart) having heights and plan dimensions generally between 1,5m and 10m. This category includes large airfields, open parklands or farmlands, and undeveloped outskirts of towns and suburbs, with few trees. This is the category on which the regional basic wind speed **V** is based.

iii) Category 3: Terrain having numerous closely spaced obstructions generally having the size of domestic houses. This category includes wooded areas and suburbs, towns and industrial areas, fully or substantially developed as illustrated by Figure 8.2b).

iv) Category 4: Terrain with numerous large, tall, closely-spaced obstructions. This category includes large city centres as illustrated by Figure 8.2a).

8.4.1.2c) Effect of wind direction

Depending on the direction from which the wind blows, a change in wind direction may imply a change in Terrain Category since a substation may be surrounded by obstacles of different classification. However, the regional basic wind speed **V** should be varied only if for design purposes according to specific wind directions, sufficient meteorological information is available. Such information can be obtained from the newly installed Geographic Information System (GIS) resident in the Transmission GIS Department in the form of an online information system. Wind Roses as illustrated in Figure 8.3.

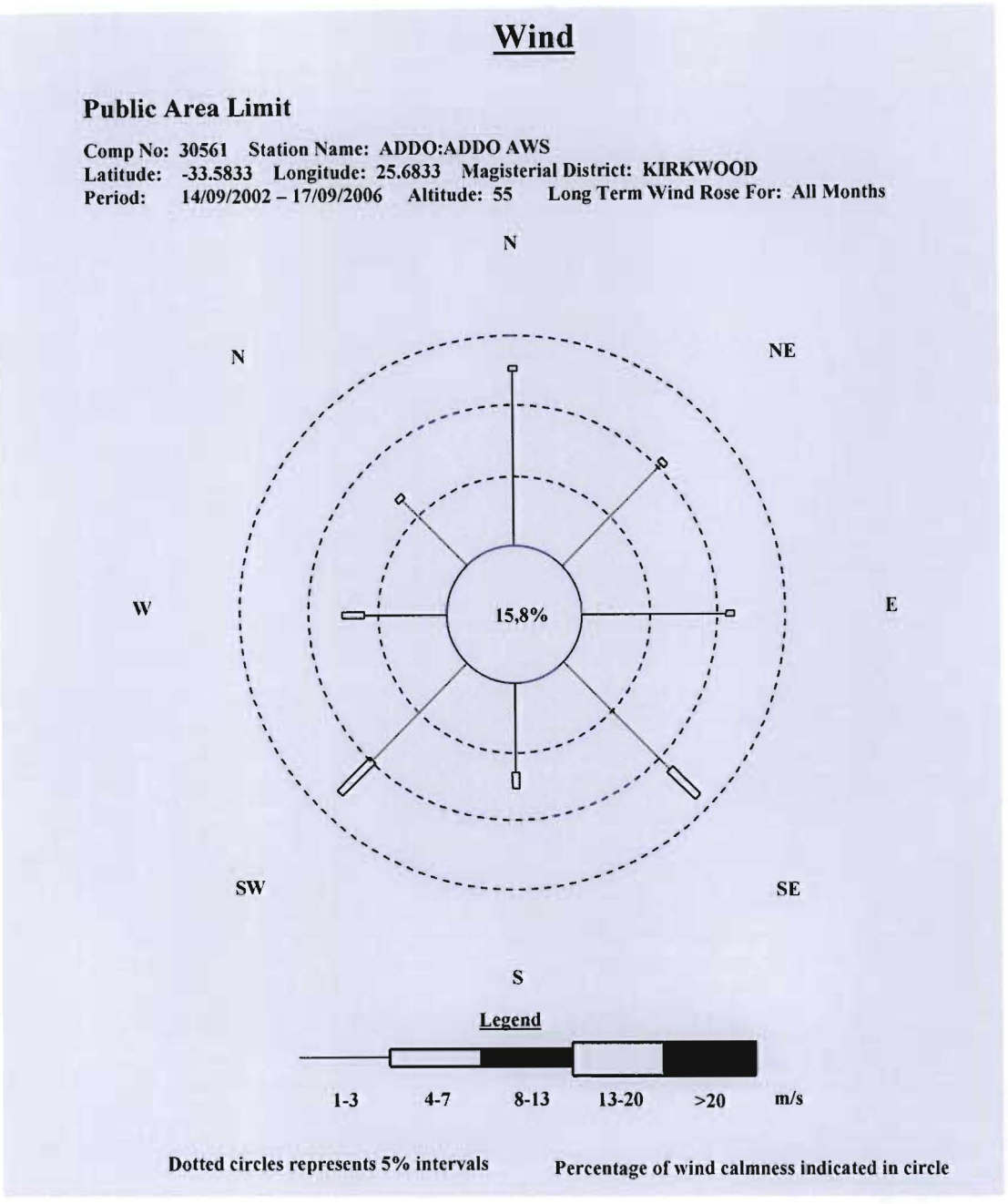

Figure 8.3: Wind Rose for the Addo Weather Station Located in Close Proximity to the Coega IDZ [23]

The Wind Rose shows that the dominating wind speed ranges from 1-3 m/s, and that the rest of the time it ranges from 4-7 m/s. It is clear that there is no dominant direction in this case, and that at least 5 different directions need to be considered.

If, however, the Wind Rose is orientated geographically correctly and superimposed on the substation layout, a clearer picture emerges. The direction of the wind approaching the substation shows that the tubular conductors do not experience the full force of some of these winds when resolved into components in-line with, and perpendicular to the busbar as illustrated in Figure 8.4. The illustration shows that none of the dominant wind directions are

perpendicular to the busbar. This offers an opportunity for an optimised techno-economic design. It is immediately apparent that the most dominant wind direction is south west (**SW**). One should, however, also investigate the easterly (**E**) and north-easterly (**NE**) wind directions.

Suppose the angle of incidence of the wind onto the busbar is χ, then the wind perpendicular to the tubular conductor is:-

$$\mathbf{V_p = V_z.cos\chi} \qquad (8.13)$$

Example:

$\chi = 16^\circ$

$\mathbf{V_p = V_z.cos16^\circ}$

$\mathbf{V_p = 0.96.V_z}$

In other words, the tubular conductor will experience a wind speed of 96% of the total wind speed. In this case, it is not that significant, however, there will be cases where this will make a big difference to the design.

The layout shown in Figure 8.4 is that of the proposed Dedisa 400/132kV Substation which is to be built in the Coega IDZ as one of the main electrical supply points into this area.
Where:-

$\mathbf{V_z}$ = Characteristic wind speed in m/s (value fixed on statistical bases to correspond to a prescribed probability of not being exceeded on the unfavourable side during the lifetime of the installation-nominal value)

$\mathbf{V_p}$ = The component of the Characteristic wind speed in m/s that is perpendicular to the bus tubing

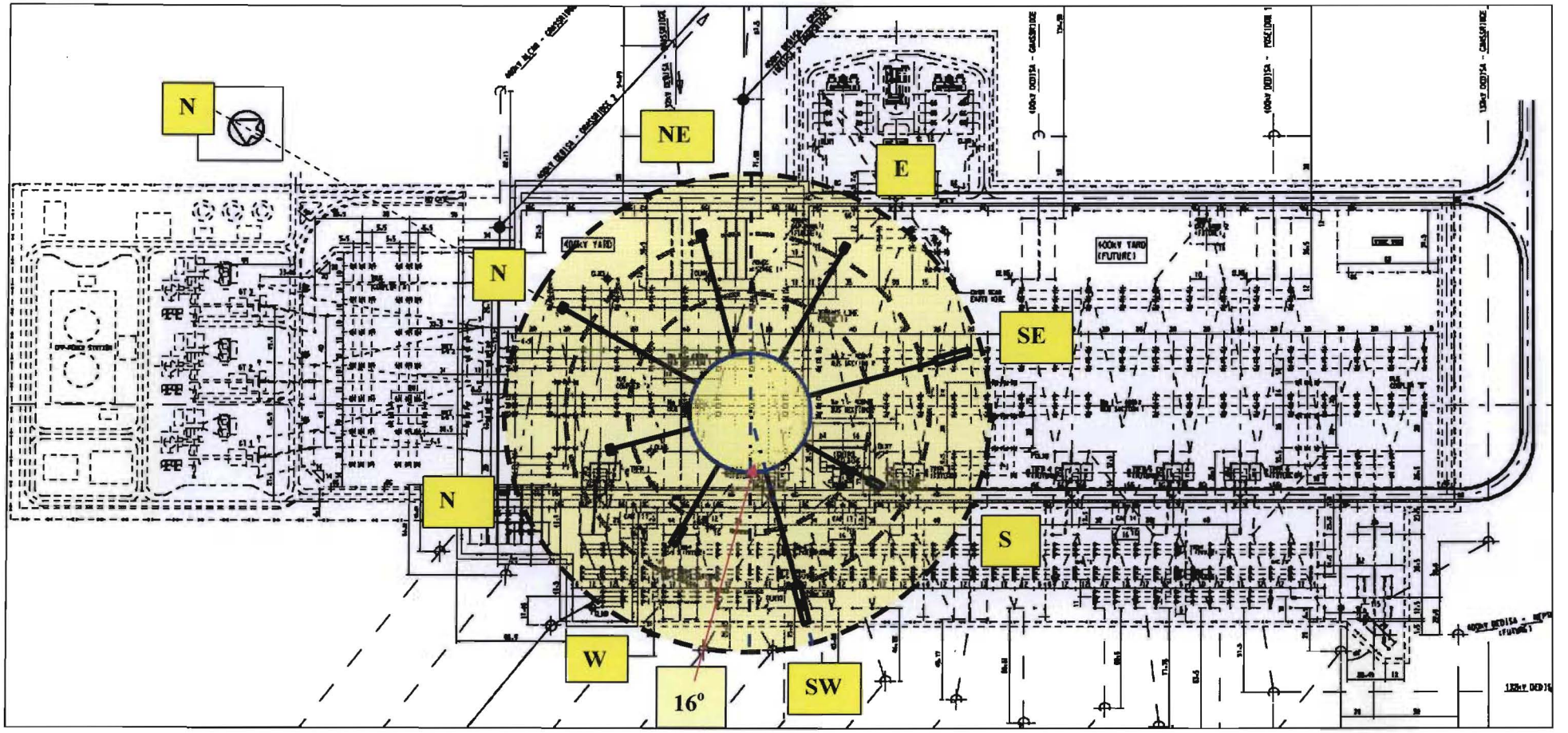

Figure 8.4: Wind Rose Geographically Orientated and Superimposed on the Proposed Dedisa Substation in the Coega IDZ

8.4.1.2d) Local effects on wind speed [18]

A number of geographical aspects need to be considered within the immediate vicinity of where the substation is to be built. These include:-

i) Shielding: Already considered under terrain categories

ii) Exposure: Important to consider effects of exposure resulting from a fetch of open (more severe) terrain in an otherwise rougher (less severe) terrain category.

iii) Local topography: Where the local topography is such that increases in wind speed may occur as a result of tunnelling or other effects, the design speed needs to be adjusted accordingly, on the basis of appropriate meteorological advice or tests

iv) Sudden change in ground level: Increased exposure due to situations on or near the edge of a cliff, bluff or escarpment.

v) Wind speed multiplier: Determine the characteristic wind speed $\mathbf{V_z}$ at height **z** above site mean ground level for the assessed terrain category and class of structure.

$$\mathbf{V_z = V.k_z} \qquad (8.14)$$

Where:-

$\mathbf{V_z}$ = Characteristic wind speed in m/s (value fixed on statistical bases to correspond to a prescribed probability of not being exceeded on the unfavourable side during the lifetime of the installation-nominal value)

$\mathbf{V}$ = Regional basic wind (gust) speed in m/s, according to regional location, for a 50-year return period (see Figure 8.5)

$\mathbf{k_z}$ = Wind speed multiplier (dimensionless), factor for converting regional wind speed into nominal wind speed for the variation of wind speed with height, according to terrain category and class of structure.

Table 8.3 gives the "Variation of Characteristic Wind Speed with Terrain, Height and Class of Structure". It is expected that the majority of design situations will fall into Terrain Category 3, and that the selection of a more severe (Categories 1 and 2) or less severe (Category 4) terrain category will be deliberate.

The table provides factors for discreet values of height (**z**). It is, however, normally required to determine a wind speed multiplier $\mathbf{k_{zn}}$ for an intermediate value of **z**, it can be estimated as follows:-

$$k_{zn} = \left(\frac{k_{z2} - k_{z1}}{z_2 - z_1}\right).(z_n - z_1) + k_{z1} \qquad (8.15)$$

Owing to the large differences in wind speeds between Terrain Categories 2 and 3, and where there is doubt whether the terrain under consideration falls into Category 2 or 3, the design wind speed may be obtained by interpolation between the two values for these categories.

$$k_{zn} = \left(\frac{k_{z2B} + k_{z3B}}{2}\right) \qquad (8.16)$$

8.4.1.2e) height above ground (z): measured from ground level in the immediate vicinity of the structures.

8.4.1.2f) class of structure or element [16]

i) **Class A**: For the determination of forces on units of cladding, roofing, glazing and their intermediate fixings, including roof battens and minor purlins supporting small areas of roofing, and on individual members of roofing.

ii) **Class B**: For the determination of forces on main structural members as well as for the overall resultant forces and for over-tuning moments on buildings, where neither the height nor the width nor the depth of the building exceeds 50m.

iii) **Class C**: For the determination of the overall resultant forces and over-turning moments on buildings where the height or the width or the depth exceeds 50m.

NB: In virtually all cases, **Class B** structures will be employed

1. A characteristic wind speed (V_z) of at least 24m/s (86,4km/hr) must be used
2. Characteristic wind pressure (p_z)

$$p_z = C_p.k_p.V_z^2 \qquad (8.17)$$

Where:-

p_z = Pressure on the surface at height z in N/m^2

C_p = Pressure coefficient for the particular surface

k_p = A constant dependent on site altitude (dimensionless)

Table 8.2: Values of k_p for a range of site altitudes [16]

Site Altitude above Sea Level (m)	k_p
0	0,60
500	0,56
1000	0,53
1500	0,50
2000	0,47

$$k_p = \frac{\text{air density}}{2} \tag{8.18}$$

Half the density of air under the relevant conditions and therefore varies with temperature and atmospheric pressure. A temperature of 20°C has been selected as appropriate for South Africa and variation of mean atmospheric pressure with altitude is allowed for above. Intermediate values of k_{pn} may be obtained by linear interpolation.

$$k_{pn} = \left(\frac{k_{p2} - k_{p1}}{H_{a2} - H_{a1}}\right).(H_{an} - H_{a1}) + k_{p1} \tag{8.19}$$

Where:-

k_{pn} = Interpolated constant dependent on site altitude (dimensionless)

k_{p1} = Lower constant dependent on site altitude (dimensionless)

k_{p2} = Upper constant dependent on site altitude (dimensionless)

H_{a2} = Altitude upper value in m

H_{a1} = Altitude lower value in m

$$F^1_w = C_d.k_{pn}(V.k_z)^2.C_c.A_e$$
$$= C_d.k_{pn}(V.k_z)^2.C_c.(d_{bo} + 2.t_i) \text{ N/m} \tag{8.20}$$

Where:-

F^1_w = Resultant force on components in N/m

C_d = Drag coefficient =1 for circular tubes

k_p = A constant dependent on site altitude (dimensionless)

k_z = Wind multiplier (dimensionless)

C_c = Curvature coefficient = 0,6

A_e = Projected or effective area of element in m^2

$$F^1_w = C_d.k_{pn}(V.k_z)^2.C_c.(d_{bo} + 2.t_i)$$

$$= 1.k_{pn}(V.k_z)^2.0,6.(d_{bo} + 2.t_i) \quad (8.21)$$

$$F^1_w = 0,6.k_{pn}(V.k_z)^2.(d_{bo} + 2.t_i) \text{ N/m}$$

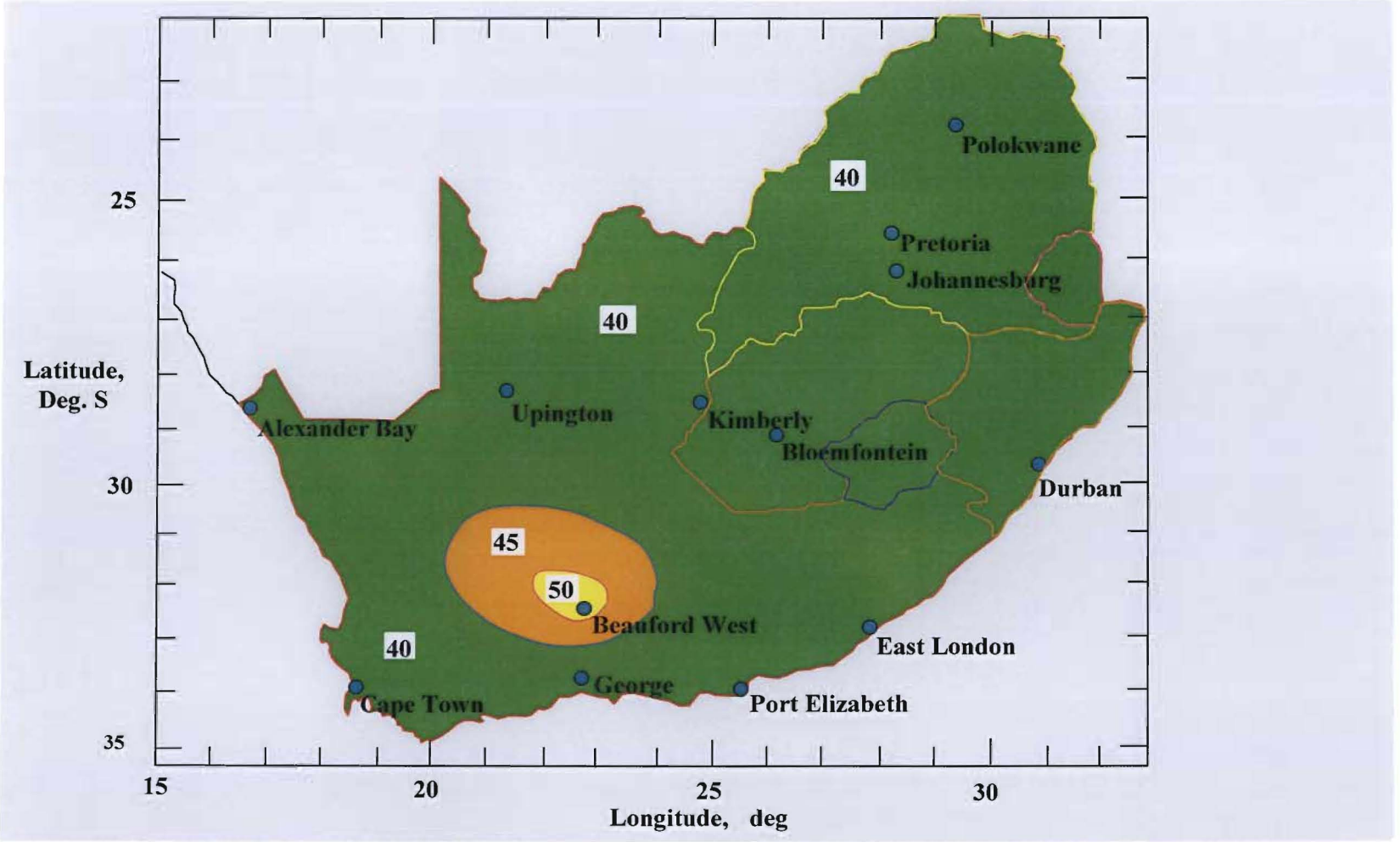

Figure 8.5: Regional Basic Wind Speed V, m/s (Isopleths of 3 Second Gust Speeds at 10m Height in Terrain of Category 2, Estimated to be exceeded on Average Only 50 Years) [16]

Table 8.3: Variation of Characteristic Wind Speed with Terrain, Height and Class of Structure [16]

1	2	3	4	5	6	7	8	9	10	11	12	13
Height z (m) Up to	**Wind Speed Multiplier - k_z**											
	Terrain Category 1			**Terrain Category 2**			**Terrain Category 3**			**Terrain Category 4**		
	Class of Structure Element											
	A	B	C	A	B	C	A	B	C	A	B	C
5	1,03	1,02	1,00	0,94	0,92	0,88	0,67	0,64	0,60	0,65	0,62	0,57
10	1,09	1,08	1,05	1,00	0,98	0,95	0,74	0,71	0,68	0,65	0,62	0,57
15	1,12	1,11	1,09	1,04	1,02	0,99	0,81	0,78	0,76	0,65	0,62	0,57
20	1,14	1,13	1,11	1,07	1,05	1,02	0,86	0,83	0,81	0,65	0,62	0,57
50	1,22	1.21	1,20	1,16	1,15	1,13	1,00	0,98	0,96	0,86	0,84	0,80
100	1,28	1,27	1,27	1,23	1,22	1,21	1,11	1,10	1,08	1,00	0,98	0,95

There are essentially four separate climatic conditions to be considered when determining the contribution of wind force on the tubular conductor. They comprise studying the effect of firstly, the average wind force and secondly, a 50 year extreme wind force, exerted on tubes with no ice covering, and then for the case where tubes have an ice covering. The later two studies are done for cases where ice covering could be expected since the added weight of the ice and the larger effective diameter of the tube changes the dynamic performance of the tube.

Tubular conductors, together with supports, may be subjected to a wind pressure of **700Pa** or more. In the case of lattice support structures the area for calculating the force due to wind pressure is **1,5** times the projected area of the members of one side and in the case of round tubular conductors, hexagonal or elliptical poles, the area is **0,6** times the projected area.

Although dynamic, the wind loading is treated as a steady continuous force in Pa or N/m^2, i.e. a static force.

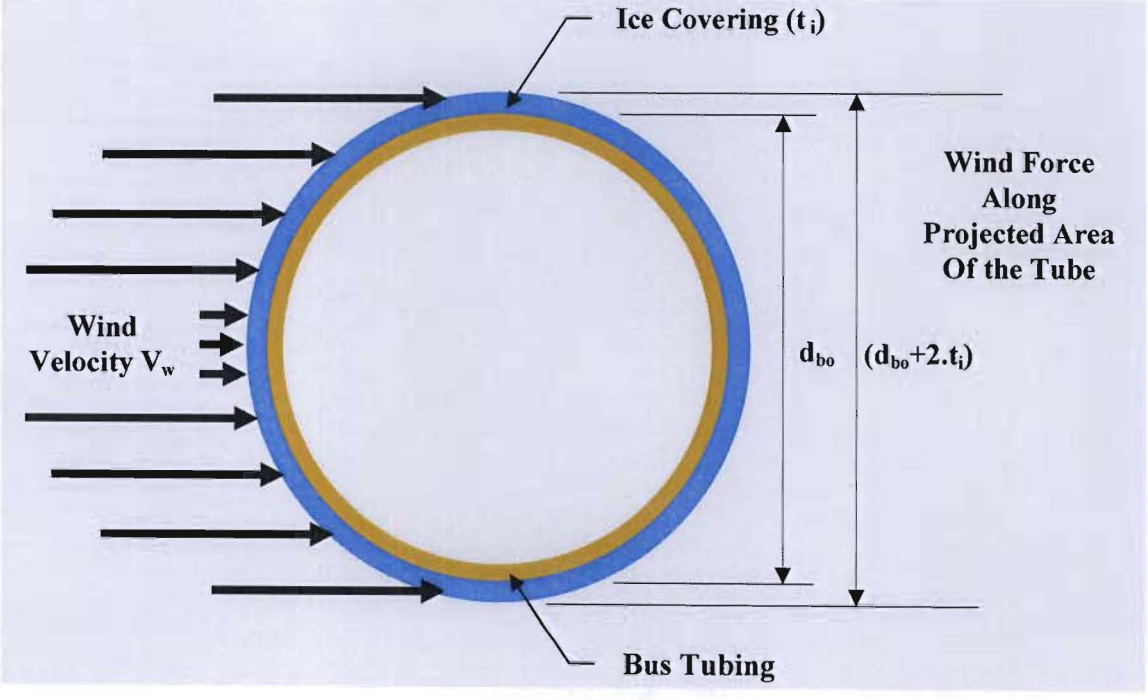

Figure 8.6: No Ice Covering (Applicable for most areas in RSA)

d_{bo} = obtained from Manufacturers tables

8.4.2 Average or Maximum Expected Wind Force

$$F^1_{wo} = P^1_w.(d_{bo} + 2.t_i).10^{-3}.C_c$$
$$= P^1_w.(d_{bo} + 2.t_i).10^{-3}.0,6 \quad (N/m) \qquad (8.23)$$

Where:-

$\mathbf{F^{l}_{wo}}$ = Force per unit length of bus tubing with no ice in N/m

$\mathbf{P^{l}_{w}}$ = Maximum wind pressure on the projected area in N/m^2

$\mathbf{C_c}$ = Curvature coefficient = 0,6 for circular tubes (used on electrical substations)

9. ELECTROMAGNETIC SHORT CIRCUIT FORCES

Objective of this Chapter:

- Determine the reference force ($\mathbf{F}^{1}_{sc}$)
- Determine the Kappa Factor (κ)
- Determine the peak short circuit forces per unit length for 3-phase fault on middle phase ($\mathbf{F}^{1}_{L2p}$) and two outer phases ($\mathbf{F}^{1}_{L1p}$ and $\mathbf{F}^{1}_{L3p}$)
- Determine the peak short circuit forces per unit length for 2-phase fault ($\mathbf{F}^{1}_{sc(L2p)}$)
- Distinguish between the applicable static and dynamic forces
- Determine the static forces on the conductor: Own weight, Ice Loading and Wind Loading
- Determine the resultant force ($\mathbf{F}_{R(\sigma)}$)
- Determine the maximum static stress imposed on the conductor σ_{ST} chosen boundary conditions
- Test against 0,2% proof stress of alloy

Although dynamic in nature, the **short circuit reference force** ($\mathbf{F}^{1}_{sc}$) and **peak short circuit force** ($\mathbf{F}^{1}_{L2p}$) is employed as the fifth component in the calculation of the resultant force ($\mathbf{F}_{R(\sigma)}$)

9.1 Theoretical Analysis

The parallel conductors in a 3 phase busbar system are subjected to time varying forces evenly distributed along the length of the conductor as a result of the time varying current flowing in the conductors. Under short circuit conditions, these time varying forces are far larger than under system healthy conditions. The magnitude of these short circuit currents can be as great as 10 times the nominal system healthy values, particularly as the distance of the parallel conductors is reduced.

The modern day trends in high voltage systems strive for compactness (smaller phase separations) which in combination with ever increasing fault levels place high demands on substation hardware for mechanical integrity. Mechanical stresses can no longer be ignored in new designs and older systems should be re-evaluated. This often results in refurbishment work being required.

These effects are the manifestations of the response of the bus system to the electromagnetic excitation forces during electrical short circuits. When rating substation hardware, the following mechanical quantities are imperative for the sound performance of the system during short circuits:-

i) Maximum bending stresses in the tubular conductor that could result in permanent deformation

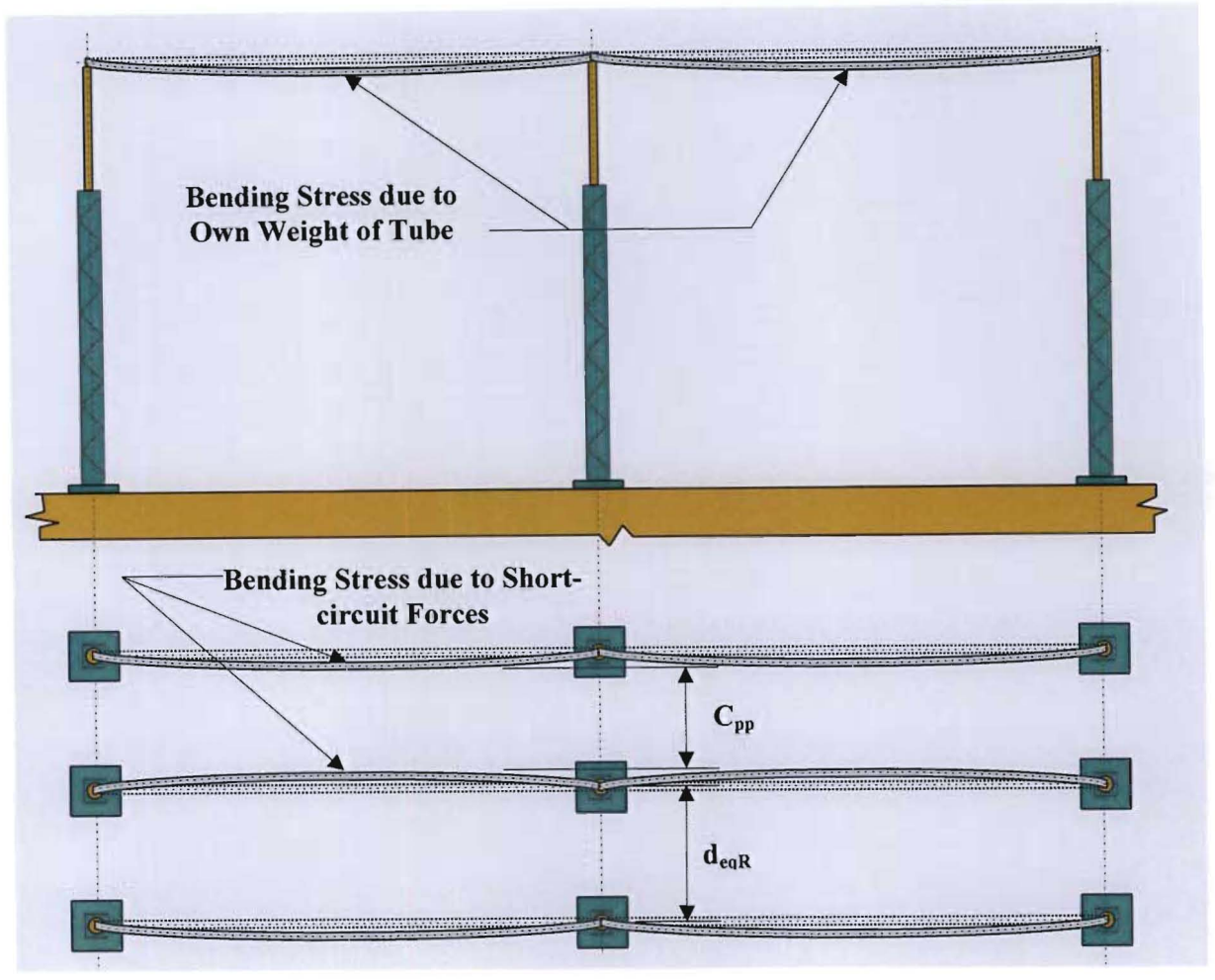

Figure 9.1: Deflection of Conductors due to Short Circuit Forces

ii) Forces transferred to the hardware (clamps and fittings)

iii) Dynamic loading which result in a maximum bending moment at the base of support insulators and steel structures

iv) Twisting (torque) effects which could lead to failure normally at the top end of porcelain support insulators

For rigid tubular conductors, the method and equations for calculating the stresses are linear [4]. Different stress components, however, may be superimposed on each other hence mechanical resonance of conductors at higher harmonic orders should not be neglected.

The simplified method for calculating the stress and forces is based on the following assumptions [6]:-

i) The centre line distance between conductors is much smaller than the conductor length so that the conductors can be regarded as being of infinite length

ii) The conductor diameter and conductor deflection during oscillations are much smaller than the centre line distance between conductors, so that the conductors can be treated as a parallel line-conductors

iii) The short circuit occurs far from rotating machines

iv) The short circuit occurs simultaneously for all faulted phases

v) Conductor support structures are rigid, implying that it will have no deflection whatsoever under any applied force.

For all calculations, the conventional arrangement of conductors (flat configuration), as shown in Figure 9.2, is taken as the basis.

The short circuit peak force is sufficient to determine the dynamic stress only if the fundamental mechanical frequency of the system is large in comparison to the excitation frequencies.

The mechanical fundamental frequency of high voltage tubular busbars is normally less than 10 Hz (see Chapter 10 of this dissertation). However, the excitation forces contain frequency components that are the same as or double the electrical frequency, with large constant components occurring as well. The exact time patterns of the electromagnetic forces are therefore of great importance; the investigation of these forces yields the time patterns of the dynamic stresses necessary for the dimensioning of the structures.

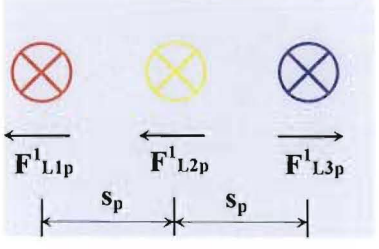

a) Three Phase Short Circuit [4]

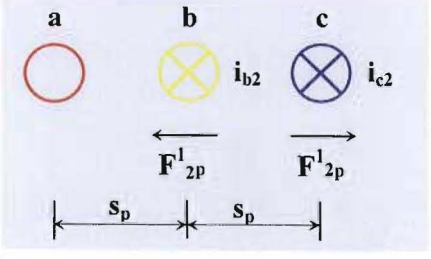

b) Phase to Phase Short Circuit

Figure 9.2: Short Circuit Forces between Conductors [4]

9.2 Reference Short Circuit Force per Unit Length

The reference short circuit force per unit length is simply the force per unit length experienced between two parallel conductors through which a short circuit current flows equal in magnitude, but not necessarily in the same direction. It can cause the either conductors to either attract or repel each other. The magnitude of the force can be derived from the following well known equation [19]:-

$$F^{1}_{sc} = \frac{\mu_0}{2.\pi.s_p}\left(\sqrt{2}.I_{sc}\right)^2$$

$$= \frac{4.10^{-7}}{s_p}.(I_{sc})^2 \qquad (9.1)$$

Where:-

F^{1}_{sc} = Reference short-circuit force per unit length of bus tubing in N/m

I_{sc} = 3 phase symmetrical short circuit current (rms) value in A.

NB: For HV yards close to or at rotating machines (power stations) the sub-transient value of the symmetrical short circuit current should be used.

s_p = phase spacing in metres

μ_0 = Permittivity of free space = $4.\pi.10^{-7}$

$$F^{1}_{sc} \alpha \frac{1}{s_p}$$

The short-circuit force is inversely proportional to the phase spacing. The larger the phase spacing, the smaller the forces acting on the bus tubing for the same short-circuit current.

9.3 Kappa Factor [6] [19]

The peak forces caused by simultaneous short circuits are proportional to the square of the factor κ for the short circuit peak current. Factor κ is the ratio of the largest asymmetric value of the short circuit current to the largest symmetric value of the short circuit current. Single phase earth faults are not taken into account since the electromagnetic forces are small.

κ is determined for the ratio $\frac{R}{X}$ from the resulting system impedance $\mathbf{Z_k}=\mathbf{R_k} + \mathbf{jX_k}$ at the fault location. The values of κ in different networks:-

Table 9.1: Limits of κ for Various Electrical Systems [19]

Network	Limits of κ
Low Voltage	1,8
High Voltage substations far from rotating machines	2,0
At or near rotating machines (generators) < 100MVA	1,8
At Rotating Machines (generators) , >100MVA	1,9

$$\kappa = 1{,}02 + 0{,}98.e^{\left(-3.\frac{R}{X}\right)} \qquad (9.2)$$

= Kappa factor for peak short circuit current

For designs of power station HV yard bus systems therefore, the value of κ becomes larger than 1.8, a fact that needs to be allowed for.

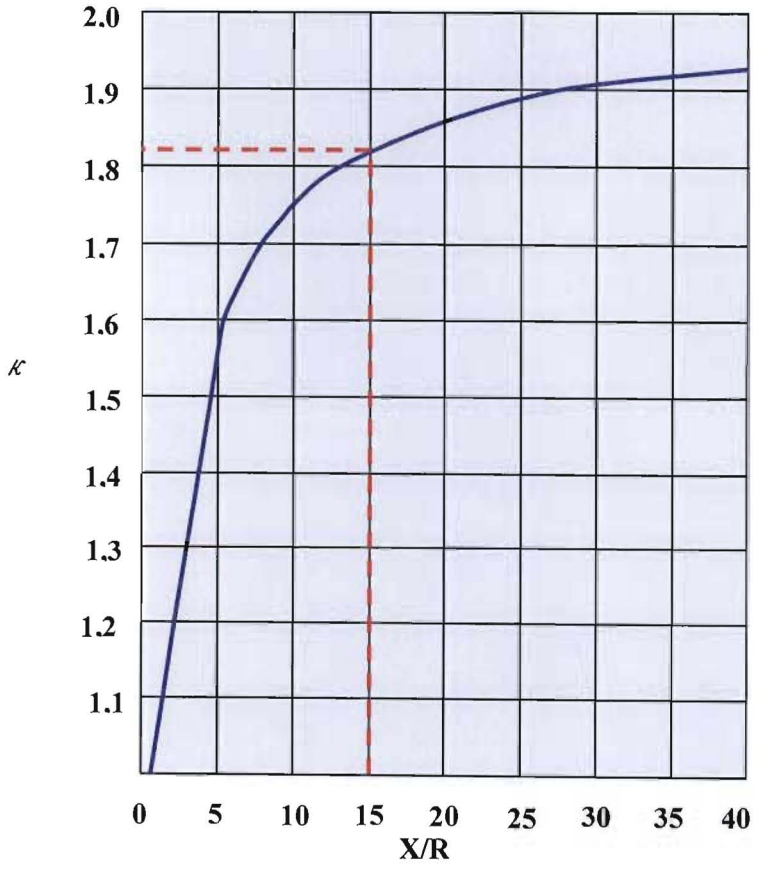

Figure 9.3: κ (Kappa) Factor [6] [19]

Time variant electromagnetic forces act on the conductors during short circuits and the whole structure performs forced oscillations for the short circuit duration and free oscillations after the fault. The resultant force consists of a steady state component (constant oscillation plus un-damped oscillation at double the electrical frequency) plus a decaying component (oscillation at electrical frequency plus exponential decaying term).

9.4 Peak Short-circuit Forces per Unit Length

Objectives:

- Determine the peak short-circuit forces on all three phases ($\mathbf{F'_{L2p}}$, $\mathbf{F'_{L1p}}$ and $\mathbf{F'_{2p}}$)
- Deflection of conductor such that phase-to-phase clearance not infringed

At the instant that the fault occurs, the current wave form lifts to be asymmetrical about the time axis, containing an alternating current component and a direct current component. This produces an initial peak value ($\mathbf{I_p}$) before settling symmetrically about this axis. Two cases are shown below, that for stations close to or at generating stations, and the other where the station is far from generation.

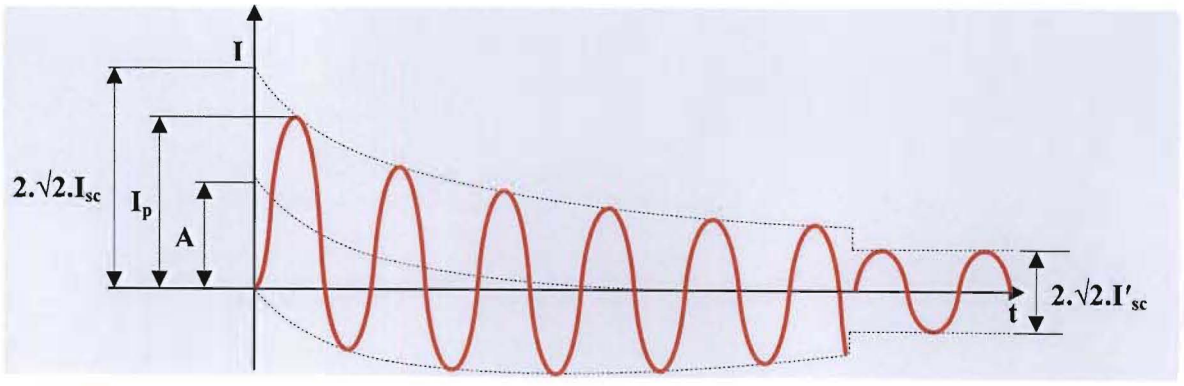

a) Short Circuit Near To Generating Plant

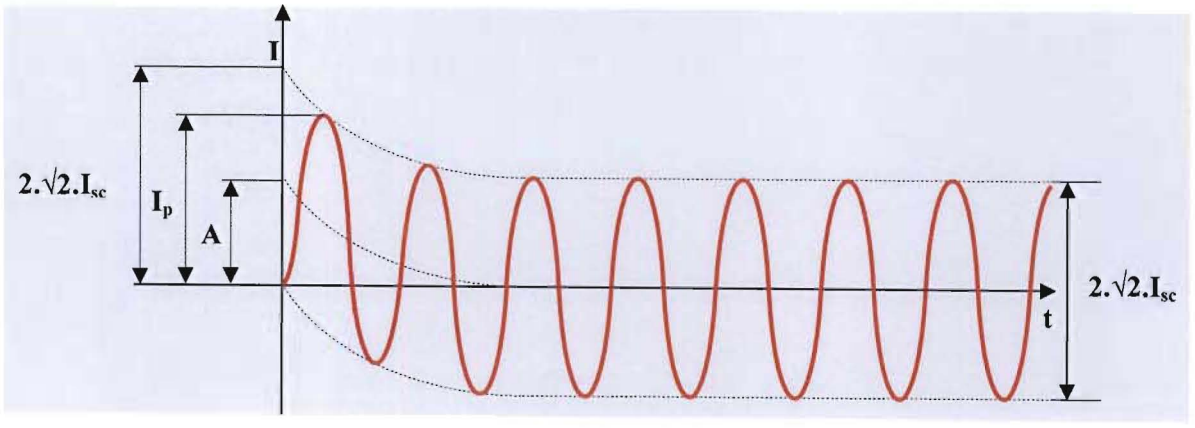

b) Short Circuit Far From Generating Plant

Figure 9.4: Curves of Short Circuit Currents [9]

In a 3-phase system, fault current flowing in all three phases has a compounded effect on the centre phase. Figure 9.4a) showing the short-circuit forces between conductors, illustrates that the force per unit length on the centre phase is larger than that on the outer phases. In the case where only two phases are subjected to the flow of fault current the peak short-circuit force is smaller than that for a 3-phase fault. The following equations have been derived to calculate the **peak short circuit forces per unit length**:-

9.4.1 Three phase short circuit [4]

9.4.1.1 Force on centre phase

$$F^{1}_{L2p} = 0{,}866.F^{1}_{sc}.\kappa^{2}\ (N/m) \tag{9.3}$$

9.4.1.2 Force on outer phases

$$F^{1}_{L1p} = F^{1}_{L3p} = 0{,}808.F^{1}_{sc}.\kappa^{2}\ (N/m) \tag{9.4}$$

9.4.2 Phase-to-phase short circuit

$$F^{1}_{sc(L2p)} = 0{,}750.F^{1}_{sc}.\kappa^{2}\ (N/m) \tag{9.5}$$

Since faults happen for a large variety of reasons, and that it is difficult to predict the occurrence of a particular type of fault, it stands to reason that a typical three phase busbar system will be designed to satisfy the worst case condition given by (9.3) and that the other two equations need not be further considered. The resultant short circuit force on the centre conductor is about 7 percent greater than that on the outer phases [4].

9.5 Maximum Static Resultant Force Imposed on the Conductor

Chapter 8 dealt with the essentially static forces imposed on the bus tubing, viz. weight of the bus tubing on its own, the weight of the damping conductor, the weight of ice that may form around the bus tubing during the winter months, and lastly the wind loading on the bus tubing.

The fifth and final component of force that needs to be considered was dealt with above, viz. the short circuit forces on the centre and outer tubes. This is essentially dynamic force, but does not take into account the natural mechanical frequency of the bus tubing. A typical tubular busbar system is subjected to a combination of static and dynamic forces and stresses (see Figure 9.5).

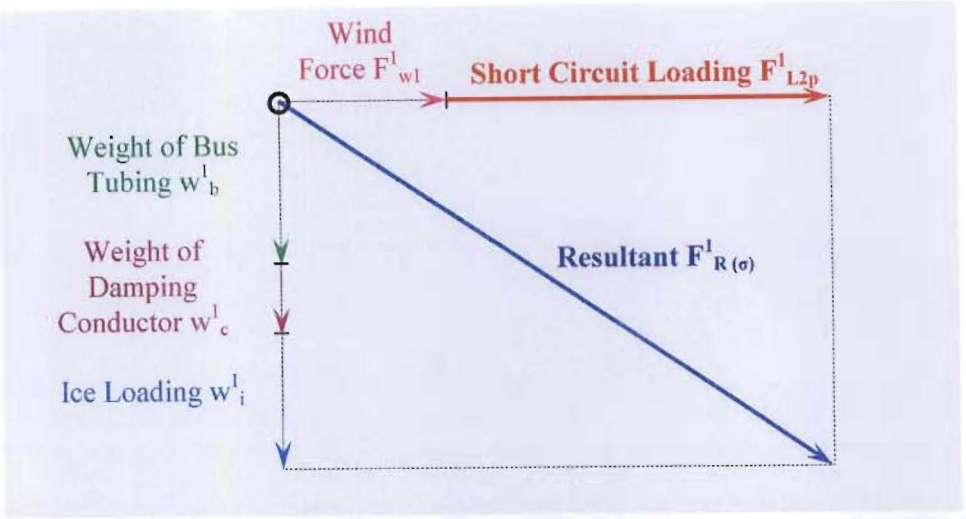

Figure 9.5: Vector Representation of the Component Forces Including the Short Force Exerted on the Tubular Conductors [9]

9.6 Resultant Force [9]

The rigid bus tube must be capable of withstanding the simultaneous application of the forces shown in Figure 9.5, viz. following forces:-

a) Weight of bare bus tubing ($\mathbf{w^1_b}$)
b) Weight of vibration damping conductor ($\mathbf{w^1_c}$)
c) Wind force ($\mathbf{F^1_{wl}}$)
d) Weight of ice if applicable ($\mathbf{w^1_i}$)
e) Short-circuit force ($\mathbf{F^1_{L2p}}$)

The vector sum of these forces is given by:-

$$\mathbf{F^1_{R(\sigma)} = \sqrt{(F^1_{L2p} + F^1_{wl})^2 + (w^1_b + w^1_c + w^1_i)^2}} \ \mathbf{(N/m)} \qquad (9.6)$$

Where:-

$\mathbf{F^1_{R(\sigma)}}$ = The resultant force due to short-circuit current, wind loading, conductor weight and ice loading if applicable in N/m

9.7 Maximum Static Stress Imposed On the Conductor [3] [4]

The **maximum static stress imposed on the conductor** σ_{ST} is calculated as follows:-

In general, the static stress is given as:

$$\sigma_{ST} = \frac{F_{R(\sigma)} \cdot \ell^2}{k.W} (N/m^2) \qquad (9.7)$$

Where:-

k = Static stress factor

Table 9.2: Static Stress Factors for Different Fixing Configurations and Spans [19]

Type of Support System	Static Stress Factor
Tube supported at both ends	8
Tube with one end supported and one end fixed	8
Tube fixed at both ends	12
Tube on three supports	8
Tube on four supports	10
Tube on more than four supports	9

9.7.1 For conductors with both ends supported [4]

$$\sigma_{ST} = \frac{F_{R(\sigma)} \cdot \ell^2}{8.W} (N/m^2) \quad (9.8)$$

9.7.2 For conductors with one end supported and one end fixed

$$\sigma_{ST} = \frac{F_{R(\sigma)} \cdot \ell^2}{8.W} (N/m^2) \quad (9.9)$$

9.7.3 For conductor with both ends fixed

$$\sigma_{ST} = \frac{F_{R(\sigma)} \cdot \ell^2}{12.W} (N/m^2) \quad (9.10)$$

Where:-

W = Moment of resistance for bending in m^3

$$W = \frac{J}{\left(\frac{d_{bo}}{2}\right)} (m^3) \quad (9.11)$$

Where:-

J = Moment of inertia in m^4

d_{bo} = outside tube diameter in mm

d_{bi} = inside tube diameter

$$J = \frac{\pi}{64} . \left(d_{bo}^4 - d_{bi}^4\right) (m^4) \quad (9.12)$$

10. FUNDAMENTAL MECHANICAL FREQUENCY OF THE SELECTED SYSTEM DUE TO TIME VARIANT ELECTROMAGNETIC FORCES - PARAMETRIC STUDIES

Objectives of this Chapter:

- Choose support system to set the boundary conditions
- Determine the fundamental mechanical frequency ($\mathbf{f_c}$)
- Determine the ratio $\mathbf{f_c/f}$
- Test $\mathbf{f_c/f>>1}$, $\mathbf{f_c/f<<1}$
- Determine the ratio between dynamic and static forces on the support insulator (v_F)
- Determine the ratio between dynamic and static conductor stress (v_σ)
- Determine the ratio between stress with and without unsuccessful auto-re-closure (v_r)
- Determine the Eigen value for the busbar support system (λ)
- Determine the dynamic conversion factors (v_F, v_σ and v_r)
- Choose ratio **X/R = 15**

The three fundamental busbar models as described in Chapter 7 are; Conductors with both ends freely supported, conductors with one end supported and one end fixed, and conductors with both ends fixed [see Figures 7.1, 7.2 and 7.3].

10.1 Fundamental Mechanical Frequency

Parametric studies carried out show that the most important parameter for the calculation of the dynamic short circuit stress is the fundamental mechanical frequency ($\mathbf{f_c}$), also referred to as the characteristic or natural frequency of the tube that is a function of the tube cross-section (diameter and wall thickness), material properties (Modulus of Elasticity) and length.

$$\mathbf{f_c = \frac{\lambda^2}{2.\pi}.\sqrt{\frac{E.J}{m^1{}_{b+c}.\ell^4}}} \qquad (10.1)$$

If the frequency of the mechanical fundamental oscillation or of a mechanical harmonic oscillation is equal to the electrical or double the electrical frequency resonance enhancements will occur.

The increases caused by resonances with electrical frequency are comparatively small when $\frac{\mathbf{X}}{\mathbf{R}} = \mathbf{15}$, but increases considerably when $\frac{\mathbf{X}}{\mathbf{R}} = \mathbf{30}$ **[7] [19]**

Fundamental frequency and dynamic factors were calculated for the simplified method and Cigré presented the results in graphic form for easy reference (see Figures 10.1 and 10.2).

The fundamental mechanical frequency for a tubular conductor is given by:-

From [19]

$$f_c = \frac{\lambda^2}{2.\pi.\ell^2} \cdot \sqrt{\frac{E.J}{m'_{b+c}}}$$

$$f_c = \frac{\gamma}{\ell^2} \cdot \sqrt{\frac{E.J}{m'_{b+c}}} (Hz) \qquad (10.2)$$

Where:-

f_c = Fundamental mechanical frequency for a tubular conductor in Hz

λ = Eigen value for busbar type (see Table 10.1)

ℓ = Span length of tubular conductor in metres

γ = Fundamental (natural) frequency factor based on rigid busbar boundary conditions (see Tables 10.1 and 10.2).

$$\gamma = \frac{\lambda^2}{2.\pi} (Hz) \qquad (10.3)$$

Table 10.1: Eigen Values for Busbar Support Systems [20]

Type	Eigen value	n = 1		n = 2		n = 3	
	λ	λ	γ	λ	γ	λ	γ
Both Ends Simple Support	**n . π**	**3,14**	**1,57**	**6,28**	**6,28**	**9,42**	**14,14**
One Simple & One Fixed	$\left(\frac{4.n+1}{4}\right).\pi$	**3,93**	**2,45**	**7,07**	**7,96**	**10,21**	**16,59**
Both Ends Fixed	$\left(\frac{2.n+1}{2}\right).\pi$	**4,71**	**3,56**	**7,85**	**9,82**	**11,00**	**19,24**

Fundamental 2 nd Harmonic 3 rd Harmonic

Table 10.2: Fundamental Frequency Factors for Various Boundary Conditions of Tubular Busbars Complete with Support Arrangements [20]

Type of beam and supports			Factor α	Factor β	Factor γ
Single span beam	A and B simple supports	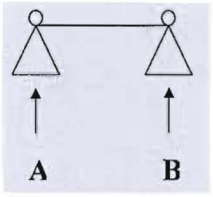	A : 0.5 B : 0,5	1,0	1,57
	A simple support B fixed support	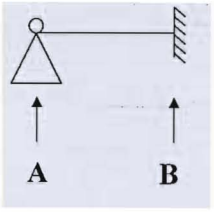	A : 0,625 B : 0,375	0,73	2,45
	A and B fixed supports	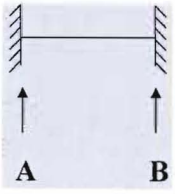	A : 0,5 B : 0,5	0,5	3,56
Continuous beams with equidistant simple supports	Two spans (simple-fixed-simple)	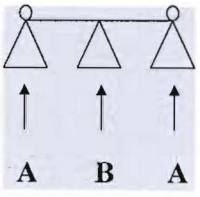	A : 0,375 B : 1,25	0,73	2,45
	Three or more spans (simple-fixed-fixed-simple)	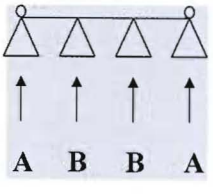	A : 0,4 B : 1,1	0,73	3,56
	Two or more spans simple supports	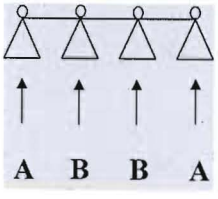	A : 0,5 B : 1,0	0,73	1,57

The three dynamic factors are determined by the ratio of fundamental mechanical frequency and the nominal electrical system frequency **f** = 50Hz.

Where:-

$$\frac{f_c}{f} = \frac{\textbf{lowest mechanical frequency of conductor}}{\textbf{nominal system frequency}} \qquad (10.4)$$

Where: $\frac{f_c}{f} >> 1$ the stress is proportional to the exciting force

and

Where: $\frac{f_c}{f} << 1$ the stress is lower, except for special harmonic resonance.

Multiphase auto re-closure at the optimally worst time with respect to mechanical vibration of the rigid tubular conductor will increase the stress significantly as compared to the case without auto-re-closure. A fitted curve was plotted by Cigré that can be used to supplement the simplified calculation procedure.

10.2 Dynamic Factors

The simplified method of calculation, which is being proposed here, makes use of **three dynamic factors** to **convert from static to dynamic conditions**. The dynamic factors are a function of the fundamental mechanical frequency of the system. Since we regard conductor support structures as rigid, only the tubular conductors determine the fundamental mechanical frequency. The three dynamic conversion factors are as follows:-

10.2.1 Dynamic factor for the support insulator system

Where:-

ν_F = ratio between dynamic and static forces on the support insulator

$$\nu_F = \frac{\textbf{dynamic force on support insulator}}{\textbf{static force on support insulator}} \qquad (10.5)$$

10.2.2 Dynamic factor for the tubular conductor system

Where:-

ν_σ = ratio between dynamic and static conductor stress

$$\nu_\sigma = \frac{\textbf{dynamic stress on conductor}}{\textbf{static stress on conductor}} \qquad (10.6)$$

The values for ν_F and ν_σ can be found by evaluating the ratio $\frac{f_c}{f}$ and using Figure 10.1 to determine these two dynamic factors.

10.2.3 Dynamic factor for unsuccessful auto re-closure on the system

Where:-

v_r = ratio between stress with and without unsuccessful auto-re-closure

$$v_r = \frac{\textbf{dynamic stress with auto - reclosure conductor}}{\textbf{dynamic stress without auto - reclosure}} \qquad (10.7)$$

From Figure 10.2 it can be seen that considerable increases in stress are to be anticipated in large high voltage systems with very low fundamental mechanical frequencies. The dynamic factor for auto-re-closure in large high voltage systems can be as high as v_r = **1,8** (80 percent increase in stress). Medium voltage substations with higher mechanical frequencies (typically $\frac{f_c}{f} > 3$) are not effected by auto-re-closure and the increased stress can be ignored.

For the simplified method, two curves are provided; one for auto-re-closure dead time ≥ 0,3 seconds and one for dead time ≥ 1,0 second.

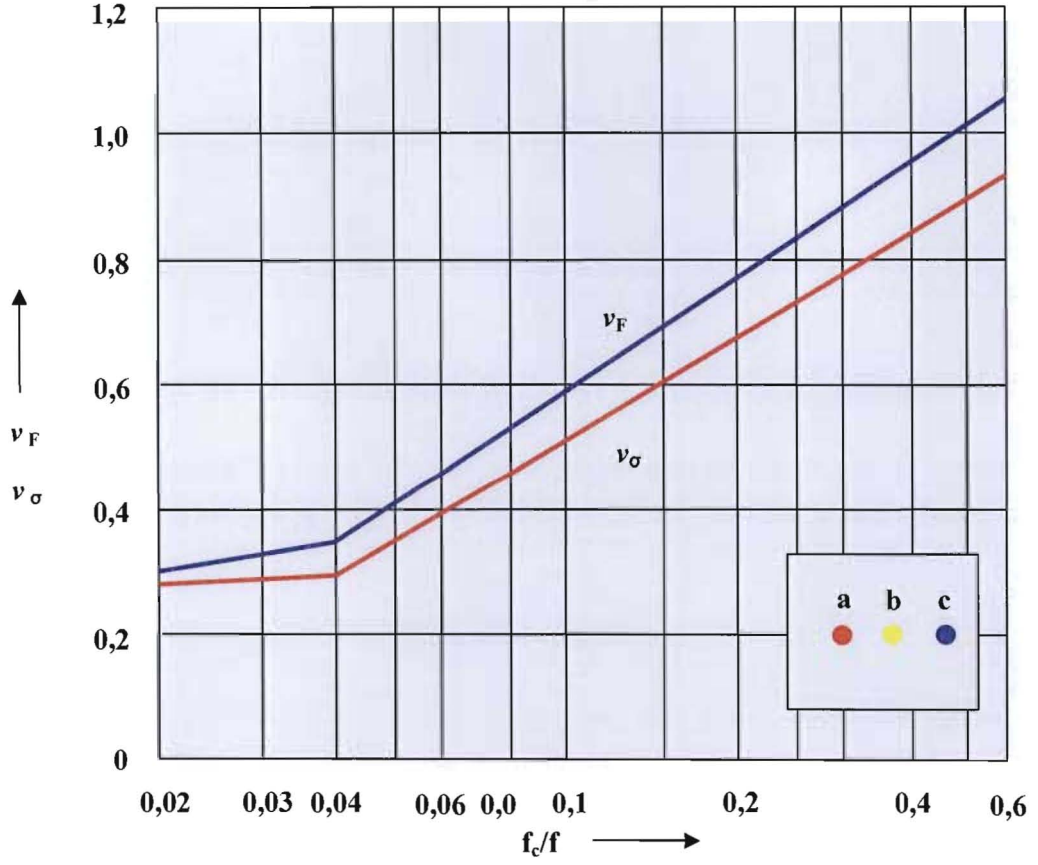

Figure 10.1: Dynamic Factors v_F (Support System) vs f_c/f and v_σ (Tubular Busbar) vs f_c/f [6] [7]

The functions given in the above graphs have been determined empirically and the value of v_F and v_σ can either be read off the graph for a calculated value of f_c/f or calculated by functions that form a close fit to the straight lines above (See Appendix B of this dissertation):

$$v_F = 0{,}1684*\text{Log}(f_c/f) + 0{,}5903 \quad \text{for } 0{,}02 \leq f_c/f \leq 0{,}04 \qquad (10.8)$$

$$v_F = 0{,}6108*\text{Log}(f_c/f) + 1{,}2087 \quad \text{for } 0{,}04 \leq f_c/f \leq 0{,}6 \qquad (10.9)$$

$$v_\sigma = 0{,}0352*\text{Log}(f_c/f) + 0{,}3471 \quad \text{for } 0{,}02 \leq f_c/f \leq 0{,}04 \qquad (11.10)$$

$$v_\sigma = 0{,}5586*\text{Log}(f_c/f) + 1{,}0788 \quad \text{for } 0{,}04 \leq f_c/f \leq 0{,}6 \qquad (10.11)$$

As with the above functions, the function for v_r given in the graph below have been determined empirically and its value can either be read off the graph for a calculated value of f_c/f or calculated by functions that form a close fit to the straight line below (See Appendix B of this dissertation):

$$v_r = 1{,}8 \quad \text{for } 0{,}02 \leq f_c/f \leq 0{,}0274;\ t_U \geq 1s \qquad (10.12)$$

$$v_r = 0{,}8009 - 0{,}6395*\text{Log}(f_c/f) \quad \text{for } 0{,}0274 \leq f_c/f \leq 0.4883;\ t_U \geq 1s \qquad (10.13)$$

$$v_r = 1{,}8 \quad \text{for } 0{,}02 \leq f_c/f \leq 0{,}05;\ t_U \geq 0{,}3s \qquad (10.14)$$

$$v_r = 1{,}0152 - 0{,}6032*\text{Log}(f_c/f) \quad \text{for } 0{,}05 \leq f_c/f \leq 0{,}6;\ t_U \geq 0{,}3s \qquad (10.15)$$

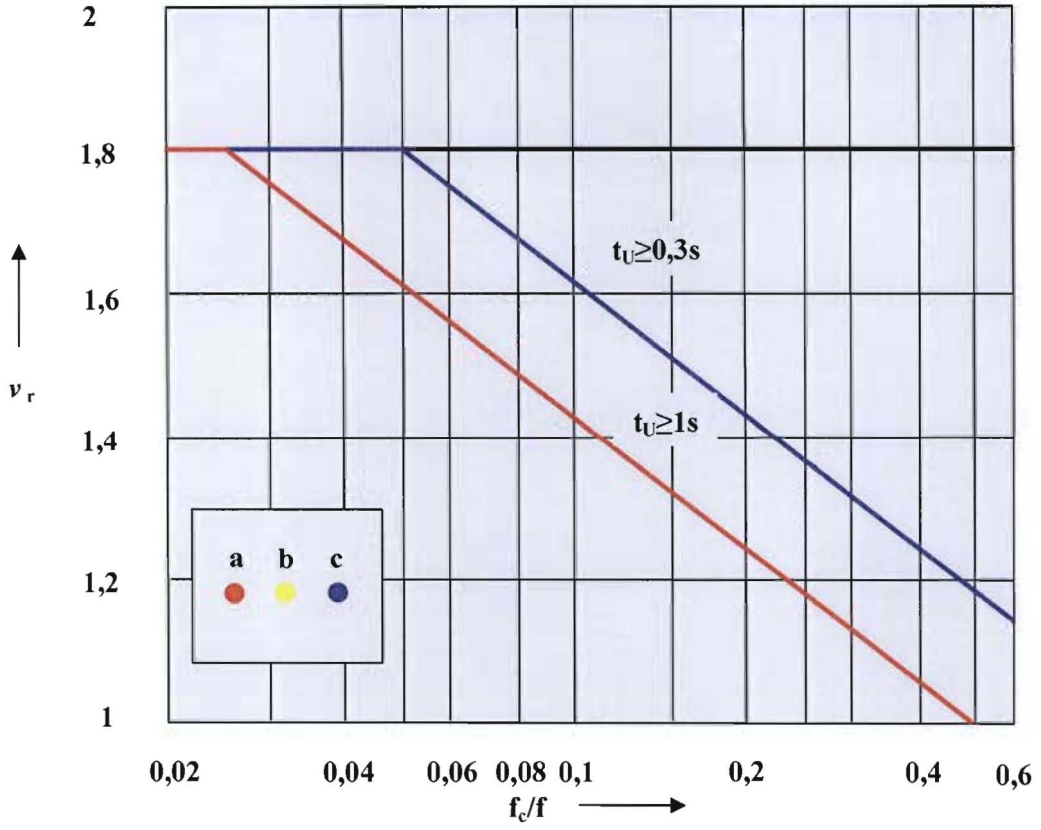

Figure 10.2: Dynamic Factor v_r (Auto-Reclosure) vs f_c/f [6] [7]

11. DIMENSIONING OF BUS TUBING BASED ON MECHANICAL RESPONSE TO LAMINAR WIND FLOW (AEOLIAN VIBRATION)

Objectives of this Chapter:

- Determine whether or not damping is required for the length of tube selected
- Types of dampers
- If damping conductor is required, determine total mass per unit length ($\mathbf{m^1_{b+c} = m^1_b + m^1_c}$)

11.1 Determine the Requirement of Damping due to Aeolian Vibrations

There are two causes of bus vibration. The first is by wind blowing across the bus tubing, the second being due to the 50Hz the bus tubing is carrying.

11.1.1 Wind Induced (Aeolian) Vibrations and Damping

Under certain conditions, wind can encourage oscillations of tubular conductors. This is known as **Aeolian** vibration. An abundance of literature is available on Aeolian vibration that substantiates the fact that some form of damping of the tubular conductors is necessary. Damping can either be in the form of tuned dampers or stranded conductors inserted in the tubes

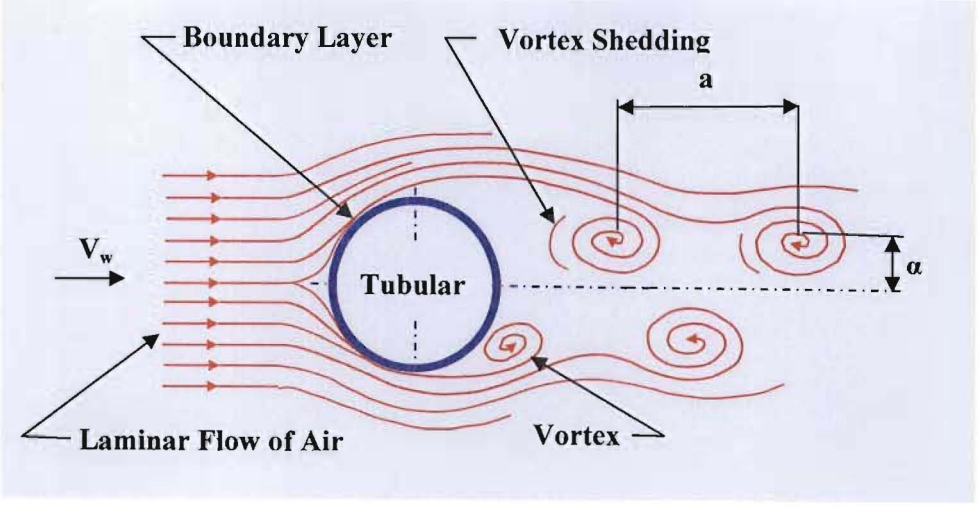

Figure 11.1: Whirl Path of Kárrén Generated at Laminar Flow around a Cylindrical Obstacle [1]

11.1.2 Maximum Frequency of the Aeolian Force

To calculate the maximum frequency of the Aeolian force, one requires meteorological information regarding wind speeds of the general area. Experience has shown that wind speeds of **24km/hr** can have laminar flow [9]. The maximum frequency is calculated as follows:

$$\mathbf{f_a} = \frac{\mathbf{51{,}75.V_w}}{\mathbf{d_{bo}}}\mathbf{(Hz)}\ [9] \qquad (11.1)$$

Where:-

$\mathbf{f_a}$ = Maximum Aeolian force frequency in Hz

$\mathbf{V_w}$ = Maximum wind speed for laminar flow in km/hr

$\mathbf{d_{bo}}$ = Outside diameter of bus tube in mm

In Chapter 10, the fundamental mechanical (or natural) frequency for a tubular conductor in Hz is given by:-

$$\mathbf{f_c} = \frac{\gamma}{\ell^2}\cdot\sqrt{\frac{\mathbf{E.J}}{\mathbf{m'_{b+c}}}}\mathbf{(Hz)} \qquad (11.2)$$

As an indication that damping may be required, $\mathbf{f_a}$ and $\mathbf{f_c}$ need to be calculated. If $\mathbf{2.f_c > f_a}$, then either the bus span length needs to be changed, or dampers are to be employed.

11.2 Types of Dampers

When determining the need for a vibration damper, whether a fixed damper which is tuned for a few frequencies, or a conductor damper on the inside of the rigid bus tubing which caters for a large spectrum of frequencies, one needs to select an appropriate bus system.

Tuned dampers are very effective over a narrow bandwidth at the design frequency. They, however, loose their effectiveness rapidly outside this bandwidth. This makes it almost necessary to tailor make a tuned damper for every different span length or clamping arrangement.

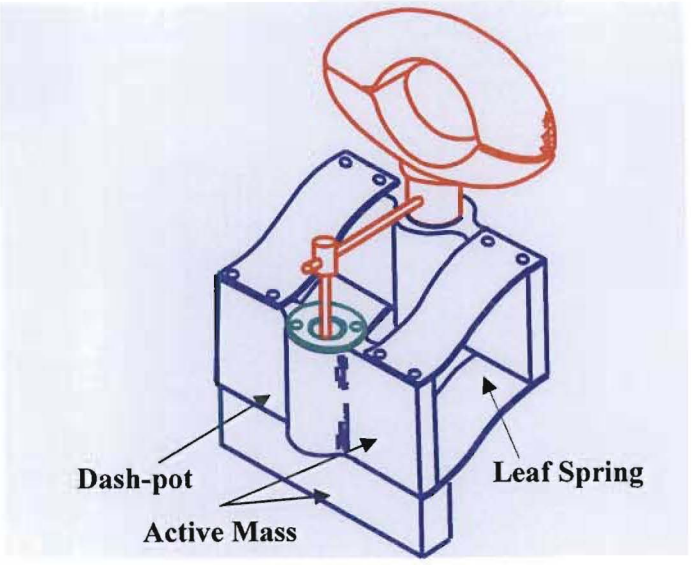

Figure 11.2: Tuned Vibration Damper [9]

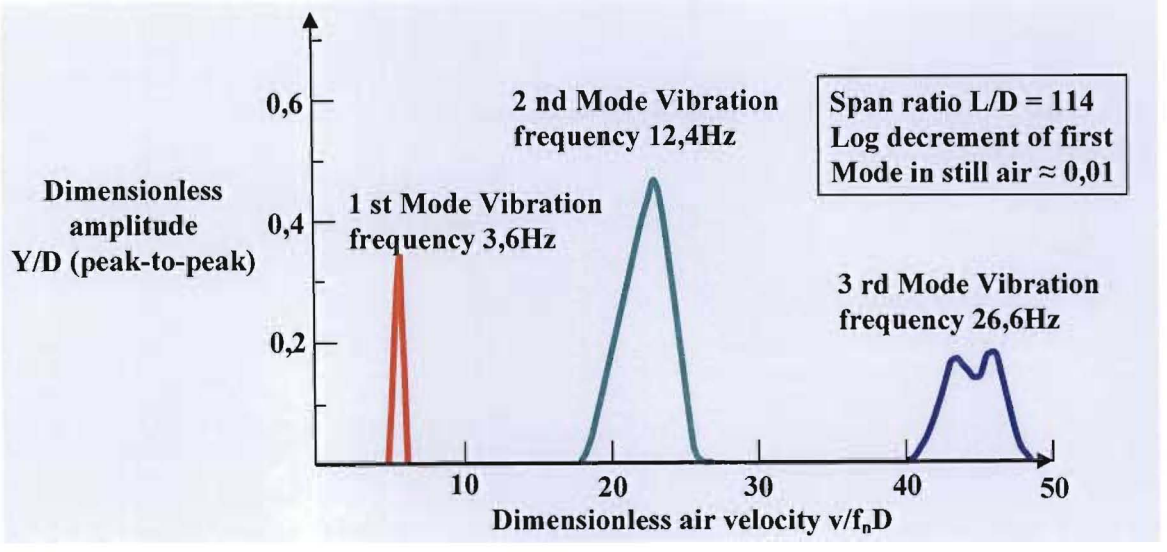

Figure 11.3: Typical Vibration Characteristics of an 8m Flexibly Mounted Span [9]

On the other hand, an inserted stranded conductor is not as effective as the tuned damper at the design frequency, but it provides a reasonable degree of damping over a much wider frequency spectrum including the second and third modes. The inserted conductor is fixed at one end to prevent partial discharge resulting from contamination that is caused by the potential differences between the conductor and the tube. The inserted stranded conductor should be of the same material as the bus tubing to prevent corrosion due to the difference in electro-potential difference. The weight of the stranded conductor should be from **10%** to **33%** of the bus conductor weight. Some applications have shown that stranded conductor weights of **25%** that of the bus conductor have worked well.

For our purposes the use of the stranded conductor is therefore preferred and the following guidelines are recommended:-

Table 11.1: Damping Conductors [1]

Tube Outer Diameter (mm)	Damping Conductor	Number of Damping Conductors	Length of Damping Conductors
80 - 120	Centipede	1	Within 100mm of tube length
160 +	Bull	1	
	Centipede	2 (see Note below)	Both ⅔ length of tube

Note: In particular disadvantageous cases, a diametrically opposite insertion of two damping conductors into the tube will become necessary. It is normal and a preferred practice to do this in any event.

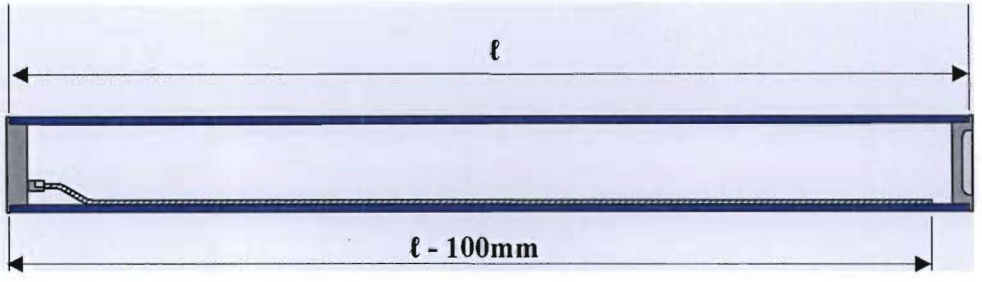

Figure 11.4: Damping Conductor Configuration for Bus Tubes with Outer Diameters 80mm to 120mm Inclusive

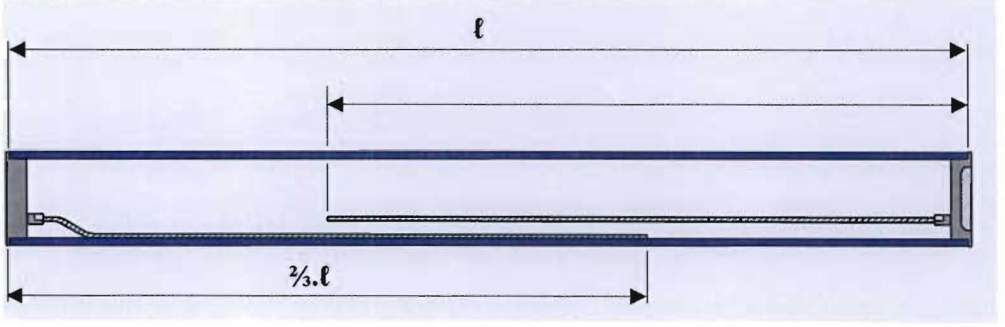

Figure 11.5: Damping Conductor Configuration for Bus Tubes with Outer Diameters in Excess of 120mm

12. MAXIMUM DYNAMIC STRESS IMPOSED ON THE CONDUCTOR DYNAMIC FACTORS v_σ AND v_r – THE TRANSITION FROM STATIC TO DYNAMIC

Dynamic electromagnetic forces resulting from short circuit current in the network add a substantial load to the system and could dominate loadings that result from own mass and wind. In certain parts of South Africa it may be necessary to add a vertical and horizontal loading component which results from seismic activity. Seismic loading is a subject on its own and is not considered in this document.

v_σ = ratio between dynamic and static conductor stress

v_r = ratio between stress with and without unsuccessful auto-re-closure

12.1 Maximum Dynamic Stress Without Auto-Re-close [3]

The maximum Dynamic stress without auto-re-close imposed on the conductor (σ_{DYN}) is calculated using the maximum static stress value and multiplying it with the ratio v_σ as follows:-

$$\sigma_{DYN} = \sigma_{ST}.v_\sigma \ (N/m^2) \qquad (12.1)$$

12.2 Maximum Dynamic Stress With Auto-Re-close [3]

The maximum Dynamic stress with auto-re-close imposed on the conductor $\sigma_{DYN+ARC}$ is calculated using the maximum dynamic stress without auto-re-close value and multiplying it with the ratio v_r as follows:-

$$\sigma_{DYN+ARC} = \sigma_{DYN}.v_r \ (N/m^2) \qquad (12.2)$$

12.3 Choice between Maximum Dynamic Stress Without or With Auto-Re-close [3]

Of the two values to employ depends on whether or not the auto-re-close function is applied to the operating regime. If it is not required, forces and stresses on components are much reduced, resulting in cost savings on equipment.

The conductor must be able to withstand the stress with a degree of safety. A number of minimum safety factors (SF_{Al}) have been suggested, from **2,5** to **2,65** [3] for aluminium conductors with respect to the 0,2 % proof stress.

$$R_{p0,2} \geq \sigma_{DYN+ARC}.SF_{Al} \ (N/m^2) \qquad (12.3)$$

Where:-

$R_{p0,2}$ = Stress resulting in permanent elongation less than 0,2% in N/m^2

SF_{Al} = Aluminium Safety Factor applied

Table 12.1 below provides the mechanical properties for a range of aluminium alloys that are widely used in tubular busbar substations.

Table 12.1: Mechanical Properties of Various Aluminium Alloys [3]

ALLOY TYPE	HULETT'S S.A.		ASA STANDARD		DIN STANDARD	
	D50S TF	**D65S TF**	**6063 T6**	**6061 T6**	**AlMgSi 0,5F22**	**AlMgSi 0,5F25**
Specific mass kg / m^3	2703	2703	2703	2703	2703	2703
Modules of elasticity E in N / m^2	$65,66.10^9$	$69,12.10^9$	69.10^9	70.10^9	70.10^9	70.10^9
0,2 % Proof stress in MPa ($R_{p0,2}$)	170	240	214	276	160	195

13. DIMENSIONING BUS TUBING TO MEET CONDUCTOR DEFLECTION UNDER DIFFERENT CRITERIA

13.1 Maximum Vertical Deflection under Static "Dead-Load" Conditions

Objectives:

- Define the support system
- Determine the deflection of the bus tube alone under its own weight
- Determine the deflection of the bus tube under its own weight and inserted damping conductor
- Various definitions of aspect ratio
- Choose Applicable Aspect Ratio y_a/d_{bo}, Acceptance criteria $y_a/d_{bo} = 0{,}5$, i.e. $y_a = ½.d_{bo}$
- Determine Maximum Vertical Deflection of a Rigid Bus Due To Own Weight (y_c)
- Test $y_c/d_{bo} \leq 0{,}5$
- Determine the deflection of the bus tube under its own weight, inserted damping conductor and ice coating

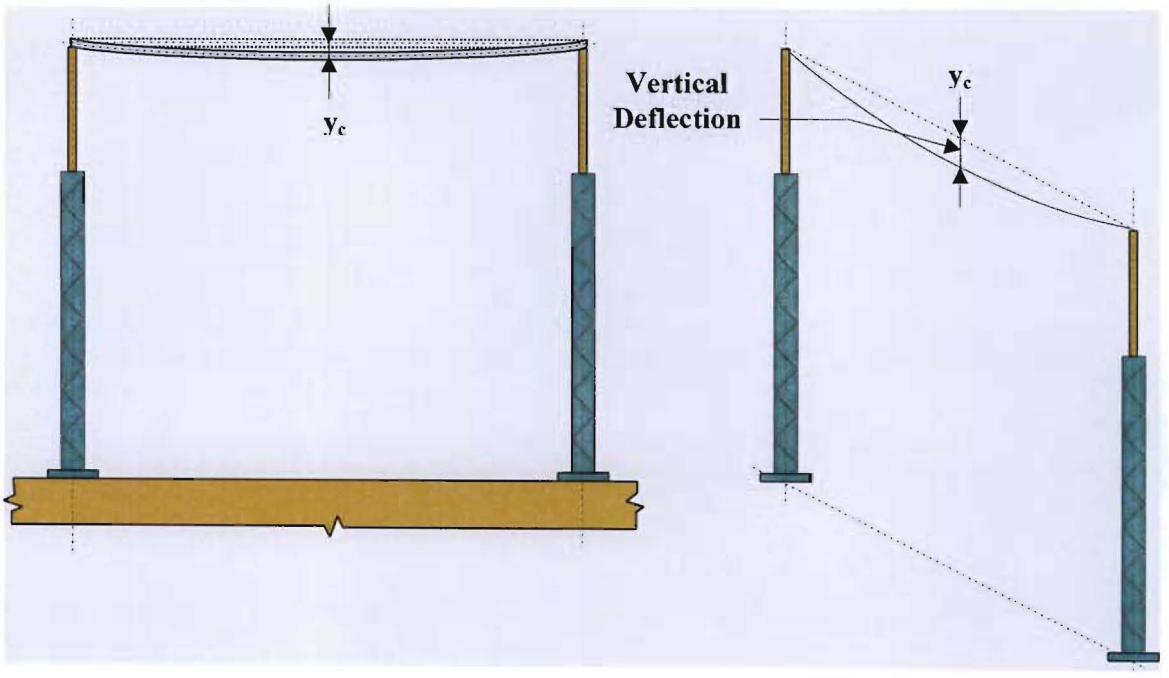

Figure 13.1: Vertical Deflection of Tube under Own Weight

13.1.1 Maximum Vertical Deflection of a Rigid Bus Due to Own Weight (Bus Tubing and Damping Conductor) [4] [19]

Refer to the three fundamental busbar models considered for calculating boundary conditions for the tubular busbars in Chapter 7.

The deflection is in the direction of the applied force, viz. vertically due to own weight, for:

13.1.1.1 Conductor with both ends supported

$$y_c = \frac{5}{384} . \frac{9{,}81.m^{1}_{b+c}.\ell^4}{E.J} \text{ (m)} \qquad (13.1)$$

13.1.1.2 Conductor with one end supported and one end fixed

$$y_c = \frac{1}{185} . \frac{9{,}81.m^{1}_{b+c}.\ell^4}{E.J} \text{ (m)} \qquad (13.2)$$

13.1.1.3 Conductor with both end fixed

$$y_c = \frac{1}{384} . \frac{9{,}81.m^{1}_{b+c}.\ell^4}{E.J} \text{ (m)} \qquad (13.3)$$

Where:-

y_c = Actual vertical deflection of chosen bus tubing in m

m^{1}_{b+c} = Mass of conductor (bus tubing and damping conductor) per unit length in kg/m

13.1.2 Allowable Vertical Deflection of a Rigid Bus [1]

The **allowable vertical deflection** of a rigid bus is usually limited by appearance and is sometimes referred to as the **aspect ratio**. The aspect ration is a subjective matter that may be defined according to the perception of the public or a utility. The following are some of the ratios used.

$$\textbf{aspect ratio} = \frac{y_a}{d_{bo}} \qquad (13.4)$$

Where:-

Aspect Ratio = 0,5 to 1,0 (dimensionless) [Eskom Transmission uses 0,5]

y_a = Allowable vertical deflection in mm

$$\textbf{aspect ratio} = \frac{\ell}{150} \quad [1] \qquad (13.5)$$

or

$$\textbf{aspect ratio} = \frac{\ell}{300} \quad [1] \qquad (13.6)$$

The aspect ratio is often not considered for icing conditions, and therefore ice weight is usually, not considered for vertical deflection.

13.1.3 Test Aspect Ratio

$$\textbf{aspect ratio} = \frac{y_a}{d_{bo}} = 0{,}5 \leq y_c \qquad (13.7)$$

If the condition is not met, either a tube of smaller wall thickness to reduce the mass per unit is chosen and retested, or a tube with a larger outer diameter can be chosen and retested.

Figure 13.2: Unacceptable Vertical Deflection of a Tube Due to Own Weight

Figure 13.3: Acceptable Vertical Deflection of a Tube Due to Own Weight

13.2 Maximum Deflection of the Tubular Conductor due to the Resultant Dynamic Force (Without Auto-Reclose)

Objectives of this Chapter:

- Definition of deflection due to resultant force ($\mathbf{F_{R(\sigma)DYN}}$)
- Determine Maximum Deflection ($\mathbf{y_{DYN}}$) of a Rigid Bus Due To the resultant force ($\mathbf{F_{R(\sigma)DYN}}$) resulting from the fault current and chosen boundary conditions
- Determine Maximum Horizontal and vertical Deflection of two Rigid Bus conductors under Dynamic Conditions (wind, fault & without ARC) ([$\mathbf{y_{DYNh1}}$,$\mathbf{y_{DYNv1}}$] and [$\mathbf{y_{DYNh2}}$,$\mathbf{y_{DYNv2}}$])
- The associated phase-to-phase clearance and ensure required phase-to-phase clearance is not infringed

The **maximum deflection** of the tubular conductor under **dynamic** conditions ($\mathbf{y_{DYN}}$) is in the direction of the applied resultant force, i.e. the force due to the weight of the conductor, the weight of the ice, the wind force and the short circuit force (no ARC). This resultant force can be determined by working backward from the calculated maximum dynamic stress without auto-re-close ($\boldsymbol{\sigma_{DYN}}$) as calculated from the maximum static stress value and multiplying it with the ratio v_σ shown in (12.1).

$$\boldsymbol{\sigma_{DYN}} = \frac{\mathbf{F^1_{R(\sigma)DYN}}.\ell^2}{\mathbf{k.W}} \ \mathbf{(N/m^2)} \qquad \text{(from 9.7)}$$

$$\mathbf{F^1_{R(\sigma)\,YN}} = \frac{\boldsymbol{\sigma_{DYN}}.\mathbf{k.W}}{\ell^2} \ \mathbf{(N/m)} \qquad (13.8)$$

Deflection of conductor must be such that phase-to-phase clearance is not infringed.

The maximum deflection of the tubular conductor under dynamic conditions due to wind, short current forces and its own weight is in the direction of the applied force, i.e. the resultant force ($\mathbf{F^1_{R(\sigma)}}$) and is given by:-

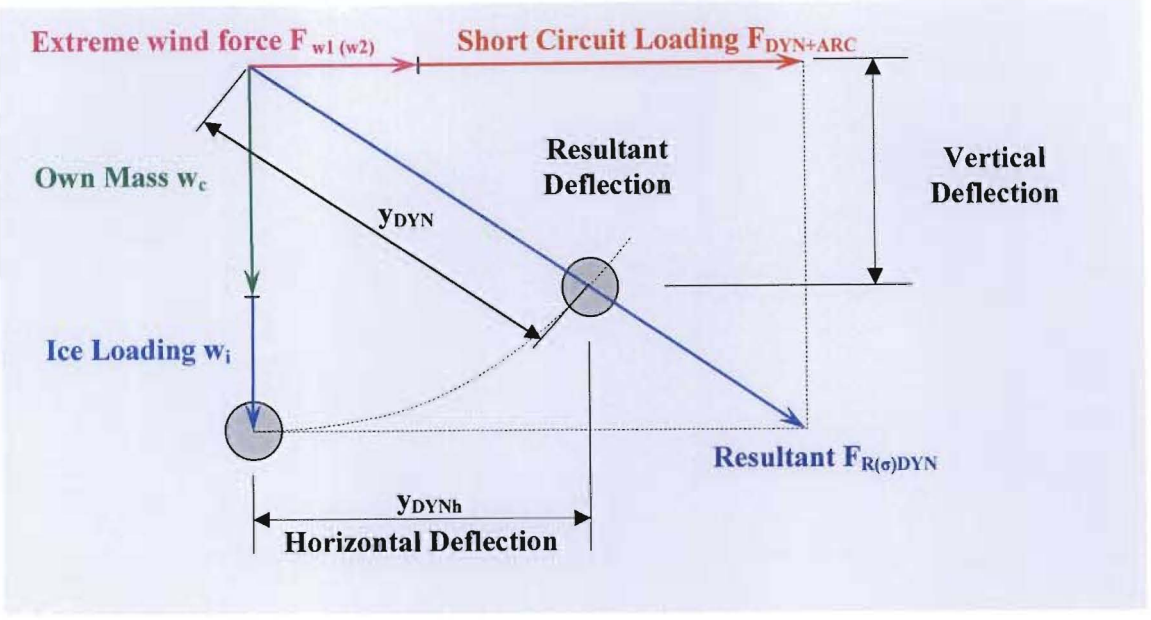

Figure 13.4: Horizontal Deflection of a Tube Due to Short-Circuit Forces

13.2.1 Conductor with both ends supported

$$y_{DYN} = \frac{5}{384} \cdot \frac{F^{1}_{R(\sigma)DYN} \cdot \ell^{4}}{E.J} \text{ (m)} \qquad (13.9)$$

13.2.2 Conductor with one end supported and one end fixed

$$y_{DYN} = \frac{1}{185} \cdot \frac{F^{1}_{R(\sigma)DYN} \cdot \ell^{4}}{E.J} \text{ (m)} \qquad (13.10)$$

13.2.3 Conductor with both ends fixed

$$y_{DYN} = \frac{1}{384} \cdot \frac{F^{1}_{R(\sigma)DYN} \cdot \ell^{4}}{E.J} \text{ (m)} \qquad (13.11)$$

13.2.4 Calculating the Phase-to-Phase Distance between the Conductors

In each of the above cases, it is important to determine how close the two attracting phases approach in order to determine whether or not phase-to-phase clearance is breached. This requires the straight line distance between the surfaces of the bus tubes ($\mathbf{C_{1,2}}$).

It must be remembered that for phase conductor 2, the short circuit force now acts in the opposite direction to that of phase conductor 1, against the wind force.

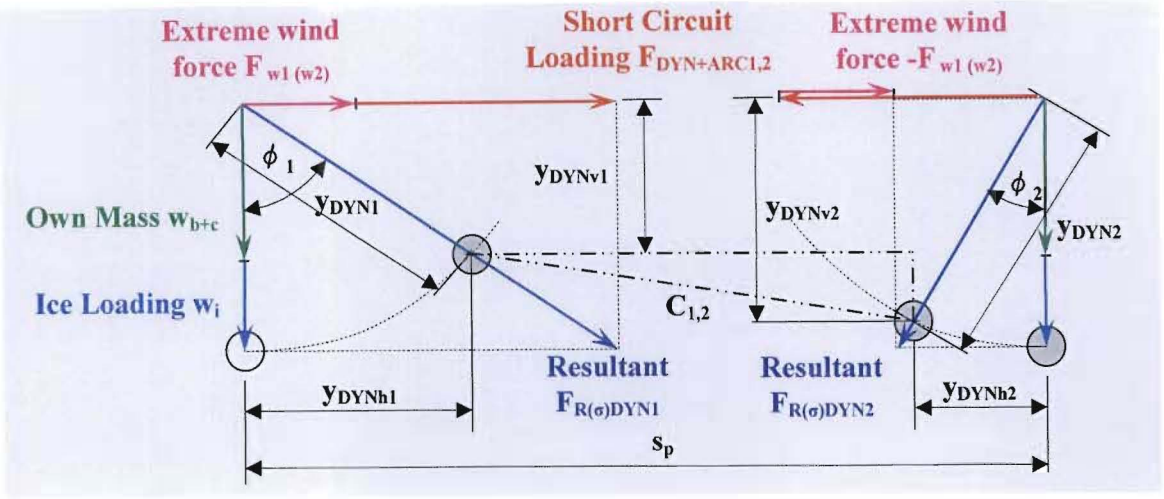

Figure 13.5: Closeness of Approach of Two Tubular Conductors Moving Towards Each Other to Short-Circuit Forces

The following parameters are known for conductor 1 as shown in Figure 13.5:

Weight of bus tubing ($\mathbf{w^1_{b+c}}$)

Weight of ice ($\mathbf{w^1_i}$)

Wind force ($\mathbf{F^1_w}$)

Resultant force ($\mathbf{F_{R(\sigma)DYN1}}$)

Phase conductor 1 deflection ($\mathbf{y_{DYN1}}$)

At this point the short circuit loading ($\mathbf{F_{DYN+ARC1,2}}$) is not known, but can be easily calculated by working backward from the resultant force equation in the form of (9.6).

For conductor 1 where the wind direction is in the same direction as the short circuit force:

$$\mathbf{F^1_{R(\sigma)DYN1}} = \sqrt{(\mathbf{F^1_{DYN}} + \mathbf{F^1_w})^2 + (\mathbf{w^1_{b+c}} + \mathbf{w^1_i})^2} \quad \mathbf{(N/m)} \qquad (13.12)$$

For conductor 2 where the wind direction is in the opposite direction as the short circuit force:

$$\mathbf{F^1_{R(\sigma)DYN2}} = \sqrt{(\mathbf{F^1_{DYN}} - \mathbf{F^1_w})^2 + (\mathbf{w^1_{b+c}} + \mathbf{w^1_i})^2} \quad \mathbf{(N/m)} \qquad (13.13)$$

The important issue here, however, is to find the relative position of phase conductor 1 due to the resultant force.

$$\cos\phi_1 = \frac{(w^1_{b+c1} + w^1_{i1})}{F^1_{R(\sigma)DYN1}}$$
$$\phi_1 = \cos^{-1}\left[\frac{(w^1_{b+c1} + w^1_{i1})}{F^1_{R(\sigma)DYN1}}\right] \quad (13.14)$$

$$y_{DYNh1} = y_{DYN1}.\sin\ \phi_1 \quad (13.15)$$

$$y_{DYNv1} = y_{DYN1}.\cos\ \phi_1 \quad (13.16)$$

The co-ordinates of phase conductor 1 is therefore ($y_{DYN1}.\sin\ \phi_1$, $y_{DYN1}.\cos\ \phi_1$)

The relative position of phase conductor 2 makes use of the magnitude of $F_{R(\sigma)DYN1}$ which must equal $F_{R(\sigma)DYN2}$. In like manner to phase conductor 1 therefore:

$$\cos\phi_2 = \frac{(w^1_{b2+c2} + w^1_{i2})}{F^1_{R(\sigma)2}}$$
$$\phi_2 = \cos^{-1}\left[\frac{(w^1_{b2+c2} + w^1_{i2})}{F^1_{R(\sigma)2}}\right] \quad (13.17)$$

$$y_{DYNh2} = y_{DYN2}.\sin\ \phi_2 \quad (13.18)$$

$$y_{DYNv2} = y_{DYN2}.\cos\ \phi_2 \quad (13.19)$$

The co-ordinates of phase conductor 2 is therefore ($y_{DYN2}.\sin\ \phi_2$, $y_{DYN2}.\cos\ \phi_2$)

From these two sets of co-ordinates then, the straight-line distance between the surfaces ($C_{1,2}$) of the two conductors can be calculated by subtracting the diameter of one tube from the calculated value.

$$C_{1,2} = \sqrt{(s_p - y_{DYN2}.\sin\phi_2 - y_{DYN1}.\sin\phi_1)^2 + (y_{DYN2}.\cos\phi_2 - y_{DYN1}.\cos\phi_1)^2} - d_{bo} \quad (13.20)$$

It must then be ensured that for the given voltage:-

$$C_{1,2} \geq C_{pp}. \quad (13.21)$$

14.3 Maximum Deflection of the Tubular Conductor due to Resultant Dynamic Force (With Unsuccessful Auto-Re-close)

Objectives of this Section:

- Definition of deflection due to resultant force ($F_{R(\sigma)DYN+ARC}$)

- Determine Maximum Deflection ($y_{DYN+ARC}$) of a Rigid Bus Due To the resultant force ($F_{R(\sigma)DYN+ARC}$) resulting from the fault current and chosen boundary conditions
- Determine Maximum Horizontal and vertical Deflection of two Rigid Bus conductors under Dynamic Conditions (wind, fault & without ARC) ([$y_{DYN+ARCh1}$,$y_{DYN+ARCv1}$] and [$y_{DYN+ARCh2}$,$y_{DYN+ARCv2}$])
- The associated phase-to-phase clearance and ensure required phase-to-phase clearance is not infringed

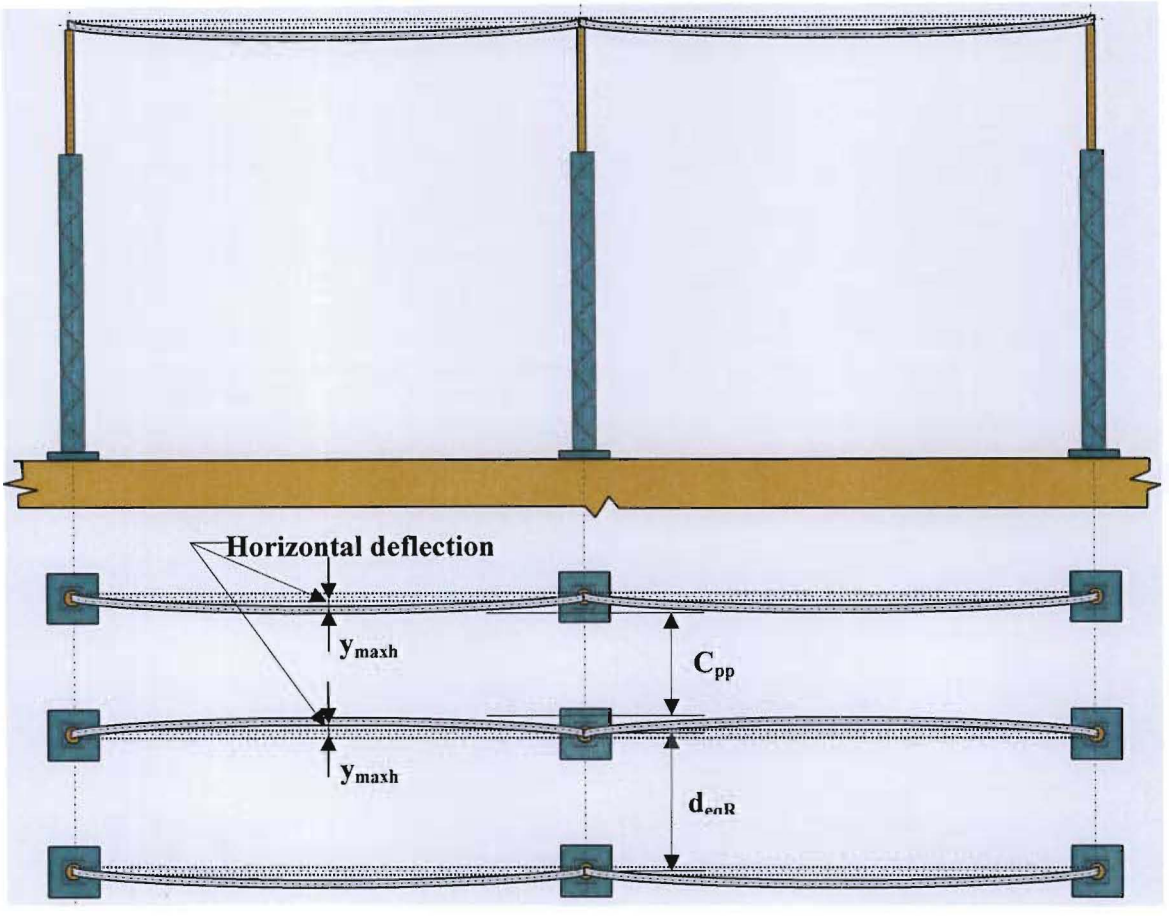

Figure 13.6: Maximum Deflection of the Tubular Conductor due to Resultant Dynamic Force (With Unsuccessful Auto-Re-close)

As in 13.4, the **maximum deflection** ($y_{DYN+ARC}$) of the tubular conductor is in the direction of the applied force, i.e. the resultant force due to the weight of the conductor, the weight of the ice, the wind force and the short circuit force (with ARC). This resultant force can be determined by working backward from the calculated maximum dynamic stress with auto-re-close ($\sigma_{DYN+ARC}$) as calculated from the maximum dynamic stress value and multiplying it with the ratio ν_r shown in (12.2)

$$F^{1}_{R(\sigma)DYN+ARC} = \frac{\sigma_{DYN+ARC}.k.W}{\ell^2} \quad (N/m) \qquad (13.22)$$

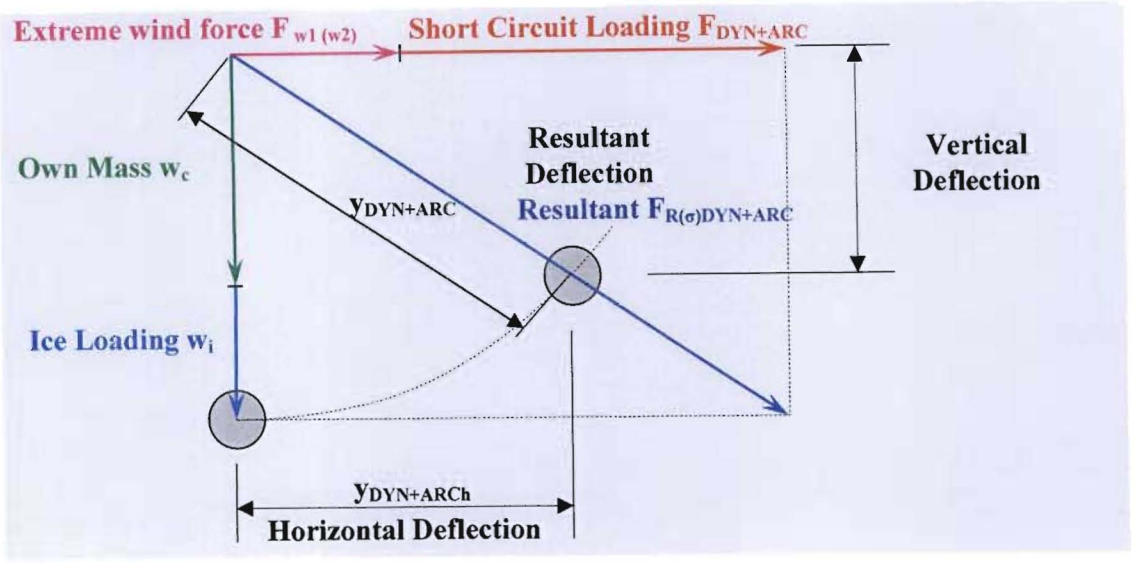

Figure 13.7: Deflection of a Tubular Conductor under Fault Conditions

13.3.1 Conductor with both ends supported [3]

$$y_{DYN+ARC} = \frac{5}{384}.\frac{F^{1}_{R(\sigma)DYN+ARC}.\ell^4}{E.J} \quad (m) \qquad (13.23)$$

13.3.2 Conductor with one end supported and one end fixed [3]

$$y_{DYN+ARC} = \frac{1}{185}.\frac{F^{1}_{R(\sigma)DYN+ARC}.\ell^4}{E.J} \quad (m) \qquad (13.24)$$

13.3.3 Conductor with both ends fixed [3]

$$y_{DYN+ARC} = \frac{1}{384}.\frac{F^{1}_{R(\sigma)DYN+ARC}.\ell^4}{E.J} \quad (m) \qquad (13.25)$$

13.3.4 Calculating the Phase-to-Phase Distance between the Conductors

The straight line distance between the surfaces of the bus tubes ($C_{1,2}$) is calculated in the same manner as in paragraph 13.2.4, but using $F_{R(\sigma)DYN+ARC}$.

13.4 Maximum Deflection Of A Rigid Bus Under Dynamic Conditions_Due To Wind, Short Current Forces, Own Weight And Bending Of Steelwork Support Structure

13.4.1 Deflection of the tubular conductor and steelwork support structure.

The combined deflection of the tube (y_{max}), the support structure (y_{ss}) and the movement of the tube due to the tilting action of the post insulator (y_{PI}), plus the outer diameter of the tube (d_{bo}) must be such that the minimum phase-to-phase clearance is not exceeded.

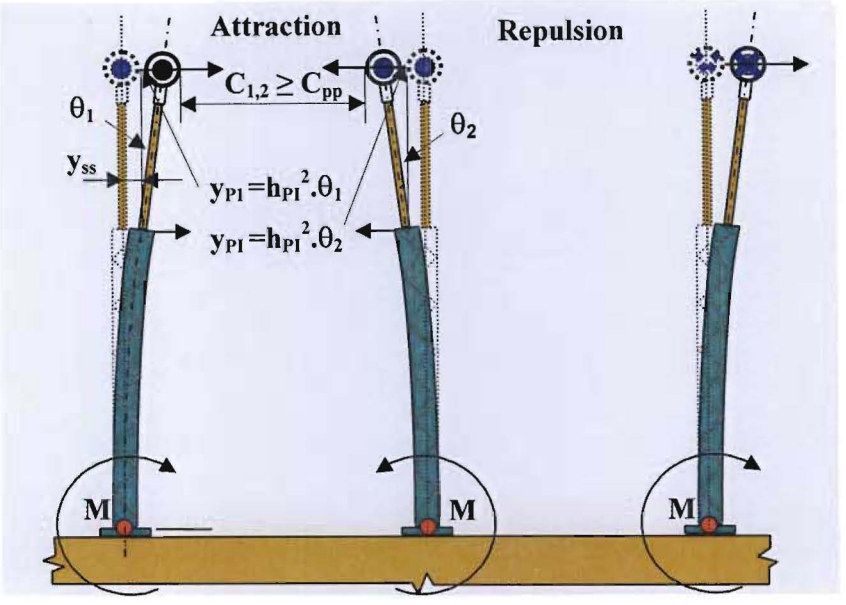

Figure 13.8: Deflection of the Insulator Steelwork Support

$$C_{pp} \geq C_{1,2} = 2.(y_{max} + y_{ss} + y_{PI}) - d_{bo} \qquad (13.26)$$

The amount by which the structure deflects is a property of the structure geometry and material e.g. lattice or tubular steel, lattice or tubular aluminium, concrete, etc. and can be determined using civil engineering software packages such as **Prokon**. The use of this software is deemed to be out of the scope of this dissertation and a more practical approach is to consider the support structure in terms of its elastic properties and ability to absorb some of the energy as demonstrated in Figure 13.8 above and so effectively reduce the fault current forces translated to the tubular conductor and post insulators. This is dealt with in the next chapter.

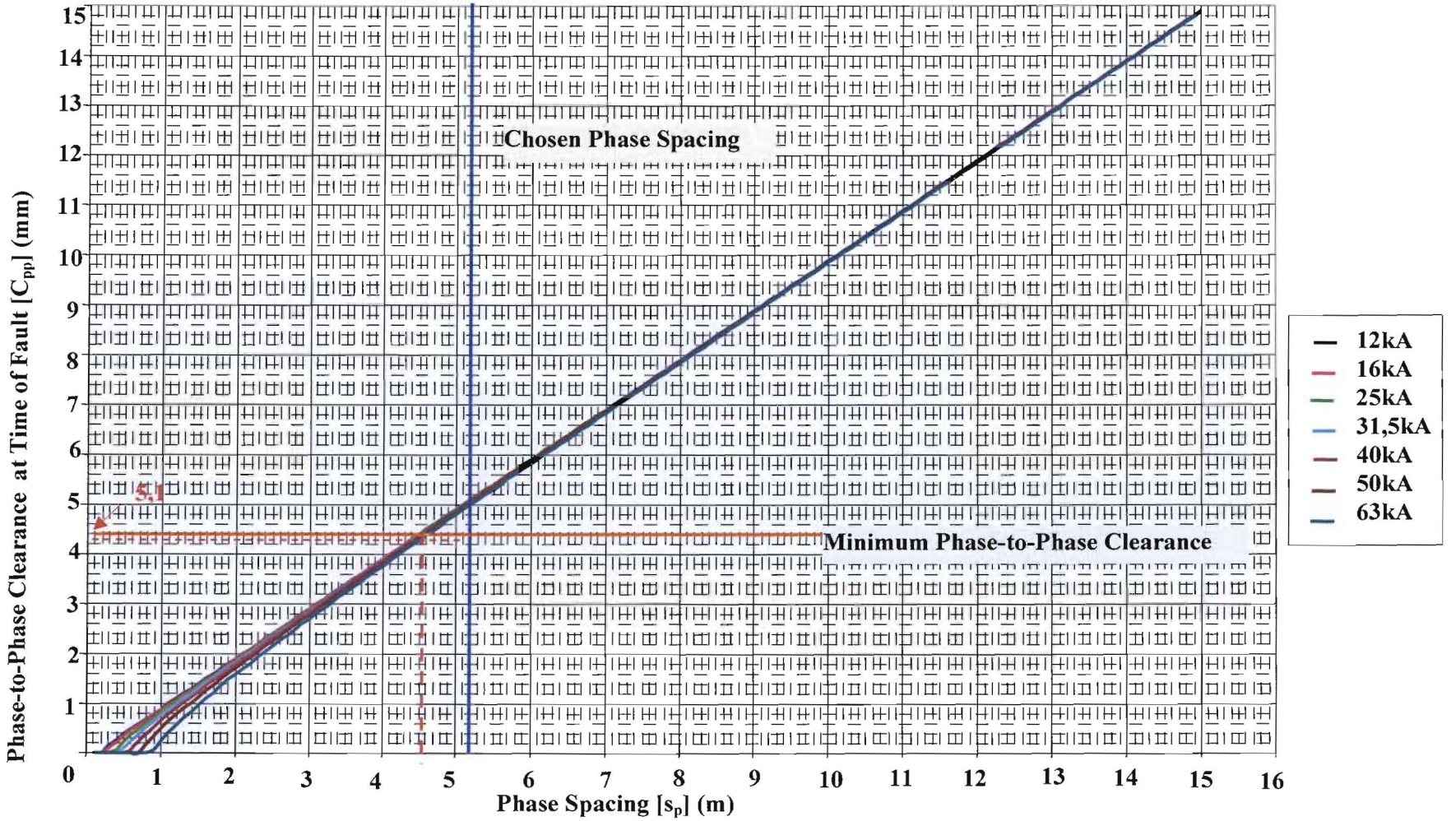

Figure 13.9: Phase-to-Phase Clearance [C_{pp}] (m) at the time of the Fault on a 20m Bus Tube Ø250mm x 6mmWT vs Phase Spacing [s_p] (m) 6063T6 aluminium alloy

13.4.2 Graphical Representation of Phase-to-Phase Distance between the Conductors

Figure 13.9 is an Excel based graphical representation of the phase-to-phase clearances expected for a Ø250mm x 6mmWT bus tube, 20m long extruded from 6063T6 aluminium alloy. This forms one of several graphical outputs from the Excel based busbar program developed by the author for carrying out the studies that forms part of this dissertation.

It is clear from this printout that for phase separations in excess of 4,5m, the differences in the phase-to-phase clearance becomes vitually negligible, perhaps 100mm or so. This shows the weakened impact of the short circuit forces as the phase separation increases and also the rigidity of this alloy.

14. MAXIMUM FORCES IMPOSED ON THE POST INSULATORS

14.1 The Maximum Static Force Imposed Onto the Insulators

Objectives of this Chapter:

- Determine the maximum static force imposed on the post insulators A ($\mathbf{F_{A(PI)ST}}$) and B ($\mathbf{F_{B(PI)ST}}$) for a chosen boundary conditions
- Choose α factor for rigid conductor boundary conditions depending the number of spans
- Determine the post insulator strength with a 1,2 Safety Factor

The force acting on the conductor as a result of short circuit current, impose a reaction force at the top of the support insulator. The insulator must be able to withstand this force with a degree of safety (a minimum safety factor of 1,2 is recommended for porcelain insulators).

The static force imposed onto the insulators for a single span is calculated as follows:-

$\mathbf{F^{I}_{L2p}}$ from (9.3)

14.1.1 Systems with both ends supported (A and B) [3]

$$\mathbf{F_{A,\,B(PI)ST} = 0{,}5.F^{I}_{L2p} \,.\, \ell\ (N)} \qquad (14.1)$$

14.1.2 Systems with one end supported and one end fixed

14.1.2.1 Supported end (A)

$$\mathbf{F_{A(PI)ST}} = \frac{3}{8}\mathbf{.F^{I}_{L2p} \,.\, \ell} = \mathbf{0{,}375.F^{I}_{L2p} \,.\, \ell\ (N)} \qquad (14.2)$$

14.1.2.2 Fixed end (B)

$$\mathbf{F_{B(PI)ST}} = \frac{5}{8}\mathbf{.F^{I}_{L2p} \,.\, \ell} = \mathbf{0{,}625.F^{I}_{L2p} \,.\, \ell\ (N)} \qquad (14.3)$$

14.1.3 Systems with both ends fixed (A and B)

$$\mathbf{F_{A,\,B(PI)ST} = 0{,}5.F^{I}_{L2p} \,.\, \ell\ (N)} \qquad (15.4)$$

Busbars, by definition, do not consist of single spans, but multiple spans that could be made up of various combinations of boundary conditions. A simplification of the various combinations

of conductor boundary conditions are provided in the form of factor α [2] as given in Table 10.2 as follows:-

$$F_{(PI)ST} = \alpha \cdot F^{1}_{L2p} \cdot \ell \text{ (N)} \quad (14.5)$$

Where:-

α = factor for rigid conductor boundary conditions (see Table 10.2)

For Supports A and B

$$F_{A(PI)ST} = \alpha_{A} \cdot F^{1}_{L2p} \cdot \ell \text{ (N)} \quad (14.6)$$

$$F_{B(PI)ST} = \alpha_{B} \cdot F^{1}_{L2p} \cdot \ell \text{ (N)} \quad (14.7)$$

14.2 Maximum Dynamic Forces Imposed On the Insulators

Objectives of this Section:

- Choose γ fundamental (natural) frequency factor based on rigid busbar boundary
- Determine the Dynamic Force Acting on the Insulator [$F_{(PI)DYN}$]
- Determine the Dynamic Force Acting with ARC on the Insulator [$F_{(PI)DYN+ARC}$]

Forces acting on the tubular busbar support post insulators [6] [7].

The forces acting in the post insulators are multiplied by 1,2 [3]. The resultant must not exceed the minimum insulator failing load (cantilever strength).

The dynamic force acting on insulators is therefore:-

14.2.1 Dynamic forces without ARC

$$F_{(PI)DYN} = \alpha \cdot F^{1}_{L2p} \cdot \ell \cdot \nu_F = F_{(PI)ST} \cdot \nu_F \text{ (N)} \quad (14.8)$$

14.2.1.1 Post Insulators A and B

$$F_{A(PI)DYN} = F_{A(PI)ST} \cdot \nu_F \text{ (N)} \quad (14.9)$$

$$F_{B(PI)DYN} = F_{B(PI)ST} \cdot \nu_F \text{ (N)} \quad (14.10)$$

14.2.2 Dynamic forces with ARC

$$F_{(PI)DYN+ ARC} = F_{(PI)DYN} \cdot \nu_r \text{ (N)} \quad (14.11)$$

14.2.2.1 Post Insulators A and B

$$F_{A(PI)DYN + ARC} = F_{A(PI)DYN}.\nu_r \ (N) \tag{14.12}$$

$$F_{B(PI)DYN + ARC} = F_{B(PI)DYN}.\nu_r \ (N) \tag{14.13}$$

14.3 Resultant Forces Imposed On the Post Insulators

Objective of this section:

- Determine the Resultant Force Acting on the Insulator [$F_{R(PI)}$]

14.3.1 Resultant Forces acting on the tubular busbar support post insulators [9]

$$F_{R(PI)} = \sqrt{(W_{b + c} + W_i)^2 + (F_{w1} + F_{DYN + ARC})^2} \tag{14.14}$$

14.3.1.1 Post Insulators A and B

$$F_{RA(PI)} = \sqrt{(W_{b + c} + W_i)^2 + (F_{w1} + F_{A(PI)DYN + ARC})^2} \tag{14.15}$$

$$F_{RB(PI)} = \sqrt{(W_{b + c} + W_i)^2 + (F_{w1} + F_{B(PI)DYN + ARC})^2} \tag{14.16}$$

14.3.2 Maximum Resultant Forces acting on the tubular busbar support post insulators

The performance of porcelain insulators subjected to dynamic forces is somewhat different to that under static conditions. This is due to the fact that an insulator inherently has microscopic deformities as a result of imperfect manufacturing processes. These deformities may cause partial rupturing within these zones when sudden changes in stress acts on structures at an atomic level. In order to prevent this from taking place and ensure enough residual strength, the insulators are oversized by a predetermined safety factor.

Initial tests conducted by Eskom have indicated that a safety factor of 1,2 [3] should be used.

14.3.2.1 Post Insulators A and B

$$\begin{aligned} F_{RA(PI)MAX} &= F_{RA(PI)}.SF \\ &= F_{RA(PI)}.1{,}2 \end{aligned} \tag{14.17}$$

$$\begin{aligned} F_{RB(PI)MAX} &= F_{RB(PI)}.SF \\ &= F_{RA(PI)}.1{,}2 \end{aligned} \tag{14.18}$$

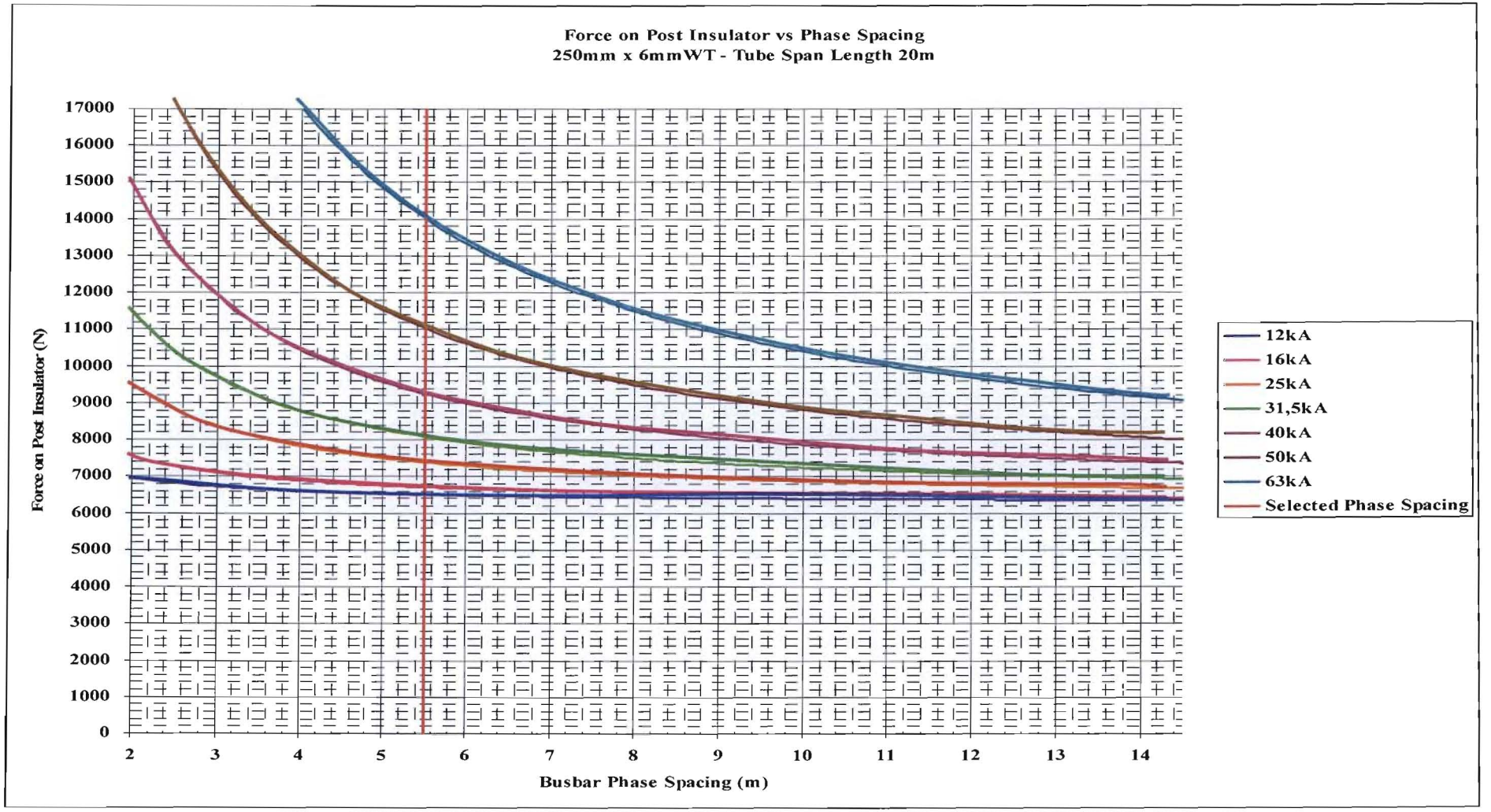

Figure 14.1: Force on Post Insulator (N) vs Busbar Phase Spacing (m) for a given Fault Current (kA) [Excel Printout from Busbar Programme]

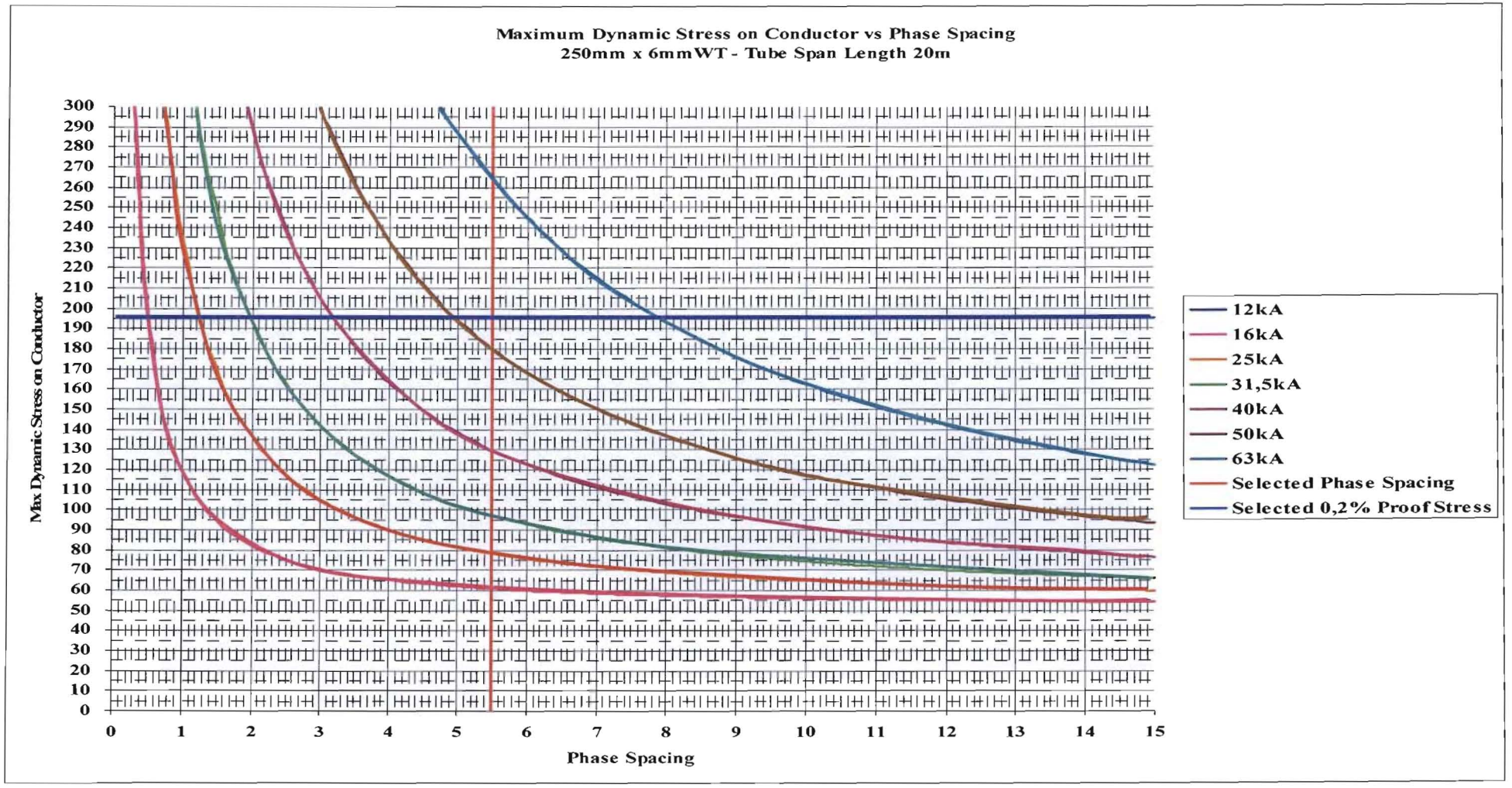

Figure 14.2: Maximum Dynamic Stress inBus Tube (MPa) vs Busbar Phase Spacing (m) for a given Fault Current (kA) [Excel Printout from Busbar Programme]

15. BENDING MOMENTS IMPOSED ON THE TUBULAR BUSBAR SYSTEM

Objectives of this Chapter:

- Calculate the bending moments exerted on the base of the support post insulator
- Calculate the bending moments exerted on the base of the post insulator support steelwork
- Demonstrate the effect that different types of support systems have on the support post insulator

15.1 Bending Moment Imposed At the Base of the Porcelain Insulators

A further requirement in the choice of the Insulator whether it be porcelain or composite is to ensure that the maximum allowable bending moment at the base is no exceeded. This is done simply by considering the maximum dynamic force at the base of each of the insulators, and the height of the centre line of the tube above the base of the insulator.

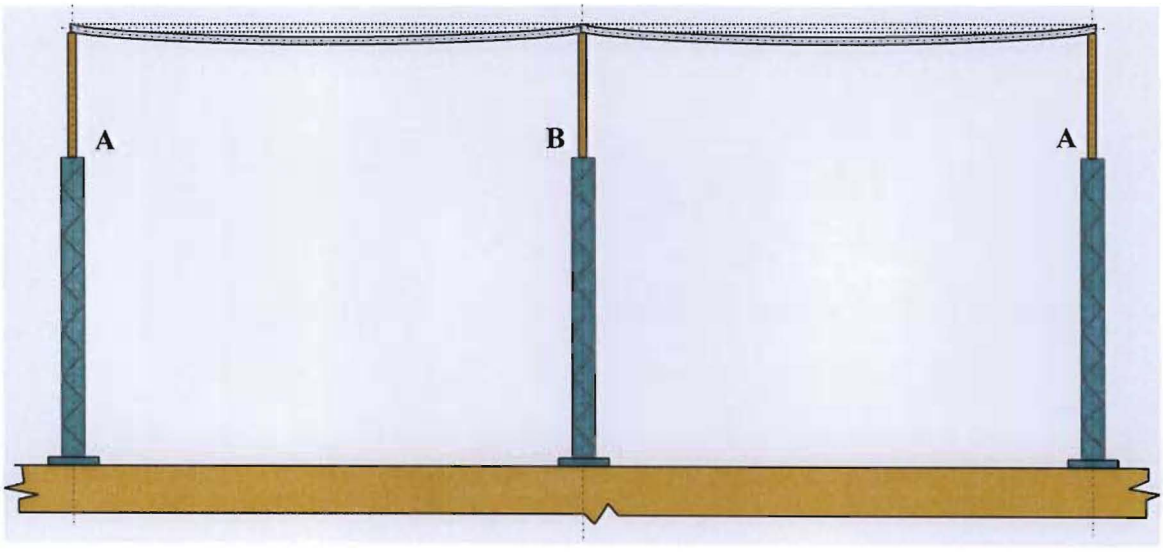

Figure 15.1: Two to Three or more spans (See Table 10.2 of this dissertation)

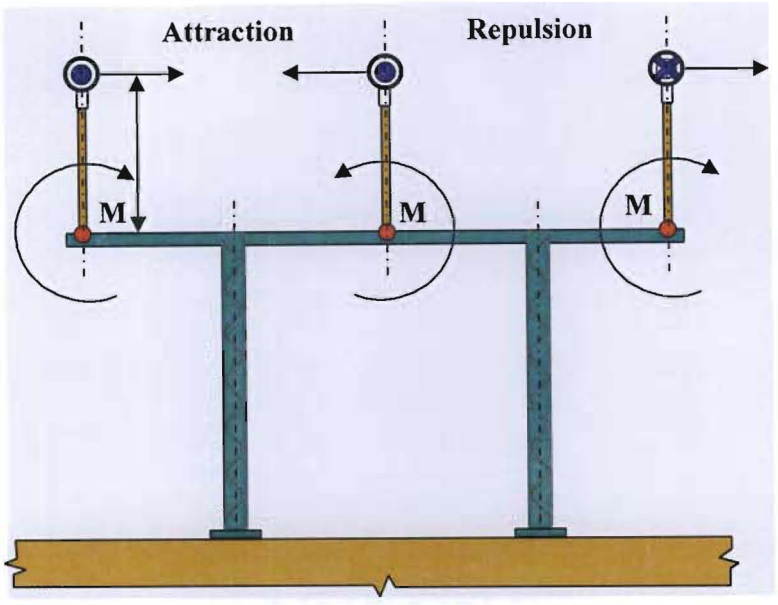

Figure 15.2: Bending moment at the base of the porcelain insulator for a single combined support structure

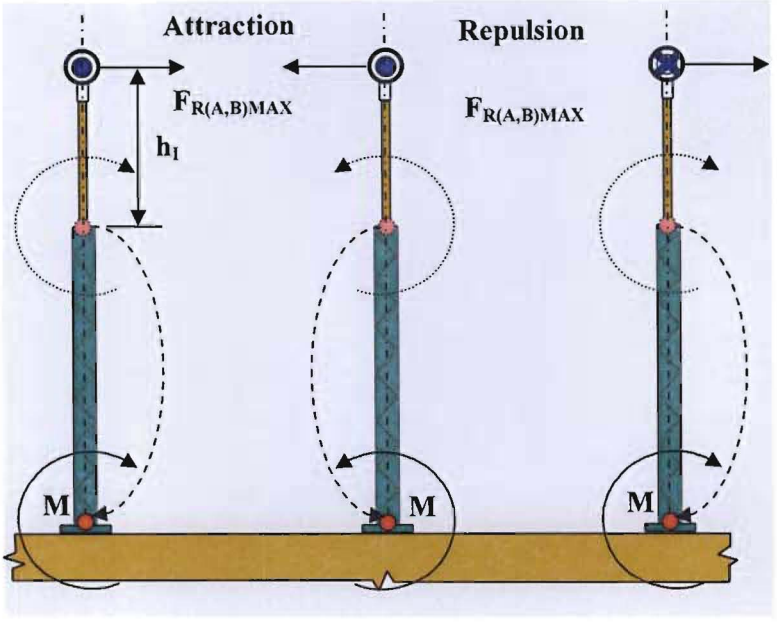

Figure 15.3: Bending moment at the base of the porcelain insulator for three single supports

$$M = F_{RMAX} \cdot h_I \text{ (N.m)} \quad (15.1)$$

Where:-

h_I = height of the centre line of the tube above the base of the insulator in m

15.1.1 Porcelain A and B:

$$M_{(A)} = F_{R(A)MAX} \cdot h_{IA} \text{ (N.m)} \quad (15.2)$$

$$M_{(B)} = F_{R(B)MAX} \cdot h_{IB} \text{ (N.m)} \quad (15.3)$$

15.2 Bending Moment Imposed At the Base of the Steelwork Structure

At EHV and UHV voltage levels, the insulators are supported on dedicated structures as shown above. The moment generated is in fact transferred to the base of the structure. It is therefore necessary to ensure that the moment at the base of the steelwork support structure does not exceed the maximum allowable bending moment. As in the case of the insulators, this is done simply by considering the maximum dynamic force on the insulators, and the height of the centre line of the tube above the base of the insulator.

15.2.1 Bending moment at the base of the insulator steelwork support structure

$$M = 1,7 \cdot F_{RMAX(DYN+ARC)} \cdot (h_i + h_s) \text{ (N.m)} \quad (15.4)$$

Where:-

h_s = height of the support above the foundation in m

15.2.1.1 Support structures A and B:

$$M_{(A)} = 1,7 \cdot F_{R(A)MAX(DYN+ARC)} \cdot (h_{iA} + h_s) \text{ (N.m)} \quad (15.5)$$

$$M_{(B)} = 1,7 \cdot F_{R(B)MAX(DYN+ARC)} \cdot (h_{iB} + h_s) \text{ (N.m)} \quad (15.6)$$

A safety factor of **1,7** is built into all steelwork structures.

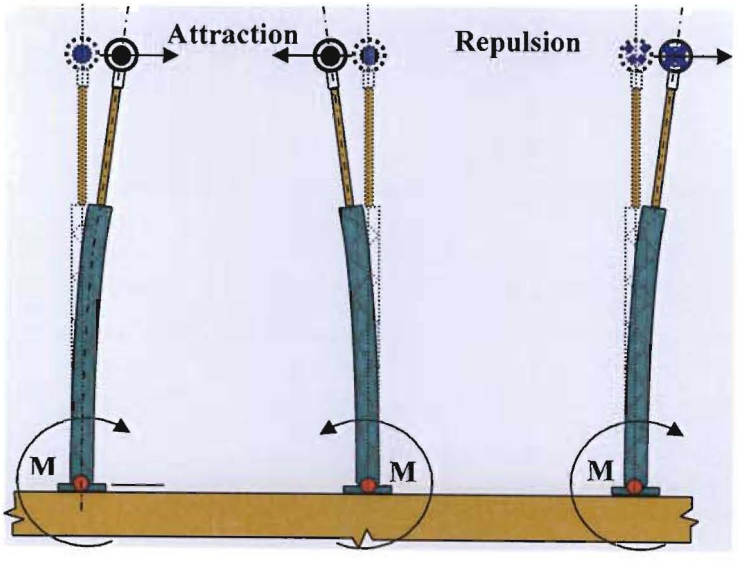

Figure 15.4: Deflection of the Insulator Steelwork Support

15.2.1.2 Steelwork Structure Flexibility

Busbar support structures can be fabricated from various types of materials and in various configurations. Due to their flexibility, these structures are capable of absorbing some of the

energy generated under fault conditions and so reduce the effective short-circuit forces. (9.1) could in effect be reworked as follows:

$$F^{1}_{sc} = K_f . \frac{4.10^{-7}}{s_p} . (I_{sc})^2 \qquad (15.7)$$

Where:-

K_f = Busbar support structure flexibility factor

Where all three phases are mounted on one structure as shown in Figure 15.5, K_f is taken as unity ($K_f = 1$)

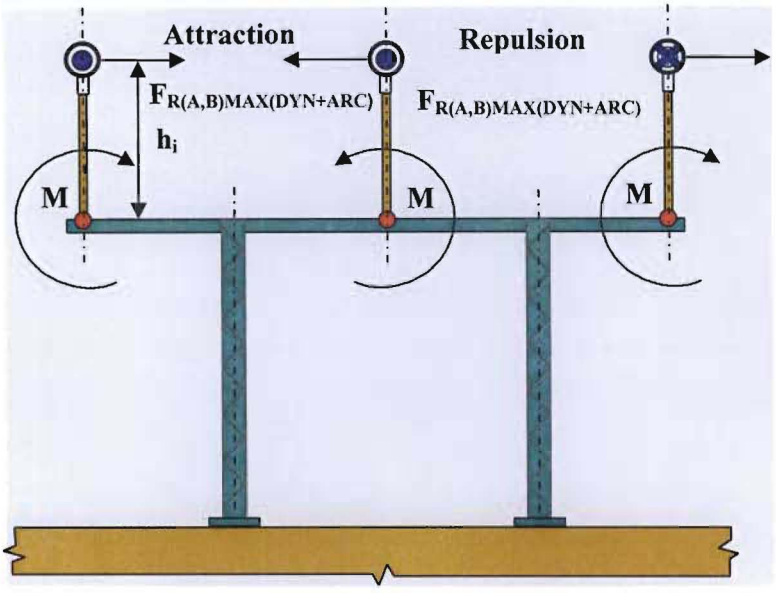

Figure 15.5: Bending moment at the base of the porcelain insulator for a single combined support structure

Where the three phases are mounted on separate support structures as illustrated in Figure 15.4 above, the K_f values can be determined from Figure 15.6 [9]

Figure 15.6: K_f vs Busbar Height [9]

The estimated parameters for the decrement factor functions are given below:

$$K_{fA} = 1,0 \qquad 0 < h_c \leq 2683m$$
$$= 1,0723 - 2,6953.10^{-5}.h_c \qquad 2683mm < h_c \leq 12192mm \qquad (15.8)$$

$$K_{fB} = 1,0 \qquad 0 < h_c \leq 4213m$$
$$= 1,1056 - 2,5066.10^{-5}.h_c \qquad 4213mm < h_c \leq 12192mm \qquad (15.9)$$

$$K_{fC} = 1,0 \qquad 0 < h_c \leq 4543m$$
$$= 1,1467 - 2,3841.10^{-5}.h_c \qquad 6152m < h_c \leq 12192m \qquad (15.10)$$

$$K_{fD} = 1,0 \qquad 0 < h_c \leq 10007m$$
$$= 1,2519 - 2,5172.10^{-5}.h_c \qquad 10007mm < h_c \leq 12192mm \qquad (15.11)$$

Where:

A	=	Lattice and tubular aluminium
B	=	Tubular and wide flange steel
C	=	Lattice steel
D	=	Solid concrete

16. THERMAL EXPANSION CONSIDERATIONS FOR BUS TUBING

Objectives of this Chapter:

- Calculate the expansion clamp slot length

When the temperature of a bus conductor changes the length of the conductor also changes. The change in length with respect to change in temperature can also be calculated as follows:-

$$\Delta \ell_i = \ell_i \left[\left(\frac{1 + \alpha_{th} T_f}{1 + \alpha_{th} T_i} \right) - 1 \right] \text{ (mm)} \qquad (16.1)$$

Where:-

ℓ_i = Span length of tubular conductor in mm

$\Delta \ell_i$ = Change in span length in mm

α_{th} = Coefficient of thermal expansion in $^{\circ}C^{-1}$

= $\alpha_{Cu} = 17.10^{-6}\ K^{-1}$, $\alpha_{Al} = 23.10^{-6}\ K^{-1}$

T_i = Initial temperature in °C

T_f = Final temperature in °C

16.1 Forces on Equipment Due To the Elongation of Rigid Conductors Fixed At Both Ends

Temperature related changes can exert considerable mechanical stresses on the conductors, their supports and connection points (equipment) if lengthy conductor runs include no means of compensation.

Example: Using the maximum emergency value of 90°C with an ambient temperature of 40°C, and assuming a tube length of typical 10 m:-

For Copper Bus Tubing

$$\Delta \ell_{Cu} = 10.10^{3} \left(\frac{17.10^{-6}.50}{1 + 17.10^{-6}.40} \right) \text{ (mm)}$$

$\Delta \ell_{Cu} = 8{,}5$ mm

For Aluminium Bus Tubing

$$\Delta\ell_{Al} = 10.10^{3}.\left(\frac{23.10^{-6}.50}{1+23.10^{-6}.40}\right) \textbf{ (mm)}$$

$\Delta\ell_{Al} = 11{,}5$ mm

The forces applied can be calculated very easily if the change of length due to temperature ΔL is put equal to the change of length caused by a mechanical force **F**

$$\Delta\ell_i = \ell_i.\left(\frac{\alpha_{th}.(T_f - T_i)}{1+\alpha_{th}T_i}\right) = \frac{F.L_i}{E.A} \qquad (16.2)$$

Where:-

F	=	Mechanical force in N
A	=	Conductor cross-sectional area in mm^2
E	=	Modulus of Elasticity in $°C^{-1}$
	=	Cu = 1,1 x 10^5 N/mm^2, Al = 0,65 x 10^5 N/mm^2
T_i	=	Initial temperature in °C

$$\frac{F}{E.A} = \left(\frac{\alpha_{th}.(T_f - T_i)}{1+\alpha_{th}T_i}\right) \qquad (16.3)$$

$$F = E.A.\left(\frac{\alpha_{th}.(T_f - T_i)}{1+\alpha_{th}T_i}\right) \qquad (16.4)$$

For $\Delta\theta$ = 1K, **A** = 1 mm^2 (specific values)

Specific loading

$$F^1 = \alpha_{th}.E \qquad (16.5)$$

$F^1_{cu} \approx \underline{2{,}53\ N/(K.mm^2)}$

$F^1_{Al} \approx \underline{1{,}50\ N/(K.mm^2)}$

16.2 Compensating For the Elongation of Rigid Conductors Fixed At Both Ends

The expansion of the tubular conductors is accommodated be installing expansion clamps into which the conductors are fixed as illustrated in Figures 16.1 and 16.2. One side may be fixed, while the other is allowed to slide, or both sides may slide. There is, however, a limit to the length of the bus that an expansion bus support can accommodate. This is due to the preset gap **D** that the expansion clamp is designed with to allow for bus expansion.

Manufacturers may specify the gap dimension **D** for 20°C installation temperature and is therefore used as temperature for T_i in the above equation. The final bus temperature used for

T_f in the above equation must consider the temperature of the bus right after the occurrence of a short-circuit condition. A value of 90°C can be assumed since this is the value used for emergency conditions.

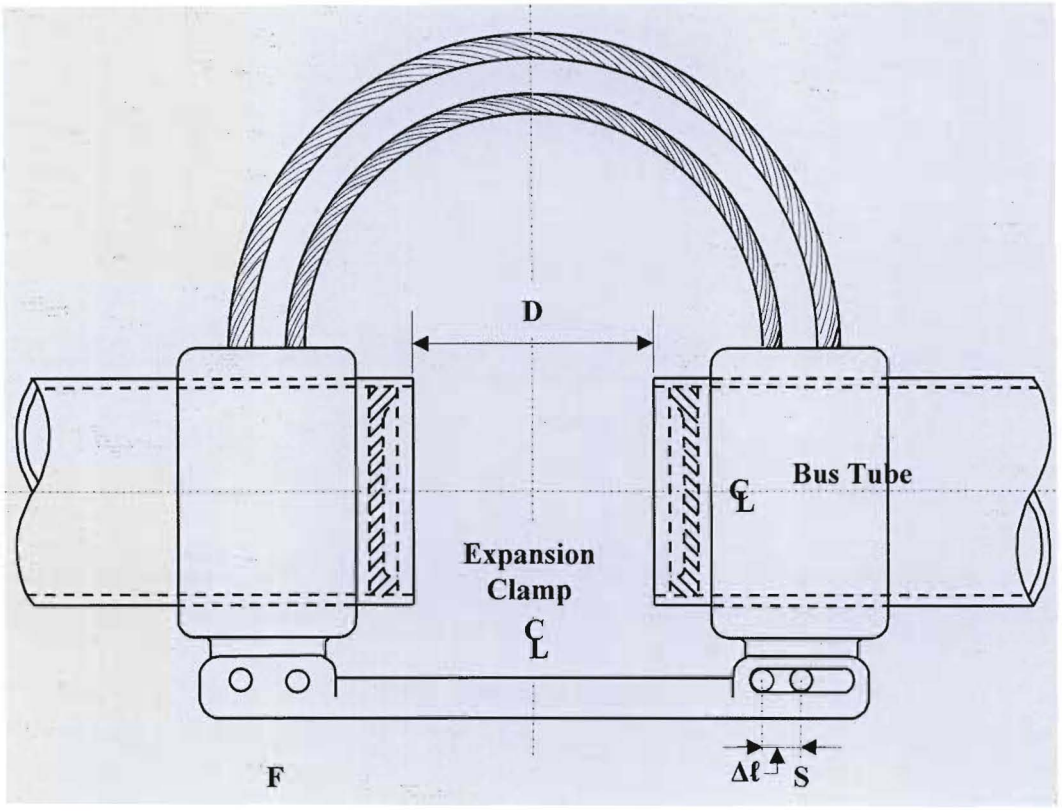

Figure 16.1: Tubular Bus Expansion Clamp

Rearranging equation 17.1 for ℓ_i:-

$$\ell_i = \Delta\ell_i.\left(\frac{1+\alpha_{th}T_i}{\alpha_{th}.(T_f-T_i)}\right) \text{ (mm)} \qquad (16.6)$$

Since α_{th} is very small (23.10^{-6} per unit length per °C), $1 + \alpha_{th} \approx 1$

$$\ell_i \approx \Delta\ell_i.\left(\frac{1}{\alpha_{th}.(T_f-T_i)}\right) \text{ (mm)} \qquad (16.7)$$

Suppose it is assumed that **D** = 100mm, then the length of a tube should not exceed:-

$$\ell_i \approx 100.\left(\frac{1}{23.10^{-6}.(90-20)}\right)$$
$$= 62112 \text{ mm}$$
$$\approx 62 \text{ m}$$

This value will generally far exceed any practical length of tube employed in tubular bus substations and should therefore not present a problem providing the correct gap is used. This

will be dictated by the width of the clamp and the amount of movement that is allowed by the sliding slot.

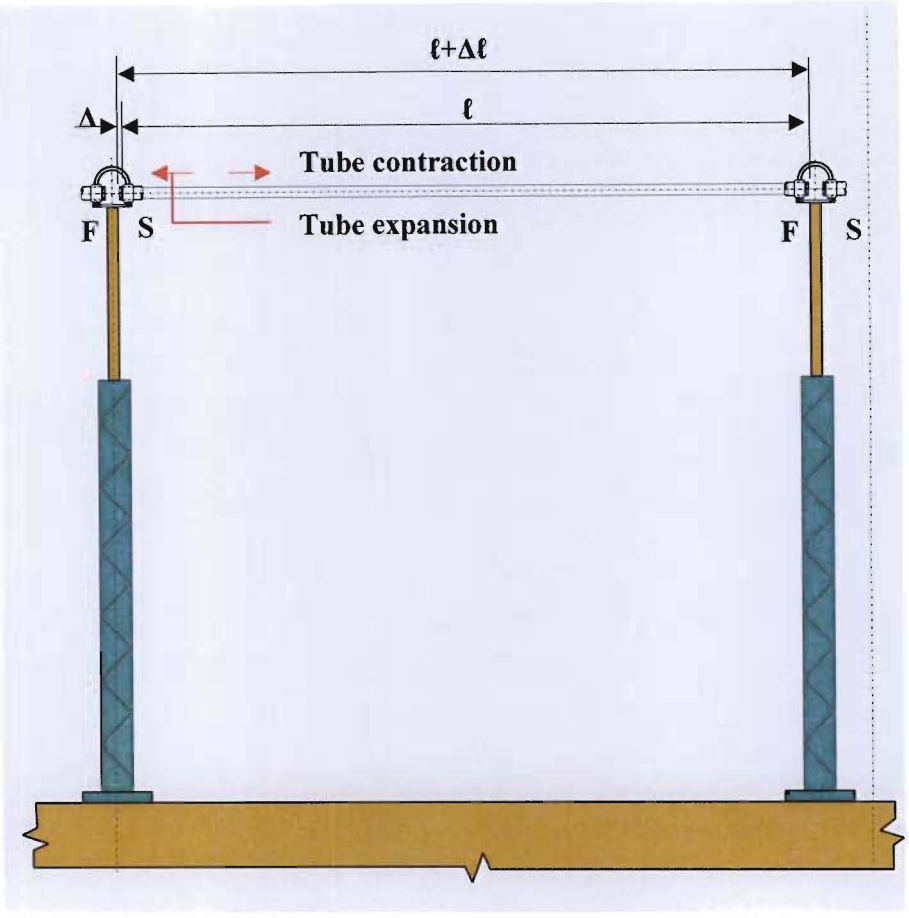

Figure 16.2: Tubular Bus Expansion System

16.3 Torsional Forces on the Post Insulators

The maximum allowable torsion on the post insulator head is usually in the region of 3kN.m and varies from manufacturer to manufacturer. For example, CERAM, a very well known and reputable insulator manufacturer offer the following products:-

Table 16.1: Post Insulator Minimum Failing Loads [24]

Type	Minimum Failing Load		
	Bending (kN)	Torsion (Static Load) (τ_{PI}) (kN.m)	Torsion (Dynamic Load) (τ_{PI}) (kN.m)
C4 - 1425	4	3	2,5
C6 - 1425	6	3	2,5
C8 - 1425	8	4	3,33
C10 - 1425	10	4	3,33
C12,5 - 1425	12,5	6	5
C16 - 1425	16	6	5
C20 - 1425	20	6	5

Under dynamic conditions, the allowable torque is only 80% that of the static value as the failure mechanism is slightly different to that under static conditions.

$$\tau_{sc} < \tau_{(PI)DYN} \qquad (16.8)$$

Where:-

τ_{sc} = Torque due to short circuit forces on the bus tubing exerted on the head of the post insulator in kN.m

$\tau_{(PI)DYN}$ = Rated maximum allowable dynamic torque on the head of the post insulator in kN.m (Manufacturers tables)

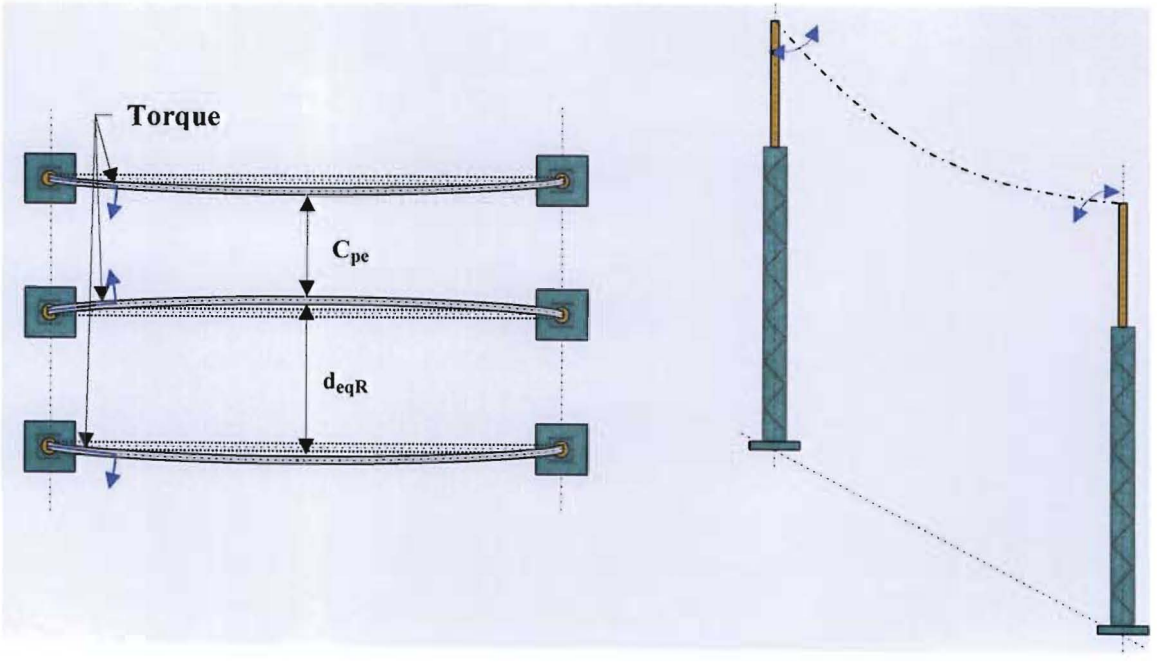

Figure 16.3: Torsional Forces

In the event that the allowable post insulator torsional forces are exceeded, the head of the insulator will shear off. This could result from excessive movement of the tubular conductor due to a fault in conjunction with high wind loading, or an incorrectly applied clamping arrangement at the end of the busbars.

If a rigidly fixed (**F**) clamp is used at the end of a bus system with no allowance for lateral movement, the force is asymmetrical, unlike the other post insulators which would have opposing moments on them that essentially cancel out the torsional moment. The former case would therefore result in a torsional force on it as indicated in the area enclosed by the chain line in Figure 16.3 above. This latter case would result in a torsional force, which if greater than the strength of the post insulator, would result in failure. The bus system would fail due to the domino effect as illustrated in Figure 16.4 below.

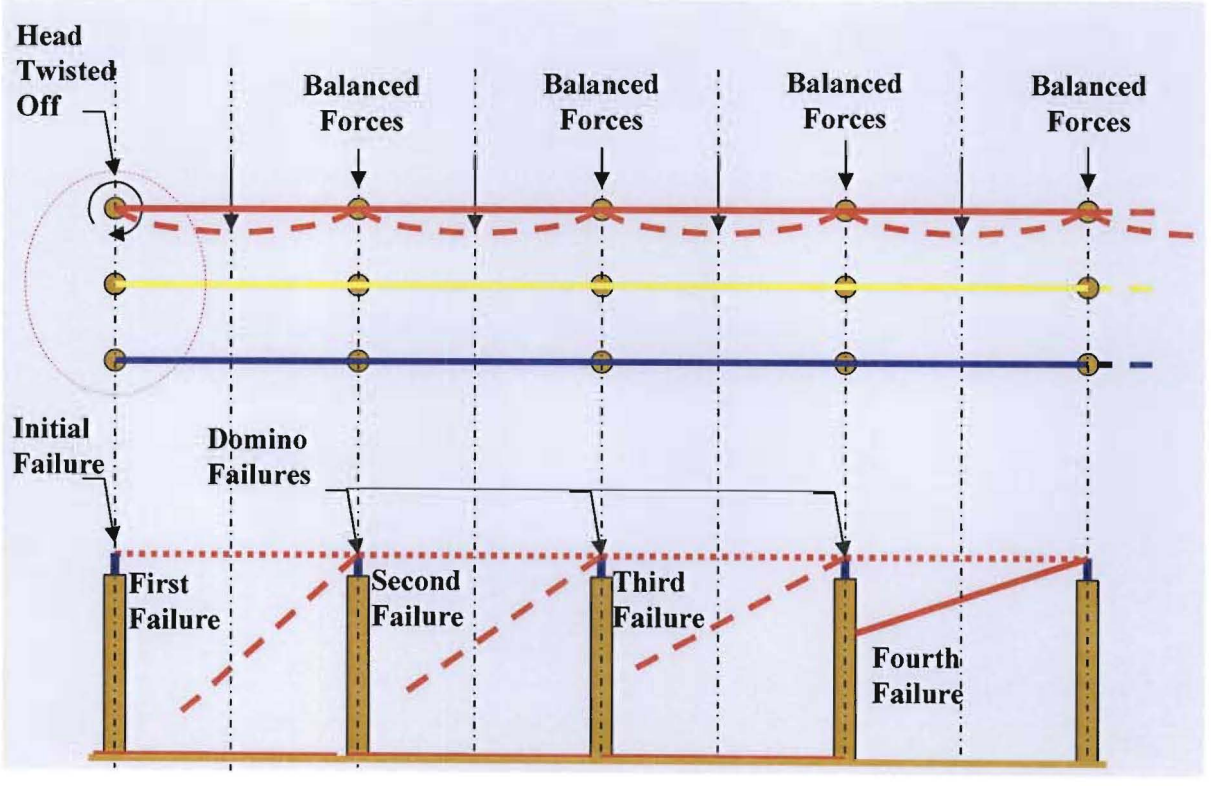

Figure 16.4: Mechanism of Catastrophic Failure

In an attempt to determine what the magnitude of the torsional force would be if one of the ends was fixed, we assume for a moment that the shape bus tube is such that it forms a sector on a circle as illustrated in Figure 16.5.

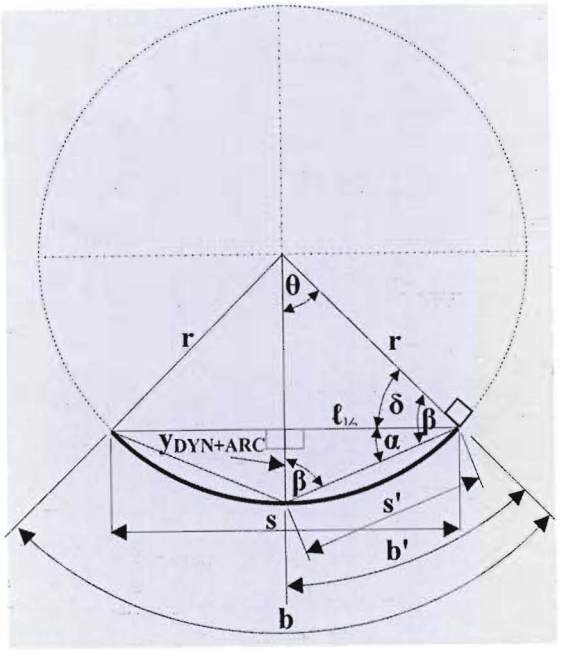

Figure 16.5: Modelling Torsional Forces

$$\alpha = \tan^{-1}\left(\frac{y_{DYN+ARC}}{\ell\frac{1}{2}}\right) \qquad (16.9)$$

Where:-

α = The angular displacement of the tube with respect to the straight line joining the two supporting post insulators in degrees

$\ell_{½}$ = Half the span length in mm

$y_{DYN+ARC}$ = The maximum displacement of the tube at its midpoint under fault conditions in mm

$$\beta = 90^{o} - \alpha \qquad (16.10)$$

$$\theta = 180^{o} - 2.\beta \qquad (16.11)$$

β and θ are merely angles within the geometry of the model measured in degrees.

$$s' = \sqrt{\left(\ell\frac{1}{2}^{2} + y_{DYN+ARC}^{2}\right)} \qquad (16.12)$$

Where:-

s' = The length of the chord subtended by angle θ measured in mm

$$\frac{s'}{\sin\theta} = \frac{r}{\sin\beta} \quad \textbf{where } \theta \textbf{ is in radians} \tag{16.13}$$

$$\therefore r = \frac{s'.\sin\beta}{\sin\theta}$$

r = The radius of the approximated circle of which the deformed tube forms a part in mm

$$b' = r.\theta \quad \textbf{where } \theta \textbf{ is in radians} \tag{16.14}$$

b' = The length of the arc subtended by angle θ measured in mm

Total amount of movement

$$d_m = b' - \ell_{½} \tag{16.15}$$

The slot must therefore accommodate a total of d_s mm from its rest position

$$d_s = d_m + \Delta\ell \tag{16.16}$$

Thermal contraction will shorten the tube length, reducing the amount the sliding pin can move. This needs to be checked in conjunction with the movement of the tube under fault conditions. Figure 16.6 shows a typical expansion clamp where the one side is fixed marked **F**, while the other side is allowed to move or slide marked **S**. The slot **S** must be long enough to cater for the worst condition with respect to either full tube expansion or contraction and then experiencing a fault condition.

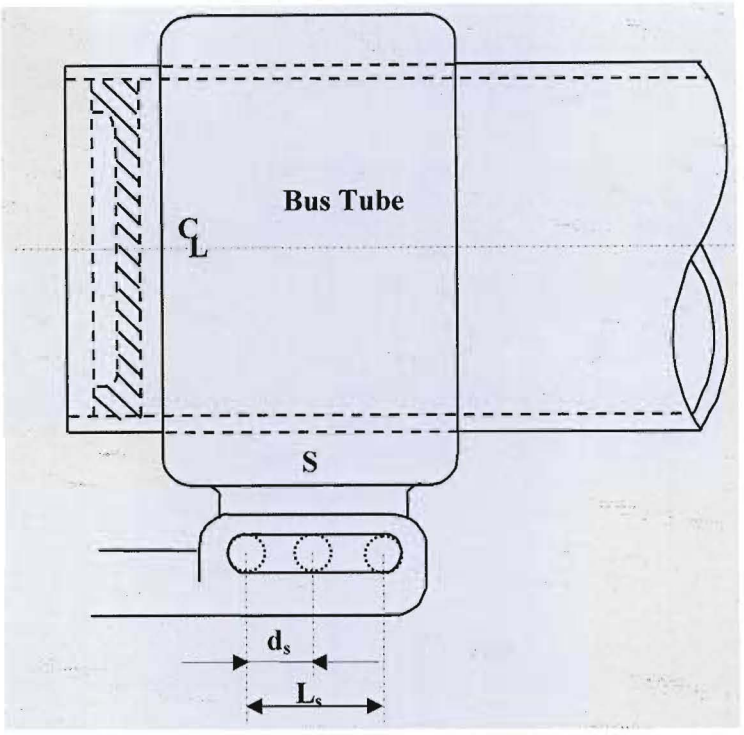

Figure 16.6: Tubular Bus Expansion Clamp Slot Length

As illustrated in Figures 16.6 and 16.7, if it is assumed that the initial position is in the centre of the slot, then accounting for contraction, it is safe to say total slot length must be at least:

$$\mathbf{L_s = 2.d_s} \qquad (16.17)$$

The problem arises when the contraction is such that when a fault occurs, there is not enough distance left in the slot to allow for the movement, causing the sliding pin to knock up against the end of the slot. Under these conditions, not only will there be a cantilever force exerted on the insulator, but also a torsional force.

Example: This clamp must is to be used for the following design:-

400kV Yard in an area close to the coast with sparse vegetation and experiencing high wind speeds of 50 m/s. Suppose the temperature difference from the installed value is 25°C. The fault current is calculated to 50kA.

ℓ= 10 000mm

$y_{DYN+ARC}$ = 335mm

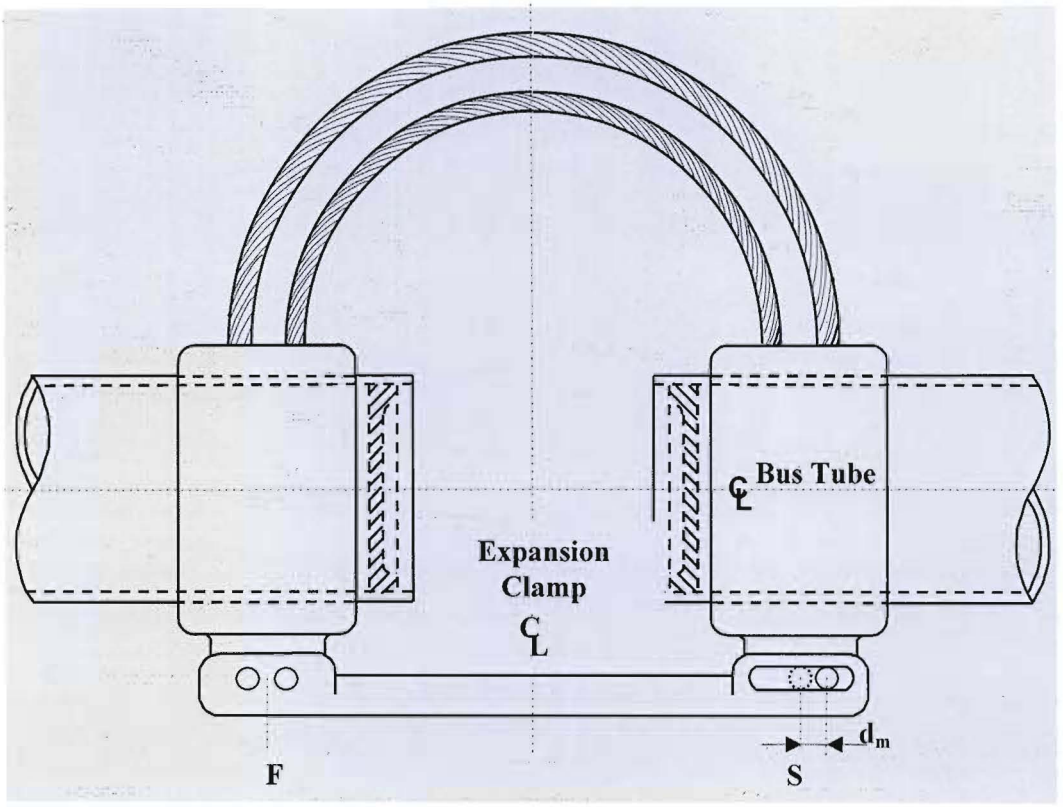

Figure 16.7: Tubular Bus Expansion Clamp

$\ell_t = \ell.(1+\alpha_{th}.\Delta\theta_{th})$ (from 7.1)

$= 10\,000.(1 + 23.10^{-6}.25)$

$\ell_t = 10\,006\text{mm}$

$$\alpha = \tan^{-1}\left(\frac{y_{DYN + ARC}}{\ell}\right)$$

$$= \tan^{-1}\left(\frac{335}{10\,006}\right)$$ (from 16.9)

$= 1{,}9175°$

$\beta = 90° - 1{,}9175°$

$= 88{,}0825°$

$\theta = 180° - 2.\ 88{,}0825°$

$= 3,\ 8350°$

$$s' = \sqrt{\left(\ell^2 + y_{DYN+ARC}^2\right)}$$

$$= \sqrt{\left(10006^2 + 335^2\right)} \qquad \text{(from 16.12)}$$

$$= 10012\,\text{mm}$$

$$\frac{s'}{\sin\theta} = \frac{r}{\sin\beta} \qquad \textbf{where } \theta \textbf{ is in radians}$$

$$r = \frac{s'.\sin\beta}{\sin\theta} \qquad \text{(from 16.13)}$$

$$= \frac{10012.\sin 88{,}0825^\circ}{\sin 3{,}8350^\circ}$$

$$= 149{,}610\,\text{m}$$

$$b' = r.\theta$$

$$= 149{,}421.3{,}8350.\frac{\pi}{180^\circ} \qquad \text{where } \theta \text{ is in radians} \qquad \text{(from 16.14)}$$

$$10{,}014\,\text{m}$$

Total amount of movement

$$d_m = b' - \ell \qquad \text{(from 16.15)}$$

$$= 10\,014 - 10\,006$$

$$d_m = 8\ \text{mm}$$

The slot must therefore allow for:-

$$d_s = d_m + \Delta\ell \qquad (16.16)$$

$$= 8\text{mm} + 16\text{mm}$$

d_s = 24mm from its original set position.

Assuming this was in the centre of the slot then it would require a slot length of

$$L_s = 2.d_s \qquad (16.17)$$

$$= 2\,.\,24\text{mm}$$

L_s = 48mm long.

It would probably best to make it 50mm in length to allow for any inaccuracies in the calculation.

In the worst case, if the end tube was fixed, the torsional force exerted on the insulator would be:-

$$\tau_{sc} = F^{1}_{R(\sigma)DYN + ARC}.\ell$$

(17.18)

$= 0,6767.10$

$= 6,767$ kN.m

The result would obviously mean failure of the insulator as the calculated torsional force exceeds the rated static and dynamic values of all the insulators.

Example: The failure of the 400kV Red phase busbar at Maputo Substation, Maputo, Mozambique.

A cyclone moved through the Maputo area and Maputo substation experienced wind speeds in the order of 50 m/s. The result of this was that part of the 400kV red phase busbar, which bore the brunt of the wind, fell to the ground as a result of insulator failure. On investigation it was found that a fixed clamp was used at the end of the busbar. The fault level at Maputo is only around 10kA.

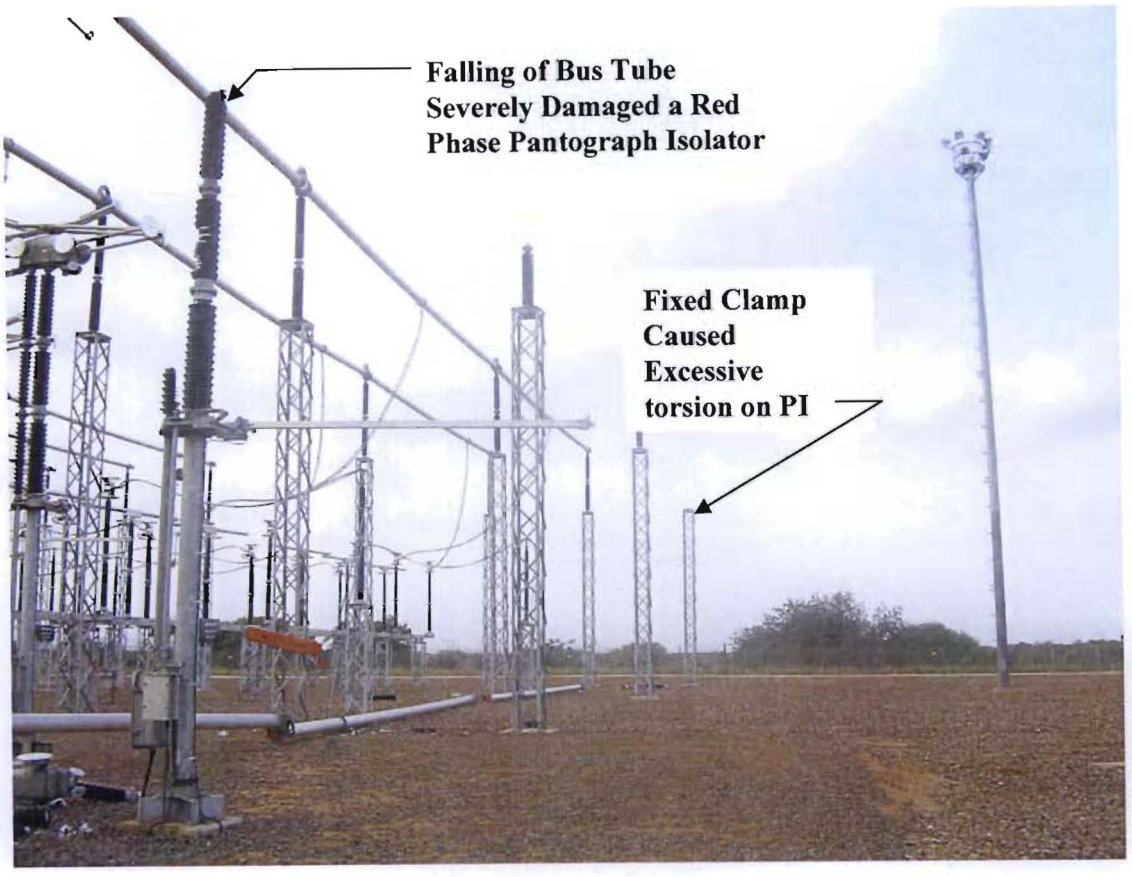

Figure 16.8: Catastrophic Failure at the End of the 400kV Red Phase Conductors

$F_{R(\sigma)DYN+ARC} = 275{,}38$ N

$\tau_{sc} = F^{1}_{R(\sigma)DYN + ARC}.\ell$ (from 16.18)

$= 0{,}27538.10$

$= 2{,}754$ kN.m

At Maputo Substation, 6kN post insulators were used which have a dynamic rating of 2,5kV.m. This value was exceeded and therefore resulted in the failure shown in Figures 16.8 and 16.9.

Figure 16.9: Catastrophic Failure of the 400kV Red Phase Conductors

17. SUBSTATION CONDUCTOR HEIGHTS DETERMINED BY CORONA PERFORMANCE

Objectives of this Chapter:

There are several factors that have an influence on the height of conductors above ground level amongst which are statutory clearances to the base of equipment porcelains, safe vertical working clearance, corona inception levels and allowable electric and magnetic field strengths within the boundaries of the substation, and on the substation perimeter edges where the public has access. At low voltage levels, vertical working clearance and possibly magnetic field strengths (assuming high current levels) would dominate. At high voltage levels (EHV and UHV) corona performance and electric field strengths would dominate. The Statutory clearance to the base of equipment porcelains applies to all voltages.

17.1 Ensuring Electrical Clearances are not Infringed

Having met all the horizontal phase-to-earth and phase-to-phase electrical clearances and thus establishing the bay width, the height of the inter-equipment conductors needs to be determined.

The equipment level conductors need to meet at least the sum of the statutory clearance to the base of the equipment porcelain ($\mathbf{h_s}$), the height from the base of the equipment porcelain to the equipment connection terminal ($\mathbf{h_{et}}$), and particularly in the case where stranded flexible conductors to interconnect items of equipment, the expected sag in the inter-equipment conductor ($\mathbf{s_c}$). This value ($\mathbf{h_c}$) needs to equal or exceed the safe vertical working clearance ($\mathbf{C_{wv}}$).

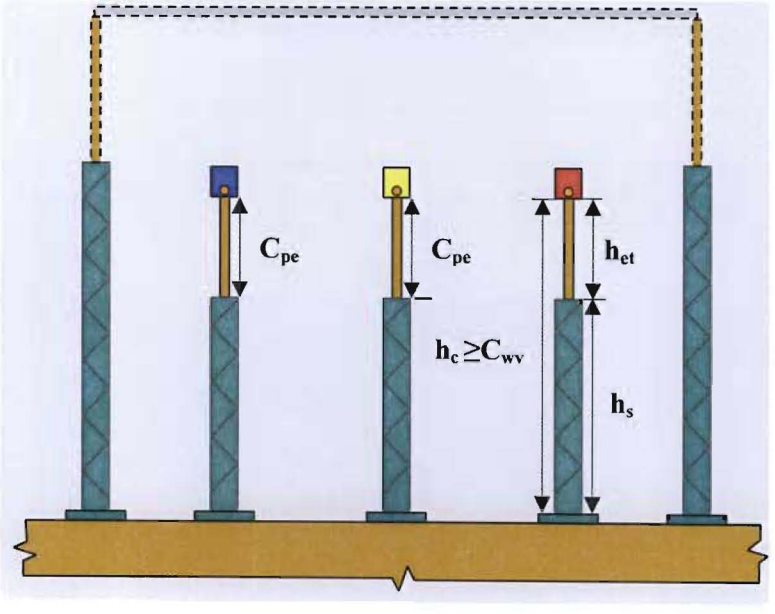

(a) Elevation transverse to an equipment bay (across the phases)

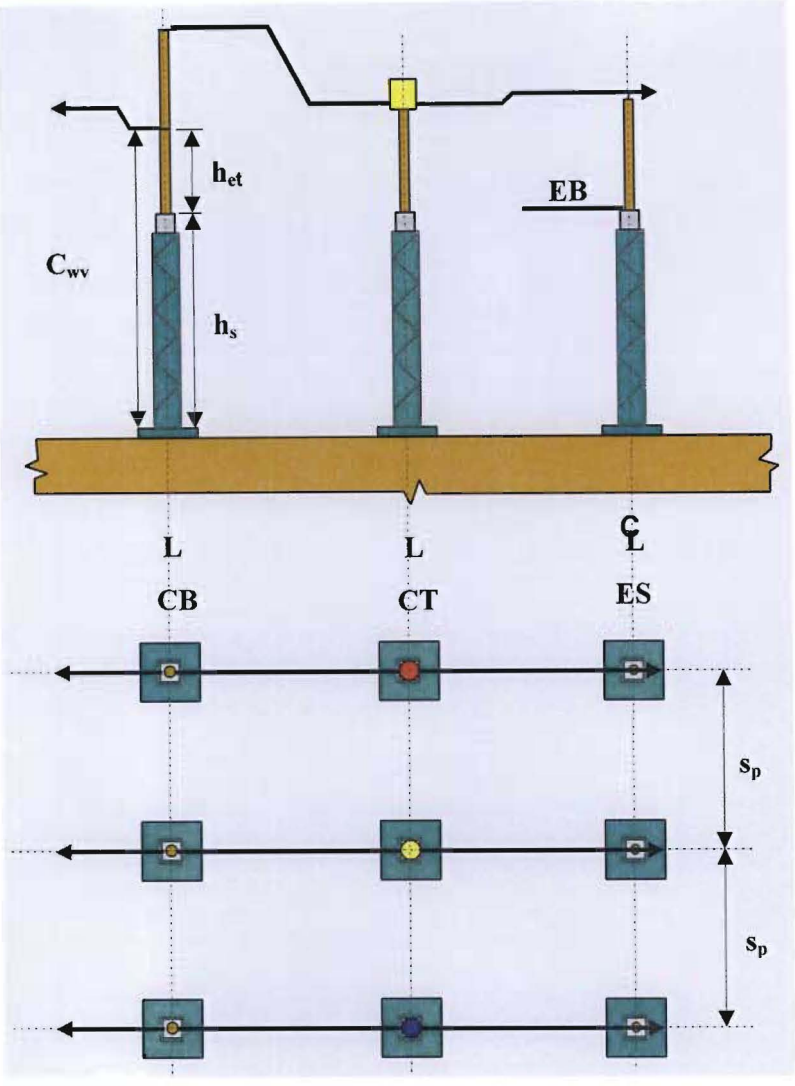

17.1: Determining the Inter- equipment Conductor Height

As a starting point therefore:-

$$h_c = h_s + h_{et} - s_c \geq C_{wv} \qquad (17.1)$$

Where:-

h_c = Height of the lowest point of the equipment interconnector conductor above the equipment foundation top of concrete in mm

h_s = Statutory clearance to the base of the equipment porcelain in mm

h_{et} = Height from the base of the equipment porcelain to the equipment connection terminal in mm

s_c = Expected sag in the inter-equipment conductors (applicable when stranded flexible conductors are used) in mm

s_p = Phase spacing in mm

(17.1) would suffice for low system voltages with low phase currents, where electric and magnetic field strengths would probably be below the recommended safe levels. However, as a general guideline, and for illustrating the complete analysis process, the remaining criteria need to be checked, viz. corona inception levels and allowable electric and magnetic field strengths within the boundaries of the substation, and on the substation perimeter edges where the public has access. These would in any event be required at EHV and UHV levels.

17.2 Corona Requirements

Objectives of this Section:

- Chosen Line Voltage $\mathbf{V_L}$
- Determine the height of the inter-equipment connection conductors ($\mathbf{h_c}$) to result in E $\leq$ 10kV/m and H $\leq$ 500μT (E and H fields)
- Determine the height of the busbars ($\mathbf{h_b}$).
- Determine the height of the stringers ($\mathbf{h_{ss}}$)
- Determine the height of the lightning protection conductors ($\mathbf{H_e}$)

17.2.1 Substation Conductor Heights (determine corona performance)

The busbar conductor needs to be corona-free during fair weather conditions. This is generally not too difficult to achieve with tubular conductors that are normally over-dimensioned for ampacity in order to meet mechanical strength requirements. In order to ensure corona-free operation, the maximum value of the surface voltage gradient on the bus conductor ($\mathbf{E_m}$) must be less than the surface voltage gradient at the corona inception or threshold limit ($\mathbf{E_c}$)

The surface field strength on a tubular conductor is dependant on various factors such as height above ground, tube diameter, and to a lesser degree, phase spacing ($\mathbf{s_p}$).

The corona inception or threshold limits for various single conductors are listed in Table 17.1. Theoretically it should be possible to reduce these figures by a reasonable safety factor and then select a suitable tube size from Table 6.1 for that particular voltage. However, another factor that should be borne in mind is the span length that might necessitate the use of a much larger tube to meet the mechanical strength requirements as discussed in Chapter 12. Under such conditions, the increased diameter would also contribute to a lower surface field strength as mentioned further on in this chapter.

To give the substation designer a bit of leeway, the recommendation would be to consider two separate sets of conditions as follows:-

- Relatively short span lengths without welds and ;
- Long span lengths where welds may be essential (today imported tubes of lengths up to 30m are possible, thus negating the requirement of welds).

17.2.2 Calculation of Conductor Surface Field Strength and Determination of Corona Inception Levels for Typical Arrangements

This section deals with the calculation of conductor surface field strength, for single and bundle conductor arrangements and compares inception levels at various voltages.

17.2.2.1 Corona threshold limits (E_c) [3]

Empirical expressions that were developed by Peek (UK) and Heymann (University of Pretoria) [4] give corona threshold field strengths for single conductors as follows:-

Peek : $$E_c = 3.m_r.\delta\left[1+\frac{0,03}{\sqrt{r_{bo}.\delta}}\right].\frac{10}{\sqrt{2}}\frac{kV}{cm}\ (rms) \qquad (17.2)$$

Heymann : $$E_c = 2,4.m_r.\delta\left[1+\frac{0,0937}{(r_{bo}.\delta)^{0,4}}\right].\frac{10}{\sqrt{2}}\frac{kV}{cm}\ (rms) \qquad (17.3)$$

Where:-

E_c = Corona threshold surface field strength

δ = Relative air density (RAD)

r_{bo} = Conductor radius in metres

m_r = Factor to allow for surface roughness

Typical values for m_r are as follows:-

Polished tubes	-	**1,0**
Extruded tubes	-	**0,95**
stranded conductor	-	**0,8**

The relative air density (RAD) can be determined from the reciprocal of equation 4.12

$$\mathbf{RAD} = \mathbf{e}^{-\left(\frac{Ha}{8150}\right)}\mathbf{(dimensionless)}\ [14] \qquad (17.4)$$

If **RAD** is taken as **0,8** typical of 1800 m above sea level, equations 17.2 and 17.3 give the values listed in Table 17.1 below for $\mathbf{E_c}$.

Table 17.1: Corona Threshold Surface Field Strength for Various Conductors

CONDUCTOR DETAILS			PEEK	HEYMANN
Type	Conductor Dia. (mm)	m_r	E_c kV / cm (rms)	E_c kV / cm (rms)
Tubular Conductor	50	0,95	19,54	18,68
Tubular Conductor	75	0,95	18,91	17,81
Tubular Conductor	100	0,95	18,54	17,28
Tubular Conductor	150	0,95	18,10	16,62
Tubular Conductor	200	0,95	17,83	16,22
Tubular Conductor	250	0,95	17,65	15,93

17.2.2.2 Calculation of conductor surface field strength (E_m) using the image method.

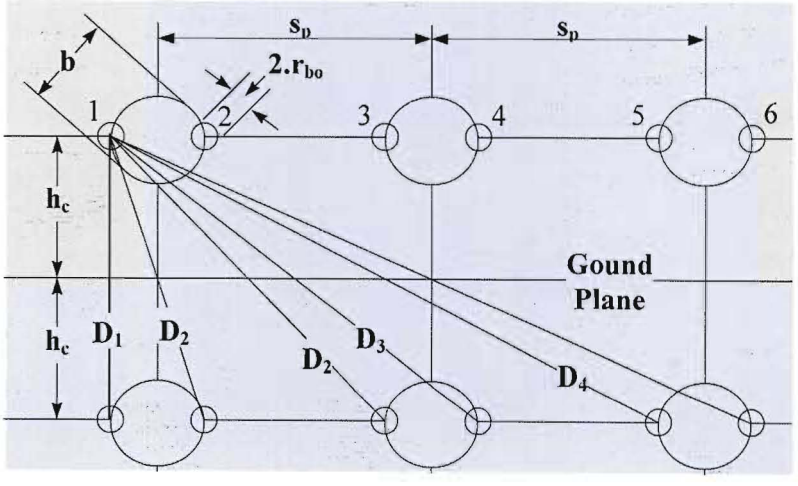

Figure 17.2: Conductor Surface Field Strength on a Conductor Bundle Using the Image Method [3]

By applying the formulae derived for a three phase transmission line to a bundle conductor arrangement as shown above, the phase to ground voltage on conductor 1 is given by:

$$V_1 = \frac{Q_1}{2.\pi\varepsilon}.\ln\left[\frac{2.h_b}{b}\right] + \frac{Q_2}{2.\pi\varepsilon}.\ln\left[\frac{D_1}{b}\right] + \frac{Q_3}{2.\pi\varepsilon}.\ln\left[\frac{D_2}{s_p}\right] + \frac{Q_4}{2.\pi\varepsilon}.\ln\left[\frac{D_3}{s_p + b}\right] \quad (17.5)$$

$$+ \frac{Q_5}{2.\pi\varepsilon}.\ln\left[\frac{D_4}{2.s_p}\right] + \frac{Q_6}{2.\pi\varepsilon}.\ln\left[\frac{D_5}{2.s_p + b}\right](\text{Volts})$$

Where:-

V_1	=	instantaneous phase to ground voltage on conductor 1 in volts
Q_1, Q_2	=	instantaneous charges on conductors
.....Q_6		1, 2 ...6 respectively in coulomb/m.
ε	=	the dielectric constant for air in C^2/Nm^2.
r_{bo}	=	the radius of the conductor in metres
h_c	=	height of conductors above ground in metres
s_p	=	phase spacing in metres
D_1, D_2	=	relative distances between conductors in metres
....D_5		

The instantaneous charge on a conductor is proportional to the instantaneous phase to ground voltage of the conductor, but due to the fact that the voltages on the three phases are displaced by 120° and the algebraic sum of the charges $\sum_{x=1}^{n} Q_x = 0$, it follows that if the charge on conductor 1 at any particular instant equals +**Q** coulomb/m, then the charges on the other two phases are **-0,5.Q** coulomb/m each. This leads to the following simplification:-

$$Q_1 \approx Q_2 = Q \quad (17.6)$$

$$Q_3 \approx Q_4 = -0,5.Q_1 = -0,5.Q \quad (17.7)$$

$$Q_5 \approx Q_6 = -0,5.Q_1 = -0,5.Q \quad (17.8)$$

Substitute in (17.6), (17.7) and (17.8) above and we get:-

$$V_1 = V_n = \frac{Q}{2.\pi\varepsilon}.\left\{\ln\left[\frac{2.h_c}{r_{bo}}\right] + \ln\left[\frac{D_1}{b}\right] - 0,5.\ln\left[\frac{D_2}{s_p}\right] + \ln\left[\frac{D_3}{s_p + b}\right] + \ln\left[\frac{D_4}{2.s_p}\right] + \ln\left[\frac{D_5}{2.s_p + b}\right]\right\}(\text{Volts})$$

$$V_1 = V_n = \frac{Q}{2.\pi\varepsilon}.[P_1](\text{Volts}) \quad (17.9)$$

Where V_n = phase to neutral voltage in volts

$$P_1 = \ln\left[\frac{2.h_c}{r_{bo}}\right] + \ln\left[\frac{D_1}{b}\right] - 0{,}5.\ln\left[\frac{D_2}{s_p}\right] + \ln\left[\frac{D_3}{s_p + b}\right] + \ln\left[\frac{D_4}{2.s_p}\right] + \ln\left[\frac{D_5}{2.s_p + b}\right] \qquad (17.10)$$

but the average field strength on the surface of any conductor with radius **r** and charge + **q** coulomb/m is given by:-

$$E_{av} = \frac{+q}{2.\pi\varepsilon .r_{bo}} \text{(Volts/m)} \qquad (17.11)$$

(17.11) applied to conductor 1 of the above arrangement gives:-

$$E_{1av} = \frac{Q}{2.\pi\varepsilon .r_{bo}} \text{(Volts/m)} \qquad (17.12)$$

Where :-

Q = charge on conductor 1 in coulomb/m

r_{bo} = radius of conductor 1 in metres

Substitute for **Q** from (17.10)

$$E_{1av} = \frac{[V_n].2\pi\varepsilon}{[P_1].2\pi\varepsilon} . \frac{1}{r_{bo}}$$

$$= \frac{V_n}{[P_1]} . \frac{1}{r_{bo}} \text{kV/m(rms)}$$

$$E_{1av} = \frac{[V_L]}{\sqrt{3}} . \frac{1}{P_{1r}} . \frac{1}{10^2} \text{kV/cm(rms)} \qquad (17.13)$$

with V_L in kV (rms) and r_{bo} in metres.

The average field strength for the other conductors can be calculated in a similar manner.

However, when wires are close together as in a bundle, the charges influence each other and bring about a spatial variation of the field. The actual variation of field strength round the circumference has been shown by several investigators to closely follow a cosine relationship given by the equation:-

$$E_e = E_{av}.\left[1 + (n - 1).\frac{d_{bo}}{b}.\cos\theta\right] \qquad (17.14)$$

Where:-

n = number of conductors in a bundle

$\mathbf{d_{bo}}$ = conductor diameter

b = bundle diameter

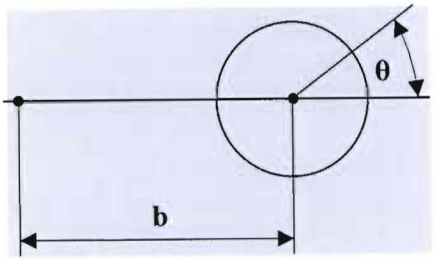

Figure 17.3: Variation of the Electric Field Strength w.r.t Angular Position Relative to a Bundle Conductor

Experimental results, however, confirm that the corona threshold is reached when the field strength reaches halfway between the average value and the maximum value, i.e. when $\theta = 45°$, and where $\cos\theta = 0{,}71$.

This is termed the effective field strength and is given by:-

$$E_e = E_{av}.\left[1 + 0{,}71.(n-1).\frac{d_{bo}}{b}\right] \qquad (17.15)$$

The above is true if each phase was made up of a bundle of conductors, however, since a single bus tube per phase ($n = 1$) is generally used, the above relationship reduces to:

$$E_e = E_{av} \qquad (17.16)$$

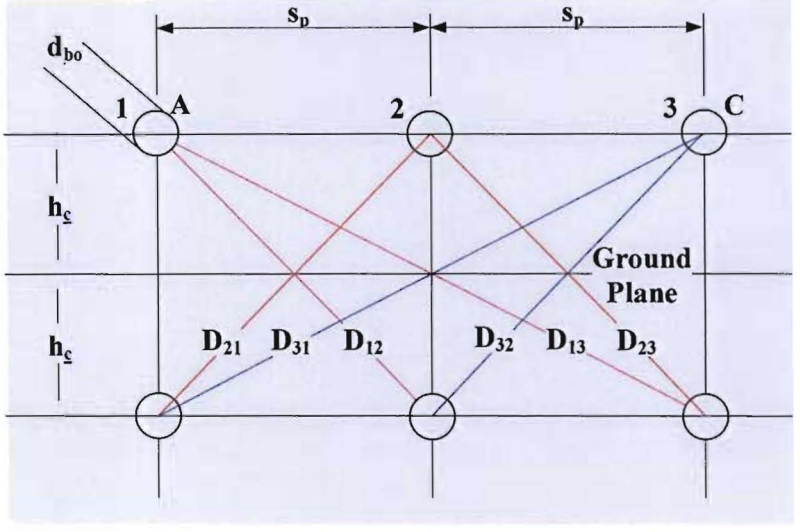

Figure 17.4: Conductor Surface Field Strength on a Bus Tube Using the Image Method

By applying the formulae derived for a three phase transmission line to a tubular conductor arrangement as shown above, the phase to ground voltage on conductor 1 is given by:

$$V_1 = \frac{Q_{11}}{2\pi\varepsilon}.\ln\left[\frac{2.h_c}{r_{bo}}\right] + \frac{Q_{12}}{2\pi\varepsilon}.\ln\left[\frac{D_{12}}{s_p}\right] + \frac{Q_{13}}{2\pi\varepsilon}.\ln\left[\frac{D_{13}}{2.s_p}\right] \text{ (Volts)} \qquad (17.17)$$

The average field strength for the other conductors can be calculated in a similar manner.

$$V_2 = \frac{Q_{21}}{2\pi\varepsilon}.\ln\left[\frac{D_{21}}{s_p}\right] + \frac{Q_{22}}{2\pi\varepsilon}.\ln\left[\frac{2.h_c}{r_{bo}}\right] + \frac{Q_{13}}{2\pi\varepsilon}.\ln\left[\frac{D_{23}}{s_p}\right] \text{ (Volts)} \qquad (17.18)$$

$$V_3 = \frac{Q_{31}}{2\pi\varepsilon}.\ln\left[\frac{D_{31}}{2.s_p}\right] + \frac{Q_{32}}{2\pi\varepsilon}.\ln\left[\frac{D_{32}}{s_p}\right] + \frac{Q_{13}}{2\pi\varepsilon}.\ln\left[\frac{2.h_c}{r_{bo}}\right] \text{ (Volts)} \qquad (17.19)$$

Where:-

V_1, V_2, V_3	=	instantaneous phase to ground voltage on conductors 1, 2 and 3 respectively in volts
Q_{11}, Q_{12}, Q_{13}, Q_{21}, Q_{22}, Q_{23}, Q_{31}, Q_{32}, Q_{33}	=	instantaneous charges on conductors 1, 2, 3 respectively in coulomb/m.
ε	=	the dielectric constant for air in C^2/Nm^2.
d_{bo}	=	the diameter of the conductor in mm
r_{bo}	=	the radius of the conductor in mm
h_c	=	height of conductors above ground in mm
s_p	=	phase spacing in mm
D_{11}, D_{12}, D_{21}, D_{22}, D_{31}, D_{32}	=	relative distances between conductors in mm

The instantaneous charge on a conductor is proportional to the instantaneous phase to ground voltage of the conductor, but due to the fact that the voltages on the three phases are displaced by 120° and the algebraic sum of the charges $\sum_{x=1}^{n} Q_x = 0$, it follows that if the charge on conductor 1 at any particular instant equals **+Q** coulomb/m, then the charges on the other two phases are **-0,5Q** coulomb/m each. This leads to the following simplification:-

$$Q_{11} \approx Q_{22} \approx Q_{33} = Q \qquad (17.20)$$

$$Q_{12} \approx Q_{13} = -0{,}5.Q_1 = -0{,}5.Q \quad (17.21)$$

$$Q_{21} \approx Q_{23} = -0{,}5.Q_1 = -0{,}5.Q \quad (17.22)$$

$$Q_{31} \approx Q_{32} = -0{,}5.Q_1 = -0{,}5.Q \quad (17.23)$$

Substitute in (17.17), (17.18) and (17.19) above and we get:-

$$V_1 = V_n = \frac{Q}{2\pi\varepsilon}.\left\{\ln\left[\frac{2.h_c}{r_{bo}}\right] + \ln\left[\frac{D_{12}}{s_p}\right].\cos 120^\circ + \ln\left[\frac{D_{13}}{2.s_p}\right].\cos 240^\circ\right\}(\text{Volts}) \quad (17.24)$$

$$V_2 = V_n = \frac{Q}{2\pi\varepsilon}.\left\{\ln\left[\frac{D_{21}}{s_p}\right].\cos 120^\circ + \ln\left[\frac{2.h_c}{r_{bo}}\right] + \ln\left[\frac{D_{23}}{s_p}\right].\cos 240^\circ\right\}(\text{Volts}) \quad (17.25)$$

$$V_3 = V_n = \frac{Q}{2\pi\varepsilon}.\left\{\ln\left[\frac{D_{31}}{2.s_p}\right].\cos 120^\circ + \ln\left[\frac{D_{32}}{s_p}\right].\cos 240^\circ + \ln\left[\frac{2.h_c}{r_{bo}}\right]\right\}(\text{Volts}) \quad (17.26)$$

Simplified

$$V_1 = V_n = \frac{Q}{2\pi\varepsilon}.\left\{\ln\left[\frac{2.h_c}{r_{bo}}\right] - 0{,}5.\ln\left[\frac{D_{12}}{s_p}\right] - 0{,}5.\ln\left[\frac{D_{13}}{2.s_p}\right]\right\}(\text{Volts}) \quad (17.27)$$

$$V_2 = V_n = \frac{Q}{2\pi\varepsilon}.\left\{-0{,}5.\ln\left[\frac{D_{21}}{s_p}\right] + \ln\left[\frac{2.h_c}{r_{bo}}\right] - 0{,}5.\ln\left[\frac{D_{23}}{s_p}\right]\right\}(\text{Volts}) \quad (17.28)$$

$$V_3 = V_n = \frac{Q}{2\pi\varepsilon}.\left\{-0{,}5.\ln\left[\frac{D_{31}}{2.s_p}\right] - 0{,}5.\ln\left[\frac{D_{32}}{s_p}\right] + \ln\left[\frac{2.h_c}{r_{bo}}\right]\right\}(\text{Volts}) \quad (17.29)$$

$$V_1 = V_n = \frac{Q}{2\pi\varepsilon}.[P_1](\text{Volts}) \quad (17.30)$$

$$V_2 = V_n = \frac{Q}{2\pi\varepsilon}.[P_2](\text{Volts}) \quad (17.31)$$

$$V_3 = V_n = \frac{Q}{2\pi\varepsilon}.[P_3](\text{Volts}) \quad (17.32)$$

Where:-

V_n = phase to neutral voltage in volts

$$P_1 = \ln\left[\frac{2.h_c}{r_{bo}}\right] - 0{,}5.\ln\left[\frac{D_{12}}{s_p}\right] + -0{,}5.\ln\left[\frac{D_{13}}{2.s_p}\right] \tag{17.33}$$

$$P_2 = -0{,}5.\ln\left[\frac{D_{21}}{s_p}\right] + \ln\left[\frac{2.h_c}{r_{bo}}\right] - 0{,}5.\ln\left[\frac{D_{23}}{s_p}\right] \tag{17.34}$$

$$P_3 = -0{,}5.\ln\left[\frac{D_{31}}{s_p}\right] - 0{,}5.\ln\left[\frac{D_{32}}{s_p}\right] + \ln\left[\frac{2.h_c}{r_{bo}}\right] \tag{17.35}$$

In terms of the basic parameters

$$P_1 = \ln\left[\frac{2.h_c}{r_{bo}}\right] - 0{,}5.\ln\left[\frac{\sqrt{\left([2.h_c]^2 + s_p{}^2\right)}}{s_p}\right] - 0{,}5.\ln\left[\frac{\sqrt{\left([2.h_c]^2 + [2.s_p]^2\right)}}{2.s_p}\right] \tag{17.36}$$

$$P_2 = -0{,}5.\ln\left[\frac{\sqrt{\left([2.h_c]^2 + s_p{}^2\right)}}{s_p}\right] + \ln\left[\frac{2.h_c}{r_{bo}}\right] - 0{,}5.\ln\left[\frac{\sqrt{\left([2.h_c]^2 + s_p{}^2\right)}}{s_p}\right] \tag{17.37}$$

$$P_3 = -0{,}5.\ln\left[\frac{\sqrt{\left([2.h_c]^2 + [2.s_p]^2\right)}}{s_p}\right] - 0{,}5.\ln\left[\frac{\sqrt{\left([2.h_c]^2 + s_p{}^2\right)}}{s_p}\right] + \ln\left[\frac{2.h_c}{r_{bo}}\right] \tag{17.38}$$

but the average field strength on the surface of any conductor with radius **r** and charge + **q** coulomb/m is given by:-

$$E_{av} = \frac{+q}{2\pi\varepsilon}\text{(Volts/m)} \tag{17.39}$$

(17.39) applied to conductor 1 of the above arrangement gives:-

$$E_{1av} \approx E_{2av} \approx E_{3av} = \frac{Q}{2\pi\varepsilon.r_{bo}}\text{(Volts/m)} \tag{17.40}$$

Where:-

Q	=	charge on conductor 1 in coulomb/m
r_{bo}	=	radius of conductors 1, 2 and 3 in metres

Substitute for **Q** from (17.40)

$$E_{1av} = \frac{[V_n].2\pi\varepsilon}{[P_1].2\pi\varepsilon}.\frac{1}{r_{1bo}}$$

$$= \frac{V_n}{[P_1]}.\frac{1}{r'_{1bo}}\text{kV/cm(rms)} \tag{17.41}$$

$$E_{1av} = \frac{[V_L]}{\sqrt{3}} \cdot \frac{1}{P_{1r}} \cdot \frac{1}{r_{1bo}} \cdot \frac{1}{10^2} \text{ kV/cm(rms)} \qquad (17.42)$$

with V_L in kV (rms) and r_{bo} in metres.

Similarly for the centre phase

$$E_{2av} = \frac{[V_n].2\pi\varepsilon}{[P_2].2\pi\varepsilon} \cdot \frac{1}{r_{2bo}}$$

$$= \frac{V_n}{[P_2]} \cdot \frac{1}{r_{2bo}} \text{ kV/cm(rms)} \qquad (17.43)$$

$$E_{2av} = \frac{[V_L]}{\sqrt{3}} \cdot \frac{1}{P_{1r}} \cdot \frac{1}{r_{2bo}} \cdot \frac{1}{10^2} \text{ kV/cm(rms)} \qquad (17.44)$$

For the outer phase

$$E_{3av} = \frac{[V_n].2\pi\varepsilon}{[P_3].2\pi\varepsilon} \cdot \frac{1}{r_{3bo}}$$

$$= \frac{V_n}{[P_3]} \cdot \frac{1}{r_{3bo}} \text{ kV/cm(rms)} \qquad (17.45)$$

$$E_{3av} = \frac{[V_L]}{\sqrt{3}} \cdot \frac{1}{P_{3r}} \cdot \frac{1}{r_{3bo}} \cdot \frac{1}{10^2} \text{ kV/cm(rms)} \qquad (17.46)$$

17.2.2.3 Effective field strength for typical outdoor busbar configurations

Equation 17.14 applied to horizontal busbar arrangements, using single, double and bundle conductors give values for effective field strengths at line voltages of 765 kV, 400 kV and 275 kV respectively. Results are shown in Tables 24.3 to 24.9 in Appendix D of this dissertation.

For the conductor system to be corona free, the effective field strength (average voltage gradient at the surface of the bus conductor) E_e must be less than the corona threshold surface field strength E_c.

$E_e < E_c \Rightarrow$ no corona

The program **BUSBAR** was developed to calculate the effective field strength E_e and compare it to the value E_c, the equation of which was determined experimentally and fitted with the equations 17.2 and 17.3. A typical **BUSBAR** report sheet is shown below.

BUSBAR REPORT SHEET

CORONA CALCULATION PROGRAM

INTRODUCTION

A computer program based on the image method as discussed in the previous section was developed for **calculation of conductor surface field strengths**, as well as corona threshold limits.

The corona calculation program will calculate the maximum electric field strength as well as the corona threshold limit for single and bundle stranded conductors as well as tubular conductors.

An example of the input and output of the program is shown below for a 200 mm diameter tubular conductor at 1800 m above sea level.

CORONA CALCULATION PROGRAM

System Voltage (kV) 400.00000000
Number of Phases 3
Phase Spacing (m) 7.00000000
Height above Ground (m) 5.80000000
No of Conductors per bundle 1
Conductor Diameter (mm) 200.00000000
Centipede = 26.46 Zebra = 28.6 Bull = 38.4
Conductor on Circle Y/N N
Bundle should be centered round phase position
Input Co-ordinates should be relative to phase position
and be given in mm
X Pos. of cond. No.1 1.00000000
Y Pos. of cond. No.1 1.00000000
Input effective bundle diameter in mm 1.00000000
CORONA THRESHOLD LIMITS
Relative Air Density 0.80000000
Surface Factor: 0.95000000
Polished Tubes = 1.0
Extruded Tubes = 0.95
Stranded Conductor = 0.8

Maximum Electric Field Strength

Corona Threshold limit = **17.024 kV/cm**

Phase 1: **5.3797 kV/cm Corona Absent**

Phase 2: **5.6419 kV/cm Corona Absent**

Phase 3: **5.3797 kV/cm Corona Absent**

Another try? Y/N Y

If the equipment conductor height ($\mathbf{h_c}$) as determined in (18.1) meets the corona performance criterion $\mathbf{E_e < E_c}$, then as far as corona performance is concerned, that height is fixed. If, however, $\mathbf{E_e}$ is very close to $\mathbf{E_c}$ or $\mathbf{E_e \geq E_c}$, corona will result, requiring the conductor height ($\mathbf{h_c}$) to be increased. $\mathbf{E_e}$ is recalculated for a larger value of $\mathbf{h_c}$. $\mathbf{E_e}$ should be at least 5-6kV/m less than $\mathbf{E_c}$ to allow for slight variations in the conductor height. A suitable conductor height can be determined through iteration, increasing $\mathbf{h_c}$ until $\mathbf{E_c = (E_e + 5)\ kV/m}$

18. SUBSTATION CONDUCTOR HEIGHTS DETERMINED BY ALLOWABLE ELECTRIC AND MAGNETIC FIELD STRENGTHS

18.1 Background

For some time now, there is an international perception that electromagnetic fields at power frequencies present a health hazard to living tissue, particularly humans where it has been claimed that these fields can cause certain types of cancers, i.e. brain tumours and leukaemia. There has been much publicity and research to establish links between cause and effect, but no conclusive evidence has been found.

NRPB Advisory Group on non-ionising radiation power frequency electromagnetic fields and risk of cancer, issue a statement in March 2001 as follows:-

"Laboratory experiments have provided no good evidence that extremely low frequency electromagnetic fields are capable of producing cancer, nor do human epidemiological studies suggests that they cause cancer in general. There is, however, some epidemiological evidence that prolonged exposure to higher levels of power frequency magnetic fields is associated with a small risk of leukaemia in children. In practice, such levels of exposure are seldom encountered by the general public in the UK. In the absence of clear evidence of a carcinogenic effect in adults, or of a plausible explanation from experiments on animals or isolated cells, the epidemiological evidence is currently not enough to justify a firm conclusion that such fields cause leukaemia in children. Unless, however, further research indicates that the finding is due to chance or some currently unrecognised artefact, the possibility remains that intense prolonged exposures to magnetic fields can increase the risk of leukaemia in children."

Eskom's has taken a middle of the road stance on this issue is explained in the following statement made:-

"**1. Preamble**

"The health, safety and well-being of the general public, our customers and staff are of prime concern to Eskom

"Research into the possible biological effects of exposure to EMF has thus far yielded inconclusive results. However, some epidemiological studies indicate a possible link between long term exposure to EMF and certain types of cancer. It is widely agreed that research should continue until firm conclusions are reached as to whether any detrimental health effects exist.

"Internationally, power utilities are increasingly finding it necessary to inform their staff and the studies are often contradictory and difficult to replicate.

"A national EMF forum, linked to the international EMF Research Co-ordinators Group was established in 1990, with Eskom as a member.

"**2. Policy**

"Eskom will continue to actively participate in national and international initiatives on the biological effects of EMF. Eskom will continue to review the findings to EMF research and, **through the design and operation of its plant, to mitigate any possible adverse effects on the general public, its customers and its staff.**

"**3. Strategy**

"Eskom supports the view that the medical research council will select and co-ordinate appropriate research on the biological effects of EMF in South Africa.

"Eskom supports the view that South Africa should support international studies on the biological effects of EMF, but confine research to areas where local expertise and unique conditions can complement international efforts. Eskom enjoys support on this view from relevant environmental bodies and municipalities.

"Eskom will measure and calculate electric and magnetic field intensities and related exposure levels associated with the provision and use of electrical energy. This information will be made available upon request. Eskom will continue to take part in the National EMF Forum.

"Eskom will endeavour to inform its staff on EMF topics.

"**Eskom will be guided by the limits for magnetic fields as given by the 'International Radiation Protection Association (IRPA) when designing transmission lines" which will include substations at the terminal ends.**

"Eskom will use an electric field limit of 10kV/m in the design of transmission lines.

"Live line work will continue.

"Eskom will review its policy on EMF as new information becomes available."

18.2 Electric Field Limits

The electric field from overhead live conductors, typically measured at 1 to 1,7m above the ground level, is a function of the busbar configuration, and is directly proportional to the system voltage. The busbar configuration includes conductor height above the ground,

conductor phase arrangement, conductor diameter, number of sub-conductors per phase and the presence and size of ground wires. Electric fields are measured in kV/m.

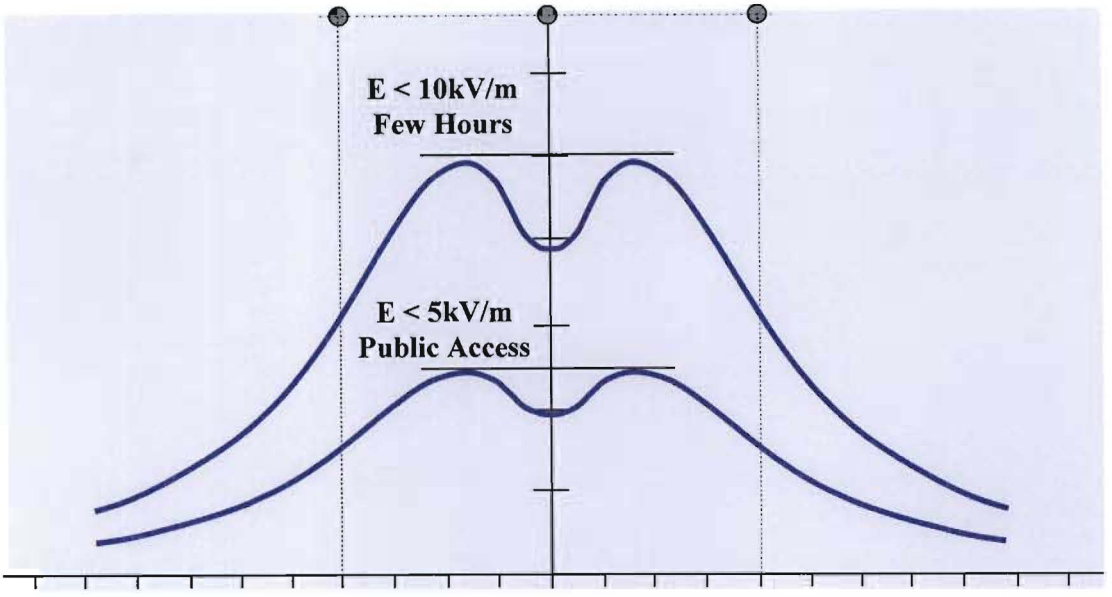

Figure 18.1: Recommended Safe Levels of Electric Field Strength for Different Periods of Exposure

The recommended safe electric field strengths are given as 10kV/m within a live chamber where it is envisaged that electrical personnel would not spend more than a few hours carrying out maintenance work, and so limiting exposure to slightly higher fields than that is recommended for areas where the public has access, viz 5kV/m. This is summarised in Figures 18.1 and 18.2 showing the recommended maximum values for various positions in and around the substation.

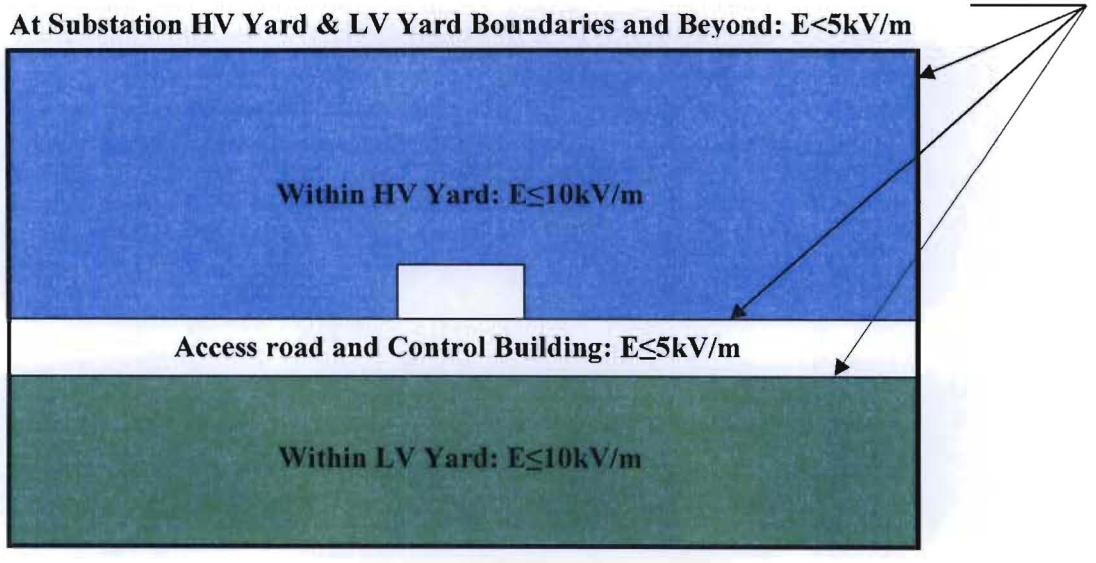

Figure 18.2: Allowable Electric Field Strength (E) in Designated Areas

The electric field strength for a given system voltage is dependent upon a number of factors, one of which is the height of the conductors above the ground. In order to determine the minimum heights of the first level of conductor, the electric field strength must satisfy the above criterion of 10kV/m at any point in the substation. Figure 18.3 shows a typical elevation on an equipment bay. The tubular conductor will vary in height due to the different equipment connection heights one should use the average height of the conductor as a starting point.

$$\mathbf{h_{avec}} = \frac{\mathbf{1}}{\ell_{tot}} \sum_{1}^{n} \mathbf{h_{ai}}.\ell_{ai} \qquad (18.1)$$

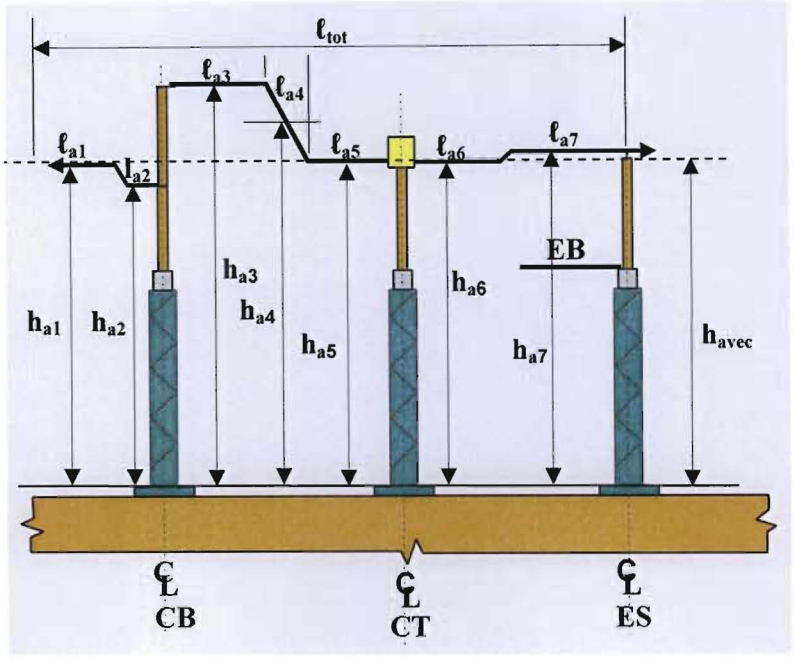

Figure 18.3: Minimum Height of First Level of Conductor (h_{avec})

There are a number of software packages available that can be used to model the different substation conductor configurations, taking into account the various conductor levels. The software package CDEGS (Current Distribution Electromagnetic and Grounding Systems) was used to determine the electric field strengths for a 3-phase bus conductor system at different conductor heights (h_c), a given maximum system voltage (U_m), conductor outer diameter (d_{bo}) and bus phase spacing (s_p). The results are plotted in terms of Electric Field Strength in kilo-volts per metre (kV/m) verses conductor height above 1,8m above ground level as shown in Figure 18.4. The value of 1,8m above ground level is chosen as this represents the height of the head of an average man, the head being the highest point of a human and is the part of the human anatomy that would be most sensitive to electromagnetic fields.

Figure 18.4 represents only one system voltage, at a given phase spacing, for a given conductor size. In order to provide as much information as possible in the choice of the tubular conductor, a series of curves have been developed. From the data used to develop this series of curves, one can develop curves for determining the electric field strengths for a 3-phase bus conductor system at different bus phase spacings (s_p), a given maximum system voltage (U_m), conductor outer diameter (d_o) and conductor height (h_c) such as shown in Figure 18.5. The results are plotted in terms of Electric Field Strength in kilo-volts per metre (kV/m) verses conductor phase spacing in metres (m) (See Appendix E).

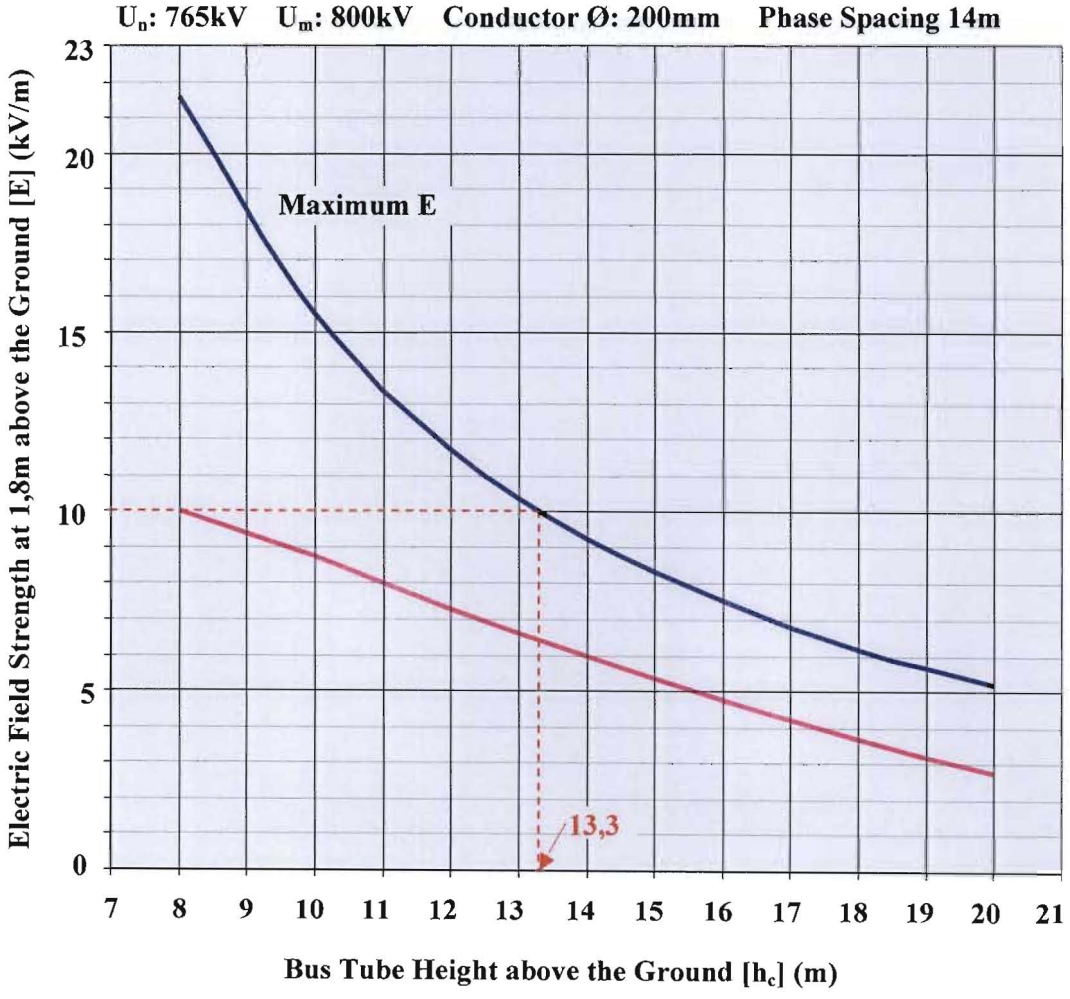

Figure 18.4: Maximum Electric Field Strength (kV/m) vs Bus Conductor Height (m)

[Printout from Excel based Busbar Programme]

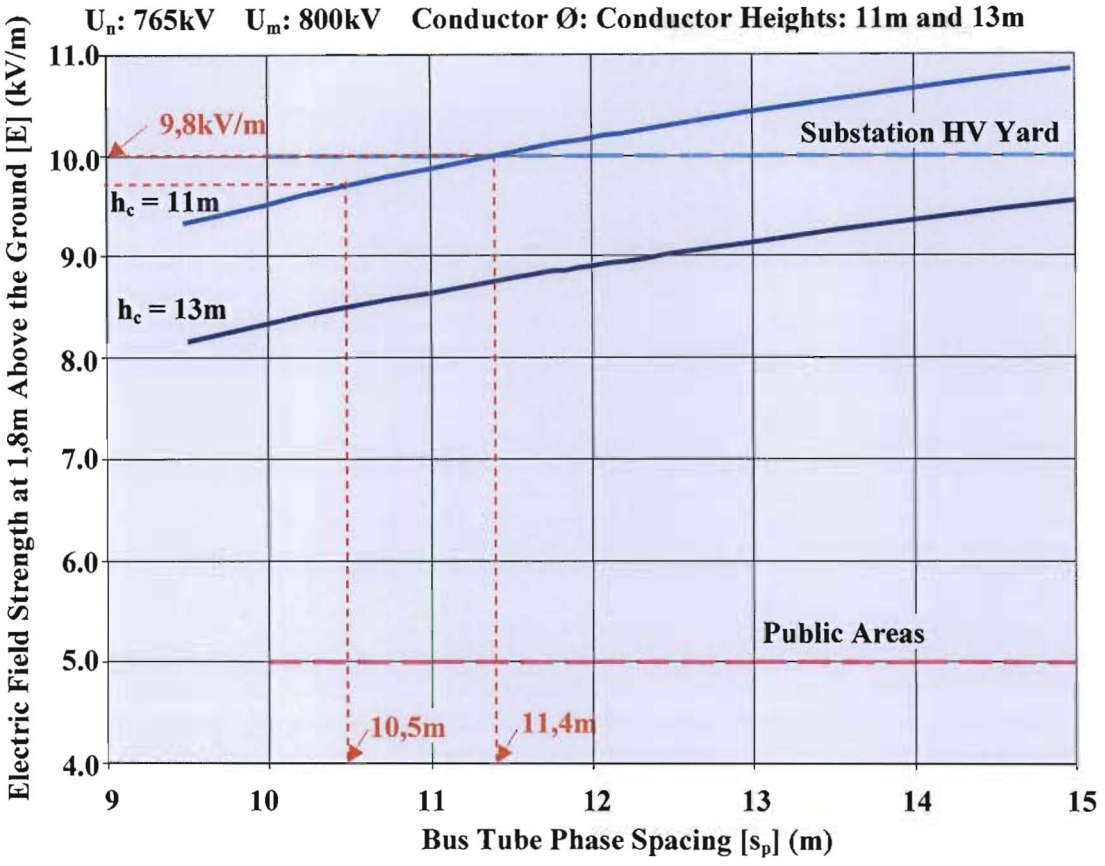

Figure 18.5: Maximum Electric Field Strength (kV/m) vs Phase Spacing (m)

[Printout from Excel based Busbar Programme]

The increase in electric field strength with increase in phase spacing is due to the weaker cancellation effect (destructive interference) as the phases move further apart from each other. The electric fields are 120° out of phase with each other. As illustarated above, the higher the conductors are above the ground, the lower is the electric field strength.

In order to ensure an electric field strength of 10kV and below, the 765kV busbar phases require to be no more than 11,4m apart. Any value more than this will lead to higher phase electric field strengths, and any value less than this will obviously have lower electric field strengths.. In the latter case, however, phase-to-phase clearance is to be maintained. If a phase-to-phase value of 10,5m is used, for example, the electric field strength will be within the limits and the phase-to-phase clearance will be satisfied.

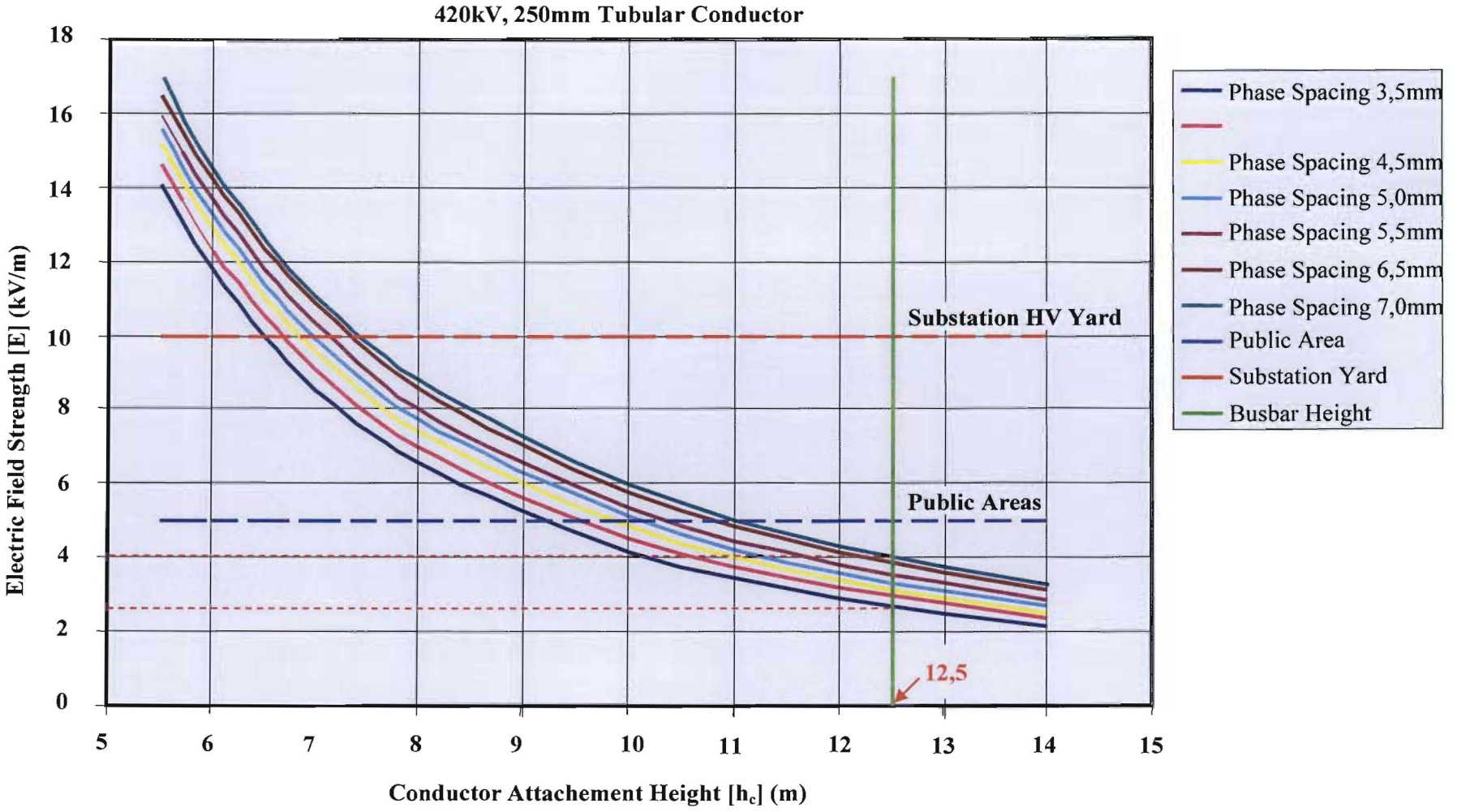

Figure 18.6: Electric Field Strength [E] (kV/m) at 1,8m vs Conductor Height [h_c] (m)

[Printout from Excel based Busbar Programme]

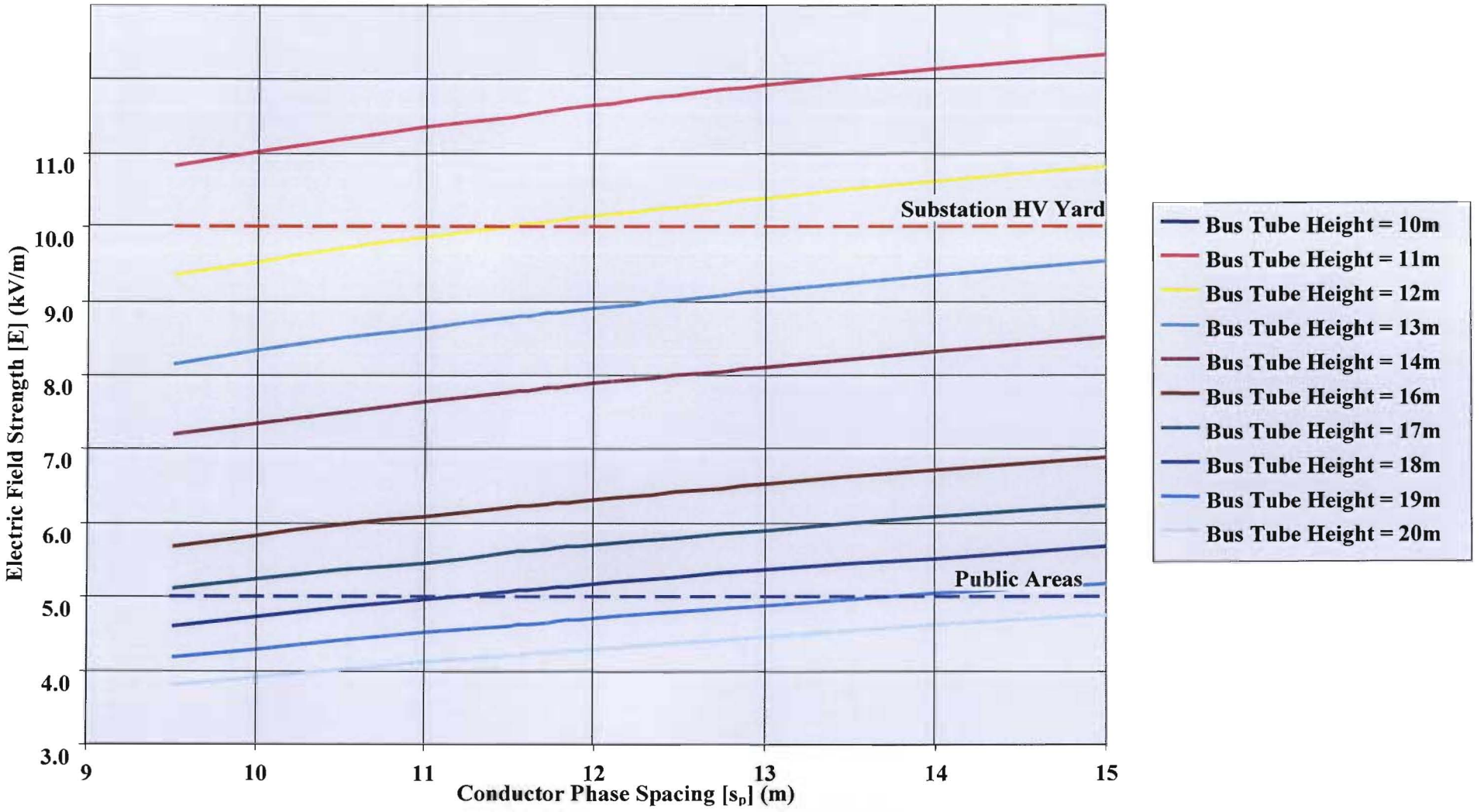

Figure 18.7: Printout for Excel based Busbar Programme of Electric Field Strength [E] (kV/m) at 1,8m vs Phase Spacing [s] (m)

[Printout from Excel based Busbar Programme]

18.3 Functional Forms of Regression Analysis on Electric and Magnetic Field Study Data

Having modelled the 3-phase bus ducting system using CEDEGS and obtained the data from the electric and magnetic field studies it is necessary to 'fit' a curve to represent the data in functional form. It is necessary to determine how well the sample regression line fits the data. If all the observations were to lie on the regression line, one would obtain a perfect fit, but this is more the exception than the rule. Generally, there will be some deviation from this regression line measured as positive and negative errors ($\mathbf{e}^i$). The resulting regression function will then aid the designer in obtaining intermediate values rapidly for use in the design of the bursar system. Considering regression models that are nonlinear in the variables and are either linear in the parameters or can be made so by suitable transformations of the variables.

18.3.1 Electric Field Study Data

The two nonlinear functions illustrated in Figure 18.4 and Figure 18.5 is of the form:

$$\mathbf{E}_i = \beta_1 . \mathbf{h}_{ci}^{\beta 2} . \mathbf{e}^{ui} \qquad (18.2)$$

Where:-

$\mathbf{E}_i$ = The electric field as measured at a height of 1,8m above the ground for a given bus ducting height ($\mathbf{h}_i$) above the ground level or the electric field as measured at a height of 1,8m above the ground for a given bus duct phase spacing keeping the height of the bus ducting above the ground constant (one of a number of such stimuli – response observations) (kV/m)

$\mathbf{h}_{ci}$ = The height of the bus duct above ground level keeping the phase spacing constant, or the phase spacing of the three phases keeping the height of the bus ducting above the ground constant (m)

β_1 = Intercept coefficient

β_2 = Slope or gradient coefficient

$\mathbf{u}_i$ = The stochastic distribution term substituting for all excluded or omitted variables

Having carried out the required electric and magnetic field studies and obtained the applicable data ($\mathbf{h}_{ci}$,$\mathbf{E}_i$), the next step is to try and fit a curve to the data. In order to do this, the above function must be transformed to appear as a linear relationship. Applying the natural logarithm to both sides

$$\ln E_i = \ln\left(\beta_1 . h_{ci}^{\beta_2} . e^{u_i}\right) \tag{18.3}$$

$$\ln E_i = \ln\beta_1 + \beta_2 . \ln . h_{ci} + u_i \tag{18.4}$$

$$\hat{E}_i = \hat{\beta}_1 + \beta_2 . \hat{h}_{ci} + u_i \tag{18.5}$$

Where:-

$\hat{E}_i$ = The transformed electric field strength (again one of a number of such transformed stimuli – response observations)

$\hat{h}_{ci}$ = The transformed bus duct height above ground level (phase spacing constant) or phase spacing (height above the ground constant)

$\hat{\beta}_1$ = The Intercept coefficient of the transformed function

β_2 = Slope or gradient coefficient of the transformed function

u_i = The transformed stochastic distribution term

Equation (18.5) then becomes the transformed function through which the intercept and slope parameters are to be determined. β_2 can obviously be determined directly, however, the intercept value requires a reverse transformation

$$\beta_1 = e^{\hat{\beta}_1} \tag{18.6}$$

From regression analysis

$$\hat{\beta}_1 = \frac{\sum_1^{Ne} \hat{h}_{ci}^2 \sum_1^{Ne} \hat{E}_i - \sum_1^{Ne} \hat{H}_i . \sum_1^{Ne} \hat{h}_{ci} . \hat{E}_i}{N_e . \sum_1^{Ne} \hat{h}_{ci}^2 - \left(\sum_1^{Ne} \hat{h}_{ci}\right)^2} \tag{18.7}$$

Where:-

N_e = The number of 'height – electric field' observations

$$\beta_2 = \frac{N_e . \sum_1^{Ne} \hat{h}_{ci} . \hat{E}_i - \sum_1^{Ne} \hat{h}_{ci} . \sum_1^{Ne} \hat{E}_i}{N_e . \sum_1^{Ne} \hat{h}_{ci}^2 - \left(\sum_1^{Ne} \hat{h}_{ci}\right)^2} \tag{18.8}$$

In order to determine the degree of correlation between the two variables $\hat{h}_{ci}$ and $\hat{E}_i$, it is necessary to first calculate the sample correlation coefficient **r**.

$$r = \frac{Ne.\sum_{1}^{Ne} \hat{h}_{ci}.\hat{E}_i - \sum_{1}^{Ne} \hat{h}_{ci}.\sum_{1}^{Ne} \hat{E}_i}{\sqrt{\left(\left[Ne.\sum_{1}^{Ne} \hat{h}_{ci}^2 - \left(\sum_{1}^{Ne} \hat{h}_{ci}\right)^2\right].\left[N.\sum_{1}^{Ne} \hat{E}_i^2 - \left(\sum_{1}^{Ne} \hat{E}_i\right)^2\right]\right)}} \quad (18.9)$$

The coefficient of determination r^2 on the other hand measures the proportion or percentage of the total variation in **E** explained by the regression model.

$$r^2 = \frac{\left(Ne.\sum_{1}^{Ne} \hat{h}_{ci}.\hat{E}_i - \sum_{1}^{Ne} \hat{h}_{ci}.\sum_{1}^{Ne} \hat{E}_i\right)^2}{\left[Ne.\sum_{1}^{Ne} \hat{h}_{ci}^2 - \left(\sum_{1}^{Ne} \hat{h}_{ci}\right)^2\right].\left[Ne.\sum_{1}^{Ne} \hat{E}_i^2 - \left(\sum_{1}^{Ne} \hat{E}_i\right)^2\right]} \quad (18.10)$$

Once it has been determined that the model used fits the observed data sufficiently well, the resulting relationship can be used within the programme developed in parallel with this text in order to chose the bus duct size and determine the required conductor heights to meet the electric (**E**) and magnetic field (**B**) limits.

18.3.2 The Matrix Form

As part of the whole design process, it is necessary to be able to predict what the electric field strength (E_i) would be at 1,8m above the ground for any set of parameters of height of conductor above the ground (h_{aveci}), conductor phase spacing (s_{pi}), tube diameter (d_{oi}) and system voltage (V_i). The single variable regression model is now generalised as a multi-variable regression model. It is assumed that a function of the form shown in (18.11) most appropriately fits the data, implying that a four variable regression model is applicable here.

$$E_i = \beta_1.h_{ci}^{\beta 2}.s_{pi}^{\beta 3}.d_{oi}^{\beta 4}.V_i^{\beta 5}.e^{u_i} \quad (18.11)$$

$$\ln E_i = \ln\left(\beta_1.h_{ci}^{\beta 2}.s_{pi}^{\beta 3}.d_{oi}^{\beta 4}.V_i^{\beta 5}.e^{u_i}\right) \quad (18.12)$$

$$\ln E_i = \ln\beta_1 + \beta_2.\ln(h_{ci}) + \beta_3.\ln(s_{pi}) + \beta_4.\ln(d_{oi}) + \beta_5.\ln(V_i) + u_i \quad (18.13)$$

$$\hat{E}_i = \hat{\beta}_1 + \beta_2.\hat{h}_{ci} + \beta_3.\hat{s}_{pi} + \beta_4.\hat{d}_{oi} + \beta_5.\hat{V}_i + u_i \quad (18.14)$$

Where:-

$\hat{E}_i$	=	The transformed electric field strength
$\hat{h}_{ci}$	=	The transformed bus duct height
$\hat{s}_{pi}$	=	The transformed phase spacing

$\hat{d}_{oi}$ = The transformed bus duct outer diameter

$\hat{V}_i$ = The transformed system voltage

u_i = The transformed stochastic distribution term which becomes very small as the "fit" becomes better

The above expressions illustrated in paragraph 18.3.1 are adequate for two or three variable functions, however, when there are multiple variables as in (18.11) and a large amount of data is available, it becomes too complex to solve in this manner. The best approach is to apply the matrix form.

$$[\beta] = [[X]^T.[X]]^{-1}.[[X]^T.[E]] \qquad (18.15)$$

Where:-

$[\beta]$ = A 5x1 matrix of coefficients defined above

$[X]$ = A Nx5 matrix of the variables $\hat{h}_{ci}$, $\hat{s}_{pi}$, $\hat{d}_{oi}$, and $\hat{V}_i$

$[X]^T$ = The 5xN transposed matrix $[X]$ of the variables $\hat{h}_{ci}$, $\hat{s}_{pi}$, $\hat{d}_{oi}$, and $\hat{V}_i$

$[E]$ = A Nx1 matrix of the electric field values

It is necessary to transform the data obtained from the studies and find the natural logarithms of each value as required by (18.12)

$$\begin{bmatrix} \ln\beta_1 \\ \beta_2 \\ \beta_3 \\ \beta_4 \\ \beta_5 \end{bmatrix} = \left[\begin{bmatrix} 1 & 1 & 1 & . & 1 \\ \ln(h_{ave12}) & \ln(h_{ave22}) & \ln(h_{ave32}) & . & \ln(h_{aveN2}) \\ \ln(s_{p13}) & \ln(s_{p23}) & \ln(s_{p33}) & . & \ln(s_{pN3}) \\ \ln(d_{o14}) & \ln(d_{o24}) & \ln(d_{o34}) & . & \ln(d_{oN4}) \\ \ln(V_{15}) & \ln(V_{25}) & \ln(V_{35}) & . & \ln(V_{Nk}) \end{bmatrix} . \begin{bmatrix} 1 & \ln(h_{ave12}) & \ln(s_{p13}) & \ln(d_{o14}) & \ln(V_{15}) \\ 1 & \ln(h_{ave22}) & \ln(s_{p23}) & \ln(d_{o24}) & \ln(V_{25}) \\ 1 & \ln(h_{ave32}) & \ln(s_{p33}) & \ln(d_{o34}) & \ln(V_{35}) \\ . & . & . & . & . \\ 1 & \ln(h_{aveN2}) & \ln(s_{pN3}) & \ln(d_{oN4}) & \ln(V_{N5}) \end{bmatrix}\right]^{-1}$$

$$. \left[\begin{bmatrix} 1 & 1 & 1 & . & 1 \\ \ln(h_{ave12}) & \ln(h_{ave22}) & \ln(h_{ave32}) & . & \ln(h_{aveN2}) \\ \ln(s_{p13}) & \ln(s_{p23}) & \ln(s_{p33}) & . & \ln(s_{pN3}) \\ \ln(d_{o14}) & \ln(d_{o24}) & \ln(d_{o34}) & . & \ln(d_{oN4}) \\ \ln(V_{15}) & \ln(V_{25}) & \ln(V_{35}) & . & \ln(V_{Nk}) \end{bmatrix} . \begin{bmatrix} \ln E_1 \\ \ln E_2 \\ \ln E_3 \\ . \\ \ln E_N \end{bmatrix}\right] \qquad (18.16)$$

To simplify the above matrix, the cap is applied to the symbols to suit the series of equations generalised by (18.15).

$$\begin{bmatrix}\hat{\beta}_1\\ \beta_2\\ \beta_3\\ \beta_4\\ \beta_5\end{bmatrix} = \left[\begin{bmatrix}1 & 1 & 1 & . & 1\\ \hat{h}_{ave12} & \hat{h}_{ave22} & \hat{h}_{ave32} & . & \hat{h}_{aveN2}\\ \hat{s}_{p13} & \hat{s}_{p23} & \hat{s}_{p33} & . & \hat{s}_{pN3}\\ \hat{d}_{o14} & \hat{d}_{o24} & \hat{d}_{o34} & . & \hat{d}_{oN3}\\ \hat{V}_{15} & \hat{V}_{25} & \hat{V}_{35} & . & \hat{V}_{N5}\end{bmatrix}\cdot\begin{bmatrix}1 & \hat{h}_{ave12} & \hat{s}_{p13} & \hat{d}_{o14} & \hat{V}_{15}\\ 1 & \hat{h}_{ave22} & \hat{s}_{p23} & \hat{d}_{o24} & \hat{V}_{25}\\ 1 & \hat{h}_{ave32} & \hat{s}_{p33} & \hat{d}_{o34} & \hat{V}_{35}\\ . & . & . & . & .\\ 1 & \hat{h}_{aveN2} & \hat{s}_{pN3} & \hat{d}_{oN4} & \hat{V}_{N5}\end{bmatrix}\right]^{-1} \cdot \left[\begin{bmatrix}1 & 1 & 1 & . & 1\\ \hat{h}_{ave12} & \hat{h}_{ave22} & \hat{h}_{ave32} & . & \hat{h}_{aveN2}\\ \hat{s}_{p13} & \hat{s}_{p23} & \hat{s}_{p33} & . & \hat{s}_{pN3}\\ \hat{d}_{o14} & \hat{d}_{o24} & \hat{d}_{o34} & . & \hat{d}_{oN3}\\ \hat{V}_{15} & \hat{V}_{25} & \hat{V}_{35} & . & \hat{V}_{N5}\end{bmatrix}\cdot\begin{bmatrix}\hat{E}_1\\ \hat{E}_2\\ \hat{E}_3\\ .\\ \hat{E}_N\end{bmatrix}\right] \quad (18.17)$$

Once the $[\beta]$ matrix has been determined, the values of β_2, β_3, β_4 and β_5 can be read off directly. For β_1, however, the value $\hat{\beta}_1$ needs to be converted back in the following manner:

$$\beta_1 = e^{\hat{\beta}1} \quad (18.18)$$

Having determined all the β values, it is a matter of substituting them back into (18.11). If the curve "fits" the data to a high degree, i.e. there is a high degree of correlation between the data and the "fitted" curve, the stochastic distribution term tends to zero. The value for the electric field for any set of parameters can then be determined.

18.3.3 The "Goodness" of Fit

In order to access how well the data fits the curve, it is necessary to arrive at the Coefficient of Determination $\mathbf{R^2}$

$$\mathbf{r^2} = \left(\frac{[\beta].[X]^T[E] - N_e.\overline{E}^2}{[E]^T.[E] - N_e.\overline{E}^2}\right) \quad (18.19)$$

18.3.4 Reporting the results of the Study

The study input data was arranged in rows and columns of conductor height (has required by the N x 4 matrix '**X**' and output data (the calculated electric field) in a single column as required by the N x 1 matrix **E** given in (18.17)

$$[\beta] = \left[[X]^T . [X]\right]^{-1} . \left[[X]^T . [E]\right] \quad \text{(from 18.15)}$$

5 x 1 5 x N N x 5 5 x N N x 1

In this study, 369 sets of data were produced, providing sufficient elements to accurately fit a curve of the form given in (18.11). With the aid of the "MATHCAD" software package and, importing the **[X]** and **[E]** matrices from an Excel spreadsheet, the following results were obtained:

$$\begin{bmatrix} \hat{\beta}_1 \\ \beta_2 \\ \beta_3 \\ \beta_4 \\ \beta_5 \end{bmatrix} = \begin{bmatrix} -2.177 \\ -1.798 \\ 0.43 \\ 0.22 \\ 1.003 \end{bmatrix}$$

$\hat{\beta}_1 = -2.177$

$\beta_1 = e^{-2.177}$

$= 0.133$

$\beta_2 = -1.789$

$\beta_3 = 0.43$

$\beta_4 = 0.22$

$\beta_5 = 1.003$

The "goodness" of the fit

$$\mathbf{r}^2 = \left(\frac{[\beta].[\mathbf{X}]^T[\mathbf{E}] - \mathbf{N_e}.\overline{\mathbf{E}}^2}{[\mathbf{E}]^T.[\mathbf{E}] - \mathbf{N_e}.\overline{\mathbf{E}}^2} \right) \quad \text{(from 18.19)}$$

$$\mathbf{r}^2 = \left(\frac{\mathbf{A} - \mathbf{C}}{\mathbf{B} - \mathbf{C}} \right) \quad (18.20)$$

$$\mathbf{A} = [\beta].[\mathbf{X}]^T[\mathbf{E}] \quad (18.21)$$

$= 2.618.10^3$

$$\mathbf{B} = [\mathbf{E}]^T.[\mathbf{E}] \quad (18.22)$$

$= 2.619.10^3$

$$\mathbf{C} = \mathbf{N_e}.\overline{\mathbf{E}}^2 \quad (18.23)$$

$N = 675$

$\overline{\mathbf{E}} = 1.89$

$\mathbf{C} = 675.1.89$

$= 1.276.10^3$

$$\mathbf{r}^2 = \left(\frac{\mathbf{A} - \mathbf{C}}{\mathbf{B} - \mathbf{C}} \right)$$

$$= \left(\frac{2.618.10^3 - 1.276.10^3}{2.619.10^3 - 1.276.10^3} \right) \quad \text{(from 18.20)}$$

$= 0.999$

The value of 0.999 for $\mathbf{R^2}$ implies an exceptionally good fit of the curve to the data, hence the stochastic term $\mathbf{u_i}$ is virtually zero and $\mathbf{e^{ui}}$=1

$$\mathbf{E_i = 0.133.h_{bi}^{-1.789}.s_{pi}^{0.43}.d_{boi}^{0.22}.V_{mi}^{1.003}} \quad (18.24)$$

Where:-

$\mathbf{E_i}$ = The electric field as measured at a height of 1,8m above the ground for a given bus ducting height ($\mathbf{h_{bi}}$) above the ground level or the electric field as measured at a height of 1,8m above the ground for a given bus duct phase spacing keeping the height of the bus ducting above the ground constant (one of a number of such stimuli – response observations) (kV/m)

$\mathbf{h_{bi}}$ = The height of the bus duct above ground level keeping the phase spacing constant, or the phase spacing of the three phases keeping the height of the bus ducting above the ground constant (m)

$\mathbf{s_{pi}}$ = Phase spacing (m)

$\mathbf{d_{boi}}$ = Diameter of bus tube (mm)

$\mathbf{V_{mi}}$ = System maximum voltage (kV)

(18.24) can now be applied to calculate the value of **E** for any combination of $\mathbf{h_{ci}}$, $\mathbf{s_{pi}}$, $\mathbf{d_{oi}}$ and $\mathbf{V_i}$ that may be required in accordance with the evaluations of all the preceding chapters. These values would have been determined by the time that the value of the electric field is to be calculated. Providing the electric field limits for public exposure and substation live yards are not exceeded, no further iterations would be required.

18.3.5 Variation of Electric Field with Bus Tube Diameter

Having established the relationship of electric field **E** verses $\mathbf{h_c}$, $\mathbf{s_p}$, $\mathbf{d_{bo}}$ and $\mathbf{V_m}$, it is now possible to analyse how **E** varies with $\mathbf{d_{bo}}$ alone, keeping $\mathbf{h_c}$, $\mathbf{s_p}$ and $\mathbf{V_m}$ constant. As an example:-

$\mathbf{h_c}$= 14m, $\mathbf{s_p}$ = 15m, $\mathbf{V_m}$ = 800kV and vary 100mm $\leq \mathbf{d_{bo}} \leq$ 320mm

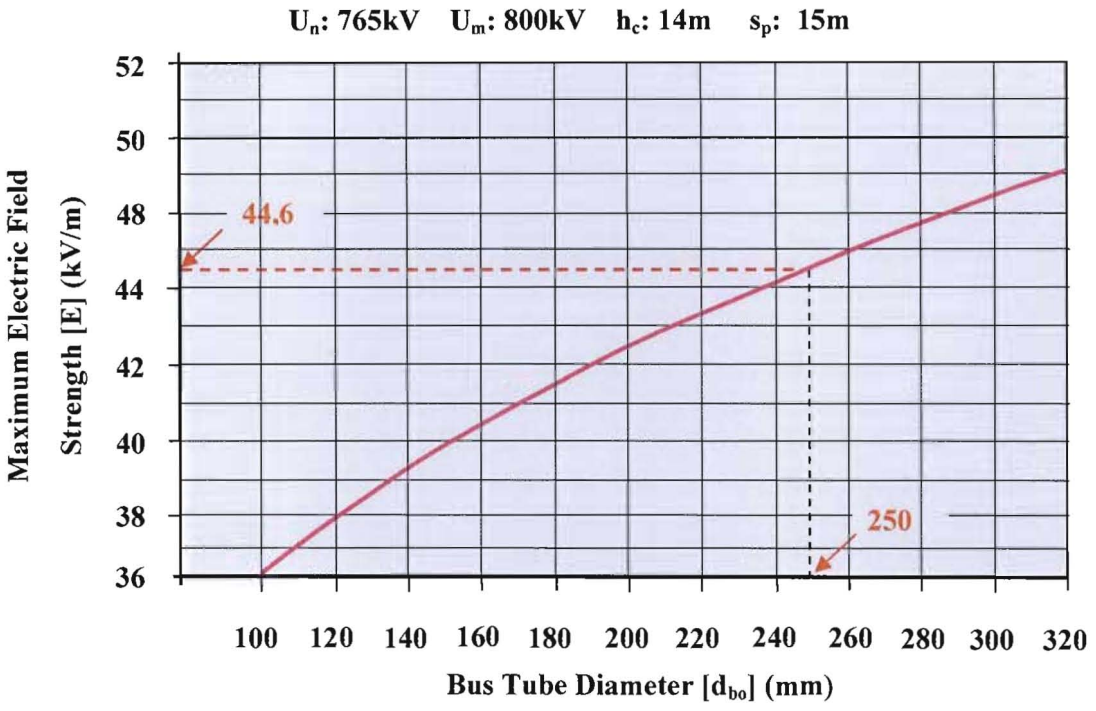

Figure 18.8: Maximum Electric Field Strength [E] (kV/m) vs Bus Tube Diameter [d_{bo}] (mm)

[Printout for Excel based Busbar Programme]

From the above study, it is clear that the magnitude of the electric field is affected by the diameter of the tube, but not to the extent as the other parameters since the practical size of the tubes vary within a relatively narrower range.

18.4 Magnetic Field Limits

The magnetic field at ground level is also a function of busbar configuration, but is directly proportional to the current flowing in the busbar conductors. The magnetic field may be influenced by secondary field sources, such as current carrying underground metallic pipelines and fences in the close proximity to the substation. Other aspects such as current imbalance and earth resistivity may further affect the magnetic field measured at ground level.

A magnetic field can be expressed in two ways, as magnetic flux density (**B**), expressed in tesla (T), or as magnetic field strength (**H**), expressed in ampere per metre (A/m). The two quantities are related by the following expression $\mathbf{B} = \mu.\mathbf{H}$ (T). μ is the permeability of free space (including non-magnet and biological material = $4\pi.10\text{-}7$ H/m)

In describing a magnetic field for protection purposes, only one of these two quantities needs to be specified.

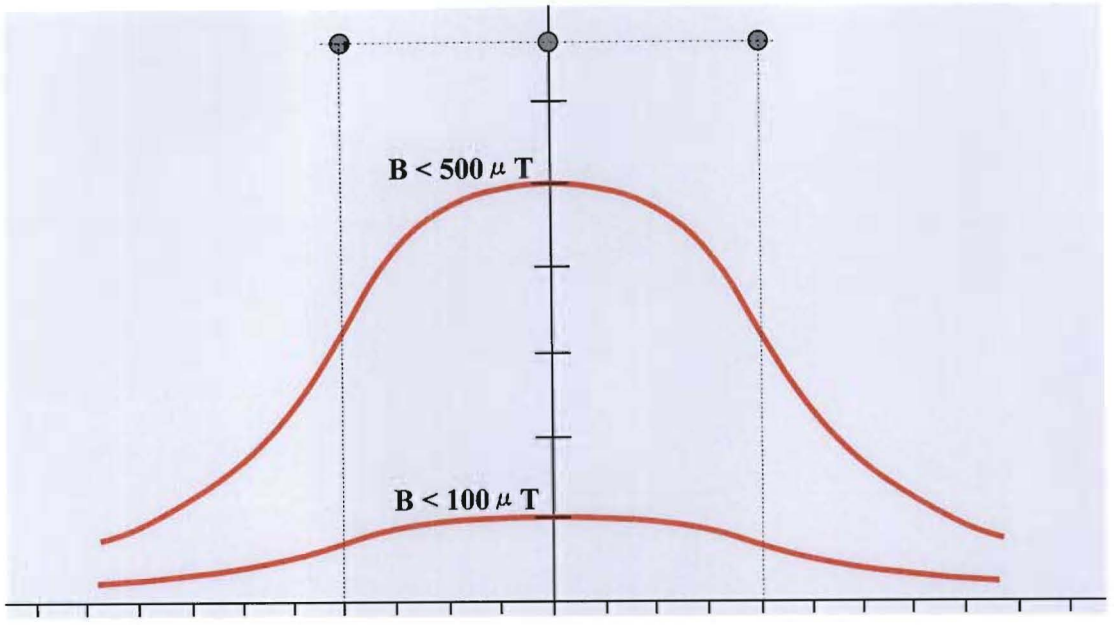

Figure 18.9: Recommended Safe Levels of Magnetic Flux Density for Different Periods of Exposure

The recommended safe magnetic flux densities are given as 500μT within a live chamber where it is envisaged that electrical personnel would not spend more than a few hours carrying out maintenance work, and so limiting exposure to slightly higher fields than that is recommended for areas where the public has access, viz. 100μT. This is summarised in Figure 18.9 showing the recommended maximum values for various positions in and around the substation.

18.4.1 ICNIRP 50Hz Exposure Guidelines

The ICNIRP 50Hz exposure guidelines are:-

Table 18.1: Electromagnetic Field Reference Levels [25]

Affected Area	Electric Field kV/m	Magnetic Field μT
Occupational	10	500
Public	5	100
Occupational	Basic restriction	10mA/m^2 **not** to be exceeded!
Public		2mA/m^2 **not** to be exceeded!

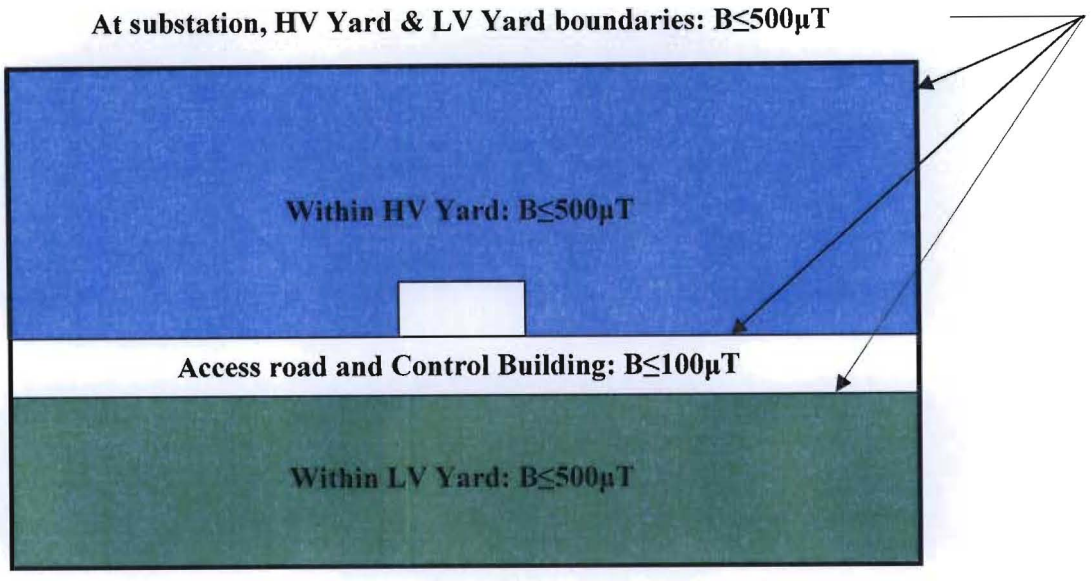

Figure 18.10: Recommended Safe Levels of Magnetic Flux Density at Various Positions in and Around a Substation for Different Durations of Exposure

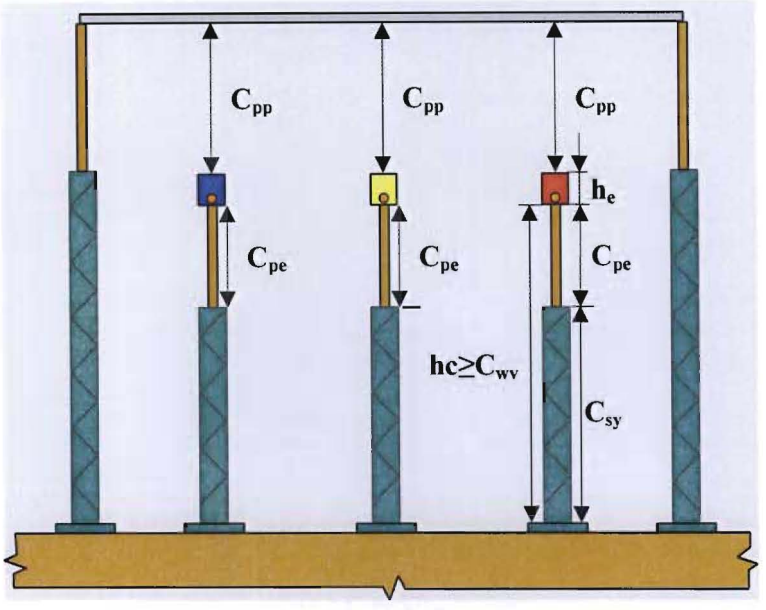

Figure 18.11: Determining the Bus Conductor Height

As with the electric field studies, the software package CDEGS was used to determine the magnetic flux density for a 3-phase bus conductor system at different conductor heights ($\mathbf{h_c}$), a given maximum system phase current ($\mathbf{I_m}$) and bus phase spacing ($\mathbf{s_p}$). The results are plotted in terms of Magnetic Flux Density in micro-Tesla (**μT**) verses conductor height above 1,8m above ground level as shown in Figure 18.10. As before, a value of 1,8m above ground level is chosen.

Figure 18.12 represents only one value of phase current ($\mathbf{I_m}$), at a given phase spacing ($\mathbf{s_p}$), for a given conductor. In order to provide as much information as possible in the choice of the tubular conductor, a series of curves have been developed. Again, from the data used to develop this series of curves, one can develop curves for determining the magnetic flux densities for a 3-phase bus conductor system at different bus phase spacing ($\mathbf{s_p}$), a given maximum phase current ($\mathbf{I_m}$) and conductor height ($\mathbf{h_c}$) such as shown in Figure 18.11. The results are plotted in terms of Magnetic Flux Density in micro-Tesla (μT) verses conductor phase spacing in metres (m) (See Appendix E).

$$B_i = \lambda_1 . h_{ci}^{\lambda 2} . s_{pi}^{\lambda 3} . I_m^{\lambda 4} . e^{ui} \qquad (18.25)$$

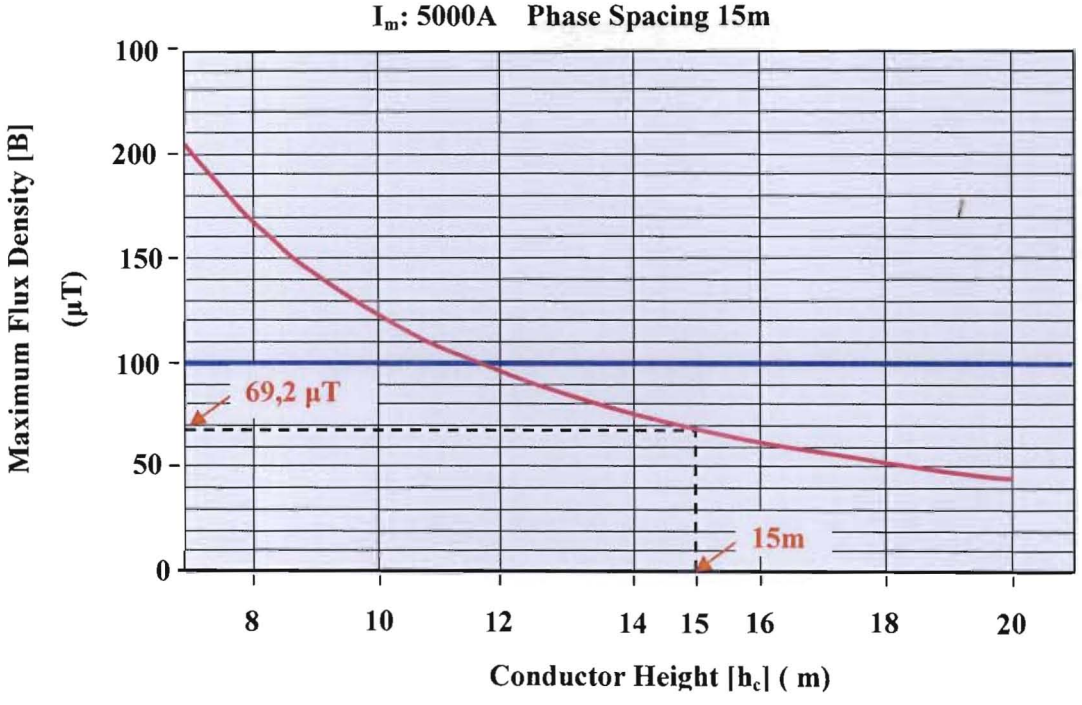

Figure 18.12: Maximum Magnetic Flux Density [B] (μT) vs Bus Conductor Height [h_c] (m) – A Single Phase Spacing

[Printout for Excel based Busbar Programme]

Applying the matrix form to (18.25):

$$[\lambda] = \left[[X]^T . [X]\right]^{-1} . \left[[X]^T . [B]\right] \qquad (18.26)$$

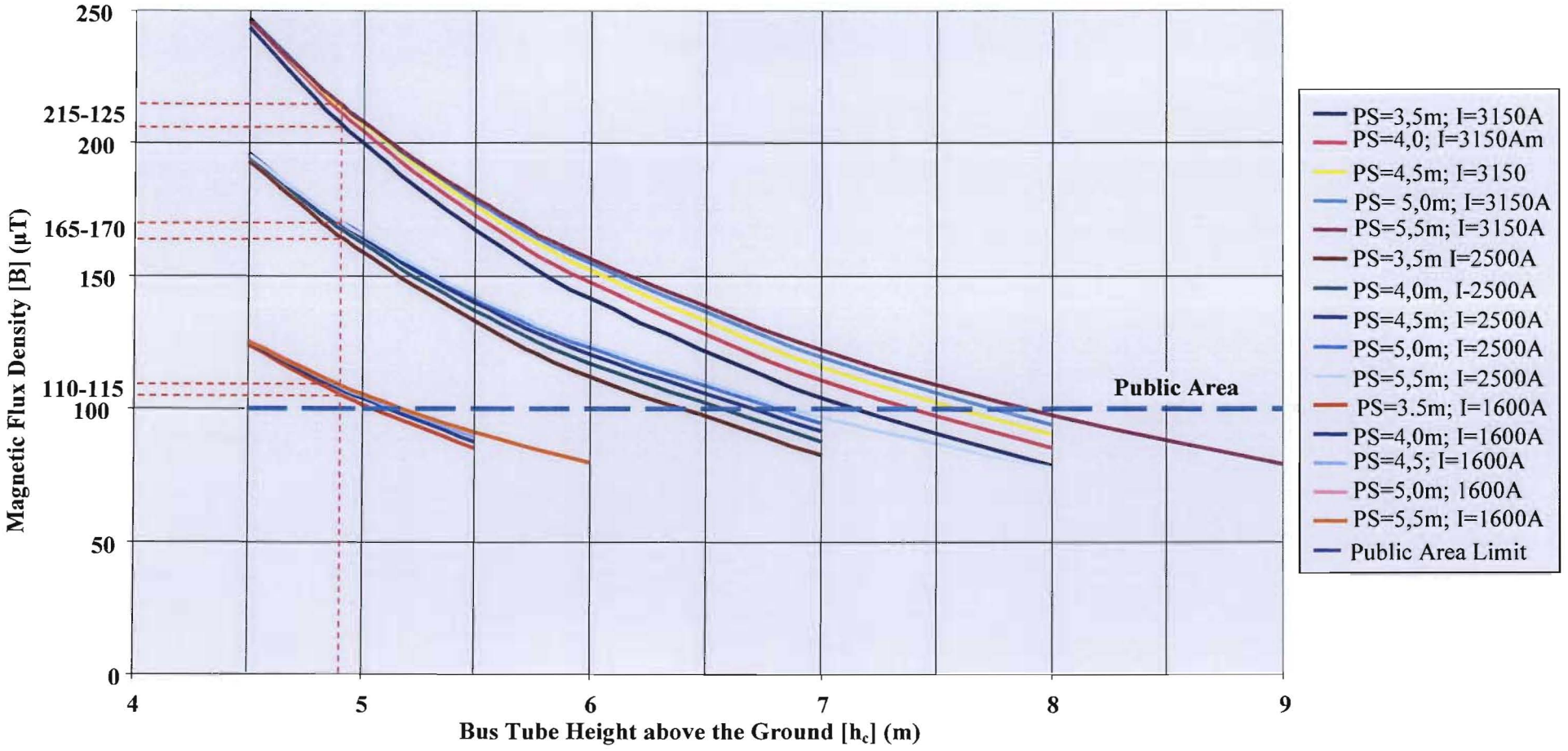

Figure 18.13: Maximum Magnetic Flux Density [B] (µT) vs Bus Conductor Height [h_c] (m) – Multiple Phase Spacings

(See Appendix E for Study Data)

[Printout from Excel based Busbar Programme]

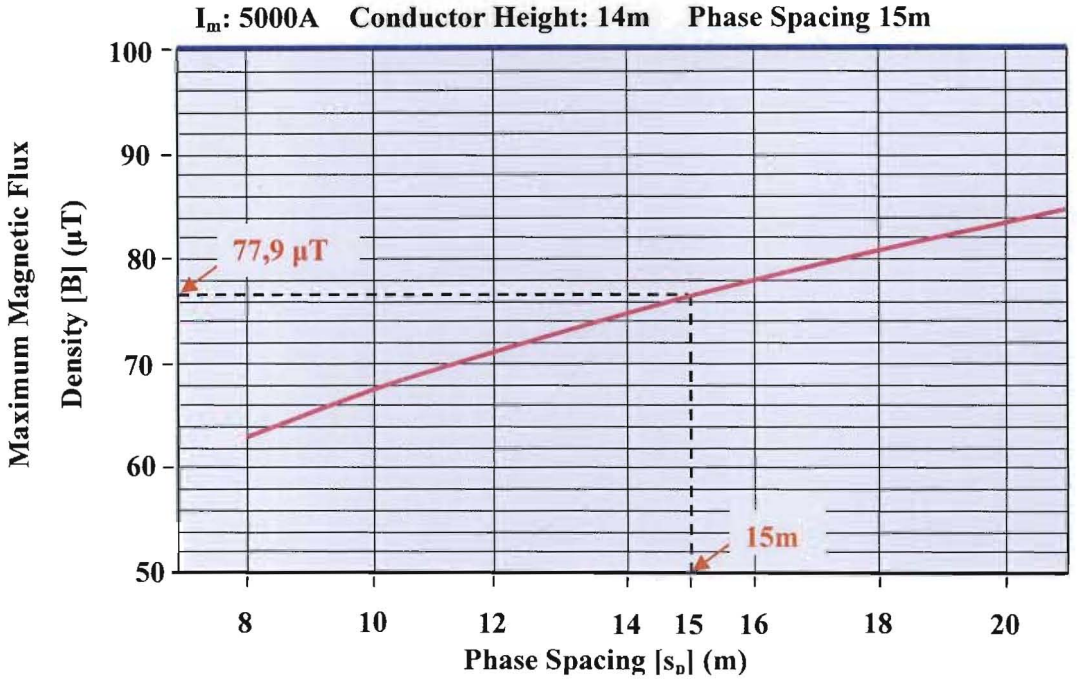

Figure 18.14: Maximum Magnetic Flux Density [B] (µT) vs Phase Spacing [s_p] (m)

A Single Bus Tube Height

[Printout from Excel based Busbar Programme]

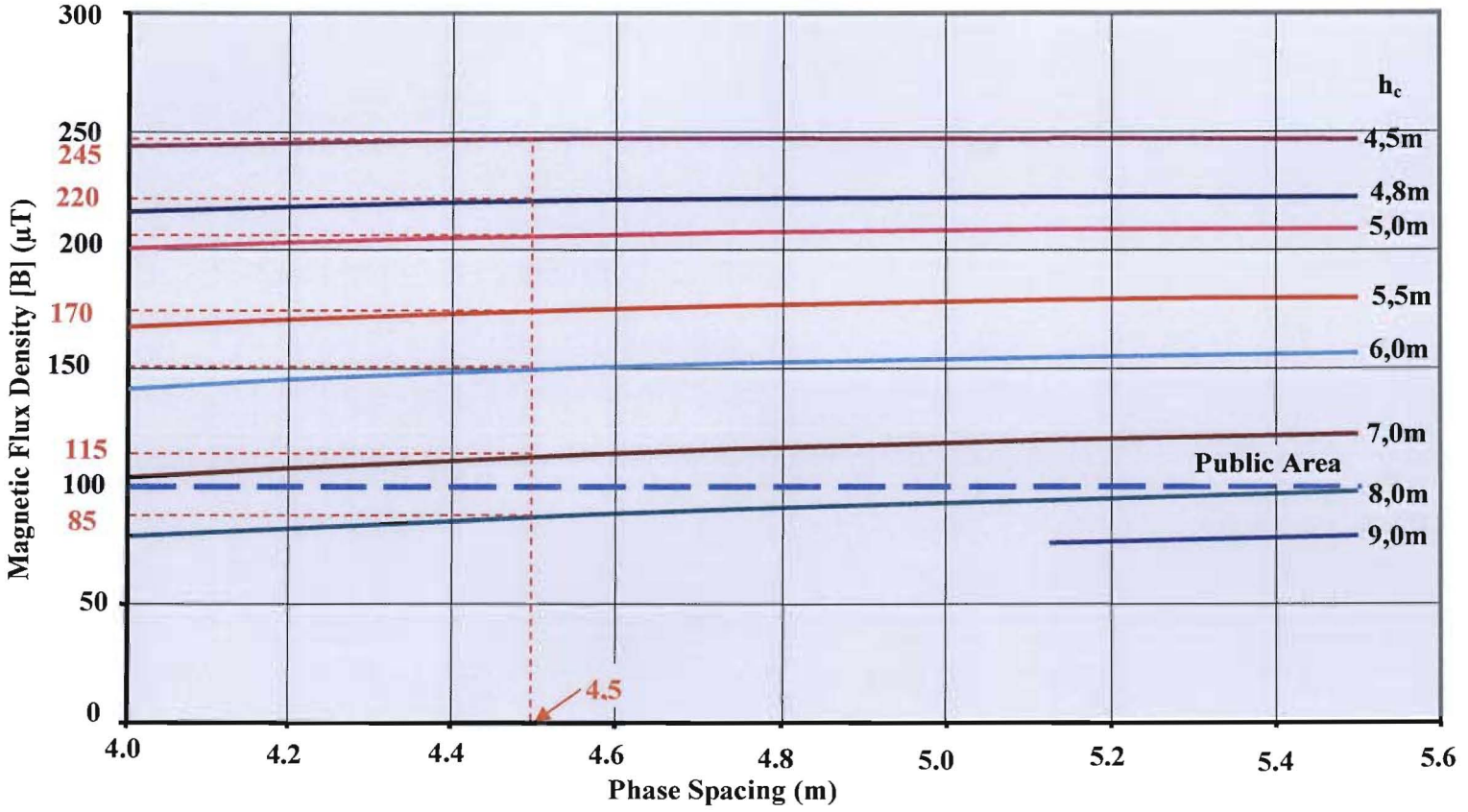

Figure 18.15: Maximum Magnetic Flux Density [B] (µT) vs Phase Spacing [s_p] (m) for I_n = 3150A - Multiple Bus Tube Heights

[Printout from Excel based Busbar Programme]

It is necessary to transform the data obtained from the studies and find the natural logarithms of each value as required by (18.27)

$$\begin{bmatrix} \ln\lambda_1 \\ \lambda_2 \\ \lambda_3 \\ \lambda_4 \end{bmatrix} = \left[\begin{bmatrix} 1 & 1 & 1 & . & 1 \\ \ln(h_{c12}) & \ln(h_{c22}) & \ln(h_{c32}) & . & \ln(h_{cN2}) \\ \ln(s_{p13}) & \ln(s_{p23}) & \ln(s_{p33}) & . & \ln(s_{pN3}) \\ \ln(I_{15}) & \ln(I_{25}) & \ln(I_{35}) & . & \ln(I_{Nk}) \end{bmatrix} \cdot \begin{bmatrix} 1 & \ln(h_{c12}) & \ln(s_{p13}) & \ln(I_{15}) \\ 1 & \ln(h_{c22}) & \ln(s_{p23}) & \ln(I_{25}) \\ 1 & \ln(h_{c32}) & \ln(s_{p33}) & \ln(I_{35}) \\ . & . & . & . \\ 1 & \ln(h_{cN2}) & \ln(s_{pN3}) & \ln(I_{N5}) \end{bmatrix} \right]^{-1} \cdot \left[\begin{bmatrix} 1 & 1 & 1 & . & 1 \\ \ln(h_{c12}) & \ln(h_{c22}) & \ln(h_{c32}) & . & \ln(h_{cN2}) \\ \ln(s_{p13}) & \ln(s_{p23}) & \ln(s_{p33}) & . & \ln(s_{pN3}) \\ \ln(I_{15}) & \ln(I_{25}) & \ln(I_{35}) & . & \ln(I_{Nk}) \end{bmatrix} \cdot \begin{bmatrix} \ln B_1 \\ \ln B_2 \\ \ln B_3 \\ . \\ \ln B_N \end{bmatrix} \right] \quad (18.27)$$

To simplify the above matrix, the cap is applied to the symbols to suit the series of equations generalised by (18.27).

$$\begin{bmatrix} \hat{\lambda}_1 \\ \lambda_2 \\ \lambda_3 \\ \lambda_4 \end{bmatrix} = \left[\begin{bmatrix} 1 & 1 & 1 & . & 1 \\ \hat{h}_{c12} & \hat{h}_{c22} & \hat{h}_{c32} & . & \hat{h}_{cN2} \\ \hat{s}_{p13} & \hat{s}_{p23} & \hat{s}_{p33} & . & \hat{s}_{pN3} \\ \hat{I}_{14} & \hat{I}_{24} & \hat{I}_{34} & . & \hat{I}_{N4} \end{bmatrix} \cdot \begin{bmatrix} 1 & \hat{h}_{c12} & \hat{s}_{p13} & \hat{I}_{14} \\ 1 & \hat{h}_{c22} & \hat{s}_{p23} & \hat{I}_{24} \\ 1 & \hat{h}_{c32} & \hat{s}_{p33} & \hat{I}_{34} \\ . & . & . & . \\ 1 & \hat{h}_{cN2} & \hat{s}_{pN3} & \hat{I}_{N4} \end{bmatrix} \right]^{-1} \cdot \left[\begin{bmatrix} 1 & 1 & 1 & . & 1 \\ \hat{h}_{c12} & \hat{h}_{c22} & \hat{h}_{c32} & . & \hat{h}_{cN2} \\ \hat{s}_{p13} & \hat{s}_{p23} & \hat{s}_{p33} & . & \hat{s}_{pN3} \\ \hat{I}_{14} & \hat{I}_{24} & \hat{I}_{34} & . & \hat{I}_{N4} \end{bmatrix} \cdot \begin{bmatrix} \hat{B}_1 \\ \hat{B}_2 \\ \hat{B}_3 \\ . \\ \hat{B}_N \end{bmatrix} \right] \quad (18.28)$$

Once the [λ] matrix has been determined, the values of λ_2, λ_3 and λ_4 can be read off directly. For λ_1, however, the value $\hat{\lambda}_1$ needs to be converted back in the following manner:

$$\lambda_1 = e^{\hat{\lambda}1} \quad (18.29)$$

Having determined all the λ_i values, it is a matter of substituting them back into (18.25). If the curve "fits" the data to a high degree, i.e. there is a high degree of correlation between the data and the "fitted" curve, the stochastic distribution term tends to zero. The value for the magnetic field for any set of parameters can then be determined.

18.4.2 The "Goodness" of Fit

In order to access how well the data fits the curve, it is necessary to arrive at the Coefficient of Determination $\mathbf{R}^2$ Matrix

$$r^2 = \left(\frac{[\lambda].[X]^T[B] - N_e.\overline{B}^2}{[B]^T.[B] - N_e.\overline{B}^2} \right) \qquad (18.30)$$

15.4.3 Reporting the results of the Study

The study input data was arranged in rows and columns of conductor height (has required by the N x 4 matrix '**X**' and output data (the calculated magnetic field) in a single column as required by the N x 1 matrix **B** given in (18.25) and (18.27)

$$[\lambda] = \left[[X]^T . [X]\right]^{-1} . \left[[X]^T . [B]\right] \qquad (18.31)$$

4 x 1 4 x N N x 4 4 x N N x 1

In this study, 369 sets of data were produced, providing sufficient elements to accurately fit a curve of the form given in (18.27). With the aid of the "MATHCAD" software package and, importing the **[X]** and **[B]** matrices from an Excel spreadsheet, the following results were obtained:

$$\begin{bmatrix} \hat{\lambda}_1 \\ \lambda_2 \\ \lambda_3 \\ \lambda_4 \end{bmatrix} = \begin{bmatrix} -0.361 \\ -1.728 \\ 0.29 \\ 0.997 \end{bmatrix}$$

$\hat{\lambda}_1 = -0.361$

$\lambda_1 = e^{-1.728}$

$= 0.697$

$\lambda_2 = -1.789$

$\lambda_3 = 0.29$

$\lambda_4 = 0.997$

The "goodness" of the fit

$$r^2 = \left(\frac{[\lambda].[X]^T[B] - N_e.\overline{B}^2}{[B]^T.[B] - N_e.\overline{B}^2} \right) \qquad \text{(from 18.30)}$$

$$r^2 = \left(\frac{A - C}{D - C} \right) \qquad (18.32)$$

$$A = [\lambda_i.[X]^T[B] \qquad (18.33)$$

$$= 9.128.10^3$$

$$\mathbf{D} = [\mathbf{B}]^{T}.[\mathbf{B}] \qquad (18.34)$$
$$= 9.129.10^{3}$$

$$\mathbf{C} = \mathbf{N}.\overline{\mathbf{H}}^{2} \qquad (18.35)$$

$\mathbf{N_e} = 369$

$\overline{\mathbf{B}} = 5.0$

$\mathbf{C} = 369.5.0$

$= 1.845.10^{3}$

$$\mathbf{r}^{2} = \left(\frac{\mathbf{A}-\mathbf{C}}{\mathbf{B}-\mathbf{C}}\right)$$
$$= \left(\frac{9.128.10^{3} - 1.845.10^{3}}{9.129.10^{3} - 1.845.10^{3}}\right) \qquad \text{(from 18.30)}$$
$$= 0.999$$

Again, the value of 0.999 for R^2 implies an exceptionally good fit of the curve to the data, hence the stochastic term $\mathbf{u_i}$ is virtually zero and $\mathbf{e^{ui}}=1$

$$\mathbf{B_i} = \mathbf{0.697.h_{ci}^{-1.728}.s_{pi}^{0.29}.I_{mi}^{0.997}} \qquad (18.36)$$

Where:-

$\mathbf{B_i}$ = The magnetic field as measured at a height of 1,8m above the ground for a given bus ducting height ($\mathbf{h_{ci}}$) above the ground level or the electric field as measured at a height of 1,8m above the ground for a given bus duct phase spacing keeping the height of the bus ducting above the ground constant (one of a number of such stimuli – response observations) (μT)

$\mathbf{h_{ci}}$ = The height of the bus duct above ground level keeping the phase spacing constant, or the phase spacing of the three phases keeping the height of the bus ducting above the ground constant (m)

$\mathbf{s_{pi}}$ = Phase spacing (m)

$\mathbf{I_{mi}}$ = System maximum current (A)

Equation (18.36) can now be applied to calculate the value of **B** for any combination of $\mathbf{h_{ci}}$, $\mathbf{s_{pi}}$ and $\mathbf{I_i}$ that may be required in accordance with the evaluations of all the preceding chapters. These values would have been determined by the time that the value of the electric field is to be calculated. Providing the electric field limits for public exposure and substation live yards are not exceeded, no further iterations would be required.

19. SENSITIVITY ANALYSIS

The graghs depicted in this section, unless otherwise referenced, are as a result of the studies that were performed using the Excel based Busbar Programme that the author developed for the purpose of the studies.

Objectives of this Chapter:

- To study how deviations in material parameters due to tolerances and error in estimating dynamic and other factors affect the selection of tubular conductors and support post insulators

19.1 Conductor Diameter and Wall Thickness

Manufacturing tolerances that should normally not be exceeded are given as follows:-

Outside diameter **-1 %, +1 % of diameter**

Wall thickness **-0,4 mm, +0,4 mm**

Due to manufacturing tolerances, a sensitivity analysis needs to be carried out to determine the effect on mechanical strength of the tubular conductor and the forces on the post insulators.

Table 19.1: Schedule of Combinations for Tolerances in Aluminium Tube Dimensions

Case 1	Case 2	Case 3	Case 4	Case 5	Case 6	Case 7	Case 8	Case 9
$0,99.d_{bo}$	$0,99.d_{bo}$	$0,99.d_{bo}$	d_{bo}	d_{bo}	d_{bo}	$1,01.d_{bo}$	$1,01.d_{bo}$	$1,01.d_{bo}$
$t_{bw} - 0,4$	t_{bw}	$t_{bw} + 0,4$	$t_{bw} - 0,4$	t_{bw}	$t_{bw} + 0,4$	$t_{bw} - 0,4$	t_{bw}	$t_{bw} + 0,4$

The tube wall thickness has a direct impact not only on the strength of the tube and stiffness of the tube, but also the strength of the post insulator required. The thicker the tube wall, the stiffer the tube resulting in less movement and whiplash of the tube translating to a lower cantilever force on the post insulators. (Produce a graph of PI strength vs tube thickness)

19.1.1 Effect of Conductor Tolerances on Post Insulator Strength

Figure 19.1 shows that all the case studies clearly pointed out that the greatest impact on the post insulators occurs when the tube diameter is slightly larger than nominal ($\mathbf{d_{bo}+1\%}$) and the wall thickness is slightly less than nominal ($\mathbf{t_w - 0,4mm}$). If this combination occurs, the forces on the post insulators can lead to values between 1,2% to 2% higher than the nominal values.

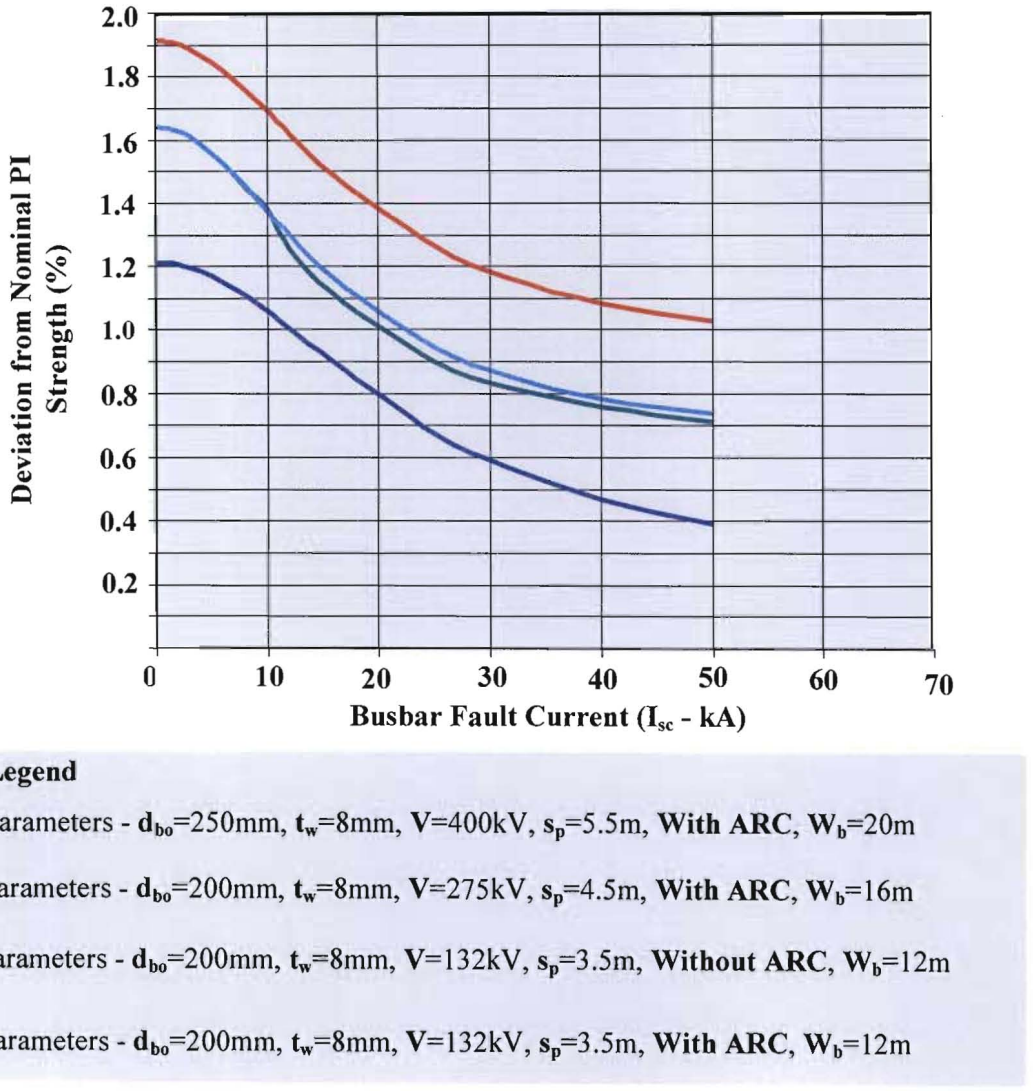

Figure 19.1: Deviation from Nominal PI Strength (%) vs Fault Current (I_{sc} - kA)

[Printout from Excel based Busbar Programme]

19.1.2 Effect of Conductor Tolerances on Stress in the Bus Tube

Figure 19.2 shows that in the cases studied, that the greatest impact on the conductor stress occurs when both the tube diameter and wall thickness is less than nominal, viz. **(d_{bo}-1%)** and **(t_w- 0,4mm)** respectively. This is relatively obvious if one considers that stress **(σ)** is measured in N/m^2, i.e. force per unit area. A smaller diameter and thinner wall thickness will result in a smaller area for the same force, hence a larger force per unit area. If this combination occurs, the stress in the conductor can lead to values between 0,6% to 1% higher than the nominal values. This becomes particularly significant when dealing with tubes with smaller wall thicknesses and higher fault currents. This is shown by the divergence of the two upper curves. Acceptable tolerances should be stated clearly in the conductor specifications. By

implementing a decrement factor (k_f) equal to unity, i.e. no flexibility in the support structure, one observes that when employing a lattice structure, only a marginal improvement is realised.

It is also interesting to note that the rate of % increase is more pronounced and relatively linear for $10kA \leq I_{sc} \leq 30kA$, after which it starts to decrease. The decrease implies that the short circuit forces now start to over dominate the rigidity of the tube.

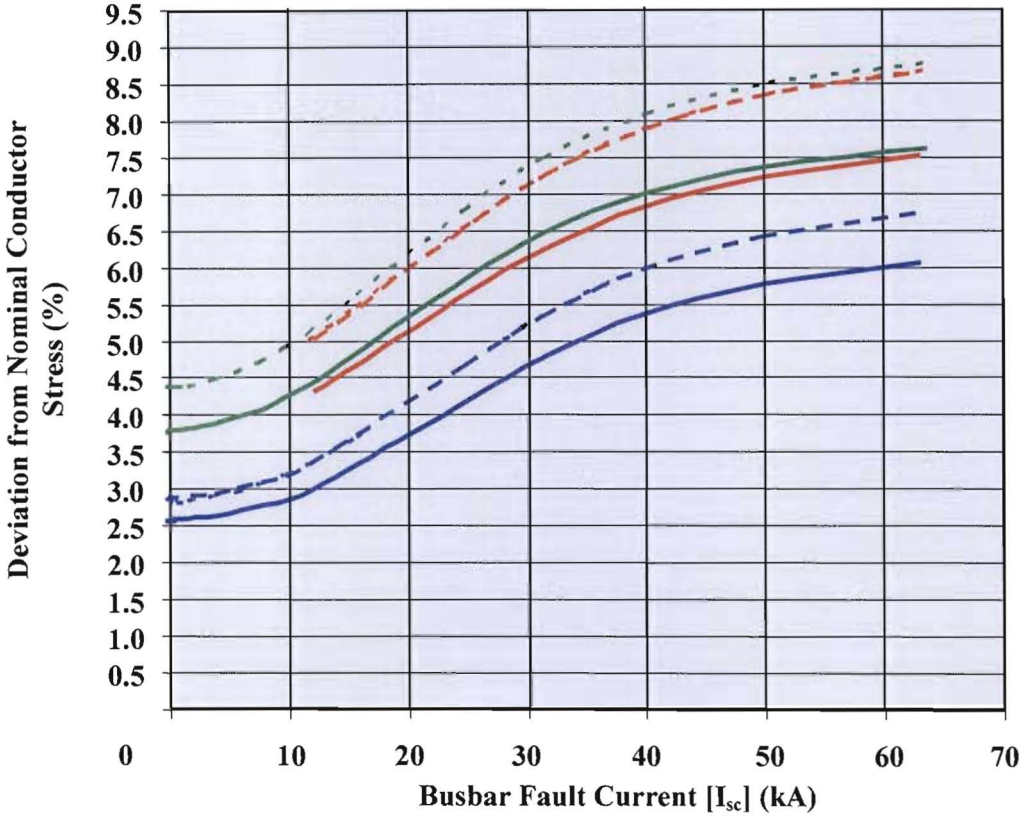

Figure 19.2: Deviation from Nominal Conductor Stress (%) vs Fault Current [I_{sc}] (kA)

[Printout from Excel based Busbar Programme]

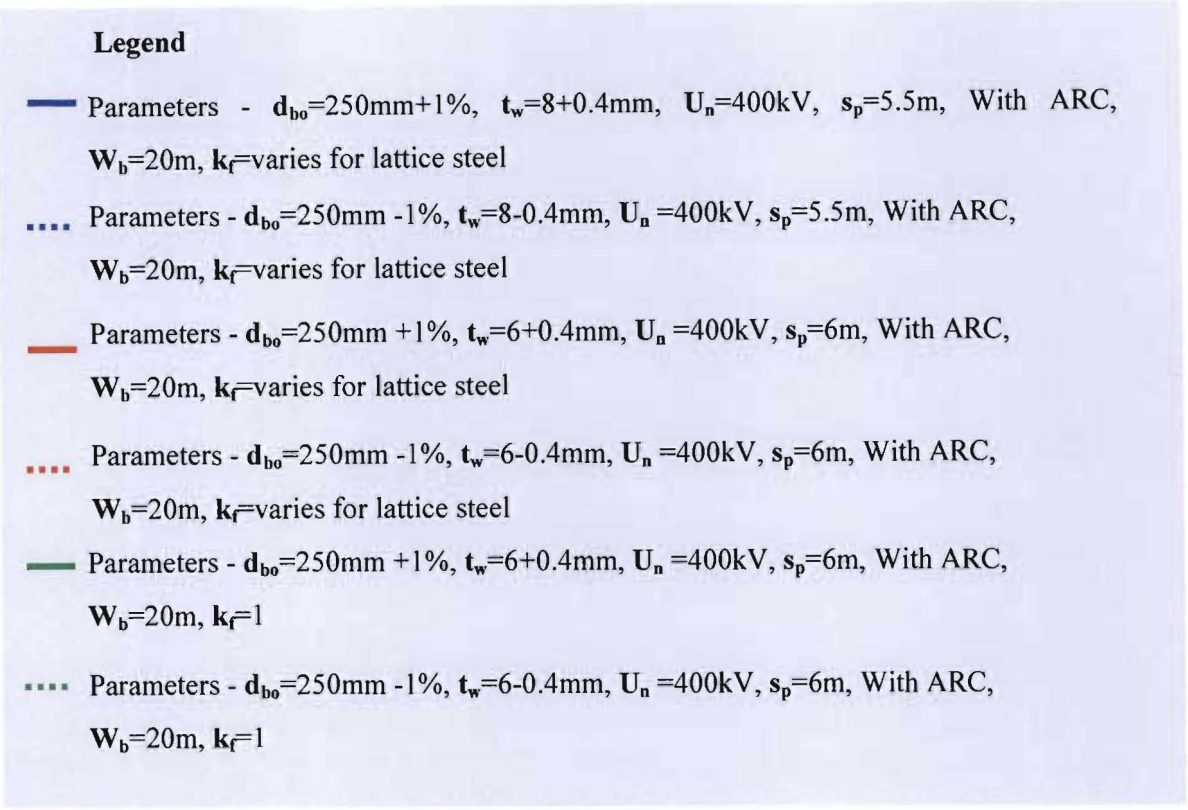

19.2 Variation of Linear Density of the Bus Tubing

Related to this is the in the variation of the linear density, or mass per unit length of the bus tubing again due to allowable manufacturing tolerance. Linear density (mass per unit length) can vary ±2% [20]

This doubles the number of cases to be considered

Table 19.2: Schedule of Combinations for Tolerances in Aluminium Tube Linear Density

Case 1 -2%	Case 1 0%	Case 2 +2%
0,98.m_b	**1,00.m_b**	**1.02.m_b**

In order to obtain a perspective on the impact of linear density on the strength of the insulator, a small diameter tube with small wall thickness, and a large diameter tube with a large wall thickness was investigated. In both cases, there did not appear to be an distinctive separation of the 3 sets of curves as is depicted in the two cases below. In fact it was found that a variation in the linear density of the tube by ±2% had only a marginal effect of ±0,18% on the nominal force on the post insulator.

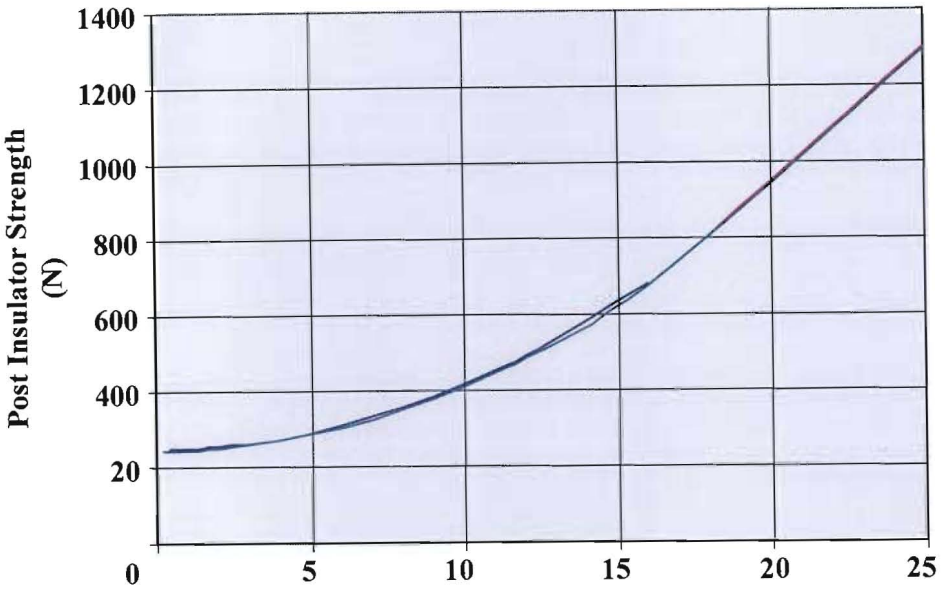

Figure 19.3: Post Insulator Strength (N) vs Short Circuit Current [I_{sc}] (kA)

Ø120mm x 4mmWT, AlMgSi.0,5F25, Terrain Category 1

[Printout from Excel based Busbar Programme]

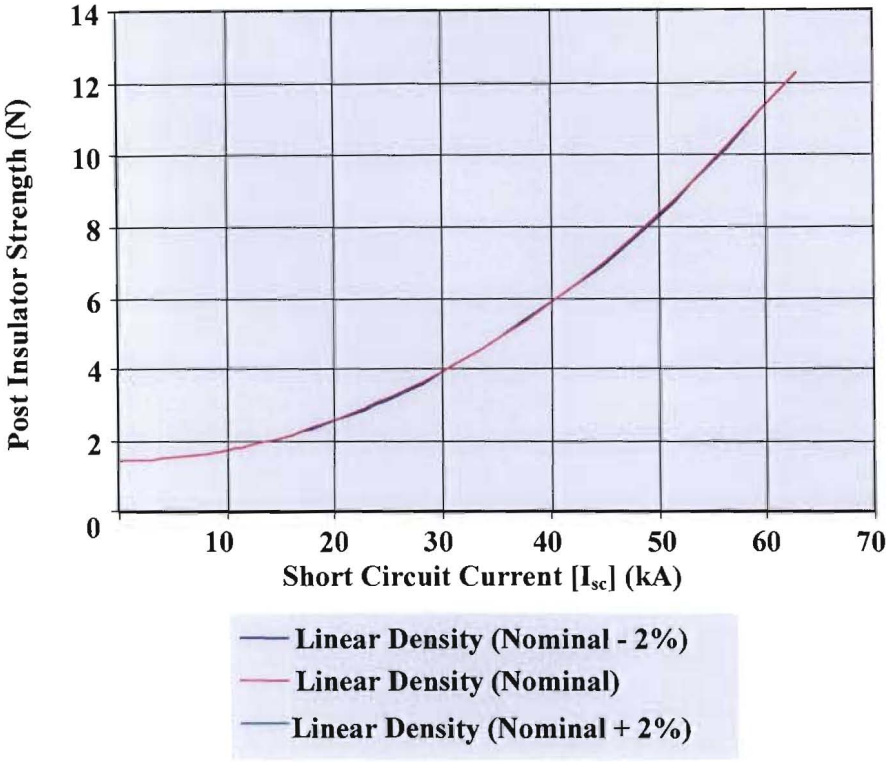

Figure 19.4: Post Insulator Strength (kN) vs Short Circuit Current [I_{sc}] (kA)

Ø250mm x 8mmWT, AlMgSi.0,5F25, Terrain Category 1

[Printout from Excel based Busbar Programme]

19.3 Error in the estimation of the Wind Speed

A study was carried out on four different tube sizes to determine the significance of an error in the wind speed. The combinations chosen were as follows:

Ø120mm x 6mmWT (small outer diameter bus tube with a small wall thickness)
Ø200mm x 8mmWT (larger diameter tube with a large wall thickness),
Ø250mm x 6mmW T (large outer diameter and small wall thickness)
Ø250mm x 8mmWT (large outer diameter and large wall thickness)

The results are depicted in Figures 19.5, 19.6, 19.7 and 20.8 respectively.

In all four cases, an error in the wind speed for values below 50km/h will result in relatively small error in the value of the post insulator, <0,5kN. For wind speeds in excess of 40km/h, and particularly >100km/h, the error becomes much more significant and care needs to be taken to choose an insulator with a safety margin of 0,5kN per 10km/h of being uncertain of the wind speed in the positive.

It is be recommended that such a study to be carried out for each design in order to provide the designer with a means of making an informed decision on what would be an appropriate value that should be added to the resulting calculation of post insulator strength to ensure a sound design.

All four scenarios were based on the worst case exposure factor, viz. 'Terrain Category 1'. Other terrain categories will result in a lesser impact of wind forces on the determination of the strength of the post insulators due to partial shielding offered by obstacles as defined in Chapter 8.

120mm x 6mmWT, Terrain Category 1, Alloy: F25, 2% Proof Stress: 195MPa

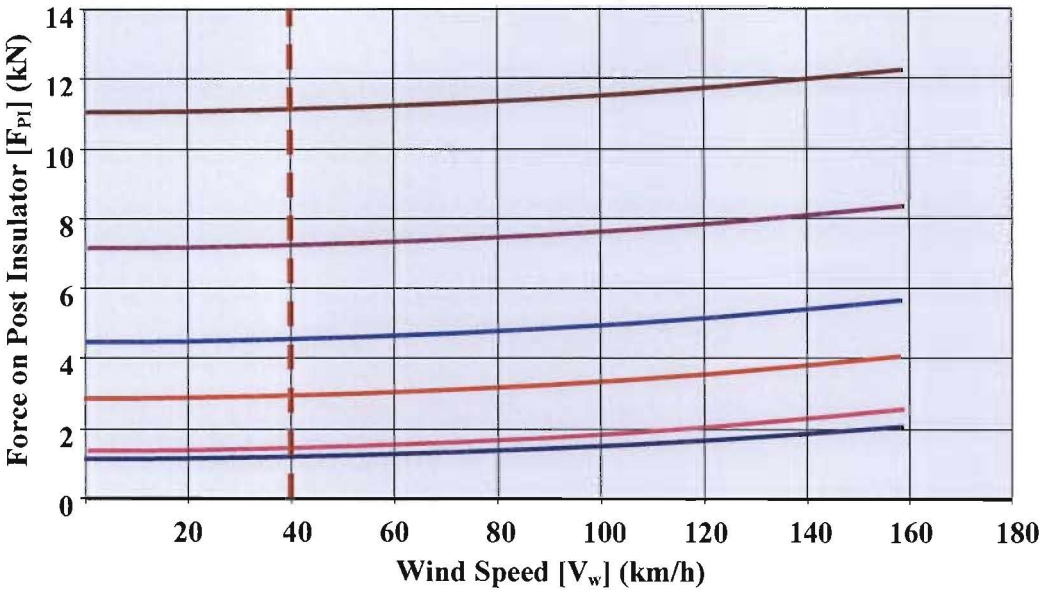

Figure 19.5: Force on Post Insulator [F_{PI}] (kN) vs Wind Speed [V_w] (km/h)

[Printout from Excel based Busbar Programme]

200mm x 8mmWT, Terrain Category 1, Alloy: F25, 2% Proof Stress: 195MPa

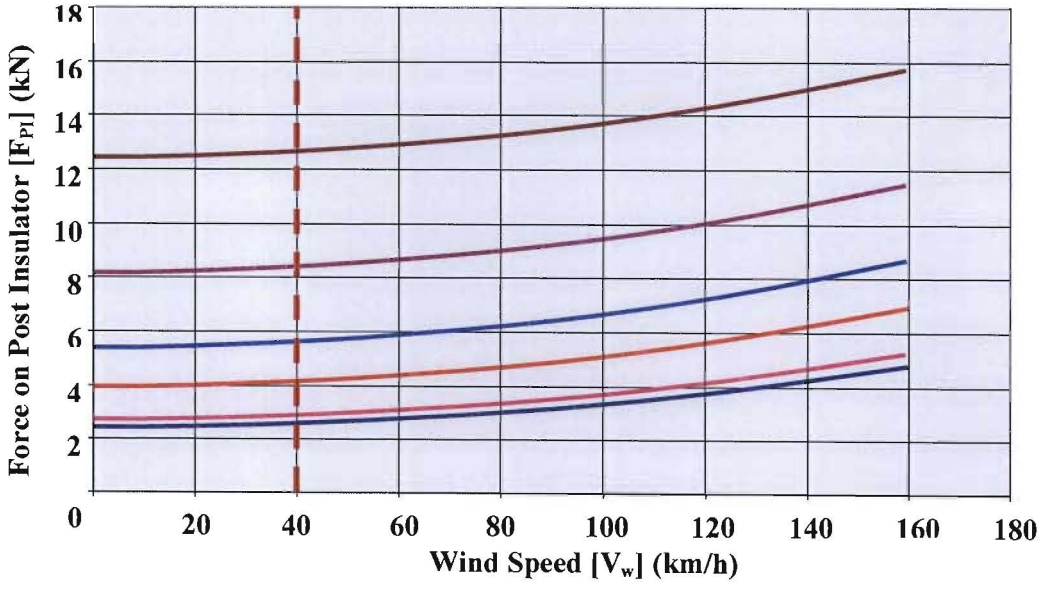

Figure 19.6: Force on Post Insulator (kN) vs Wind Speed [V_{w}] (km/h) for a Ø200mm x 8mmWT Bus Tube

[Printout from Excel based Busbar Programme]

250mm x 6mmWT, Terrain Category 1, Alloy: F25, 2% Proof Stress: 195MPa, Phase Spacing: 5,5m

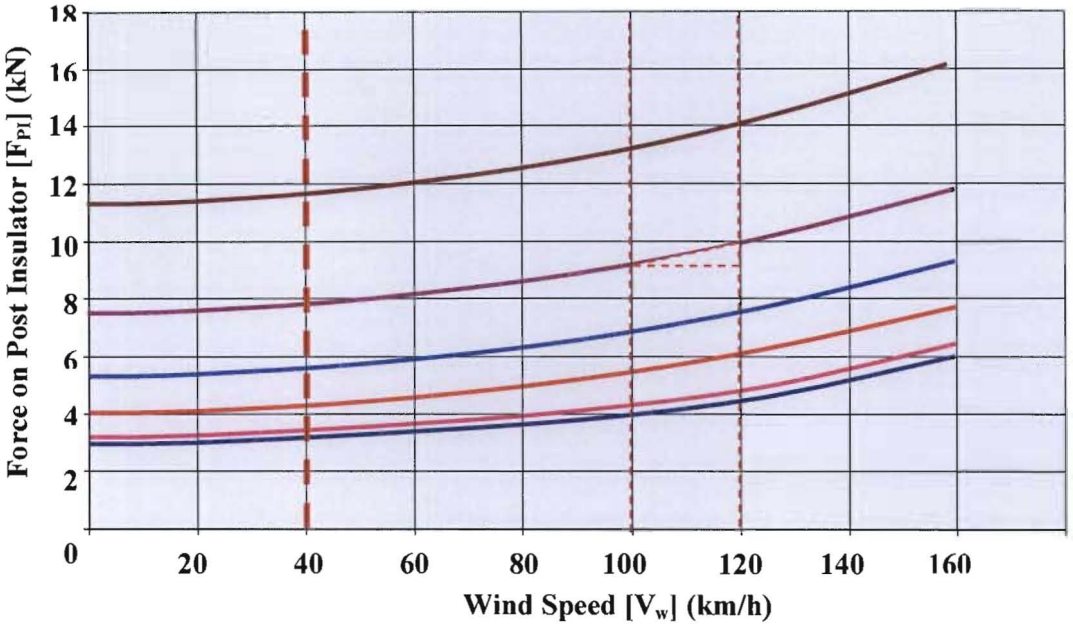

Figure 19.7: Force on Post Insulator (kN) vs Wind Speed [V_w] (km/h) for a Ø250mm x 6mmWT Bus Tube

[Printout from Excel based Busbar Programme]

250mm x 8mmWT, Terrain Category 1, Alloy: F25, 2% Proof Stress: 195MPa, Phase Spacing: 5,5m

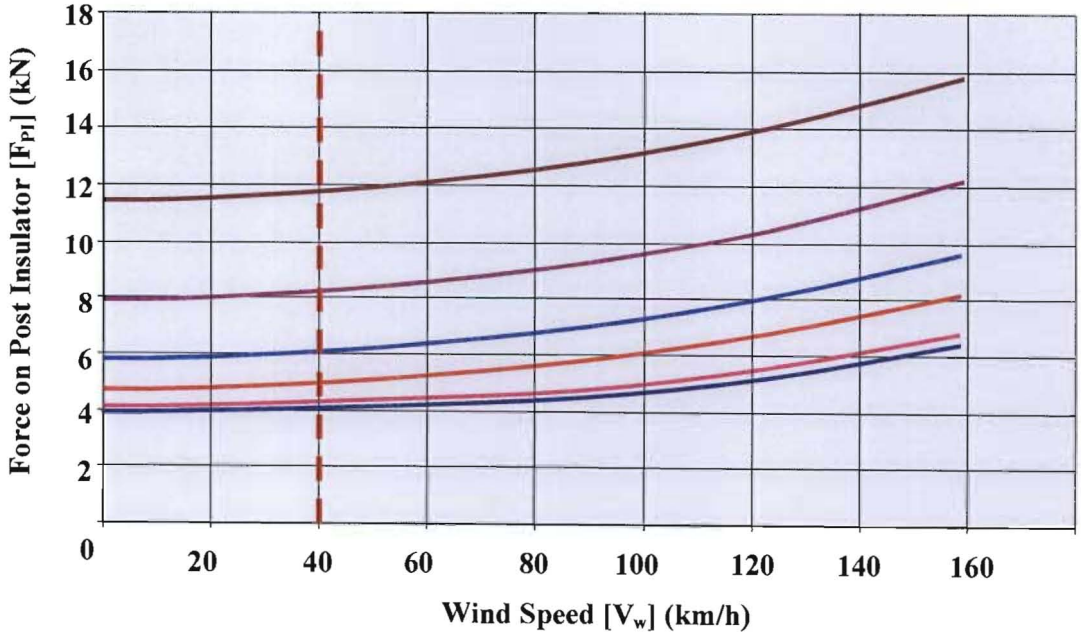

Figure 19.8: Force on Post Insulator [F_{PI}] (kN) vs Wind Speed [V_w] (km/h) for a Ø250mm x 8mmWT Bus Tube

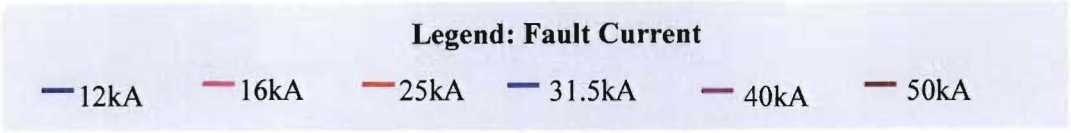

[Printout from Excel based Busbar Programme]

19.4 Uncertainty of Terrain Category Classification

Owing to the large differences in wind speeds between Terrain Categories 2 and 3, and where there is doubt whether the terrain under consideration falls into Category 2 or 3, the design wind speed may be obtained by interpolation between the two values for these categories.

$$k_{zn} = \left(\frac{k_{z2B} + k_{z3B}}{2} \right) \qquad \text{(from 8.16)}$$

It is, however, then advisable to apply the criteria discussed in paragraph 16.3 to allow for any additional uncertainty.

19.5 Error in the estimation of the Dynamic Factors

Different authors have arrived at different curves which essentially follow the same trend. The differences in the factors, however, can have a significant impact on the choice of tubular busbar infrastructure such as the size of the tube required for mechanical strength, and the class of insulator strength. These differences impact on the cost of the bus system and may make the infrastructure unnecessarily expensive.

The aim of this section is to determine the degree to which these differences can impact on the design and provide a degree of confidence that the values chosen will not result in unexpected failure of the support system.

19.4.1 Error in the estimation of the Dynamic Factor for Post Insulators (ν_F)

The results presented by the various authors' shows a wide spread in the values of the dynamic factors ν_F and ν_σ. The spread is much less pronounced at the lower end for $\mathbf{0{,}02 \leq f_c/f \leq 0{,}04}$. However, for $\mathbf{f_c/f > 0{,}04}$ the values diverge quite significantly. Some authors' concluded a constant values for ν_F and ν_σ, while others provided wildly fluctuating values.

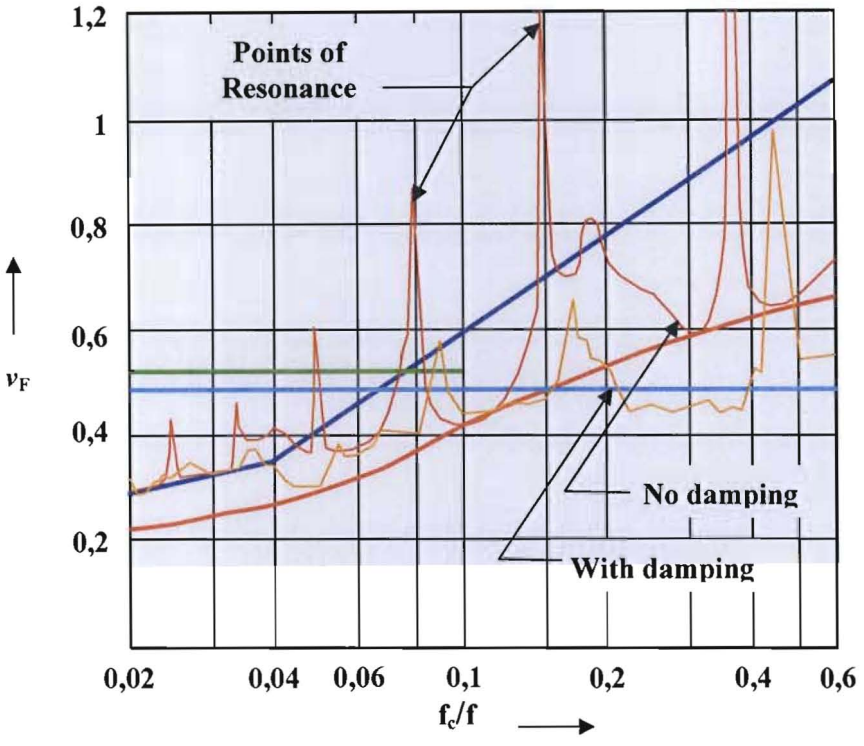

Figure 19.9: Ratio between Dynamic and Static Forces on the Support Insulator (ν_F) vs Ratio of Natural Frequency and System Frequency (f_c/f) [6]

From (14.12) and (14.13), the dynamic force on the post insulator without auto re-closure is merely the product of the static force and the dynamic factor for post insulators.

$$\mathbf{F_{A(PI)DYN + ARC} = F_{A(PI)DYN}.\nu_r \ (N)} \qquad \text{(from 14.12)}$$

$$\mathbf{F_{B(PI)DYN + ARC} = F_{B(PI)DYN}.\nu_r \ (N)} \qquad \text{(from 14.13)}$$

The above therefore indicates that an error in the determination of the dynamic force on the post insulator could very well be under estimated if the error in estimating ν_F is negative. Figure 19.10 below illustrates how the effect becomes more pronounced as the fault level increases. The graphs are relatively flat for low fault levels, the gradients of lines becoming steeper as the fault level increases.

Since there is always some uncertainty of the level of accuracy, when calculations provide results that are close to the maximum value of the standard post insulator, particularly at high system fault levels, one must rather to err on the side of caution and choose the next size up of standard post insulator value, Table 19.3 showing standard IEC insulator strengths..

Table 19.3: Standard IEC Post Insulator Strengths [24]

Strength Class	**C4**	**C6**	**C8**	**C10**	**C12**	**C14**	**C16**	**C18**
Strength (kN)	**4**	**6**	**8**	**10**	**12**	**14**	**16**	**18**

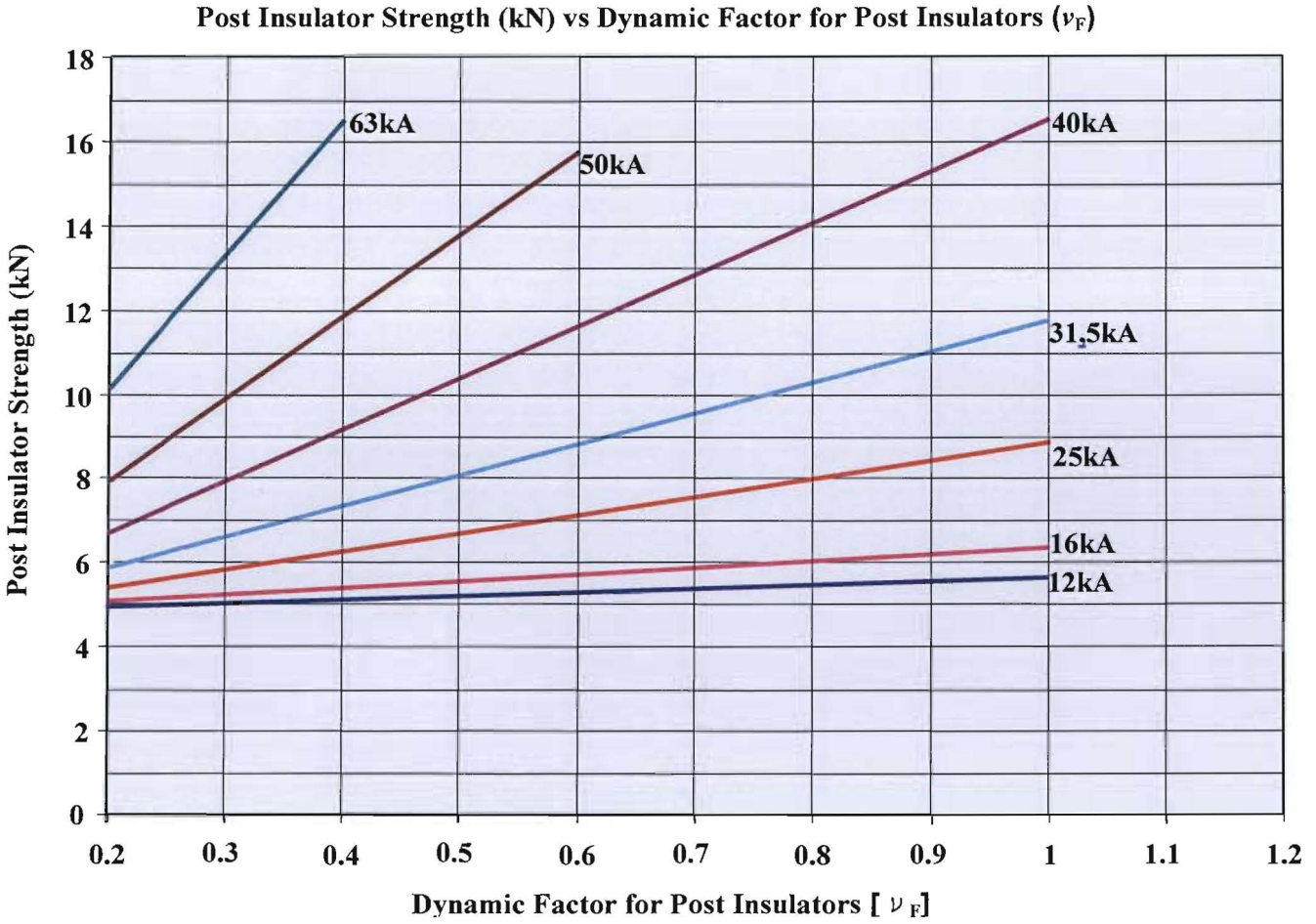

Figure 19.10: Post Insulator Strength (kN) vs Dynamic Factor for Post Insulators [v_F]

[Printout from Excel based Busbar Programme]

19.4.2 Error in the Estimation of the Dynamic Factor for Tubular Conductor (v_σ)

As with the post insulator dynamic factor, the results presented by the various authors' shows a wide spread in the values of the dynamic factors v_σ. Again, the spread is much less pronounced at the lower end for $\mathbf{0{,}02 \leq f_c/f \leq 0{,}04}$. However, for $\mathbf{f_c/f > 0{,}04}$ the values diverge quite significantly. Some authors' concluded constant values for v_F and v_σ, while others provided wildly fluctuating values

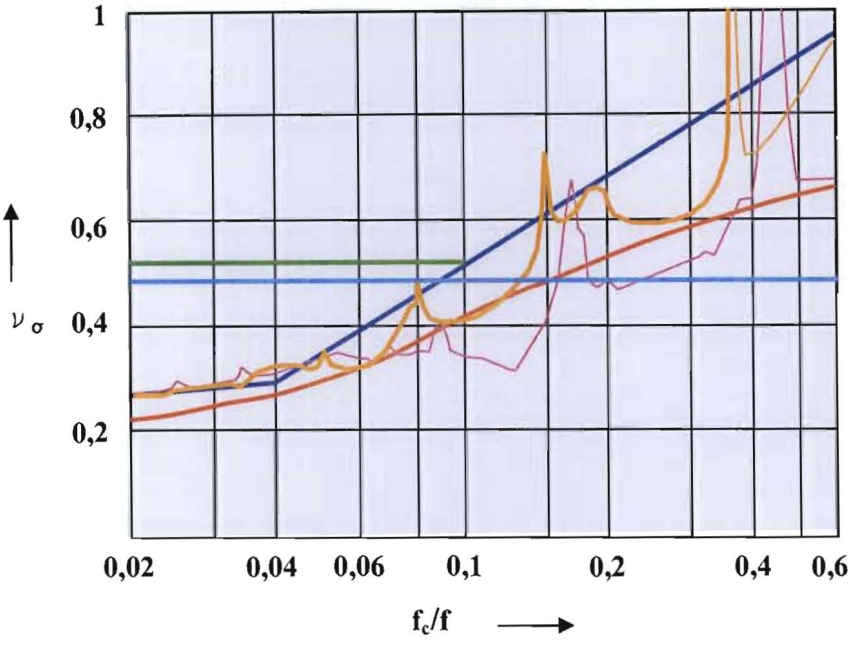

Figure 19.11: Ratio between Dynamic and Static Conductor Stress (ν_σ) vs Ratio of Natural Frequency and System Frequency (f_C/f) [6]

From (12.1) the dynamic stress in the bus tubing without auto re-closure is merely the product of the static stress and the dynamic factor for conductors.

$$\sigma_{DYN} = \sigma_{ST}.v_\sigma \ (N/m^2) \qquad \text{(from 12.1)}$$

Once again, the above indicates that an error in the determination of the dynamic stress in the bus tube could be under estimated if the error in estimating v_σ is negative. Since σ_{ST} is also fault current dependent, Figure 19.12 illustrates how the effect becomes more pronounced as the fault level increases. The graphs are relatively flat for low fault levels, the gradients of lines becoming steeper as the fault level increases.

Due to the uncertainty of the level of accuracy, when calculations provide results that are close to the proof stress of a particular alloy, especially at high system fault levels, rather err on the side of caution and choose an alloy where the Proof Stress is at least 10% greater than the

calculated dynamic stress developed in the tube. Table 19.4 provides the Proof Stresses ($\mathbf{R_{p0,2}}$) for some allows that are available on the market.

Table 19.4: Aluminium Alloy Proof Stress

Alloy Type	**HULETT'S S.A.**		**ASA STANDARD**		**DIN STANDARD**	
	D50STF	**D65STF**	**6063T6**	**6061T6**	**AlMgSi, 5F22**	**AlMgSi,5F25**
0,2 % Proof Stress in MPa $R_{p0,2}$	170	240	214	276	160	195

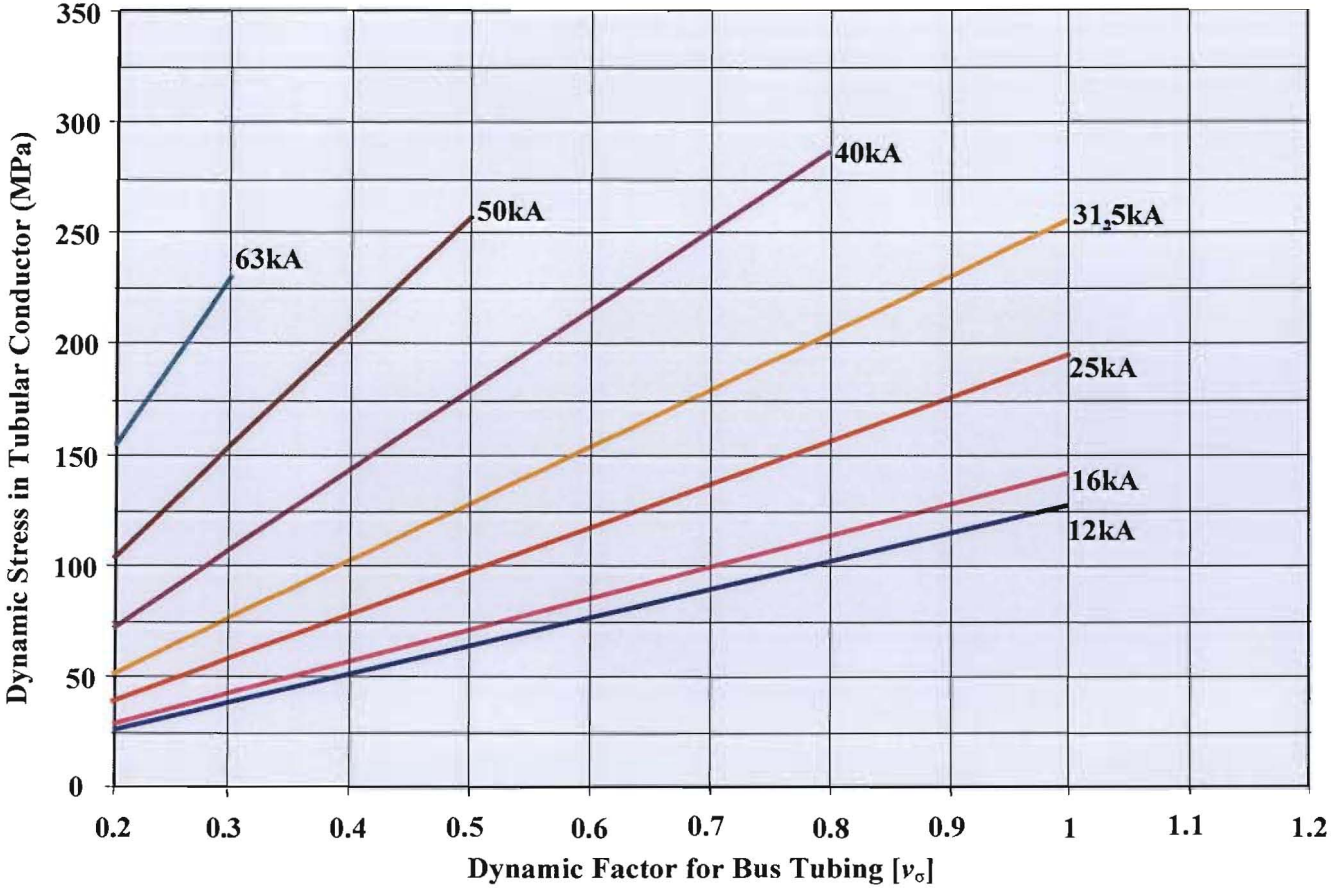

Figure 19.12: Post Dynamic Stress in Tubular Conductor (MPa) vs Dynamic Factor for Tubular Conductor (v_σ)

[Printout from Excel based Busbar Programme]

19.4.3 Error in the estimation of the Dynamic Factor for Auto Re-closure (ν_r)

As with the post insulator and tubular conductor dynamic factors, the results presented by the various authors' shows a wide spread in the values of the dynamic factors ν_r. It appears to be spread within a linear band for both lower end for $0{,}02 \leq f_c/f \leq 0{,}05$ and $0{,}05 \leq f_c/f \leq 1{,}8$.

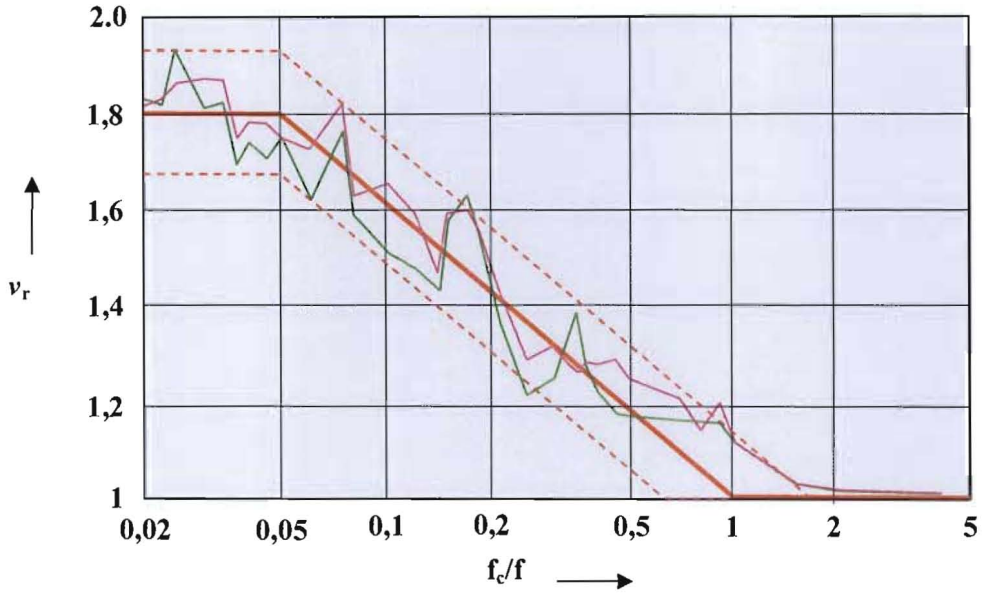

Figure 19.13: Ratio between Stress With and Without Unsuccessful Auto-Re-closure [ν_r] vs Ratio of Natural Frequency and System Frequency [f_c/f] [6]

From (12.2) and (14.11) the dynamic stress in the bus tubing and force on the post insulator with auto re-closure is as before the product of the dynamic values without auto-reclosure and the dynamic factor for auto-reclosure (ν_r).

$$\sigma_{DYN + ARC} = \sigma_{DYN}.\nu_r \ (N/m^2) \qquad \text{(from 12.2)}$$

$$F_{(PI)DYN+ ARC} = F_{(PI)DYN}.\nu_r \ (N) \qquad \text{(from 14.11)}$$

As with the preceeding dynamic factors, the above indicates that an error in the determination of the dynamic stress in the bus tube could be under estimated if the error in estimating ν_r is negative. Since σ_{DYN} is also fault current dependent as it is a linear multiple of σ_{ST}, Figure 19.14 shows the effect becomes more pronounced as the fault level increases. The graphs are relatively flat for low fault levels, the gradients of lines becoming steeper as the fault level increases.

As before, due to the uncertainty of the level of accuracy, when calculations provide results that are close to the margins of the materials, especially at high system fault levels, rather err on the

side of caution and choose mateials with higher Proof Stresses ($\mathbf{R}_{p0,2}$) and standard insulator strengths were these are applicable.

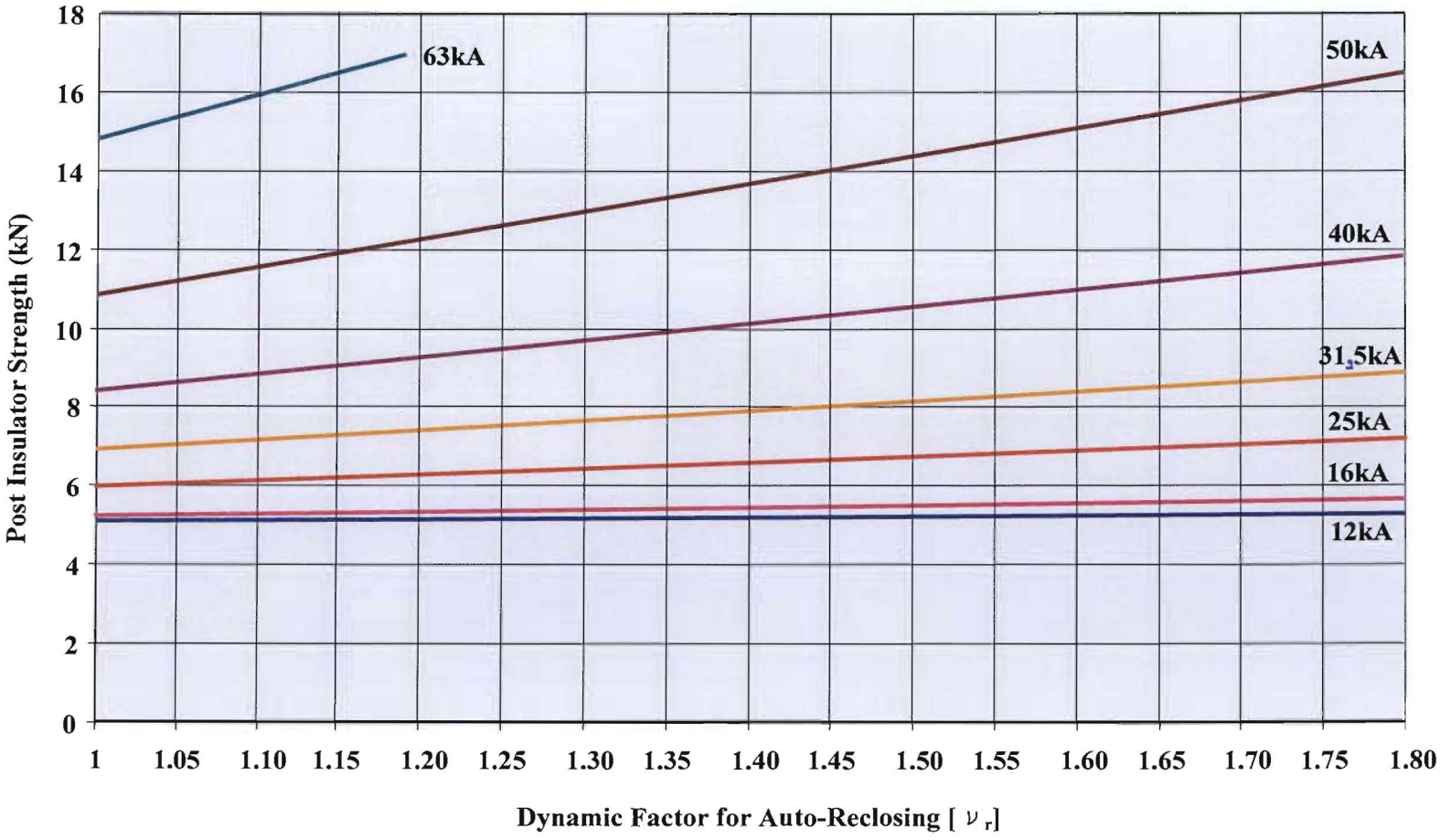

Figure 19.14: Post Insulator Strength (kN) vs Dynamic Factor for Auto-Re-closing [v_r]

[Printout from Excel based Busbar Programme]

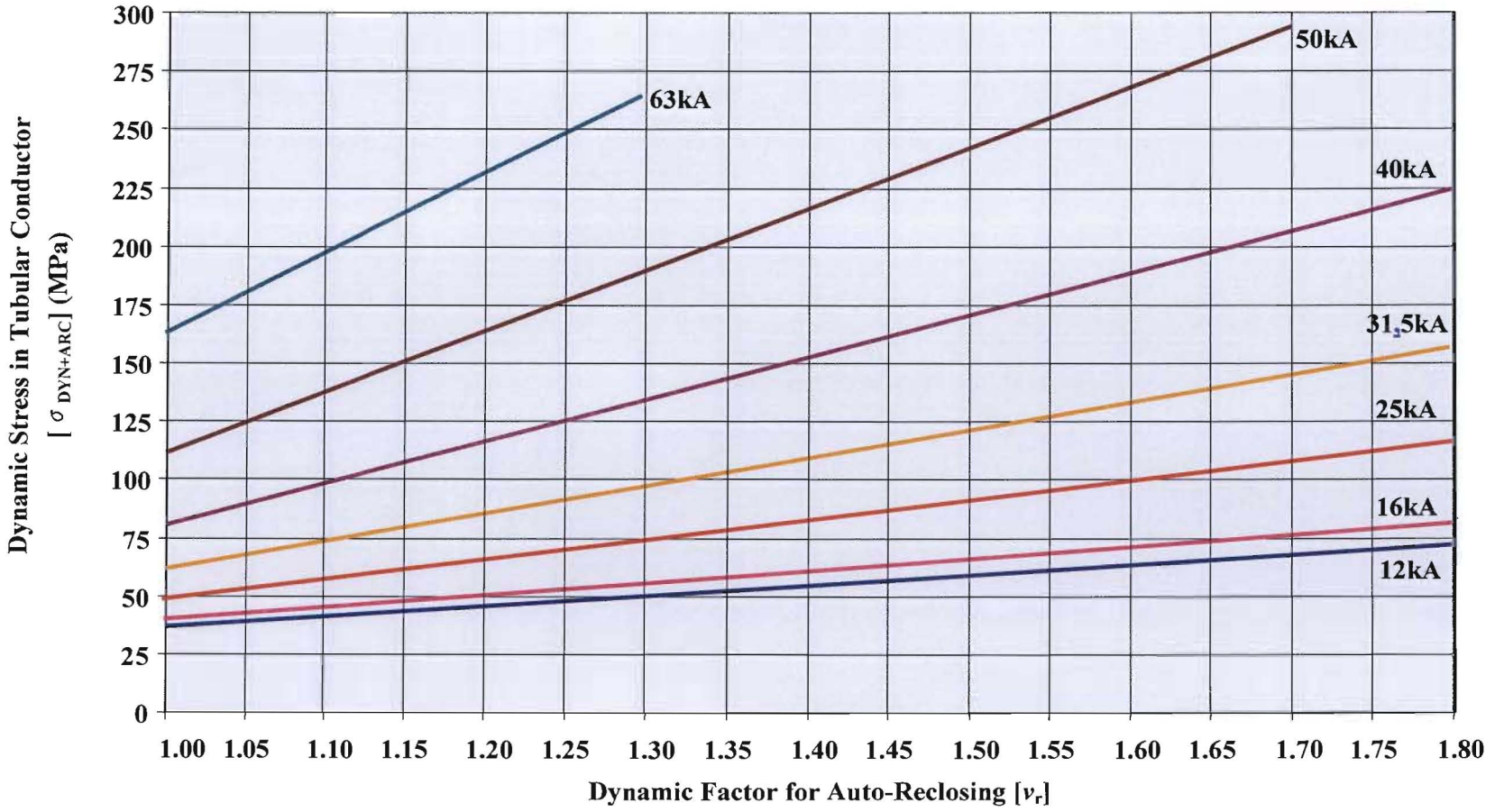

Figure 19.15: Dynamic Stress in Tubular Conductor [$\sigma_{DYN+ARC}$] (MPa) vs Dynamic Factor for Auto-Reclosing [v_r]

[Printout from Excel based Busbar Programme]

19.4.4 The Impact of Safety Factors on the Final Results

Safety factors are included in the design of substructures or systems in order to account for the amount of risk that unknown variables or factors that may lead to the failure of that substructure or system. The more data one has available for modelling purposes and the more confident one is that the proposed model being employed accurately represents the substructure or system, the smaller the safety factors need to be. Safety factors can also be reduced if there is confidence that the processes employed in the manufacturing of components minimises the probability of latent defects, or that stringent routine tests are adhered to.

19.4.4.1 Porcelain Post Insulator Safety Factor

For porcelain, safety factors are as high as **2,5** have been used. These values where applicable when manufacturing processes where not monitored very precisely. Today, reputable manufacturers employ scientists and ceramic engineers in the formulation of these manufacturing processes. Subsequently, safety factors as low as **1,2** are currently used to account for the dynamic cantilever loading on the porcelain insulators.

As an example it is determined from a study that a post insulator of 5409,8 kN is required to support a tubular conductor. Applying the safety factors above:

$\mathbf{PI_{2,5}}$ = 5,410.2,5

= 13,525 kN (standard size is 14kN)

$\mathbf{PI_{1,2}}$ = 5,410.1,2

= 6,492 kN (standard size is 8kN)

The difference in the strength required in the two scenarios is almost by a factor of 2. This obviously leads to cost for delivery to site. When large numbers of insulators are involved as is normally required by tubular bus designs, as many as 100 at a time and more, the costs could lead to a project being given the green light or being cancelled.

19.4.4.2 Tubular Conductor Safety Factor

For tubular conductor safety factors that have been used are as high as **2,65**. Figure 19.16 below is a plot of Dynamic Stress in the aluminium conductor against the applied safety factor for a Ø250mm x 8mmWT tube. These are linear relationships since the dynamic conductor stress is merely multiplied by the safety factor.

The 0,2% proof stress ($\mathbf{R_{p0,2}}$) for each of 6 alloys commonly used for this application, are plotted on the graph to provide an visual indication of which alloys should be employed. The electrical and mechanical properties of these alloys are illustrated in Table 6.2. It is very

evident that the lower the fault current, the less the impact of the safety factor is on the design value, and even the softer, lower resistivity alloys such as AlMgSi.0,5F22 ($\mathbf{R}_{p0,2}$=160MPa)and D50S TF ($\mathbf{R}_{p0,2}$=170MPa)can be employed. However, for the higher busbar fault levels, the safety factor significantly impacts on the design value and harder, higher resistivity alloys such as AlMgSi.0,5F25 ($\mathbf{R}_{p0,2}$=195MPa) and D65S TF ($\mathbf{R}_{p0,2}$=240MPa) should be employed. It is even more significant when the fault levels start exceeding 50kA and approach 63kA. Here one needs to look at special alloys with the characteristics shown by 6061T6, which has a proof stress of 276MPa.

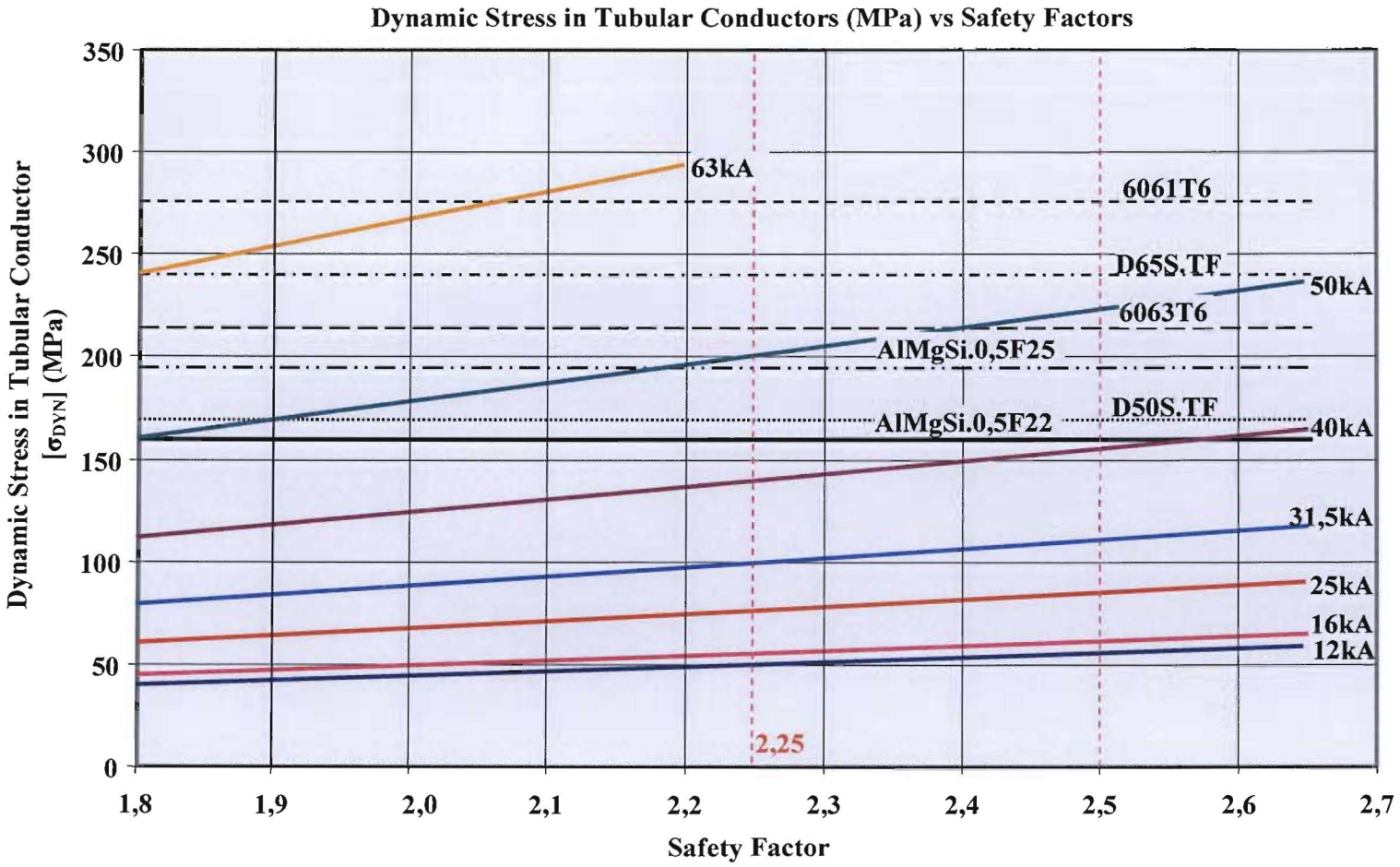

Figure 19.16: Impact of the Tubular Conductor Safety Factor on the Dynamic Stress Withstand Design Value [σ_{DYN}]

[Printout from Excel Based Busbar Programme]

20. SAMPLE CALCULATIONS

Objectives of this Chapter:

- Provide step-by-step hand calculations utilising most or all the concepts discussed in the foregoing chapters
- Illustrate the effect of different parameters on the end result
- To check the accuracy and correctness of the Excel based software programme developed to study the sensitivity of the end results due to material tolerances and parameter estimates.

20.1 Sample Calculation 1:-

20.1.1 System Parameters

Tubular conductor: 120 mm x 6 mm Alloy D65S TF.

$\mathbf{I_{sc}}$	=	25 kA
$\frac{\mathbf{X}}{\mathbf{R}}$	=	15
Wind force	=	700 Pa
3φARC	=	1 second dead time

Boundary conditions:-

one end supported ⅄ and one end fixed △

ℓ	=	10 000 mm
$\mathbf{s_p}$	=	3 000 mm
LIWL	=	550kV

Terrain having numerous closely spaced obstructions generally having the size of houses

	=	category 3
Class of structure	=	B
Assume structure rigid ($\mathbf{K_f}$)	=	1 (decrement factor)
Altitude ($\mathbf{H_a}$)	=	1800m
Regional wind velocity (**V**)	=	40m/s

The sample chosen is a typical arrangement for 132 kV with a continuous current rating of 2500A and a short time current rating of 25kA.

Table 6.2: Electrical and Mechanical Properties of Various Aluminium Alloys

Alloy Type	HULETT'S S.A.		ASA Standard		DIN Standard	
	D50S TF	**D65S TF**	**6063 T6**	**6061 T6**	**AlMgSi 0,5F22**	**AlMgSi 0,5F25**
Electrical resistivity at 20 °C (max.) in Ω mm^2 / m	0,03133	0,037	0,0325	0,0431	0,03333	0,03571
Specific mass kg/m^3	2703	2703	2703	2703	2703	2703
Modules of elasticity E in N / m^2	$65,66.10^9$	$69,12.10^9$	69.10^9	70.10^9	70.10^9	70.10^9
Thermal co-efficient of expansion per °C	23.10^{-6}	23.10^{-6}	23.10^{-6}	23.10^{-6}	23.10^{-6}	23.10^{-6}
0,2 % Proof Stress in Mpa Rp0,2	170	240	214	276	160	195

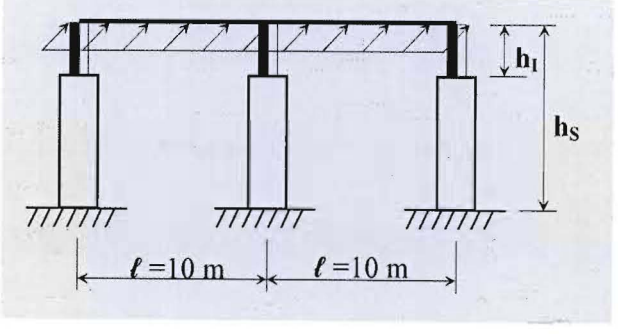

a) Wind and Dynamic Short Circuit Force

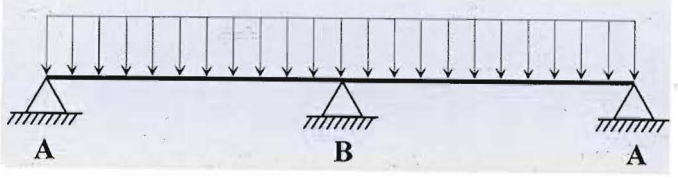

b) Mass of Conductor

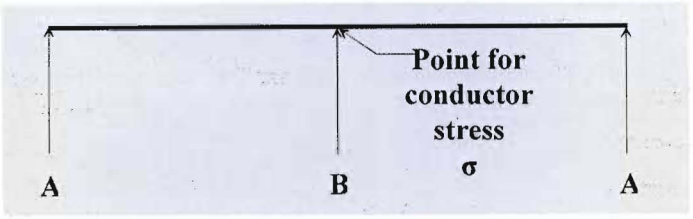

c) Stress

h_S = 6 500 mm
h_I = 1 500 mm
ℓ = 10 000 mm

Figure 20.1: Diagrammatic Illustration of Component Forces on Tubular Conductors for Example 1

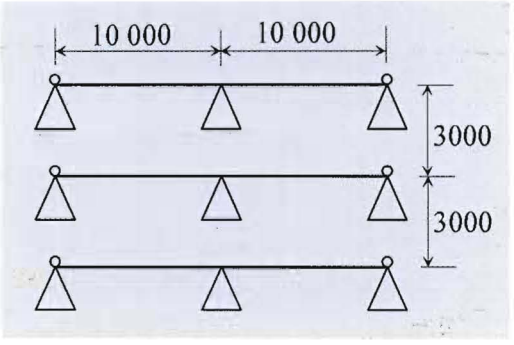

Figure 20.2: Busbar System for Analysis for Example 1

20.1.2 Support System (Post Insulator and Structure)

20.1.2.1 Reference force per unit length.

$$F_{ref} = K_f.\frac{4.10^{-7}}{s_p}.(I_{cc})^2 \qquad \text{(from 15.7)}$$

$$F_{ref} = 1.\frac{4.10^{-7}}{3}.\left(25.10^3\right)^2$$

$$= 83{,}3 \text{ (N/m)}$$

20.1.2.2 Kappa factor.

$$\kappa = 1{,}02 + 0{,}98.e^{\left(-3.\frac{R}{X}\right)} \qquad \text{(from 9.2)}$$

$$\kappa = 1{,}02 + 0{,}98.e^{\left(-3.\frac{1}{15}\right)}$$

$= \quad 1{,}02 + 0{,}98 \,.\, e^{(-0{,}2)}$

$= \quad 1{,}02 + 0{,}8024$

$= \quad \underline{1{,}8224}$

20.1.2.3 Peak force on centre phase.

$$F^{1}_{L2p} = 0{,}866.F_{ref}\kappa^{2} \text{ (N/m)} \qquad \text{(from 9.3)}$$

$$F^{1}_{L2p} = 0{,}866.83{,}3.(1{,}8442)^2$$

$= \underline{239{,}6}$ (N/m)

20.1.2.4 Mechanical frequency

$$f_c = \frac{\gamma}{\ell^2}.\sqrt{\frac{E.J}{m^1}} \text{ (Hz)} \qquad \text{(from 10.2)}$$

$\mathbf{E} \quad = \quad \underline{69{,}12 \,.\, 10^9}$ (N/m^2) Table 6.2

$$J = \frac{\pi}{64}.\left(d_o^{\,4} - d_i^{\,4}\right) \qquad \text{(from 9.12)}$$

$$J = \frac{\pi}{64}.\left(0{,}12^4 - [0{,}12 - 2.0{,}006]^4\right)$$

$= \quad 3{,}46.10^{-6}$ (m^4)

$\gamma \quad = \quad \underline{2{,}45}$ Table 10.2

(Boundary condition for post insulator (A) supported and post insulator (B) fixed).

20.1.2.5 Tubular conductor mass per unit length

$\mathbf{m}_{120.6} \quad = \quad 5{,}805$ (kg/m) Table 6.1

$$f_c = \frac{2{,}45}{(10)^2}.\sqrt{\frac{69{,}12.10^9.3{,}46.10^{-6}}{6{,}95}} \text{ (Hz)}$$

$= \quad 0{,}0245 \,.\, 185{,}50$

$= \quad \underline{4{,}54 \text{ Hz}}$

20.1.2.6 Ratio of mechanical frequency

$$\frac{f_c}{f} = \frac{\textbf{lowest mechanical frequency of conductor}}{\textbf{nominal system frequency}} \qquad \text{(from 10.4)}$$

where $\frac{f_c}{f} >> 1$ the stress is proportional to the exciting force

and

where $\frac{f_c}{f} << 1$ the stress is lower, except for special harmonic resonance.

$$\frac{f_c}{f} = \frac{4,45}{50}$$
$$= 0,09$$

20.1.2.7 Aeolian Vibration Frequency

$$f_a = \frac{51,75.V_a}{d_{bo}} \text{ (Hz)} \qquad \text{(from 11.1)}$$

$$f_a = \frac{51,75.24}{120}$$
$$= 10,35 \text{ (Hz)}$$

To test if $2.f_c > f_a$

$2.f_c = 2.4,84 = 9,68 < 10,35 = f_a$

Already has damping conductor in.

20.1.2.8 Static forces

Table 10.2: Extract from Fundamental Frequency Factors for Various Boundary Conditions of Tubular Busbars Complete with Support Arrangements

Type of beam and supports			Factor α	Factor γ
Single span beam	**A fixed support** **B simple support**	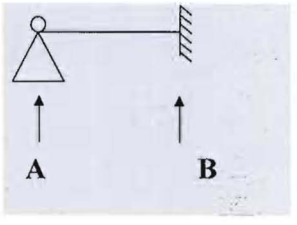	**A : 0,625** **B : 0,375**	**2,45**

$F_{(PI)ST} = \alpha . F^1_{L2p} . \ell$ (N) (from 14.5)

20.1.2.8a) End A fixed

$F_{A(PI)ST} = 0,625.239,6.10$
$= 1498$ N
$= 1,498$ kN

20.1.2.8b) End B supported (2.[5/8]=1,25) Fixed end with force either side x2

$F_{B(PI)ST}$ = 0,325.239,6.10

= 899 N

= 0,899 kN

The larger of the two values is $F_{A(PI)ST}$ = 1498 (N)

20.1.2.9 Dynamic factors

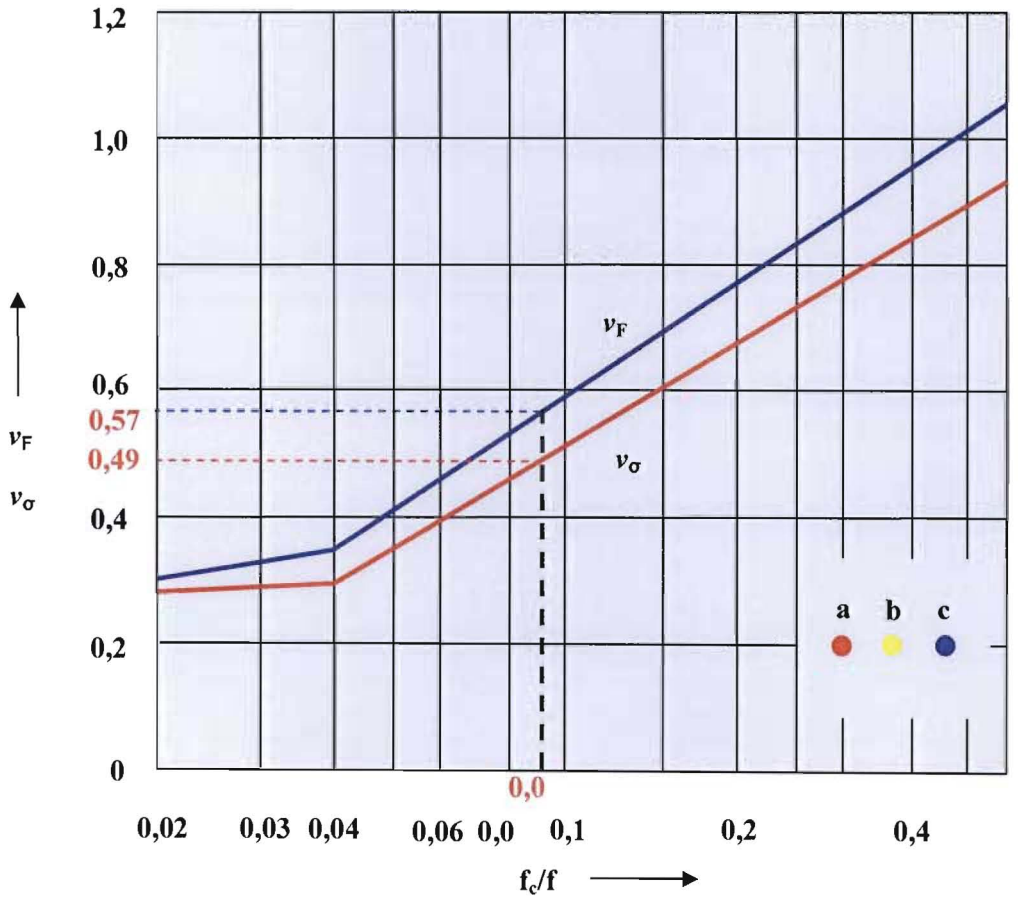

Figure 20.3: Dynamic Factors ν_F and ν_σ vs f_c/f for Example 1

Support system

ν_F = 0,57 (Figure 20.3)

Tubular conductor

ν_σ = 0,49 (Figure 20.3)

Three phase ARC

(≥ 1 second)

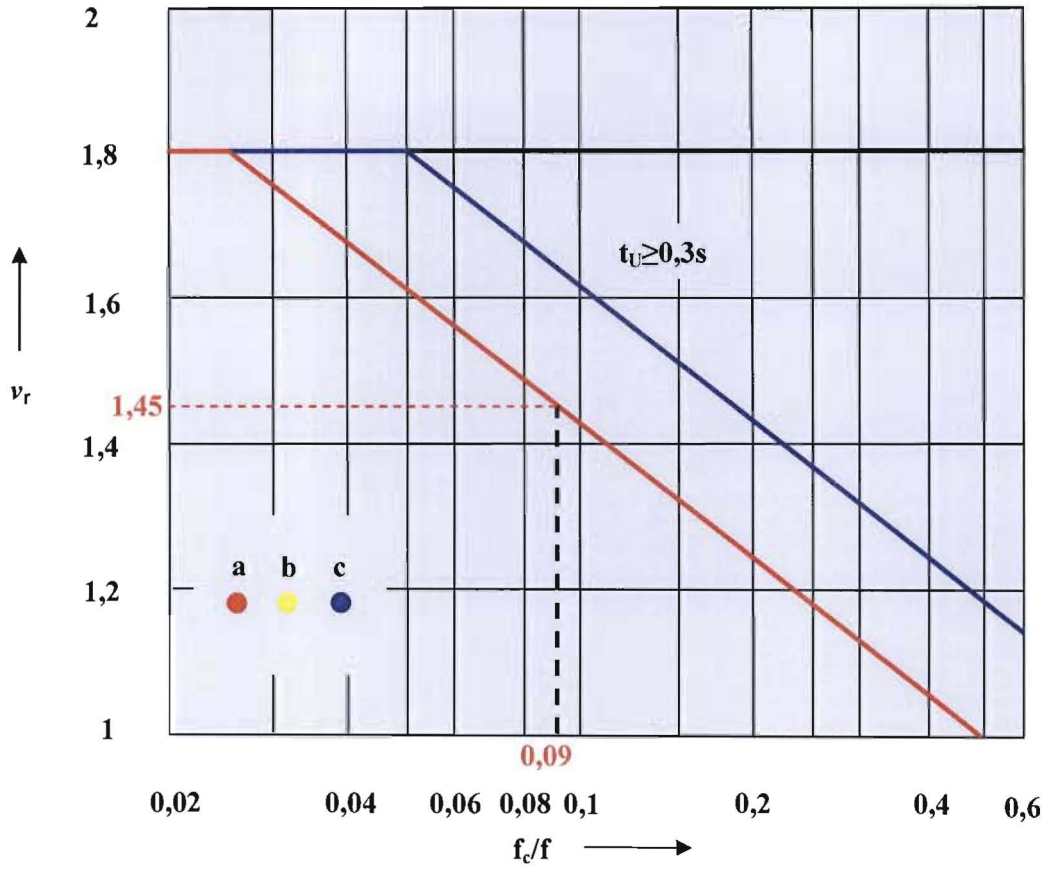

Figure 20.4: Dynamic Factor v_r vs f_c/f for Example 1

v_r = 1,45 (Figure 20.4)

20.1.2.10 Dynamic forces

$$F_{(PI)DYN} = \alpha.F^{I}_{L2p} \,.\, \ell \,.v_F$$
$$= F_{(PI)ST}.v_F$$

(from 14.8)

20.1.2.10a) End A fixed

$F_{A(PI)DYN} = 1,498 .0,57$
$= 0,835$ kN

20.1.2.10b) End B supported

$F_{B(PI)DYN} = 0,899.0,57$
$= 0,512$ kN

20.1.2.11 Dynamic forces with ARC

$$F_{(PI)DYN+\,ARC} = F_{DYN} \,.\, v_r$$

(from 14.11)

20.1.2.11a) End A fixed

$F_{A(PI)DYN+ARC} = 0{,}853.1{,}45$

$= 1{,}238$ kN

20.1.2.11b) End B supported

$F_{B(PI)DYN+ARC} = 1{,}512.1{,}45$

$= 0{,}742$ kN

20.1.2.12 Weight of tubular conductor

$m_b = m_c^1.\ell(kg)$ (from 14.8)

$= 6{,}95.10$

$= 69{,}5$ kg

$w_b = 682$ N ($g = 9{,}81$ m/s^2)

$= 0{,}682$ kN

20.1.2.13 Wind force on tubular conductor

Assuming tubular support structures

w_ℓ = **(wind force) . (projected area) . 0,6**

$= 700.0{,}12.10.0{,}6$

$= 504$ N

20.1.2.14 Resultant force F_R

$$F_{R(A)} = \sqrt{\left[(w_c + w_i)^2 + (\text{wind force} + F_{A(DYN+ARC)})^2\right]}$$ (from 14.15)

$= \sqrt{682^2 + (504 + 1238)^2}$

$= 1871$ N

$= 1{,}871$ kN

Safety factor for porcelain **S.F** = 1,2

$F_{R(A)MAX} = F_{R(A)} . S.F$ (from 14.17)

$= 1871.1{,}2$

$= 2245$ N

$= 2{,}245$ kN

$$F_{R(B)} = \sqrt{\left[(w_c + w_i)^2 + (\text{wind force} + F_{B(DYN+ARC)})^2\right]}$$ (from 14.16)

$= \sqrt{682^2 + (504 + 742)^2}$

$= 1420$ N

$= 1{,}42$ kN

$F_{R(B)MAX} = F_{R(B)} . S.F$ (from 14.18)

= 1420.1,2

= 1705

= 1,705 kN

The greater force is exerted on support B insulator, viz. **2,245 kN**. A standard porcelain insulator with **4 kN** cantilever strength would suffice.

20.1.2.15 Bending moment at the base of the porcelain insulator

$\mathbf{h_1}$ (height of insulator) = 1,2 m

$\mathbf{M_{(A)}} = \mathbf{F_{R(A)MAX}} \cdot \mathbf{h_1}$ (from 15.2)

= 1871.1,2

= 2245 Nm

= 2,245 kNm

$\mathbf{M_{(B)}} = \mathbf{F_{R(B)MAX}} \cdot \mathbf{h_1}$ (from 15.3)

= 1420.1,2

= 1704 Nm

= 1,704 kNm

20.1.2.16 Bending moment at base of support structure

For steel support structure: $\mathbf{h_s}$. = 6,42

$\mathbf{M_{(A)}} = \mathbf{F_{R(A)}} \cdot (\mathbf{h_s} + \mathbf{h_i})$ (from 15.5)

= 1871.(6,42 + 1,2)

= 14,257 kNm

$\mathbf{M_{(B)}} = \mathbf{F_{R(B)}} \cdot (\mathbf{h_s} + \mathbf{h_i})$ (from 15.6)

= 1420 .(6,42 + 1,2)

= 10,82 kNm

20.1.3 Tubular Conductor System

Stress in the Tubular Conductor:

20.1.3.1 Short circuit forces per unit length including ARC

20.1.3.1a) Weight of bus tubing and damping conductor per unit length

$\mathbf{w^1_{b+c}}$ = 68,2 N/m

20.1.3.1b) Wind loading per unit length

$(\mathbf{w^1}.\boldsymbol{\ell})$ = 50,4 N/m

20.1.3.2 Resultant force F_R per unit length

$$F_{R(\sigma)} = \sqrt{(\text{weight conductor} + \text{weight ice})^2 + (\text{wind force} + F^1_{(L2p)})^2}$$

$$= \sqrt{(68,2+0)^2 + (50,4+239,66)^2} \qquad \text{(from 9.6)}$$

$$= 298 \text{ N/m}$$

20.1.3.3 Section modulus

$$J = \frac{\pi}{64}.\left(d_o^4 - d_i^4\right)$$

$$= \frac{\pi}{64}.\left(0,120^4 - 0,108^4\right) \qquad \text{(from 9.12)}$$

$$= 3,501.10^{-6} \text{ (m)}$$

$$W = \frac{J}{\left(\frac{d_o}{2}\right)}$$

$$= \frac{3,501.10^{-6}}{\left(\frac{0,12}{2}\right)} \qquad \text{(from 9.11)}$$

$$= 58,35.10^{-6} \text{ (m}^3\text{)}$$

$$= 58,35 \text{ cm}^3$$

20.1.3.4 Static stress (from 9.8)

$$\sigma_{ST} = \frac{F_{R(\sigma)}.\ell^2}{8.W}$$

$$= \frac{298.10^2}{8.58,35} \text{ N/mm}^2$$

$$= \underline{63,83} \text{ N/mm}^2 \text{ (or MPa)}$$

20.1.3.5 Dynamic stress excluding ARC: (from 12.1)

$$\sigma_{DYN} = \sigma_{ST}.\nu_\sigma$$

$$= 63,83 \text{ . } 0,49$$

$$= \underline{31,28} \text{ MPa}$$

20.1.3.6 Dynamic stress including ARC:

$$\sigma_{DYN+ARC} = \sigma_{DYN} \cdot \nu_r \qquad \text{(from 12.2)}$$

$$= 63,83 \text{ . } 1,45$$

$$= \underline{45,4} \text{ MPa}$$

20.1.3.7 Dynamic stress including ARC and S.F.

Safety factor for aluminium tubular conductor **SF = 2,65**

$\sigma_{(DYN+ARC)\,MAX}$ = $\sigma_{DYN+ARC}$. 2,65 (from 12.3)

= 45,4 . 2,65

= $\xrightarrow{120,2\ MPa}$

0,2 % Proof stress for D65S

$\mathbf{R_{p0,2}}$ = 240 Mpa (Table 12.3)

i.e. the tubular conductor will not be over stressed or permanently deformed.

$\sigma_{(DYN+ARC)\,MAX}$ = $\xrightarrow{\mathbf{120,2 < R_{p0,2}}}$

20.1.4 Maximum deflection

For conductor with one end supported and one end fixed:-

$$y_{max} = \frac{1}{185} . \frac{F^{1}_{L2p} . \ell^{4}}{E.J}\ (m) \qquad \text{(from 13.10)}$$

20.1.4.1 Maximum deflection under own weight

The maximum deflection of the tubular conductor under static conditions due to its own weight (force)

$$y_{max} = \frac{1}{185} . \frac{(9,81.m^{1}).\ell^{4}}{E.J}\ (m) \qquad \text{(from 13.2)}$$

$$= \frac{9,8 . 6,95 . 10^{4}}{185 . 69,12 . 10^{9} . 3,46 . 10^{-6}}$$

$= 15,41 . 10^{-3}$ m

= 0,0154 m

≈ 15 mm

20.1.4.2 Maximum deflection under dynamic conditions (wind, short current forces and its own weight)

The maximum deflection of the tubular conductor under dynamic conditions due to wind, short current forces and its own weight is:-

$$y_{max} = \frac{1}{185} . \frac{F^{1}_{L2p} . \ell^{4}}{E.J}\ (m) \qquad \text{(from 13.10)}$$

$$y_{max} = \frac{1}{185} . \frac{F_{R(A)} . \ell^{3}}{E.J}\ (m)$$

$$= \frac{2245.10^3}{185.69,12.10^9 .3,46.10^{-6}}$$

$$= 67,94 \; . \; 10^{-3} \text{ m}$$

$$= \underrightarrow{51 \text{ mm}}$$

20.1.5 Calculation of Conductor Surface Field Strength and Determination of Corona Inception Levels for Typical Arrangements

20.1.5.1 Corona threshold limits (E_c)

Polished tubes	-	**1,0**
Extruded tubes	-	**0,95**
stranded conductor	-	**0,8**

E_c = Corona threshold surface field strength

δ = 0,8 (Relative air density (RAD))

r'_{bo} = 0,06 (Conductor radius in metres)

m = 0,95 (Factor to allow for surface roughness)

Peek :

$$\mathbf{E_c = 3.m.\delta\left[1 + \frac{0,03}{\sqrt{r_o.\delta}}\right].\frac{10}{\sqrt{2}}\frac{kV}{cm}\ (rms)} \qquad \text{(from 17.2)}$$

$$E_c = 3.0,95.0,8\left[1 + \frac{0,03}{\sqrt{0,06.0,8}}\right].\frac{10}{\sqrt{2}}$$

$$= 18,33 \ \frac{kV}{cm} \text{ (rms)}$$

Heymann :

$$\mathbf{E_c = 2,4.m.\delta\left[1 + \frac{0,0937}{(r_o.\delta)^{0,4}}\right].\frac{10}{\sqrt{2}}\frac{kV}{cm}\ (rms)} \qquad \text{(from 17.3)}$$

$$E_c = 2,4.0,95.0,8\left[1 + \frac{0,0937}{(0,06.0,8)^{0,4}}\right].\frac{10}{\sqrt{2}}$$

$$= 16,97 \ \frac{kV}{cm} \text{ (rms)}$$

$E_{cave} = (18,33 + 16,97)/2$

$= 17,65$ kV/cm (rms)

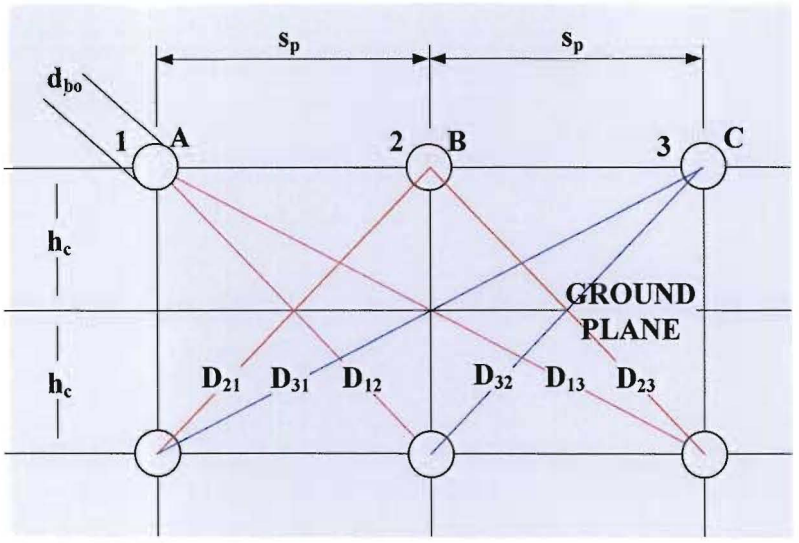

Figure 20.5: Conductor Surface Field Strength using the Image Method for Example 1

$$P_1 = \ln\left[\frac{2.h_c}{r}\right] - 0{,}5.\ln\left[\frac{\sqrt{\left([2.h_c]^2 + s_p{}^2\right)}}{s_p}\right] - 0{,}5.\ln\left[\frac{\sqrt{\left([2.h_c]^2 + [2.s_p]^2\right)}}{2.s_p}\right]$$

$$= \ln\left[\frac{2.6}{0{,}06}\right] - 0{,}5.\ln\left[\frac{\sqrt{(2.6)^2 + 3^2}}{3}\right] - 0{,}5.\ln\left[\frac{\sqrt{(2.6)^2 + (2.3)^2}}{2.3}\right} \quad \text{(from 17.36)}$$

$$= 5{,}2983 - 0{,}7083 - 0{,}4024$$

$$= 4{,}1867$$

$$P_2 = -0{,}5.\ln\left[\frac{\sqrt{\left([2.h_c]^2 + s_p{}^2\right)}}{s_p}\right] + \ln\left[\frac{2.h_c}{r_{bo}}\right] - 0{,}5.\ln\left[\frac{\sqrt{\left([2.h_c]^2 + s_p{}^2\right)}}{s_p}\right]$$

$$= -0{,}5.\ln\left[\frac{\sqrt{\left([2.6]^2 + 3^2\right)}}{3}\right] + \ln\left[\frac{2.6}{0{,}06}\right] - 0{,}5.\ln\left[\frac{\sqrt{\left([2.6]^2 + 3^2\right)}}{3}\right] \quad \text{(from 17.37)}$$

$$= -0{,}7083 + 5{,}2983 - 0{,}7083$$

$$= 3{,}8817$$

$$\mathbf{P_3 = -0{,}5.\ln\left[\frac{\sqrt{\left([2.h_c]^2 + [2.s_p]^2\right)}}{2.s_p}\right] - 0{,}5.\ln\left[\frac{\sqrt{\left([2.h_c]^2 + s_p^2\right)}}{s_p}\right] + \ln\left[\frac{2.h_c}{r_{bo}}\right]}$$

$$= -0{,}5.\ln\left[\frac{\sqrt{\left([2.6]^2 + [2.3^2]\right)}}{2.3}\right] - 0{,}5.\ln\left[\frac{\sqrt{\left([2.8]^2 + 3^2\right)}}{3}\right] + \ln\left[\frac{2.6}{0{,}06}\right] \quad \text{(from 17.38)}$$

$$= -0{,}4024 - 0{,}7083 + 5{,}2983$$

$$= 4{,}1876$$

$$\mathbf{E_{1av} = \frac{[V_L]}{\sqrt{3}}.\frac{1}{P_{1r}}.\frac{1}{r_{1bo}}.\frac{1}{10^2}}$$

$$= \frac{[132]}{\sqrt{3}}.\frac{1}{4{,}1876}.\frac{1}{0{,}06}.\frac{1}{10^2} \quad \text{(from 17.42)}$$

$$= 3{,}0332 \text{kV/cm(rms)}$$

$$\mathbf{E_{1av} = \frac{[V_L]}{\sqrt{3}}.\frac{1}{P_{1r}}.\frac{1}{r_{2bo}}.\frac{1}{10^2}}$$

$$= \frac{[132]}{\sqrt{3}}.\frac{1}{3{,}8817}.\frac{1}{0{,}06}.\frac{1}{10^2} \quad \text{(from 17.44)}$$

$$= 3{,}2722 \text{ kV/cm(rms)}$$

$$\mathbf{E_{3av} = \frac{[V_L]}{\sqrt{3}}.\frac{1}{P_{1r}}.\frac{1}{r_{3bo}}.\frac{1}{10^2}}$$

$$= \frac{[132]}{\sqrt{3}}.\frac{1}{4{,}1876}.\frac{1}{0{,}06}.\frac{1}{10^2} \quad \text{(from 17.46)}$$

$$= 3{,}0332 \text{ kV/cm(rms))}$$

$$\mathbf{E_c = E_{av}.\left[1 + 0{,}71.(n-1).\frac{d}{b}\right]} \quad \text{(from17.14)}$$

$\mathbf{E_e}$=3,2kV/cm<<<18,3 kV/cm =$\mathbf{E_c}$, therefore **no corona** will be present

20.1.5.2 Electric Field Strength (E_i)

$$\mathbf{E_i = 0.133.h_{ci}^{-1.789}.s_{pi}^{0.43}.d_{oi}^{0.22}.V_i^{1.003}} \quad \text{(from 18.24)}$$

From (19.24) therefore;

$$\mathbf{E_i} = 0{,}133.6{,}5^{-1.789}.3^{0.43}.120^{0.22}.145^{1.003}$$

$$= 2{,}7\text{kV/m}$$

The magnitude of the electric field is less that the 5kV/m limit required for public areas, and far less than the 10kV/m limit required for HV yards.

20.1.5.3 Magnetic Field Strength (H_i)

$$H_i = 0.697.h_{ci}^{-1.728}.s_{pi}^{0.29}.I_i^{0.997} \quad (18.36)$$

From eq.18.36 therefore;

$$H_i = 0.697.6{,}5^{-1.728}.3^{0.29}.2500^{0.997}$$

$$= 92{,}2\mu T$$

The magnitude of the magnetic field is less that the 100μT limit required for public areas, and far less than the 500μT limit required for HV yards.

20.2 Sample Calculation 2:- Comprises a series of calculations for a variety of conditions for the same bus tube

20.2.1 System Parameters

Description	Case 1	Case 2	Case 3	Case 4
System Voltage (kV)	400	400	400	400
SIWL (U_{rse}) (kV)	950	950	950	950
Ratio pp/pe	1,5	1,5	1,5	1,5
SIWL (U_{rsp}) (kV)	1425	1425	1425	1425
Electrode Configuration	R-C	R-C	R-C	R-C
Tube	250 mm x 6 mm	250 mm x 6 mm	250 mm x 6 mm	250 mm x 6 mm
Alloy	D65S TF	6061T6	AlMgSi0,5F25	6063T6
I_{sc} (kA)	50	63	40	50
I_n (A)	3500	4500	4000	3750
3φARC dead time (s)	1	0,3	1	1
Boundary Conditions	Multiple spans all supported	3-spans 2 ends supported , 2-centre fixed	2-spans 2 ends supported , centre fixed	Single span 1 end supported , 1 end fixed
ℓ (mm)	20 000	21 000	18 500	19 000
s_p(mm)	5 500	6 000	5 000	5 200
h_s (mm)	9 290	8 400	9 750	8 100
h_l (mm)	3250	3 600	3 250	3 400
h_b (mm)	12 540	12 000	13 000	11 500

Support Type	Lattice Steel	Tubular or Wide Flange Steel	Lattice or Tubular Aluminium	Solid Concrete
Structure Class	B	B	B	B
Description	**Case 1**	**Case 2**	**Case 3**	**Case 4**
Terrain Category	-	1	2	4
Wind Speed (m/s)	-	40	45	50
Wind force	750 Pa	-	-	-
Ice	Light	Heavy	Medium	None
Thickness of Ice(t_i) (mm)	0	12,7	6,4	0

$$\frac{X}{R} = 15$$

Table 6.2: Electrical and Mechanical Properties of Various Aluminium Alloys

Alloy Type	HULETT'S S.A.		ASA STANDARD		DIN STANDARD	
	D50S TF	D65S TF	6063 T6	6061 T6	AlMgSi0,5 F22	AlMgSi0,5 F25
Electrical resistivity at 20 °C (max.) in Ω mm² / m	0,03133	0,037	0,0325	0,0431	0,03333	0,03571
Specific mass kg/m³	2703	2703	2703	2703	2703	2703
Modules of elasticity E in N / m²	$65,66.10^9$	$69,12.10^9$	69.10^9	70.10^9	70.10^9	70.10^9
Thermal co-efficient of expansion per °C	23.10^{-6}	23.10^{-6}	23.10^{-6}	23.10^{-6}	23.10^{-6}	23.10^{-6}
0,2 % Proof Stress in Mpa Rp0,2	170	240	214	276	160	195

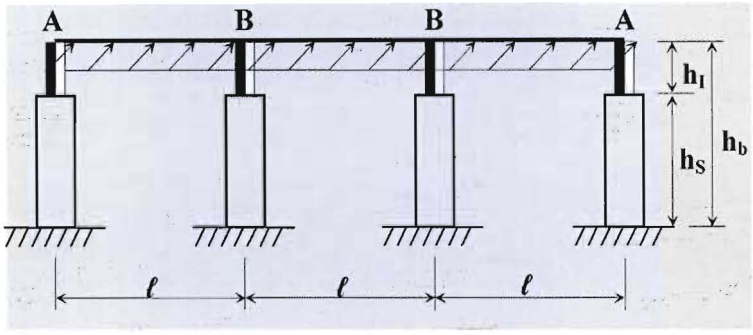

a) Wind and Dynamic Short Circuit Force

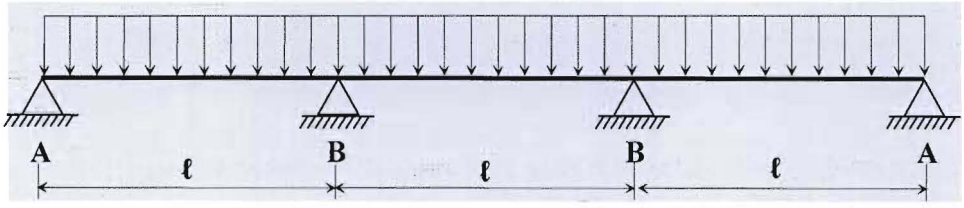

b) Mass of Conductor

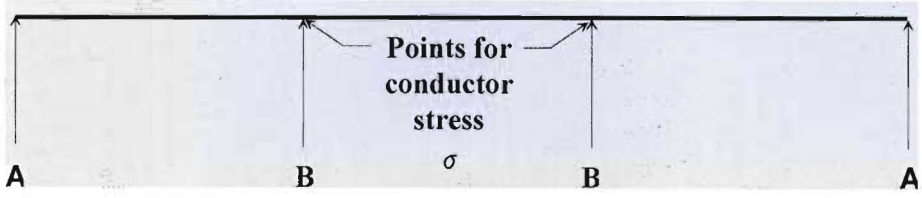

c) Stress

Figure 20.6: Diagrammatic Illustration of Component Forces on Tubular Conductors

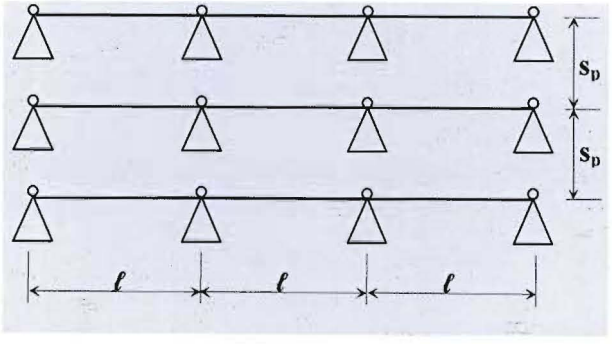

Figure 21.7: Multi-Support Busbar System for Example 2

20.2.2 Support System (Post Insulator and Structure) (See Figures 20.6 and 20.7)

20.2.2.1 Reference force per unit length.

$$F^{1}_{sc} = K_f . \frac{4.10^{-7}}{s_p} . (I_{sc})^2$$ (from 15.7)

Support Type	Case 1	Case 2	Case 3	Case 4
	Lattice Steel (**C**)	Tubular or Wide Flange Steel (**B**)	Lattice or Tubular Aluminium (**A**)	Solid Concrete (**D**)
h_c (mm)	9 290	8 400	9 750	8 100
K_f	0,820	0,805	0,715	0,960
I_{sc} (kA)	50	63	40	50
s_p (mm)	5,5	6,0	5,0	5,2
F^1_{sc} (N/m)	149,09	213,00	91,52	184,62

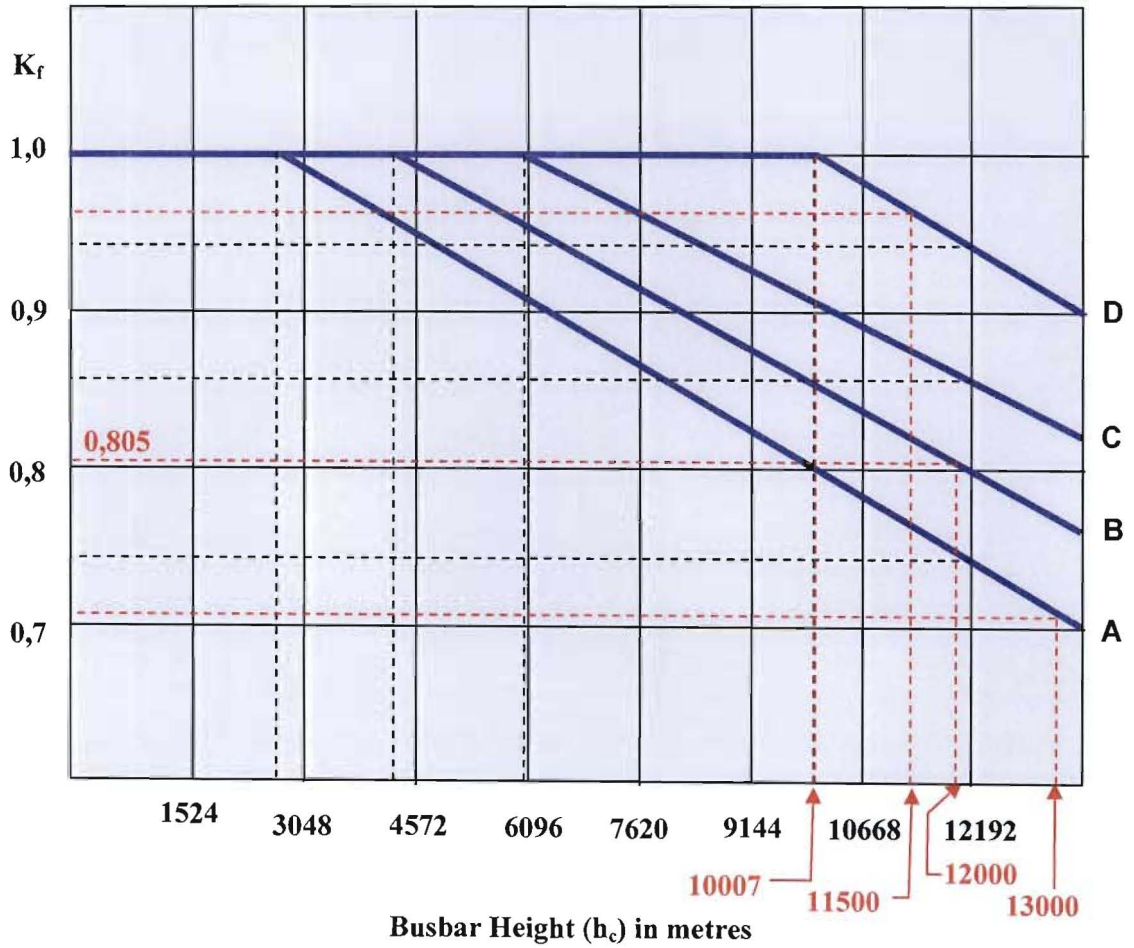

Figure 20.8: Structure Flexibility Factor (K_f) vs Busbar Height (h_c) for Example 2

20.2.2.2 Kappa Factor (κ)

$$\kappa = 1{,}02 + 0{,}98.e^{\left(-3.\frac{R}{X}\right)}$$ (from 9.2)

$$\kappa = 1{,}02 + 0{,}98.e^{\left(-3.\frac{1}{15}\right)}$$

$$= \quad 1{,}02 + 0{,}98 \,.\, e^{(-0{,}2)}$$

$$= \quad 1{,}02 + 0{,}8024$$

$$= \quad \underline{1{,}8224}$$

20.2.2.3 Peak force on centre phase.

$F_{sc(L2p)} = K_f.0{,}866.F_{sc}\kappa^{2}$ (N/m) (from 9.3)

Support Type	Case 1	Case 2	Case 3	Case 4
	Lattice Steel (C)	Tubular or Wide Flange Steel (B)	Lattice or Tubular Aluminium (A)	Solid Concrete (D)
K_f				
F^{1}_{L2p} (N/m)	0,866.149,09. $(1{,}8224)^2$	0,866.213,00. $(1{,}8224)^2$	0,866.91,52. $(1{,}8224)^2$	0,866.84,62. $(1{,}8224)^2$
	428,80	612,62	263,22	530,97

20.2.2.4 Mechanical frequency

$$f_c = \frac{\gamma}{\ell^2}.\sqrt{\frac{E.J}{m^1}}\,(Hz) \qquad \text{(from 10.2)}$$

Table 10.2: Extract from Fundamental Frequency Factors for Various Boundary Conditions of Tubular Busbars Complete with Support Arrangements

Support Type	Case 1	Case 2	Case 3	Case 4
	Lattice Steel (C)	Tubular or Wide Flange Steel (B)	Lattice or Tubular Aluminium (A)	Solid Concrete (D)
Boundary Conditions	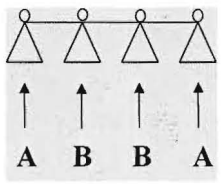	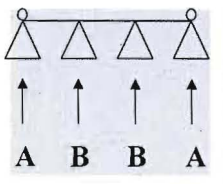	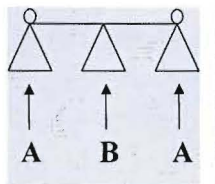	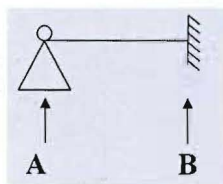
PI Force Factor (α)	A : 0,5 B : 1,0	A : 0,4 B : 1,1	A : 0,375 B : 1,25	A : 0,625 B : 0,375
Stress Factor (β)	0,73	0,73	0,73	0,73

Relevant Characteristic Factor (γ)	**1,57**	**3,56**	**2,45**	**2,45**

$\mathbf{E} = \underline{69,12 \cdot 10^9}\ (N/m^2)$ (Table 6.2)

$\mathbf{J} = \frac{\pi}{64}.\left(d_o^4 - d_i^4\right)$ (from 9.12)

$= \frac{\pi}{64}.\left(0,25^4 - [0,25 - 2.0,006]^4\right)$

$= 34,26.10^{-6}\ (m^4)$

20.2.2.5 Ice on tubular conductor (mass per unit length)

$\mathbf{m^1}_i = \rho_i.\pi.\left(d_{bo} + t_i\right).t_i.10^{-6}\ (kg/m)$ (from 8.10 & 8.11)

Density of Ice = $714 kg/m^3$

Support Type	**Case 1** Lattice Steel (**C**)	**Case 2** Tubular or Wide Flange Steel (**B**)	**Case 3** Lattice or Tubular Aluminium (**A**)	**Case 4** Solid Concrete (**D**)
Ice	Light	Heavy	Medium	None
Thickness of Ice(t_i) (mm)	0	12,7	6,4	0
Mass if Ice per unit length (kg/m)	0	$714.\pi.(250+12,7).12,7.10^{-6}$	$714.\pi.(250+6,4).12,7.10^{-6}$	0
	0	7,48	3,68	0

20.2.2.6 Tubular and damping conductors (mass per unit length)

Support Type	**Case 1** Lattice Steel (**C**)	**Case 2** Tubular or Wide Flange Steel (**B**)	**Case 3** Lattice or Tubular Aluminium (**A**)	**Case 4** Solid Concrete (**D**)
Mass per unit length of bus tube +	12,4 + 2.1,15 + 0	12,4 + 2.1,15 + 7,48	12,4 + 2.1,15 + 3,68	12,4 + 2.1,15 + 0

damping conductor + ice	14,70	22,18	18,38	14,70

$$f_c = \frac{\gamma}{\ell^2} \cdot \sqrt{\frac{E.J}{m^1{}_{b+c}}} \text{ (Hz)}$$ (from 10.2)

Support Type	Case 1	Case 2	Case 3	Case 4
	Lattice Steel (C)	Tubular or Wide Flange Steel (B)	Lattice or Tubular Aluminium (A)	Solid Concrete (D)
Factor γ	**1,57**	**3,56**	**2,45**	**2,45**
ℓ (m)	20	21	18,5	19
Natural frequency (without Ice) (f_c) (Hz)	$\frac{1,57}{(20)^2} \cdot \sqrt{\frac{69,12.10^9.34,26.10^{-6}}{14,7}}$	$\frac{3,56}{(21)^2} \cdot \sqrt{\frac{70.10^9.34,26.10^{-6}}{14,7}}$	$\frac{2,45}{(18,5)^2} \cdot \sqrt{\frac{69,12.10^9.34,26.10^{-6}}{14,7}}$	$\frac{2,45}{(19)^2} \cdot \sqrt{\frac{69.10^9.34,26.10^{-6}}{14,7}}$
	1,58	3,24	2,87	2,72
Natural frequency (with Ice) (f_{ci}) (Hz)	**No Ice**	$\frac{3,56}{(21)^2} \cdot \sqrt{\frac{69,12.10^9.34,26.10^{-6}}{22,18}}$	$\frac{2,45}{(18,5)^2} \cdot \sqrt{\frac{69,12.10^9.34,26.10^{-6}}{18,38}}$	**No Ice**
	1,58	2,64	2,57	2,72

20.2.3 Ratio of mechanical frequency

$$\frac{fc}{f} = \frac{\text{lowest mechanical frequency of conductor}}{\text{nominal system frequency}} \qquad \text{(from 10.4)}$$

where $\frac{f_c}{f} >> 1$ the stress is proportional to the exciting force

and

where $\frac{f_c}{f} << 1$ the stress is lower, except for special harmonic resonance.

Support Type	Case 1	Case 2	Case 3	Case 4
	Lattice Steel (**C**)	Tubular or Wide Flange Steel (**B**)	Lattice or Tubular Aluminium (**A**)	Solid Concrete (**D**)
Frequency Ratio (without Ice)	$\frac{1,58}{50}$	$\frac{3,24}{50}$	$\frac{2,87}{50}$	$\frac{2,72}{50}$
$\frac{f_c}{f}$	0,0316	0,0648	0,0574	0,0544
Natural frequency (with Ice)	$\frac{1,58}{50}$	$\frac{2,64}{50}$	$\frac{2,57}{50}$	$\frac{2,72}{50}$
$\frac{f_c}{f}$	0,0316	0,0528	0,0514	0,0544

$\nu_F = 0,1684.\text{Log}(f_c/f) + 0,5903$ **for** $0,02 \leq f_c/f \leq 0,04$ (from 10.8)

$\nu_F = 0,6108.\text{Log}(f_c/f) + 1,2087$ **for** $0,04 \leq f_c/f \leq 0,6$ (from 10.9)

$\nu_\sigma = 0,0352.\text{Log}(f_c/f) + 0,3471$ **for** $0,02 \leq f_c/f \leq 0,04$ (from 10.10)

$\nu_\sigma = 0,5586.\text{Log}(f_c/f) + 1,0788$ **for** $0,04 \leq f_c/f \leq 0,6$ (from 10.11)

$\nu_r = 1,8$ **for** $0,02 \leq f_c/f \leq 0,0274$; $t_U \geq 1s$ (from 10.12)

$\nu_r = 0,8009 - 0,6395.\text{Log}(f_c/f)$ **for** $0,0274 \leq f_c/f \leq 0.4883$; $t_U \geq 1s$ (from 10.13)

$\nu_r = 1,8$ **for** $0,02 \leq f_c/f \leq 0,05$; $t_U \geq 0,3s$ (from 10.14)

$\nu_r = 1,0152 - 0,6032.\text{Log}(f_c/f)$ **for** $0,05 \leq f_c/f \leq 0,6$; $t_U \geq 0,3s$ (from 10.15)

Support Type	**Case 1**	**Case 2**	**Case 3**	**Case 4**
	Lattice Steel (**C**)	Tubular or Wide Flange Steel (**B**)	Lattice or Tubular Aluminium (**A**)	Solid Concrete (**D**)
3φARC dead time (s)	1	3	1	1
v_F	0,1684.Log(0,0316) + 0,5903	0, 6108.Log(0,0648) + 1,2087	0, 6108.Log(0,0574) + 1,2087	0, 6108.Log(0,0544) + 1,2087
	0,3376	0,4828	0,4506	0,4364
v_σ	0,0352.Log(0,0316) + 0,3471	0, 5586.Log(0,0648) + 1, 0788	0, 5586.Log(0,0574) + 1, 0788	0, 5586.Log(0,0544) + 1, 0788
	0,2943	0,4149	0,3855	0,3725
v_r	0,8009 - 0, 6395.Log(0,0316)	1,0152 - 0, 6032.Log(0,0648)	0,8009 - 0, 6395.Log(0,0574)	0,8009 - 0, 6395.Log(0,0544)
	1,7604	1,7321	1,5946	1,6095

20.2.3.1 Dynamic factors

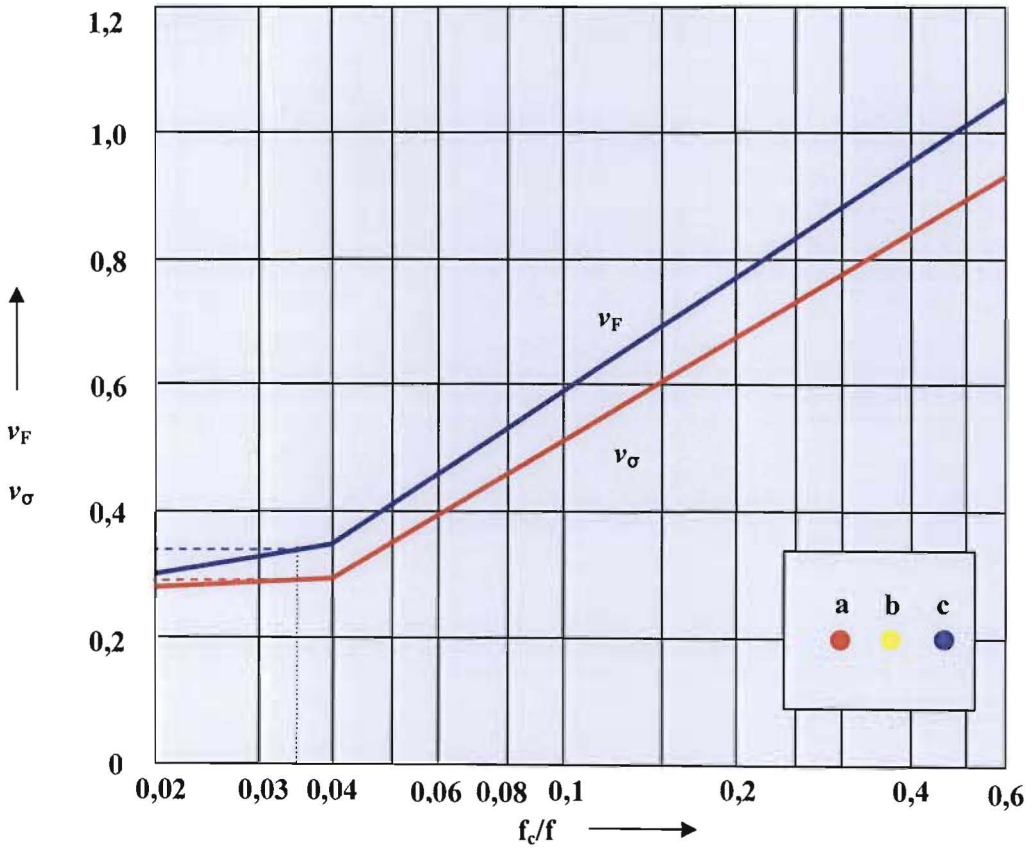

Figure 20.9: Dynamic Factors v_F and v_σ vs f_c/f for Example 2

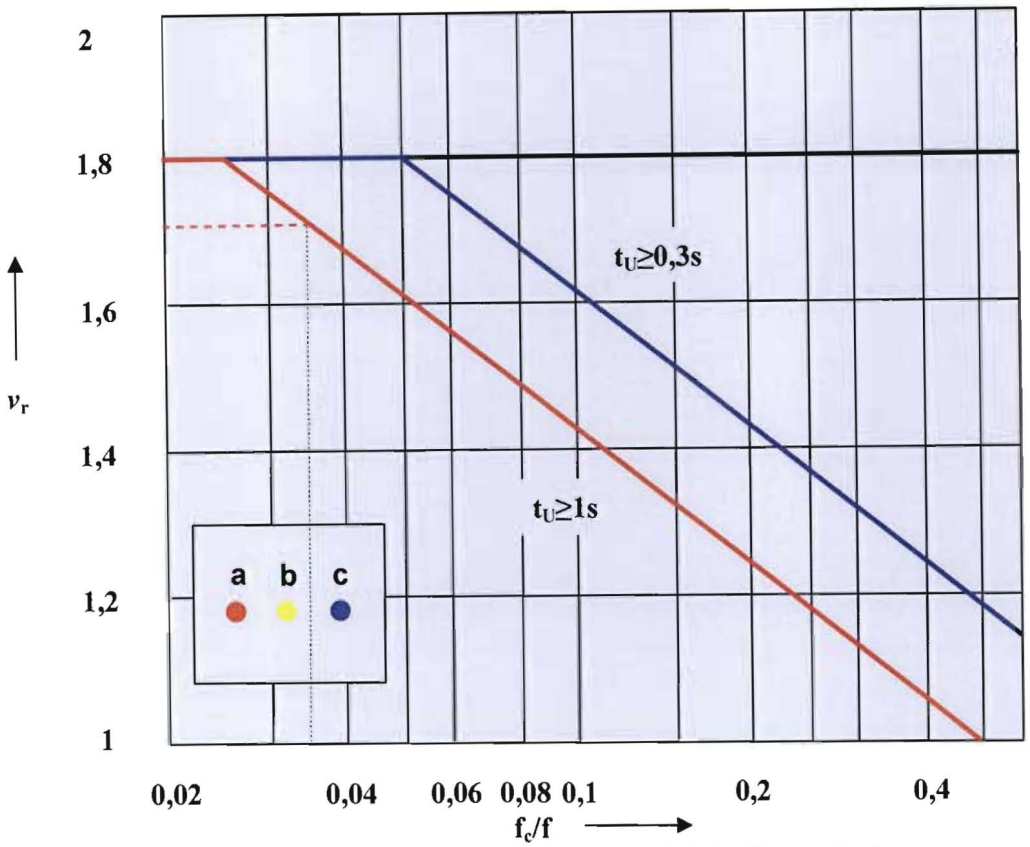

Figure 20.10: Dynamic Factor v_r vs f_c/f for Example 2

20.2.4 Static forces (pertaining to the post insulator alone)

$F_{(PI)ST} = \alpha . F^1_{L2p}$ (N/m)

$F_{(PI)ST} = \alpha . F^1_{L2p} . \ell$ (N) (from 14.5)

Support Type	**Case 1** Lattice Steel (**C**)	**Case 2** Tubular or Wide Flange Steel (**B**)	**Case 3** Lattice or Tubular Aluminium (**A**)	**Case 4** Solid Concrete (**D**)
Boundary Conditions	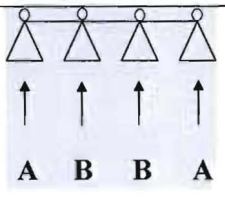	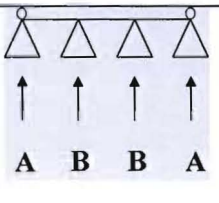	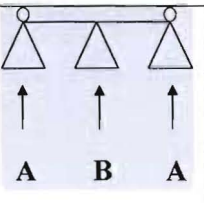	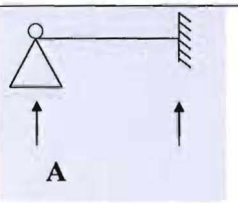
Factor α	A : 0,5 **B : 1,0**	A : 0,4 **B : 1,1**	A : 0,375 **B : 1,25**	**A : 0,625** B : 0,375
ℓ (m)	20	21	18,5	19
Support	**Case 1**	**Case 2**	**Case 3**	**Case 4**

Type	Lattice Steel (C)	Tubular or Wide Flange Steel (B)	Lattice or Tubular Aluminium (A)	Solid Concrete (D)
$F_{A(PI)ST}$	0,5. 428,80	0,4. 612,62	0,375. 263,22	0,625. 530,97
(N/m)	214,40	245,04	98,71	331,86
$F_{A(PI)ST}$	214,40.20	245,04.21	98,71.18,5	331,86.19
(N)	4288	5146	1826	6305
$F_{B(PI)ST}$	1,0. 428,80	1,1. 612,62	1,25. 263,22	0,375. 530,97
(N/m)	428,80	673,88	329,03	199,12
$F_{B(PI)ST}$	428,80.20	673,88.21	329,03.18,5	199,12.19
(N)	8576	14151	6087	3783

The larger of the two values is indicated in green highlight

20.2.5 Dynamic forces <u>without ARC</u> (dynamic factor pertaining to the post insulator alone)

$F_{(PI)DYN} = \alpha.F^{1}_{L2p} . \ell . \nu_F$ (from 14.8)

$= F_{(PI)ST}.\nu_F$ (N)

Support Type	Case 1	Case 2	Case 3	Case 4
	Lattice Steel (C)	Tubular or Wide Flange Steel (B)	Lattice or Tubular Aluminium (A)	Solid Concrete (D)
$F_{A(PI)DYN}$	214,40.0,3376	245,64. 0,4828	98,71. 0,4506	331,86. 0,4364
(N/m)	72,38	118,60	44,48	144,82
$F_{A(PI)DYN}$	4288. 0,3376	5146. 0,4828	1826,09. 0,4506	6305,32.0,4364
(N)	1447,63	2484,49	822,84	2751,64
$F_{B(PI)DYN}$	428,80. 0,3376	673,88. 0,4828	329,03. 0,4506	199,12. 0,4364
(N/m)	144,76	325,34	148,26	86,90

20.2.6 Dynamic forces <u>with ARC</u> (dynamic factor pertaining to the post insulator alone)

$F_{(PI)DYN+ ARC} = F_{DYN} . \nu_r$ (from 14.11)

Support Type	Case 1	Case 2	Case 3	Case 4
	Lattice Steel (C)	Tubular or Wide Flange Steel (B)	Lattice or Tubular Aluminium (A)	Solid Concrete (D)
$F_{B(PI)DYN}$	8576. 0,3376	14151. 0,4828	6086,96. 0,4506	3783,19. 0,4364
(N)	2895,26	6832,10	2742,78	1650,98
$F_{A(PI)DYN+ARC}$	72,38. 1,7604	118,60. 1,7321	44,48. 1,5946	144,82. 1,6095

(N/m)	127,42	205,43	70,93	222,85
$F_{A(PI)DYN+ARC}$	1447,63. 1,7604	2484,49. 1,7321	822,84. 1,5946	2751,64. 1,6095
(N)	2548,41	4303,39	1312,10	4428,77
$F_{B(PI)DYN+ARC}$	144,76. 1,7604	325,34. 1,7321	148,26. 1,5946	86,90. 1,6095
(N/m)	254,84	563,52	236,42	139,86
$F_{B(PI)DYN+ARC}$	2895,26. 1,7604	6832,10. 1,7321	2742,78. 1,5946	1650,98. 1,6095
(N)	5096,82	11833,88	4373,64	2657,26

20.2.7 Weight of tubular conductor

$m_c = m_c^{l}.\ell(kg)$ (14.8)

Support Type	Case 1	Case 2	Case 3	Case 4
	Lattice Steel (**C**)	Tubular or Wide Flange Steel (**B**)	Lattice or Tubular Aluminium (**A**)	Solid Concrete (**D**)
Weight per unit length of bus tube + damping conductor (N/m)	14,7.9,81	14,7.9,81	14,7.9,81	14,7.9,81
W_{b+c} (N/m)	144,21	144,21	144,21	144,21
Weight per unit length of bus tube + damping conductor + ice (N/m)	14,70.9,81	22,18.9,81	18,38.9,81	14,70.9,81
W_{b+c+I} (N/m)	144,21	217,59	180,31	144,21

21.2.8 Wind force on tubular conductor (see Chapter 8)

Support Type	Case 1	Case 2	Case 3	Case 4
	Lattice Steel (**C**)	Tubular or Wide Flange Steel (**B**)	Lattice or Tubular Aluminium (**A**)	Solid Concrete (**D**)
Terrain Category	-	1	2	4
Characteristic Wind Speed (**V**) (m/s)	-	40	45	50
Wind force	750 Pa	-	-	-
Class of Structure	-	B	B	B
Height of Bus Tubing (m)	12,54	12	13	11,5
Wind Multiplier Factor $\mathbf{k_{z1}}$	-	1,08	0,98	0,62
Wind Multiplier Factor $\mathbf{k_{z2}}$	-	1,11	1,02	0,62
Wind Multiplier Factor $\mathbf{k_{zn}}$	-	$\left(\frac{1,11-1,08}{15-10}\right).(15-12)+1,08$	$\left(\frac{1,02-0,98}{15-10}\right).(15-13)+0,98$	$\left(\frac{0,62-0,62}{15-10}\right).(15-11,5)+0,62$
	-	1,0920	0,9960	0,62
$\mathbf{k_{p1}}$	0,50			
$\mathbf{k_{p2}}$	0,47			
$\mathbf{H_{a1}}$	1500			
$\mathbf{H_{a2}}$	2000			
$\mathbf{H_{an}}$	1800			

Support Type	**Case 1**	**Case 2**	**Case 3**	**Case 4**
	Lattice Steel (**C**)	Tubular or Wide Flange Steel (**B**)	Lattice or Tubular Aluminium (**A**)	Solid Concrete (**D**)
Exposure Factor $\mathbf{k_{pn}}$	$\left(\frac{0,47-0,50}{2000-1500}\right).(1800-1500)+0,50$			
	0,4820			
Wind Speed at given Height ($\mathbf{V_z}$) (m/s)	0	1,0920.40	0,9933.45	0,62.50
	0	43,68	44,70	31,00
Thickness of Ice($\mathbf{t_i}$) (mm)	0	12,7	6,4	0
Wind Loading per unit length of bus tube (N/m)	0	$0,6.0,4820.43,68^2$. (0,25+2.0,0127)	$0,6.0,4820.44,70^2$. (0,25+2.0,0064)	$0,6.0,4820.31,00^2$. (0,25+2.0)
$\mathbf{f_{W(b+c+i)}}$ (N/m)	112,5	151,96	148,16	69,48
$\boldsymbol{\ell}$ (m)	20	21	18,5	19
$\mathbf{F_{W(b+c+i)}}$ (N)	2250	3191,15	2740,96	1320,12

From Table 8.3: Variation of Characteristic Wind Speed with Terrain, Height and Class of Structure

1	2	3	4	5	6	7	8	9	10	11	12	13
Height z (m) Up to	**Wind Speed Multiplier - k_z**											
	Terrain Category 1			**Terrain Category 2**			**Terrain Category 3**			**Terrain Category 4**		
	Class of Structure Element											
	A	B	C	A	B	C	A	B	C	A	B	C
5	1,03	1,02	1,00	0,94	0,92	0,88	0,67	0,64	0,60	0,65	0,62	0,57
10	1,09	1,08	1,05	1,00	0,98	0,95	0,74	0,71	0,68	0,65	0,62	0,57
15	1,12	1,11	1,09	1,04	1,02	0,99	0,81	0,78	0,76	0,65	0,62	0,57
20	1,14	1,13	1,11	1,07	1,05	1,02	0,86	0,83	0,81	0,65	0,62	0,57
50	1,22	1.21	1,20	1,16	1,15	1,13	1,00	0,98	0,96	0,86	0,84	0,80
100	1,28	1,27	1,27	1,23	1,22	1,21	1,11	1,10	1,08	1,00	0,98	0,95

20.2.9 Resultant forces $F_{R(A)}$ and $F_{R(B)}$

(see Figure 13.5)

20.2.9.1 Resultant force $F_{RA(PI)}$

$$F_{RA,\,B(PI)} = \sqrt{(W_{b\,+\,c\,+\,i})^2 + (F_{w1} + F_{A,\,B(PI)DYN\,+\,ARC})^2}$$

from 14.15)

Suppt Type	Case 1	Case 2	Case 3	Case 4
	Lattice Steel (**C**)	Tubular or Wide Flange Steel (**B**)	Lattice or Tubular Aluminium (**A**)	Solid Concrete (**D**)
$F_{RA(PI)}$ (N/m)	$\sqrt{144,21^2 + (112,50 + 127,42)^2}$	$\sqrt{217,59^2 + (151,96 + 205,43)^2}$	$\sqrt{180,31^2 + (148,16 + 70,93)^2}$	$\sqrt{144,21^2 + (69,48 + 233,09)^2}$
	279,93	418,42	283,75	335,18
$F_{RA(PI)}$ (N)	$\sqrt{2884,2^2 + (2250 + 2548,41)^2}$	$\sqrt{4569,39^2 + (3191,15 + 4303,37)^2}$	$\sqrt{3335,74^2 + (2740,96 + 1312,10)^2}$	$\sqrt{2739,99^2 + (1320,12 + 4428,17)^2}$
	5598,51	8777.69	5249,23	6367,92
$F_{RB(PI)}$ (N/m)	$\sqrt{144,21^2 + (112,50 + 254,84)^2}$	$\sqrt{217,59^2 + (151,96 + 563,52)^2}$	$\sqrt{180,31^2 + (148,16 + 236,42)^2}$	$\sqrt{144,21^2 + (69,48 + 139,86)^2}$
	394,63	747,83	424,75	254,20
$F_{RB(PI)}$ (N)	$\sqrt{2884,2^2 + (2250 + 5096,82)^2}$	$\sqrt{4569,39^2 + (3191,15 + 13157,69)^2}$	$\sqrt{3335,74^2 + (2740,96 + 4373,11)^2}$	$\sqrt{2739,99^2 + (1320,12 + 2657,26)^2}$
	7892,68	15704,49	7857,78	4829,71

20.2.9.2 Resultant force $F_{RA,B(PI)}$ Safety factor for porcelain S.F = 1,2

Support Type	Case 1	Case 2	Case 3	Case 4
	Lattice Steel (C)	Tubular or Wide Flange Steel (B)	Lattice or Tubular Aluminium (A)	Solid Concrete (D)
$F_{RA(PI)1,2}$ (N/m)	279,93.1,2	418,42.1,2	283,75.1,2	335,80.1,2
	335,92	502,10	340,50	402,96
$F_{RA(PI)1,2}$ (N)	5598,51.1,2	8777,69.1,2	5249,23.1,2	6369,92.1,2
	6718,21	10533,23	6299,08	7643,90
$F_{RB(PI)1,2}$ (N/m)	394,63.1,2	747,83.1,2	424,75.1,2	254,20.1,2
	473,56	897,40	509,10	305,04
$F_{RB(PI)1,2}$ (N)	7892,68.1,2	15704,49.1,2	7857,78.1,2	4829,71.1,2
	9471,22	18845,39	9429,34	5795,66

20.2.9.3 The greater force is exerted on support B insulator

Support Type	A - Lattice and Tubular Aluminium	B - Tubular & Wide Flange Steel	C – Lattice Steel	D - Combination H Structure
$F_{RB(PI)1,2}$ (kN)	9,471	18845,39	9429,34	7643,90
Std PI (kN)	10	-	10	8

Remarks

In the first and third cases, a post insulator of 10kN would suffice, whilst the fourth case require 8kN units. The second case is very problematic and would require a redesign in terms of either increasing the phase spacing or reducing the bus tube span length so as to reduce the forces on the insulators.

20.2.10 Bending moment at the base of the porcelain insulators

$F_{R(A)}$ and $F_{R(B)}$ are the values without the safety factor. The substructures have their own safety factors.

Support Type	Case 1	Case 2	Case 3	Case 4
	Lattice Steel (**C**)	Tubular or Wide Flange Steel (**B**)	Lattice or Tubular Aluminium (**A**)	Solid Concrete (**D**)
h_s (m)	9,29	8,4	9,75	8,1
h_I (m)	3,25	3,6	3,25	3,4
h_b (m)	12,54	12	13	11,5
$F_{R(A)}$	6,718	8,778	5,249	6,368
M_{Ai} (kN.m)	21,83	31,60	17,06	21,65
M_{As} (kN.m)	84,24	105,34	68,24	73,23
$F_{R(B)}$	9,471	15,704	7,858	4,830
M_{Bi} (kN.m)	30,78	56,53	25,54	16,42
M_{Bs} (kN.m)	118,77	188,45	102,15	55,55

Safety factor = 1,7

Design value $= M_{a,b(i,s)} \cdot 1,7$ (from 15.5 & 15.6)

Support Type	Case 1	Case 2	Case 3	Case 4
	Lattice Steel (**C**)	Tubular or Wide Flange Steel (**B**)	Lattice or Tubular Aluminium (**A**)	Solid Concrete (**D**)
M_{As} (kN.m)	143,21	179,08	116,01	124,49
M_{Bs} (kN.m)	201,91	320,37	173,66	94,43

20.2.11 Tubular Conductor System

Stress in the tubular conductor:

20.2.11.1 Short circuit forces per unit length including ARC

Support Type	Case 1	Case 2	Case 3	Case 4
	Lattice Steel (**C**)	Tubular or Wide Flange Steel (**B**)	Lattice or Tubular Aluminium (**A**)	Solid Concrete (**D**)
F^{1}_{L2p} (N/m)	428,80	612,62	263,22	530,97
f_{b+c+i} (N/m)	112,5	151,96	148,16	69,48
w_{b+c+i} (N/m)	144,21	217,59	180,31	144,21
v_σ	0,2943	0,4149	0,3855	0,3725
v_r	1,7604	1,7321	1,5946	1,6095

20.2.11.2 Resultant force on the tubular conductor F_R per unit length

$$F_{R(\sigma)} = \sqrt{(\text{weight conductor} + \text{weight ice})^2 + (\text{wind force} + F^{1}_{(L2p)})^2} \qquad \text{(from 9.6)}$$

Section modulus

$$J = 34{,}25.10^{-6}\ (m) \qquad \text{(from 9.12)}$$

$$W = \frac{J}{\left(\frac{d_o}{2}\right)}$$

$$= \frac{34{,}25.10^{-6}}{\left(\frac{0{,}25}{2}\right)} \qquad \text{(from 9.11)}$$

$$= 274.10^{-6}\ (m^3)$$

$$\sigma_{ST} = \frac{F_{R(\sigma)}.\ell^2}{k.W} \qquad \text{(from 9.8)}$$

Support Type	**Case 1**	**Case 2**	**Case 3**	**Case 4**
	Lattice Steel (**C**)	Tubular or Wide Flange Steel (**B**)	Lattice or Tubular Aluminium (**A**)	Solid Concrete (**D**)
$f_{W(b+c+i)}$ (N/m)	112,5	151,96	148,16	69,48
F^{1}_{L2p} (N/m)	428,80	612,62	263,22	530,97
$F_{R(\sigma)1}$ (N/m)	$\sqrt{144,21^2 + (112,50 + 428,80)^2}$	$\sqrt{217,59^2 + (151,96.612,62)^2}$	$\sqrt{180,31^2 + (148,16 + 263,22)^2}$	$\sqrt{144,21^2 + (69,48 + 530,97)^2}$
	560,18	794,94	449,16	617,52
$F_{R(\sigma)2}$ (N/m)	$\sqrt{144,21^2 + (-112,50 + 428,80)^2}$	$\sqrt{217,59^2 + (-151,96.612,62)^2}$	$\sqrt{180,31^2 + (-148,16 + 263,22)^2}$	$\sqrt{144,21^2 + (-69,48 + 530,97)^2}$
	347,62	509,46	213,89	483,50
Boundary Conditions	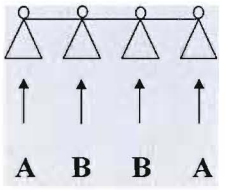	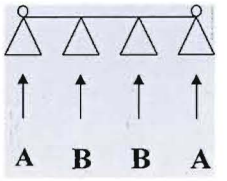	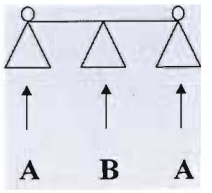	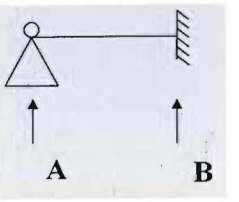
ℓ (m)	20	21	18,5	19

Support Type	Case 1	Case 2	Case 3	Case 4
	Lattice Steel (**C**)	Tubular or Wide Flange Steel (**B**)	Lattice or Tubular Aluminium (**A**)	Solid Concrete (**D**)
σ_{ST1} (MPa)	$\frac{560,18.20^2}{9.274.10^{-6}}$	$\frac{794,94,58.21^2}{10.274.10^{-6}}$	$\frac{449,16.18,5^2}{8.274.10^{-6}}$	$\frac{617,52.19^2}{8.274.10^{-6}}$
	90,86	127,94	70,13	101,70
σ_{ST2} (Mpa)	$\frac{347,62.20^2}{9.274.10^{-6}}$	$\frac{509,46,58.21^2}{10.274.10^{-6}}$	$\frac{213,89.18,5^2}{8.274.10^{-6}}$	$\frac{483,50.19^2}{8.274.10^{-6}}$
	56,39	82,00	33,40	79,63
ν_σ	0,2943	0,4149	0,3855	0,3725
σ_{DYN1} (Mpa)	90,86. 0,2943	127,94. 0,4149	70,13. 0,3855	101,70. 0,3725
	26,74	53,08	27,04	37,88
σ_{DYN2} (Mpa)	56,39. 0,2943	82,00. 0,4149	33,40. 0,3855	79,63. 0,3725
	16,60	34,02	12,87	29,66

Support Type	**Case 1**	**Case 2**	**Case 3**	**Case 4**
	Lattice Steel (**C**)	Tubular or Wide Flange Steel (**B**)	Lattice or Tubular Aluminium (**A**)	Solid Concrete (**D**)
v_r	1,7604	1,7321	1,5946	1,6095
$\sigma_{DYN+ARC1}$ (MPa)	26,74. 1,7604	53,08. 1,7321	27,04. 1,5946	37,88. 1,6095
	47,07	91,95	43,11	60,97
$\sigma_{DYN+ARC2}$ (MPa)	16,60. 1,7604	34,02. 1,7321	12,87. 1,5946	29,66. 1,6095
	29,21	58,93	20,53	47,74
2,65. $\sigma_{DYN+ARC1}$ (MPa)	124,74	243,66	114,24	161,58
2,65. $\sigma_{DYN+ARC2}$ (MPa)	77,41	156,16	54,40	126,51
Alloy	$\sigma_{(DYN+ARC)\,2,65} = 124,74 <$ All $\mathbf{R_{p0,2}}$	$\sigma_{(DYN+ARC)\,2,65} = 243,66 <$ $\mathbf{R_{p0,2}}$ **6061T6**	$\sigma_{(DYN+ARC)\,2,65} = 114,24 <$ All $\mathbf{R_{p0,2}}$	$\sigma_{(DYN+ARC)\,2,65} = 161,58 <$ Most $\mathbf{R_{p0,2}}$ except **AlMgSi0,5F22** (only just outside range)

From Table 6.2: Electrical and Mechanical Properties of Various Aluminium Alloys

ALLOY TYPE	HULETT'S S.A.		ASA STANDARD		DIN STANDARD	
	D50STF	D65STF	6063T6	6061T6	AlMgSi0,5F22	AlMgSi0,5F25
0,2 % Proof Stress in Mpa Rp0,2	170	240	214	276	160	195

20.2.12 Maximum deflection

For conductor with both ends supported:-

$$y_c = \frac{5}{384} . \frac{F^1_{L2p} . \ell^4}{E.J} \text{ (m)} \qquad \text{(from 13.10)}$$

20.2.12.1 Maximum deflection under own weight

The maximum deflection of the tubular conductor under static conditions due to its own weight (force)

$$y_c = \frac{5}{384} . \frac{(9{,}81.m^1) . \ell^4}{E.J} \text{ (m)} \qquad \text{(from 13.2)}$$

Support Type	**Case 1**	**Case 2**	**Case 3**	**Case 4**
	Lattice Steel (**C**)	Tubular or Wide Flange Steel (**B**)	Lattice or Tubular Aluminium (**A**)	Solid Concrete (**D**)
Mass per unit length of bus tube + damping conductor	14,70	14,70	14,70	14,70
+ ice	14,70	22,18	18,38	14,70
Boundary Conditions	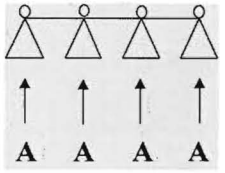	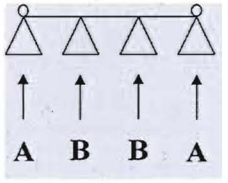	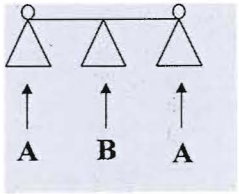	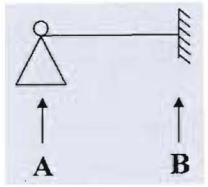
Deflection factor	0.0069	0.0069	0.0054	0.0054
ℓ (m)	20	21	18,5	19
Alloy	D65S TF	6061T6	AlMgSi0,5F25	6063T6
E	$69{,}12.10^{9}$	70.10^{9}	70.10^{9}	69.10^{9}
J (m^4)	$34{,}26.10^{-6}$			

Support Type	Case 1	Case 2	Case 3	Case 4
	Lattice Steel (**C**)	Tubular or Wide Flange Steel (**B**)	Lattice or Tubular Aluminium (**A**)	Solid Concrete (**D**)
Deflection y_c (m)	$0{,}0069.\frac{(9{,}81.14{,}7).20^4}{69{,}12.10^9.34{,}26.10^{-6}}$	$0{,}0069.\frac{(9{,}81.14{,}7).21^4}{70.10^9.34{,}26.10^{-6}}$	$0{,}0054.\frac{(9{,}81.14{,}7).18{,}5^4}{60.10^9.34{,}26.10^{-6}}$	$0{,}0054.\frac{(9{,}81.14{,}7).19^4}{69.10^9.34{,}26.10^{-6}}$
Deflection y_c (mm)	≈ 62	≈ 81	≈ 44	≈ 43

20.2.12.2 Maximum deflection under dynamic conditions (wind, short current forces and its own weight)

The maximum deflection of the tubular conductor under dynamic conditions due to wind, short current forces and its own weight is:-

$$\mathbf{F^1_{R(\sigma)DYN+ARC}} = \frac{\sigma_{DYN}.\mathbf{k}.\mathbf{W}}{\ell^2}\ \mathbf{(N/m)} \qquad \text{(from 13.22)}$$

$$\mathbf{y_{DYN\,+\,ARC}} = \frac{\mathbf{5}}{\mathbf{384}}.\frac{\mathbf{F^1_{R(\sigma)DYN+ARC}}.\ell^4}{\mathbf{E.J}}\ \mathbf{(m)} \qquad \text{(from 13.23)}$$

Support Type	**Case 1**	**Case 2**	**Case 3**	**Case 4**
	Lattice Steel (**C**)	Tubular or Wide Flange Steel (**B**)	Lattice or Tubular Aluminium (**A**)	Solid Concrete (**D**)
$\mathbf{F^{l}_{R(\sigma)DYN+ARC1}}$ (N/m)	$\frac{47{,}07.10^{6}.9.274.10^{-6}}{20^{2}}$	$\frac{91{,}95.10^{6}.10.274.10^{-6}}{21^{2}}$	$\frac{43{,}11.10^{6}.8.274.10^{-6}}{18{,}5^{2}}$	$\frac{60{,}97.10^{6}.9.274.10^{-6}}{19^{2}}$
	290,19	571,30	276,11	370,21
$\mathbf{F^{l}_{R(\sigma)DYN+ARC2}}$ (N/m)	$\frac{29{,}21.10^{6}.9.274.10^{-6}}{20^{2}}$	$\frac{58{,}93.10^{6}.10.274.10^{-6}}{21^{2}}$	$\frac{20{,}53.10^{6}.8.274.10^{-6}}{18{,}5^{2}}$	$\frac{47{,}74.10^{6}.9.274.10^{-6}}{19^{2}}$
	180,08	366,14	131,49	289,89
Deflection $\mathbf{y_{DYN+ARC1}}$ **(m)**	$0{,}0069.\frac{290{,}18.20^{4}}{69{,}12.10^{9}.34{,}26.10^{-6}}$	$0{,}0069.\frac{571{,}30.21^{4}}{70.10^{9}.34{,}26.10^{-6}}$	$0{,}0054.\frac{276{,}11.18{,}5^{4}}{70.10^{9}.34{,}26.10^{-6}}$	$0{,}0054.\frac{370{,}21.19^{4}}{69.10^{9}.34{,}26.10^{-6}}$
	0,1353	0,3197	0,0728	0,1102
Deflection $\mathbf{y_{DYN+ARC2}}$ **(m)**	$0{,}0069.\frac{180{,}08.20^{4}}{69{,}12.10^{9}.34{,}26.10^{-6}}$	$0{,}0069.\frac{366{,}14.21^{4}}{70.10^{9}.34{,}26.10^{-6}}$	$0{,}0054.\frac{131{,}49.18{,}5^{4}}{70.10^{9}.34{,}26.10^{-6}}$	$0{,}0054.\frac{289{,}89.19^{4}}{69.10^{9}.34{,}26.10^{-6}}$
	0,084	0,190	0,0347	0,0863

$$\varphi_1 = \cos^{-1}\left(\frac{W_{b+c+i}}{F_{R(\sigma)DYN+ARC1}}\right) \quad \text{(from 13.14)}$$

$$y_{DYN+ARCH1} = y_{DYN+ARC1}.\sin(\varphi_1) \quad \text{(from 13.15)}$$

$$y_{DYN+ARCV1} = y_{DYN+ARC1}.\cos(\varphi_1) \quad \text{(from 13.16)}$$

Support Type	**Case 1**	**Case 2**	**Case 3**	**Case 4**
	Lattice Steel (**C**)	Tubular or Wide Flange Steel (**B**)	Lattice or Tubular Aluminium (**A**)	Solid Concrete (**D**)
φ_1	$\cos^{-1}\left(\frac{144,21}{290,19}\right)$	$\cos^{-1}\left(\frac{217,59}{570,30}\right)$	$\cos^{-1}\left(\frac{180,31}{276,11}\right)$	$\cos^{-1}\left(\frac{180,31}{276,11}\right)$
	60,20	67,57	49,23	49,23
Deflection $y_{DYN+ARCH1}$ **(mm)**	135,3.sin 60,2°	319,7.sin 67,57°	72,8.sin 49,23°	72,8.sin 49,23°
	117,41	295,51	55,13	101,49
Deflection $y_{DYN+ARCV1}$ **(mm)**	135,3.cos 60,2°	319,7.cos 67,57°	72,8.cos 49,23°	72,8.cos 49,23°
	67,24	121,98	47,54	42,93

$$\varphi_2 = \cos^{-1}\left(\frac{W_{b+c+i}}{F_{R(\sigma)\ DYN+ARC2}}\right)$$ (from 13.17)

$$y_{DYN+ARCH2} = y_{DYN+ARC2}.\sin(\varphi_2)$$ (from 13.18)

$$y_{DYN+ARCV2} = y_{DYN+ARC2}.\cos(\varphi_2)$$ (from 13.19)

Support Type	**Case 1**	**Case 2**	**Case 3**	**Case 4**
	Lattice Steel (**C**)	Tubular or Wide Flange Steel (**B**)	Lattice or Tubular Aluminium (**A**)	Solid Concrete (**D**)
φ_2	$\cos^{-1}\left(\frac{144,21}{290,19}\right)$	$\cos^{-1}\left(\frac{217,59}{570,30}\right)$	$\cos^{-1}\left(\frac{180,31}{131,49}\right)$	$\cos^{-1}\left(\frac{144,21}{370,20}\right)$
	60,20	67,57	**Invalid – use** $\varphi_1 = 49,23$	49,23
Deflection $y_{DYN+ARCH2}$ **(mm)**	$84,0.\sin 60,2°$	$190,0.\sin\left[\cos^{-1}\left(\frac{217,59}{570,30}\right)\right]$	$34,7.\sin[49,23]$	$86,3.\sin\left[\cos^{-1}\left(\frac{144,21}{370,20}\right)\right]$
	72,89	175,63	26,28	80,19
Deflection $y_{DYN+ARCV2}$ **(mm)**	$84,0.\cos\left[\cos^{-1}\left(\frac{144,21}{290,19}\right)\right]$	$190,0.\cos\left[\cos^{-1}\left(\frac{217,59}{570,30}\right)\right]$	$34,7.\cos[49,23]$	$86,3.\cos\left[\cos^{-1}\left(\frac{144,21}{370,20}\right)\right]$
	41,74	72,49	22,66	31,89

$$C_{1,2} = \sqrt{(s_p - y_{DYN2}.\sin\varphi_2 - y_{DYN1}.\sin\varphi_1)^2 + (y_{DYN2}.\cos\varphi_2 - y_{DYN1}.\cos\varphi_1)^2} - d_{bo}$$ (from 13.20)

Support Type	**Case 1**	**Case 2**	**Case 3**	**Case 4**
	Lattice Steel (**C**)	Tubular or Wide Flange Steel (**B**)	Lattice or Tubular Aluminium (**A**)	Solid Concrete (**D**)
Phase-to-Phase Clearance (mm)	$\sqrt{\left[(5500 - 72{,}89 - 117{,}41)^2 + (41{,}74 - 67{,}24)^2\right]}$ - 250	$\sqrt{\left[(6000 - 175{,}63 - 295{,}51)^2 + (72{,}49 - 121{,}98)^2\right]}$ - 250	$\sqrt{\left[(5000 - 26{,}28 - 64{,}37)^2 + (22{,}66 - 55{,}51)^2\right]}$ - 250	$\sqrt{\left[(5200 - 80{,}19 - 101{,}419)^2 + (31{,}89 - 42{,}93)^2\right]}$ - 250
	≈ 5709	≈ 5279	≈ 4659	≈ 4768

In all 4 cases, $C_{1,2} > 4000 = C_{pp}$ and thus meet the phase-to-phase criteria. (from 13.21)

20.2.13 Calculation of Conductor Surface Field Strength and Determination of Corona Inception Levels for Typical Arrangements

20.2.13.1 Corona threshold limits (E_c)

Polished tubes - **1,0**

Extruded tubes - **0,95**

stranded conductor - **0,8**

E_c = Corona threshold surface field strength

δ = Relative air density (RAD)

r'_{bo} = 0,125 (Conductor radius in metres)

m_r = 0,95 (Factor to allow for surface roughness)

m - Exponent in atmospheric correction factor formula for external insulation withstand

$$\delta = e^{-\left(\frac{Ha}{8150}\right)}$$

$$= e^{-\left(\frac{1800}{8150}\right)}$$

$$= 0,8018 \text{ (dimensionless)}$$

(from 4.12)

Peek : $$E_c = 3.m_r.\delta\left[1+\frac{0,03}{\sqrt{r_o.\delta}}\right].\frac{10}{\sqrt{2}}\ \frac{kV}{cm}\ \textbf{(rms)}$$ (from 17.2)

$$E_c = 3.0,95.0,8018\left[1+\frac{0,03}{\sqrt{0,125.0,8018}}\right].\frac{10}{\sqrt{2}}$$

$$= 17,6901\ \frac{kV}{cm}\ \text{(rms)}$$

Heymann : $$E_c = 2,4.m_r.\delta\left[1+\frac{0,0937}{(r_o.\delta)^{0,4}}\right].\frac{10}{\sqrt{2}}\ \frac{kV}{cm}\ \textbf{(rms)}$$ (from 17.3)

$$E_c = 2,4.0,95.0,8018\left[1+\frac{0,0937}{(0,125.0,8018)^{0,4}}\right].\frac{10}{\sqrt{2}}$$

$$= 15,9670\ \frac{kV}{cm}\ \text{(rms)}$$

$$E_{cave} = (17,6901 + 15,9670)/2$$

$$= 16,8286 \text{ kV/cm (rms)}$$

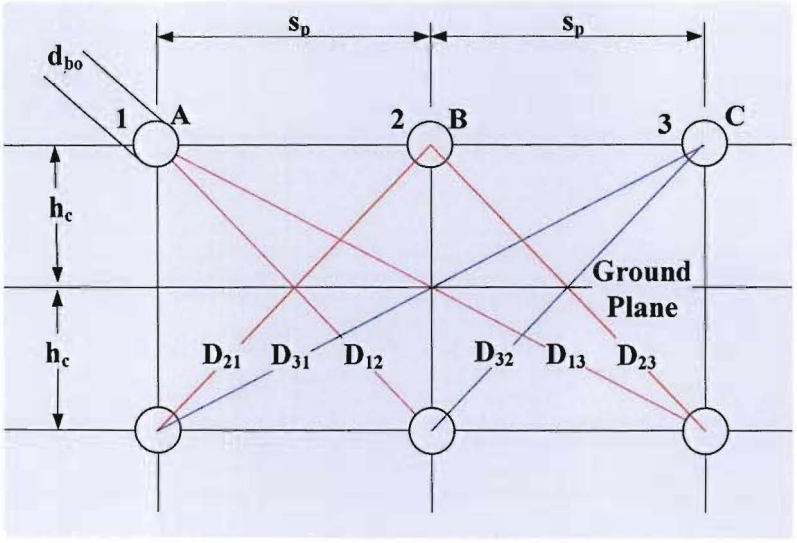

Figure 20.11 Conductor Surface Field Strength using the Image Method for Example 2

$$P_1 = \ln\left[\frac{2.h_c}{r_{bo}}\right] - 0{,}5.\ln\left[\frac{\sqrt{\left([2.h_c]^2 + {s_p}^2\right)}}{s_p}\right] - 0{,}5.\ln\left[\frac{\sqrt{\left([2.h_c]^2 + [2.s_p]^2\right)}}{2.s_p}\right] \qquad \text{(from 17.36)}$$

Support Type	Case 1	Case 2	Case 3	Case 4
	Lattice Steel (**C**)	Tubular or Wide Flange Steel (**B**)	Lattice or Tubular Aluminium (**A**)	Solid Concrete (**D**)
P_1	$\ln\left[\frac{2.12{,}4}{0{,}125}\right] - 0{,}5.\ln\left[\frac{\sqrt{(2.12{,}54)^2 + 5{,}5^2}}{5{,}5}\right] - 0{,}5.\ln\left[\frac{\sqrt{(2.12{,}54)^2 + (2.5{,}5)^2}}{2.5{,}5}\right]$	$\ln\left[\frac{2.12}{0{,}125}\right] - 0{,}5.\ln\left[\frac{\sqrt{(2.12)^2 + 6^2}}{6}\right] - 0{,}5.\ln\left[\frac{\sqrt{(2.12)^2 + (2.6)^2}}{2.6}\right]$	$\ln\left[\frac{2.13}{0{,}125}\right] - 0{,}5.\ln\left[\frac{\sqrt{(2.13)^2 + 5^2}}{5}\right] - 0{,}5.\ln\left[\frac{\sqrt{(2.13)^2 + (2.5)^2}}{2.5}\right]$	$\ln\left[\frac{2.11{,}5}{0{,}125}\right] - 0{,}5.\ln\left[\frac{\sqrt{(2.11{,}5)^2 + 5{,}2^2}}{5{,}2}\right] - 0{,}5.\ln\left[\frac{\sqrt{(2.11{,}5)^2 + (2.5{,}2)^2}}{2.5{,}2}\right]$
	= 5,3015-0,8026-0,4547	= 5,2575-0,7083-0,4024	= 5,3375-0,8334-0,5122	= 5,2149-0,7559-0,4203
	= 4,0441	= 4,1468	= 3,9919	= 4,0387

$$P_2 = -0{,}5.\ln\left[\frac{\sqrt{\left([2.h_c]^2 + s_p{}^2\right)}}{s_p}\right] + \ln\left[\frac{2.h_c}{r_{bo}}\right] - 0{,}5.\ln\left[\frac{\sqrt{\left([2.h_c]^2 + s_p{}^2\right)}}{s_p}\right] \qquad \text{(from 17.37)}$$

Support Type	Case 1	Case 2	Case 3	Case 4
	Lattice Steel (**C**)	Tubular or Wide Flange Steel (**B**)	Lattice or Tubular Aluminium (**A**)	Solid Concrete (**D**)
P_2	$= -0{,}5.\ln\left[\frac{\sqrt{\left([2.12{,}54]^2 + 5{,}5^2\right)}}{5{,}5}\right] + \ln\left[\frac{2.12{,}54}{0{,}125}\right] - 0{,}5.\ln\left[\frac{\sqrt{\left([2.12{,}54]^2 + 5{,}5^2\right)}}{5{,}5}\right]$	$= -0{,}5.\ln\left[\frac{\sqrt{\left([2.12]^2 + 6^2\right)}}{6}\right] + \ln\left[\frac{2.12}{0{,}125}\right] - 0{,}5.\ln\left[\frac{\sqrt{\left([2.12]^2 + 6^2\right)}}{6}\right]$	$= -0{,}5.\ln\left[\frac{\sqrt{\left([2.13]^2 + 5^2\right)}}{5}\right] + \ln\left[\frac{2.13}{0{,}125}\right] - 0{,}5.\ln\left[\frac{\sqrt{\left([2.13]^2 + 5^2\right)}}{5}\right]$	$= -0{,}5.\ln\left[\frac{\sqrt{\left([2.11{,}5]^2 + 5{,}2^2\right)}}{5{,}2}\right] + \ln\left[\frac{2.11{,}5}{0{,}125}\right] - 0{,}5.\ln\left[\frac{\sqrt{\left([2.11{,}5]^2 + 5{,}2^2\right)}}{5{,}2}\right]$
	= -0,7704+5,3015-0,7704	= -0,7083+5,2575-0,7083	= -0,8334+5,3375-0,8334	= -0,7559+5,2149-0,7559
	= 3,7607	= 3,8409	= 3,6707	= 3,7031

$$P_3 = -0{,}5.\ln\left[\frac{\sqrt{\left([2.h_c]^2 + [2.s_p]^2\right)}}{2.s_p}\right] - 0{,}5.\ln\left[\frac{\sqrt{\left([2.h_c]^2 + s_p{}^2\right)}}{s_p}\right] + \ln\left[\frac{2.h_c}{r_{bo}}\right] \qquad \text{(from 17.38)}$$

Support Type	Case 1	Case 2	Case 3	Case 4
	Lattice Steel (**C**)	Tubular or Wide Flange Steel (**B**)	Lattice or Tubular Aluminium (**A**)	Solid Concrete (**D**)
P_3	$= -0{,}5.\ln\left[\frac{\sqrt{\left([2.12{,}54]^2 + [2.5{,}5]^2\right)}}{2.5{,}5}\right] - 0{,}5.\ln\left[\frac{\sqrt{\left([2.12{,}54]^2 + 5{,}5^2\right)}}{5{,}5}\right] + \ln\left[\frac{2.12{,}54}{0{,}125}\right]$	$= -0{,}5.\ln\left[\frac{\sqrt{\left([2.12]^2 + [2.6]^2\right)}}{2.6}\right] - 0{,}5.\ln\left[\frac{\sqrt{\left([2.12]^2 + 6^2\right)}}{6}\right] + \ln\left[\frac{2.12}{0{,}125}\right]$	$= -0{,}5.\ln\left[\frac{\sqrt{\left([2.13]^2 + [2.5]^2\right)}}{2.5}\right] - 0{,}5.\ln\left[\frac{\sqrt{\left([2.13]^2 + 5^2\right)}}{5}\right] + \ln\left[\frac{2.13}{0{,}125}\right]$	$= -0{,}5.\ln\left[\frac{\sqrt{\left([2.11{,}5]^2 + [2.5{,}2]^2\right)}}{2.5{,}2}\right] - 0{,}5.\ln\left[\frac{\sqrt{\left([2.11{,}5]^2 + 5{,}2^2\right)}}{5{,}2}\right] + \ln\left[\frac{2.11{,}5}{0{,}125}\right]$
	= -0,4547-0,8026+5,3015	= -0,4024-0,7083+5,2575	= -0,5122-0,8334+5,3375	= -0,4203-0,7559+5,2149
	= 4,0442	= 4,1468	= 3,9919	= 4,0387

$$E_{1av} = \frac{[V_L]}{\sqrt{3}} \cdot \frac{1}{P_{1r}} \cdot \frac{1}{r_{1bo}} \cdot \frac{1}{10^2} \text{ kV/cm (rms)} \qquad (17.42)$$

Support Type	Case 1	Case 2	Case 3	Case 4
	Lattice Steel (**C**)	Tubular or Wide Flange Steel (**B**)	Lattice or Tubular Aluminium (**A**)	Solid Concrete (**D**)
E_{1av}	$= \frac{420}{\sqrt{3}} \cdot \frac{1}{4{,}0441} \cdot \frac{1}{0{,}125} \cdot \frac{1}{10^2}$	$= \frac{420}{\sqrt{3}} \cdot \frac{1}{4{,}1468} \cdot \frac{1}{0{,}125} \cdot \frac{1}{10^2}$	$= \frac{420}{\sqrt{3}} \cdot \frac{1}{3{,}9919} \cdot \frac{1}{0{,}125} \cdot \frac{1}{10^2}$	$= \frac{420}{\sqrt{3}} \cdot \frac{1}{4{,}0387} \cdot \frac{1}{0{,}125} \cdot \frac{1}{10^2}$
	= 4,7969 kV/cm (rms)	= 4,6781 kV/cm (rms)	= 4,8596 kV/cm (rms)	= 4,2132 kV/cm (rms)

$$E_{2av} = \frac{[V_L]}{\sqrt{3}} \cdot \frac{1}{P_{1r}} \cdot \frac{1}{r_{2bo}} \cdot \frac{1}{10^2} \text{ kV/cm (rms)} \qquad (17.44)$$

E_{2av}	$= \frac{420}{\sqrt{3}} \cdot \frac{1}{3{,}7607} \cdot \frac{1}{0{,}125} \cdot \frac{1}{10^2}$	$= \frac{420}{\sqrt{3}} \cdot \frac{1}{3{,}8409} \cdot \frac{1}{0{,}125} \cdot \frac{1}{10^2}$	$= \frac{420}{\sqrt{3}} \cdot \frac{1}{3{,}6707} \cdot \frac{1}{0{,}125} \cdot \frac{1}{10^2}$	$= \frac{420}{\sqrt{3}} \cdot \frac{1}{3{,}7031} \cdot \frac{1}{0{,}125} \cdot \frac{1}{10^2}$
	= 5,1695 kV/cm (rms)	= 5,0506 kV/cm (rms)	= 5,2848 kV/cm (rms)	= 5,2386 kV/cm (rms)

$$E_{3av} = \frac{[V_L]}{\sqrt{3}} \cdot \frac{1}{P_{1r}} \cdot \frac{1}{r_{3bo}} \cdot \frac{1}{10^2} \text{ kV/cm(rms)} \qquad (17.46)$$

Support Type	Case 1	Case 2	Case 3	Case 4
	Lattice Steel (**C**)	Tubular or Wide Flange Steel (**B**)	Lattice or Tubular Aluminium (**A**)	Solid Concrete (**D**)
E_{3av}	$= \frac{420}{\sqrt{3}} \cdot \frac{1}{4{,}0442} \cdot \frac{1}{0{,}125} \cdot \frac{1}{10^2}$	$= \frac{420}{\sqrt{3}} \cdot \frac{1}{4{,}1468} \cdot \frac{1}{0{,}125} \cdot \frac{1}{10^2}$	$= \frac{420}{\sqrt{3}} \cdot \frac{1}{3{,}9919} \cdot \frac{1}{0{,}125} \cdot \frac{1}{10^2}$	$= \frac{420}{\sqrt{3}} \cdot \frac{1}{4{,}087} \cdot \frac{1}{0{,}125} \cdot \frac{1}{10^2}$
	= 4,7967 kV/cm (rms)	= 4,6781 kV/cm (rms)	= 4,8596 kV/cm (rms)	= 4,2132 kV/cm (rms)

E_e = 5,2kV/cm<<<19,8 kV/cm = E_c, therefore **no corona** will be present

Electric Field Strength

$E_i = 0.133.h_{ci}^{-1.789}.s_{pi}^{0.43}.d_{boi}^{0.22}.V_i^{1.003}$ (kV/m) (from 18.24)

Support Type	Case 1	Case 2	Case 3	Case 4
	Lattice Steel (**C**)	Tubular or Wide Flange Steel (**B**)	Lattice or Tubular Aluminium (**A**)	Solid Concrete (**D**)
h_{bi} (m)	12,54	12	13	11,5
s_{pi} (m)	5,5	6	5	5,2
d_{boi} (mm)	250			
V_{mi} (kV)	420			
E_i (kV/m)	$0{,}133.12{,}54^{-1.789}.5{,}5^{0.43}$ $.250^{0.22}.420^{1.003}$	$0{,}133.12^{-1.789}.6^{0.43}$ $.250^{0.22}.420^{1.003}$	$0{,}133.13^{-1.789}.5^{0.43}$ $.250^{0.22}.420^{1.003}$	$0{,}133.11{,}5^{-1.789}.5{,}2^{0.43}$ $.250^{0.22}.420^{1.003}$
	$\approx 4{,}3$	$\approx 4{,}9$	$\approx 3{,}9$	$\approx 4{,}9$

The magnitude of the electric field in each case is just less that the 5kV/m limit required for public areas, and far less than the 10kV/m limit required for HV yards.

Magnetic Field Strength

$H_i = 0.697.h_{bi}^{-1.728}.s_{pi}^{0.29}.I_i^{0.997}$ (μ T) (from 18.36)

Support Type	Case 1	Case 2	Case 3	Case 4
	Lattice Steel (C)	Tubular or Wide Flange Steel (B)	Lattice or Tubular Aluminium (A)	Solid Concrete (D)
h_{bi} (m)	12,54	12	13	11,5
s_{pi} (m)	5,5	6	5	5,2
d_{boi} (mm)	250			
I_{mi} (A)	3500	4500	4000	3750
H_i (μT)	$0,697.12,54^{-1.789}.5,5^{0.29}.3500^{0.997}$	$0,697.12,54^{-1.789}.5,5^{0.29}.3500^{0.997}$	$0,697.12,54^{-1.789}.5,5^{0.29}.3500^{0.997}$	$0,697.12,54^{-1.789}.5,5^{0.29}.3500^{0.997}$
	≈ 42,7	≈ 60,3	≈ 44,1	≈ 52,1

The magnitude of the magnetic field in each case is less that the 100μT limit required for public areas, and far less than the 500μT limit required for HV yards.

21. CONCLUSION

The statistical nature of events combined with the improved ability to predict, minimise and control these events leading to more techno-economic compact substations when employing tubular conductors has been demonstrated. The objective of the study has been achieved in producing a "tangible" document with the development of a computer software package to assist substation design engineers in the application of tubular conductors. This package has been employed extensively in the studies relating to this dissertation, and was tested against several hand calculations that also form part of this dissertation. The graphical illustrations in this dissertation were generated using the said MicroSoft Excel programme that the author developed for the purpose of the studies. The Excel based programme was used for:-

- Modelling of a tubular bus system employing different support configurations
- Modelling of different levels of conductor in a substation
- Considering issues such as the limitation of electrical stresses (corona, voltage surges, and **self restoring** insulation) and mechanical stresses (forces due to fault current and Aeolian

As part of the research methodology, the following investigations were made:-

- Researched the original contributions from literature and note the criteria on which they were based.
- Researched current statistically based criteria relating to electrical clearances and apply these to produce a revised set of voltage based clearances
- Compared of results between deterministic and statistical approaches
- Transformed original contributions into a "**Design** Application Guide"

It is clear from the study conducted above, which covers various aspects of tubular conductor behaviour and performance under a variety of system and climatic conditions, that it is indeed possible to approach the employment of tubular conductors in a probabilistic manner and provide a methodology as "A probabilistic Based Design Application Guide for the use of Tubular Conductors in the Design of High Voltage Substations".

The IEC document IEC 71-2 on Insulation Co-ordination provides a starting point from which to work, laying out guidelines for the determination of phase-to-earth and phase-to-phase gap clearances based on the probability of a flashover for a given gap configuration. Depending on the severity of the consequences of a flashover in the given substation, one may accept the risk

of smaller electrical clearances, and control over-voltages with appropriately positioned over-voltage control devices such as metal-oxide surge arresters. These devices are in any event installed at the line terminal feeder bays, at or close to bushings for transformers, reactors and through wall units. It may mean placing surge arresters on the busbars at pre-calculated locations. This will facilitate a more compact substation in the end. It is certainly an advantage in terms of cost of land, greater awareness of the public on the sensitivity of the environment to construction, and a host of other techno-economic and social pressures that are steering utilities to become more innovative in developing new **compact** designs for outdoor air insulated substations (AIS). Tubular busbar substations aid compactness, without introducing additional **operational** risks, and at the same time producing the same or improved reliability of supply.
Rigid conductors have the inherent advantage of having no problems associated with bundle collapse as with bundled flexible conductors. Since they are supported and not under tension, far smaller steelwork structures and support foundations are required, resulting in lower civil and steelwork costs. The rigidity of the conductors restrict conductor movement under fault conditions, thus allowing smaller electrical gap clearances which in tern depend on the gap configuration.

Due to the mechanical properties of tubular conductors and the inherent high current carrying capacity they offer, smaller clearances are possible. The critical issues relating to clearances have been discussed at length throughout this dissertation and, providing the guidelines as set out in the dissertation are followed, the designer may feel quite confident that the product will withstand the climatic and fault conditions that the substation would be subjected to. It is extremely important to have a clear picture of how the system is likely to develop in the future with regard to network expansion, as fault current has a major impact on its design. This also applies to the load current that the busbar is expected to support and will be determined by the tap-off or transformed power, and the power flowing through the bus system.

The compactness achieved in tubular busbar designs by employing smaller smaller support structures and foundations translates not only into majojor cost savings, but also has a far lower visual and ecological impact on the environment (see Figure 21.1 as compared to Figure 21.2). It goes a long way to satisfy not only the investors of the infrastructure, but also those that are against large developments. South Africa needs the power for economic growth, but this needs to be done responsibly so that the environment can be preserved for future generations to enjoy.

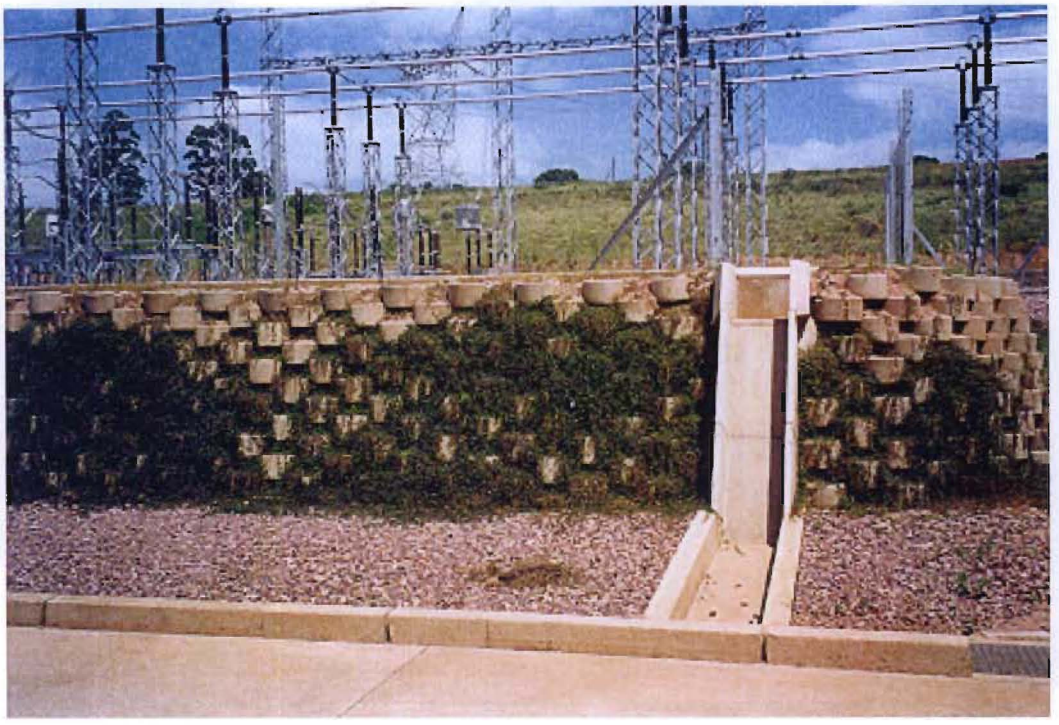

Figure 21.1: Low Visual Impact Tubular Busbar Substation (Hector Substation – Camperdown, KZN)

Figure 21.2: High Visual Impact Tubular Busbar Substation (Athene Substation – Empangeni - KZN)

22. RECOMMENDATIONS

- Although Eskom has committed itself to the IRPA guidelines, it has not made this widely known, and it is only as a result of this research project that the author has become aware of these limits.
- Further research to supplement this design guide in the form of actual measurements within the substation perimeter to determine the electric and magnetic field strengths, produce field plots, and compare these to simulated values.
- From this research, it will be possible to categories the more than 160 Main Transmission Substations into a number of categories as sujested below and try to determine means to reduce the electromagnetic field levels.

Table 22.1: Proposed Electric and Magnetic Field Measurements at Substations

Sub Stn.	Electric Field Strength			Magnetic Field Strength		
	≤5kV/m	5kV/m<E≤10kV/m	>10kV/m	≤100μT	100μT<H≤500μT	>500μT
Alpha						
Beta						

- Future work should also focus on specifying maximum percentage errors in respect of comparing simulated results and subsequent measured results.

23. REFERENCES

[1] Eskom Transmission Substation Layout Design Guide, "Electrical and Working Clearances", Vol. 1, 1995, Section 7-2

[2] William H Hayt Jr., "Engineering Electromagnetics", McGraw-Hill Kogakusha, 3 rd Edition 1974, ISBN 0-07-027390-1, pp. 382-388

[3] W.J. Meintjes, C.G.P Oliver and W.C. Van Der Merwe, "Investigation into the use of Tubular Aluminium Conductors at High Voltage Substations", Eskom Publication, July 1985

[4] CIGRE Working Group 23.03, "The Mechanical Effects of Short Circuit Currents in Open Air Substations", Part II. CIGRE Vol. 214, Paris, 2002

[5] G. Hosemann, D. Tsanakas and F.W.T Davenport, "Dynamic Short Circuit Stress of Busbar Structures with Stiff Conductors", CIGRE SC 23, WG 23-02, 1983

[6] Cigré Study Committee 23 (Working Group 23-02) report, "The Calculation Methods and Comparisons with Test Results", Electra 30, 1973

[7] Joint Brochure by Cigré SC23 and IEC TC 73, "Correctness of a Simplified Calculation Method - Parametric Studies and Simplified Calculation Methods for Dynamic Short Circuit Stresses", 1987 (Electra 68 in January 1980)

[8] R J Cakebread and H J Brown, "Integrated Mechanical Design Loading for Open Type EHV Substation Structures and Equipment", Working Group 04 of Study Committee No.23 (Substations), Electra No.60, October 1978, pp 31-55

[9] IEEE-SA Standards Board, "IEEE Guide for the Design of Substation Rigid Bus Structures", IEEE-605, August 1998

[10] IEC Standard, "High Voltage Test Tecniques – General Definitions and Test Requirements", IEC 60-1, Second Edition, 1989

[11] J D Brown, F A Fisher, wW N Neugebauer, and J Panek, "Insulation – Design Criteria", Chapter 9 of Transmission Line Reference Book, 345kV and Above, EPRI, Second Edition, Revised. 1987, pp 421-460

[12] W.C. Van Der Merwe, "Statistical Basis of Electrical Clearances", Substation Design Course Lecture Notes, 2005

[13] K J Lloyd and L E Zaffanella, "Insulation for Switching Surges", Chapter 11 of Transmission Line Reference Book, 345kV and Above, EPRI, Second Edition, Revised. 1987, pp 503-534

[14] IEC Standard, "Insulation Co-ordination – Application Guide", IEC 71-2, Third Edition, 1996-12

[15] German Standard, "Power Installations Exceeding 1kV AC", DIN VDE 0101, January 2000

[16] South African Standard, "The General Procedures and Loadings to be Adopted in the Design of Buildings", SABS 0160-1989, ISBN 0-626-09814-9, Amended 1991

[17] Damodar N. Gujarati, "Basic Econometrics", McGraw-Hill, Second Edition, ISBN 0-07-100446-7, 1988

[18] Joseph A. Edminister, "Electromagnetics", McGraw-Hill, ISBN 0-07-018990-0, 1979

[19] Asea Brown Boveri Pocket Book "Switchgear Manual", Cornelsen Girardet, Tenth Edition, ISBN 3-46-448236-7, 2001

[20] Alusingen Pamphlet 1/9/78b, "Tubular Busbars for Outdoor Substations – Aluminium", Waltzwerke Singen GmbH, Federal Republic of Germany, 1978

[21] Joseph Edward Shigley, Charles R Mischke, "Mechanical Engineering Design", McGraw-Hill International Edition, 5th Edition, 1989, ISBN 0-07-056899-5, pp743

[22] Online Eskom Transmission Geographic Information System, "TxSIS", 2000, Formerly known as "SURGIS" (Survey Geographic Information System), 1992

[23] IEEE Standard Part 2, "National Electrical Safety Code – Safety Rules for Transmission Lines", IEEE-C2, 2007, pp85

[24] PPC Insulators Brochure, "Ceramic Insulators – BIL 60kV - 2550kV", June 2006, pp 4-28

24. APPENDICES

24.1 APPENDIX A: Estimated Values Of Exponent 'M' In Atmospheric Correction Factor Formula External Insulation Withstand For Curves "a", "b", "c" and "d"

24.2 APPENDIX B: Estimation of Dynamic Factors ν_F, ν_σ and ν_r (See Chapter 15)

24.3 APPENDIX C: Estimation of Decrement Factor Functions Due To Various Insulator Supports

24.4 APPENDIX D: Effective Field Strength for Tubular Conductors in 765kV, 400kV and 275kV Three Phase Systems

24.5 APPENDIX E: Effective Electric and Magnetic Field Strengths under Different Busbar Configurations

24.6 APPENDIX F: Sensitivity of Design to Tolerances in Materials

24.1 APPENDIX A

ESTIMATED VALUES OF EXPONENT 'm' IN ATMOSPHERICCORRECTION FACTOR FORMULA EXTERNAL INSULATION WITHSTAND FOR CURVES "a", "b" , "c" and "d"

Table 24.1: Estimated Values of Exponent 'm' in Atmospheric Correction Factor Formula External Insulation Withstand for Curves "a", "b" and "c" (See Chapter 4)

U_{cw} (kV)	a	b	c
0	-	-	-
20	-	-	-
40	-	-	-
60	-	-	-
80	-	-	-
100	-	-	-
120	-	-	-
140	-	-	-
160	-	-	-
180	-	-	-
200	-	-	-
220	-	-	-
240	-	-	-
260	-	-	-
280	-	-	-
300	-	-	-
400	0,955	-	-
500	0.910	-	-
700	0,825	-	-

U_{cw} (kV)	a	b	c
800	0,785	-	-
900	0,750	-	0,975
1000	0,705	-	0,935
1100	0,665	-	0,895
1200	0,630	0,990	0,855
1300	0,595	0,950	0,815
1400	0,555	0,910	0,775
1500	0,515	0,870	0,740
1600	0,850	0,840	0,700
1700	0,445	0,815	0,675
1800	0,420	0,770	0,625
1900	0,390	0,735	0,595
2100	-	0,675	0,525
2200	-	0.630	0,495
2300	-	0,600	0,465
2400	-	0,575	0,44
-	-	-	-
-	-	-	-

Table 24.2: Estimated Values of Exponent 'm' in AtmosphericCorrection Factor Formula External Insulation Withstand for Curve "d" (See Chapter 4 of this dissertation)

r^2	0.9975	0.9915	0.9968	0.9871	0.9799	0.9861	
d	**d1-Calc**	**d2-Calc**	**d3-Calc**	**d4-Calc**	**d5-Calc**	**d6-Calc**	**Error**
0.975	-	-	-	-	-	-	-
0.930	0.951	-	-	-	-	-	2.035
0.895	0.893	-	-	-	-	-	-0.147
0.875	0.861	-	-	-	-	-	-1.200
0.850	0.839	-	-	-	-	-	-0.934
0.835	0.822	-	-	-	-	-	-1.065
0.815	0.809	-	-	-	-	-	-0.522
0.805	0.797	-	-	-	-	-	-0.614
0.790	0.788	-	-	-	-	-	-0.181
0.775	0.779	-	-	-	-	-	0.336
0.765	0.772	-	-	-	-	-	0.532
0.745	0.765	0.753	-	-	-	-	1.549
0.735	-	0.736	-	-	-	-	0.104
0.723	-	0.722	-	-	-	-	-0.082
0.710	-	0.709	-	-	-	-	-0.096
0.695	-	0.697	0.704	-	-	-	0.108
0.640	-	-	0.635	-	-	-	-0.345
0.595	-	-	0.585	-	-	-	-0.564
0.550	-	-	0.548	-	-	-	-0.109
0.510	-	-	0.518	0.517	-	-	0.430
0.475	-	-	-	0.471	-	-	-0.195
0.440	-	-	-	0.433	-	-	-0.290
0.405	-	-	-	0.402	-	-	-0.110
0.370	-	-	-	0.376	0.380	-	0.389
0.340	-	-	-	-	0.338	-	-0.067
0.310	-	-	-	-	0.303	-	-0.201
0.280	-	-	-	-	0.274	-	-0.153
0.255	-	-	-	-	0.250	-	-0.125
0.220	-	-	-	-	0.229	0.216	0.209
0.190	-	-	-	-	-	0.191	0.000

0.165	-	-	-	-	-	0.170	0.000
0.150	-	-	-	-	-	0.152	0.000
0.140	-	-	-	-	-	0.137	0.000

24.2 APPENDIX B

ESTIMATION OF DYNAMIC FACTORS v_F, v_σ AND v_r (See Chapter 10)

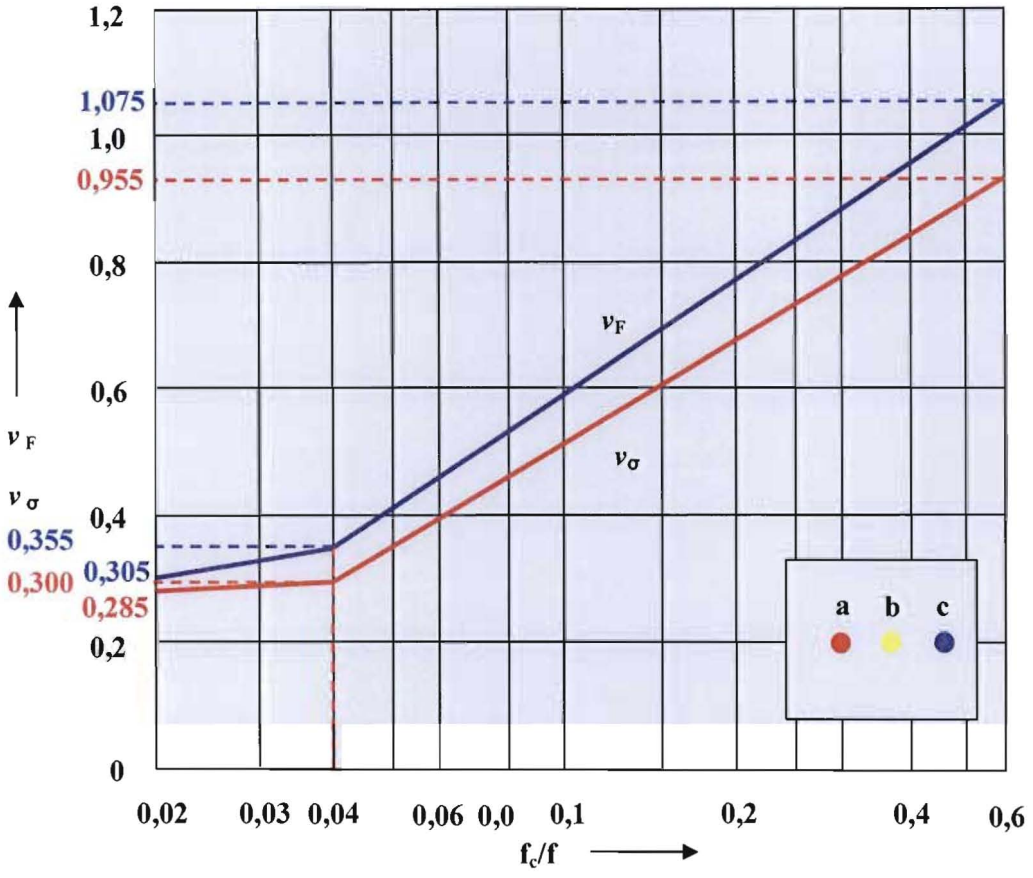

Figure 24.1: Dynamic Factors v_F, v_σ vs Frequency Ratio f_c/f

24.2.1 Estimation of Dynamic Factors v_F and v_σ

The straight line graphs are of the form:-

$$y - y_1 = \left(\frac{y_2 - y_1}{\log(x_2) - \log(x_1)} \right).\log(x) + c$$

24.2.1.1 Estimation of Dynamic Factor v_F

$$v_F = \left(\frac{v_{F2} - v_{F1}}{\left[\log\left(\frac{f_c}{f}\right)_2 - \log\left(\frac{f_c}{f}\right)_1 \right]} \right).\log\left(\frac{f_c}{f}\right) + v_{Fc}$$

a) For $0{,}02 \leq v_F \leq 0{,}04$

For $([f_c/f]_1, v_{F1}) = (0{,}02; 0{,}305)$ and $[f_c/f]_2, v_{F2}) = (0{,}04; 0{,}355)$

$$0{,}355 = \left(\frac{0{,}355 - 0{,}305}{\left[\log(0{,}04) - \log(0{,}02)\right]}\right).\log(0{,}04) + v_{FC}$$

$$0{,}355 = -0{,}232 + v_{FC}$$

$$v_{FC} = 0{,}355 + 0{,}232$$

$$v_{FC} = 0{,}587$$

$$\mathbf{'m'} = \frac{0{,}355 - 0{,}305}{\left[\log(0{,}04) - \log(0{,}02)\right]}$$

$$\mathbf{'m'} = 0{,}166$$

$$\mathbf{v_F = 0{,}166.Log(f_c/f) + 0{,}587} \qquad \mathbf{for\ 0{,}02 \le f_c/f \le 0{,}04}$$

b) For $0{,}04 \le v_F \le 0{,}06$

For $([f_c/f]_1, v_{F1}) = (0{,}04; 0{,}355)$ and $[f_c/f]_2, v_{F2}) = (0{,}6; 1{,}075)$

$$1{,}075 = \left(\frac{1{,}075 - 0{,}355}{\left[\log(0{,}6) - \log(0{,}04)\right]}\right)\log(0{,}6) + v_{FC}$$

$$1{,}075 = -0{,}136 + v_{Fc}$$

$$v_{Fc} = 1{,}075 + 0{,}136$$

$$v_{Fc} = 1{,}211$$

$$\mathbf{'m'} = \frac{1{,}075 - 0{,}355}{\left[\log(0{,}6) - \log(0{,}04)\right]}$$

$$\mathbf{'m'} = 0{,}612$$

24.2.1.2 Estimation of Dynamic Factor v_σ

$$v_\sigma = \left(\frac{v_{\sigma 2} - v_{\sigma 1}}{\left[\log\left(\frac{f_c}{f}\right)_2 - \log\left(\frac{f_c}{f}\right)_1\right]}\right).\log\left(\frac{f_c}{f}\right) + v_{\sigma C}$$

a) For $0{,}02 \le v_\sigma \le 0{,}04$

a) For $([f_c/f]_1, v_{\sigma 1}) = (0{,}02; 0{,}305)$ and $[f_c/f]_2, v_{\sigma 2}) = (0{,}04; 0{,}355)$

$$0{,}300 = \left(\frac{0{,}300 - 0{,}285}{\left[\log(0{,}04) - \log(0{,}02)\right]}\right).\log(0{,}04) + v_{\sigma c}$$

$$0{,}300 = -0{,}070 + v_{\sigma c}$$

$$v_{\sigma c} = 0{,}300 + 0{,}070$$

$$= 0{,}370$$

$$\mathbf{'m'} = \frac{0{,}300 - 0{,}285}{\left[\log(0{,}04) - \log(0{,}02)\right]}$$

$$= 0{,}050$$

$v_\sigma = 0{,}050.\text{Log}(f_c/f) + 0{,}370$ **for** $0{,}02 \leq f_c/f \leq 0{,}04$

b) For $0{,}04 \leq v_F \leq 0{,}6$

For $([f_c/f]_1, \nu_{F1}) = (0{,}04;0{,}355)$ and $[f_c/f]_2, \nu_{F2}) = (0{,}6;1{,}075)$

$$0{,}955 = \left(\frac{0{,}955 - 0{,}300}{[\log(0{,}6) - \log(0{,}04)]}\right).\log(0{,}6) + v_{\sigma c}$$

$$0{,}955 = -0{,}124 + v_{\sigma c}$$

$$v_{\sigma c} = 0{,}955 + 0{,}124$$

$$= 1{,}079$$

$$\text{'m'} = \frac{0{,}955 - 0{,}300}{[\log(0{,}6) - \log(0{,}04)]}$$

$$= 0{,}557$$

$v_\sigma = 0{,}557.\text{Log}(f_c/f) + 1{,}079$ **for** $0{,}04 \leq f_c/f \leq 0{,}6$

24.2.2 Estimation of Dynamic Factor v_r

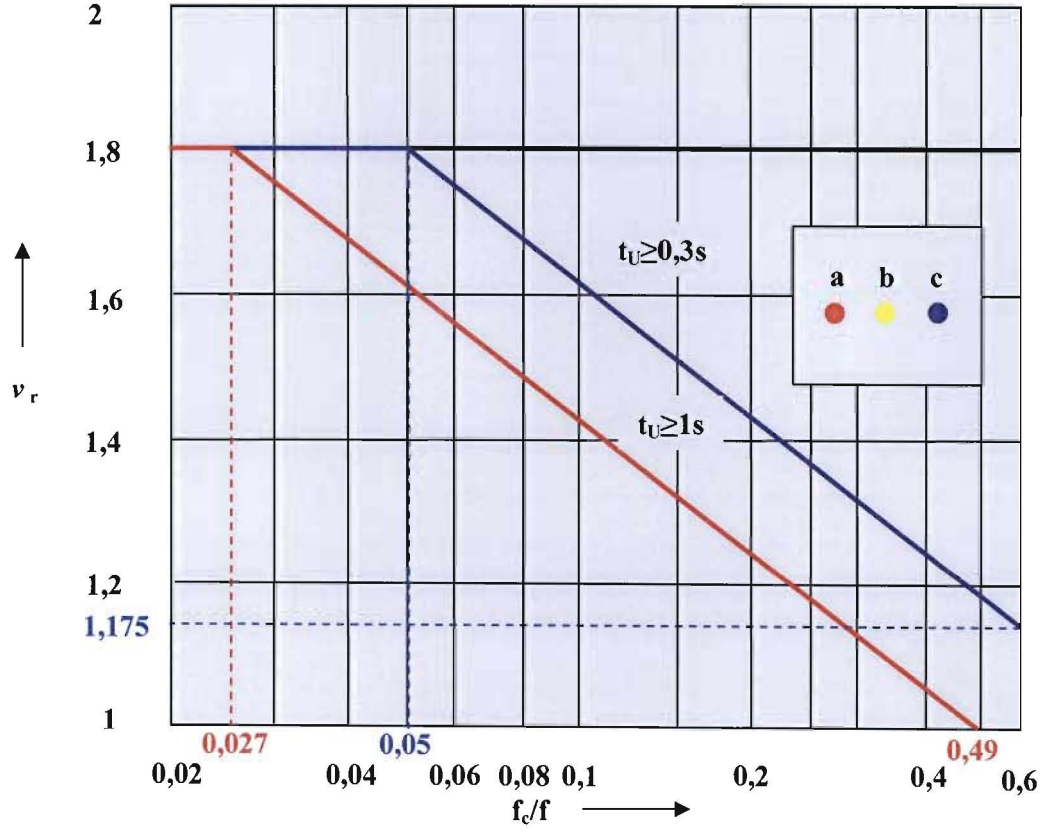

Figure 24.2: Dynamic Factor v_r vs Frequency Ratio f_c/f

$$\nu_r = \left(\frac{\nu_{r2} - \nu_{r1}}{\left[\log\left(\frac{f_c}{f}\right)_2 - \log\left(\frac{f_c}{f}\right)_1 \right]} \right) .\log\left(\frac{f_c}{f}\right) + \nu_{rc}$$

24.2.2 a) For ν_r $[0,02 \leq f_c/f \leq 0,027]$; $t_U \geq 1s$

$\nu_r = 1,8$

24.2.2 b) For ν_r $[0,027 \leq f_c/f \leq 0,49]$; $t_U \geq 1s$

For $([f_c/f]_1, \nu_{r1}) = (0,027; 1,8)$ and $[f_c/f]_2, \nu_{r2}) = (0,49; 1,00)$

$$1,8 = \frac{1,0 - 1,8}{\left[\log(0,49) - \log(0,027)\right]} \log(0,027) + \nu_{rc}$$

$$1,8 = 0,997 + \nu_{rc}$$

$$\nu_{rc} = 1,8 - 0,997$$

$$= 0,803$$

$$\text{'m'} = \frac{1,0 - 1,8}{\left[\log(0,49) - \log(0,027)\right]}$$

$$= -0,636$$

$\nu_r = 0,803 - 0,636.\text{Log}(f_c/f)$ for $0,027 \leq f_c/f \leq 0.49$

24.2.2c) For ν_r [for $0,02 \leq f_c/f \leq 0,05$] ; $t_U \geq 0,3s$

$\nu_r = 1,8$ for $0,02 \leq f_c/f \leq 0,05$

24.2.2d) For ν_r $[0,05 \leq f_c/f \leq 0,6]$; $t_U \geq 0,3s$

For $([f_c/f]_1, \nu_{r1}) = (0,05; 1,8)$ and $[f_c/f]_2, \nu_{r2}) = (0,6; 1,175)$

$$1,8 = \frac{1,175 - 1,8}{\left[\log(0,6) - \log(0,05)\right]} \log(0,05) + \nu_{rc}$$

$$1,8 = 0,753 + \nu_{rc}$$

$$\nu_{rc} = 1,8 - 0,753$$

$$= 1,047$$

$$\text{'m'} = \frac{1,175 - 1,8}{\left[\log(0,6) - \log(0,05)\right]}$$

$$= -0,579$$

$\nu_r = 1,047 - 0,579.\text{Log}(f_c/f)$ for $0,05 \leq f_c/f \leq 0,6$; $t_U \geq 0,3s$

24.3 APPENDIX C

ESTIMATION OF DECREMENT FACTOR FUNCTIONS DUE TO VARIOUS INSULATOR SUPPORTS

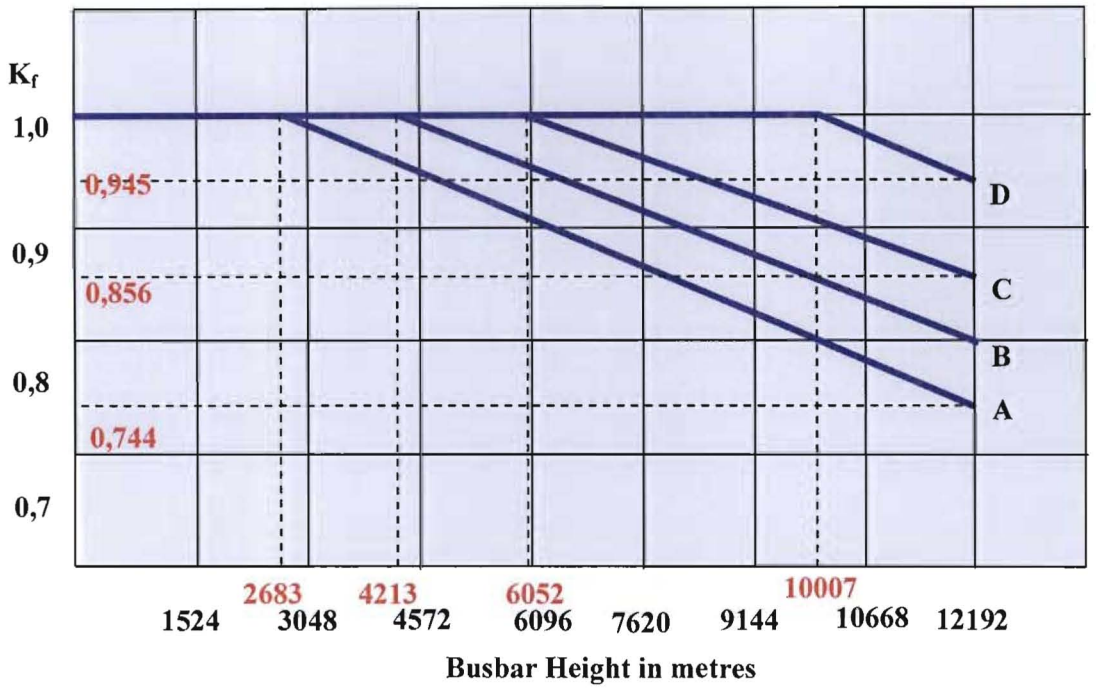

Figure 24.3: K_f vs Busbar Height [22]

24.3.1 Decrement Factor for Lattice and Tubular Aluminium Supports

The straight line graphs are of the form:-

$$y = \left(\frac{y_2 - y_1}{x_2 - x_1}\right).x + c$$

24.3.1.1 For support heights 0mm < $h_c \leq$ 2683mm

$K_{fA} = 1,0$ (from 15.8)

24.3.1.2 For support heights 2683mm < $h_c \leq$ 12192mm

For $(h_{c1}, K_{fA1}) = (2683;1,00)$ and $(h_{c1}, K_{fA2}) = (12192;0,744)$

$$1,00 = \left(\frac{0,744 - 1,000}{12192 - 2683}\right).2683 + K_{fAc}$$

$$1,00 = -0,0722 + K_{fAc}$$

$$K_{fAc} = 1,0723$$

$$m = -2,695.10^{-5}$$

$K_{fA} = 1,0723 - 2,6953.10^{-5}.h_c$ (from 15.8)

24.3.2 Decrement Factor for Tubular and Wide Flange Steel Suppotrs

24.3.2.1 For support heights $0 < h_c \leq 4213mm$

$\mathbf{K_{fB}} = \mathbf{1,0}$ (from 15.9)

24.3.2.2 For support heights $4213mm < h_c \leq 12192mm$

For $(\mathbf{h_{c1}}, \mathbf{K_{fB1}}) = (4213;1,00)$ and $(\mathbf{h_{c1}}, \mathbf{K_{fB2}}) = (12192;0,800)$

$$1,00 = \left(\frac{0,800 - 1,000}{12192 - 4213}\right).4213 + \mathbf{K_{fAc}}$$

$1,00 = -0,1056 + \mathbf{K_{fAc}}$

$\mathbf{K_{fAc}} = 1,1056$

$\mathbf{m} = -2,5066.10^{-5}$

$\mathbf{K_{fB}} = \mathbf{1,1056 - 2,5066.10^{-5}.h_c}$ (from 15.9)

24.3.3 Decrement Factor for Lattice Steel Supports

26.3.3.1 For support heights $0 < h_c \leq 4543mm$

$\mathbf{K_{fC}} = \mathbf{1,0}$ (from 15.10)

24.3.3.2 For support heights $6152mm < h_c \leq 12192mm$

For $(\mathbf{h_{c1}}, \mathbf{K_{fC1}}) = (4543;1,00)$ and $(\mathbf{h_{c1}}, \mathbf{K_{fC2}}) = (12192;0,856)$

$$1,00 = \left(\frac{0,856 - 1,000}{12192 - 6152}\right).6152 + \mathbf{K_{fAc}}$$

$1,00 = -0,1467 + \mathbf{K_{fAc}}$

$\mathbf{K_{fAc}} = 1,1467$

$\mathbf{m} = -2,3841.10^{-5}$

$\mathbf{K_{fC}} = \mathbf{1,1467 - 2,3841.10^{-5}.h_c}$ **$6152m < h_c \leq 12192m$** (from 15.10)

24.3.4 Decrement Factor for Solid Concrete Supports

24.3.4.1 For support heights $0 < h_c \leq 10007mm$

$\mathbf{K_{fD}} = \mathbf{1,0}$ **$0 < h_c \leq 10007m$** (from 15.11)

24.3.4 For support heights $10007mm < h_c \leq 12192mm$

For $(\mathbf{h_{c1}}, \mathbf{K_{fC1}}) = (10007;1,00)$ and $(\mathbf{h_{c1}}, \mathbf{K_{fC2}}) = (12192;0,945)$

$$1,00 = \left(\frac{0,945 - 1,000}{12192 - 10007}\right).10007 + \mathbf{K_{fAc}}$$

$1,00 = -0,2519 + \mathbf{K_{fAc}}$

$\mathbf{K_{fAc}} = 1,2517$

$\mathbf{m} = -2,517.10^{-5}$

$\mathbf{K_{fD}} = \mathbf{1,2519 - 2,5172.10^{-5}.h_c}$ (from 15.11)

24.4 APPENDIX D

EFFECTIVE FIELD STRENGTH ON THE SURFACE OF TUBULAR CONDUCTORS IN 765kV, 400kV AND 275kV THREE PHASE SYSTEMS

Table 24.3: Efective Surface Electric Field Strength (Voltage Gradient) on Bus Tube for Line Voltage [V_L] = 765 kV, Phase Spacing [s_p] = 14m, n = 1

h_c (m)	n	Tube 75 mm			Tube 100 mm			Tube 120 mm			Tube 150 mm			Tube 200 mm		
		E_e kV / cm (rms)			E_e kV / cm (rms)			E_e kV / cm (rms)			E_e kV / cm (rms)			E_e kV / cm (rms)		
		A	B	C	A	B	C	A	B	C	A	B	C	A	B	C
12	1	19,69	20,39	19,69	15,51	16,10	15,51	13,36	13,87	13,36	11,14	11,59	11,14	8,83	9,21	8,83
14	1	-	-	-	-	-	-	13,22	13,78	13,22	-	-	-	-	-	-

Table 24.4: Efective Surface Electric Field Strength (Voltage Gradient) on Bus Tube for Line Voltage [V_L] = 765 kV, Phase Spacing [s_p] = 14m, n = 2

h_c (m)	d_{bo} (mm)	n	Tube 50 mm			Tube 75 mm			Tube 100 mm			Tube 150 mm			Tube 200 mm		
			E_e kV / cm (rms)			E_e kV / cm (rms)			E_e kV / cm (rms)			E_e kV / cm (rms)			E_e kV / cm (rms)		
			A	B	C	A	B	C	A	B	C	A	B	C	A	B	C
12	100	2	21,02	21,80	21,02	-	-	-	-	-	-	-	-	-	-	-	-
12	125	2	-	-	-	15,61	16,23	15,61	-	-	-	-	-	-	-	-	-
12	150	2	19,90	20,70	19,90	-	-	-	12,70	13,20	12,70	-	-	-	-	-	-
12	175	2	-	-	-	14,74	15,34	14,74	-	-	-	-	-	-	-	-	-
12	200	2	-	-	-	-	-	-	12,00	12,50	12,00	9,41	9,83	9,41	-	-	-
12	250	2	-	-	-	-	-	-	-	-	-	8,96	9,37	8,96	7,62	7,98	7,62
12	300	2	-	-	-	-	-	-	-	-	-	-	-	-	7,31	7,66	7,31

Table 24.5: Efective Surface Electric Field Strength (Voltage Gradient) on Bus Tube for Line Voltage [V_L] = 400 kV, Phase Spacing [s_p] = 7m, n = 1

h_c (m)	d_{bo} (mm)	n	Tube 120 mm			Tube 150 mm			Tube 200 mm			Tube 250 mm		
			E_e kV / cm (rms)			E_e kV / cm (rms)			E_e kV / cm (rms)			E_e kV / cm (rms)		
			A	B	C	A	B	C	A	B	C	A	B	C
5,8	-	1	8,01	8,36	8,01	6,72	7,03	6,72	5,38	5,64	5,38	4,53	4,77	4,53

Table 24.6: Efective Surface Electric Field Strength (Voltage Gradient) on Bus Tube for Line Voltage [V_L] = 400 kV, Phase Spacing [s_p] = 6m, n = 1

h_c (m)	d_{bo} (mm)	n	Tube 120 mm			Tube 150 mm			Tube 200 mm			Tube 250 mm		
			E_e kV / cm (rms)			E_e kV / cm (rms)			E_e kV / cm (rms)			E_e kV / cm (rms)		
			A	B	C	A	B	C	A	B	C	A	B	C
5,8	-	1	8,17	8,58	8,17	6,86	7,22	6,86	5,50	5,81	5,50	4,65	4,92	4,65

Table 24.7: Efective Surface Electric Field Strength (Voltage Gradient) on Bus Tube for Line Voltage [V_L] = 400 kV, Phase Spacing [s_p] = 5m, n = 1

h_c (m)	d_{bo} (mm)	n	Tube 120 mm			Tube 150 mm			Tube 200 mm			Tube 250 mm		
			E_e kV / cm (rms)			E_e kV / cm (rms)			E_e kV / cm (rms)			E_e kV / cm (rms)		
			A	B	C	A	B	C	A	B	C	A	B	C
5,8	-	1	8,39	8,87	8,39	7,05	7,48	7,05	5,66	6,02	5,66	4,79	5,13	4,79

Table 24.8: Efective Surface Electric Field Strength (Voltage Gradient) on Bus Tube for Line Voltage [V_L] = 275 kV, Phase Spacing [s_p] = 4,5m, n = 1

h_c (m)	b (mm)	n	Tube 75 mm			Tube 100 mm			Tube 120 mm			Tube 150 mm			Tube 200 mm		
			E_e kV / cm (rms)			E_e kV / cm (rms)			E_e kV / cm (rms)			E_e kV / cm (rms)			E_e kV / cm (rms)		
			A	B	C	A	B	C	A	B	C	A	B	C	A	B	C
5,0	-	1	8,57	9,02	8,57	6,83	7,20	6,83	5,92	6,26	5,92	4,99	5,28	4,99	4,01	4,27	4,01

Table 24.9: Efective Surface Electric Field Strength (Voltage Gradient) on Bus Tube for Line Voltage [V_L] = 275 kV, Phase Spacing [s_p] = 4m, n = 1

h_c (m)	d_{bo} (mm)	n	Tube 75 mm			Tube 100 mm			Tube 120 mm			Tube 150 mm			Tube 200 mm		
			E_e kV / cm (rms)			E_e kV / cm (rms)			E_e kV / cm (rms)			E_e kV / cm (rms)			E_e kV / cm (rms)		
			A	B	C	A	B	C	A	B	C	A	B	C	A	B	C
5,0	-	1	8,72	9,21	8,72	6,95	7,37	6,95	6,03	6,41	6,03	5,09	5,42	5,09	4,10	4,39	4,10

h_c = Height above ground level

d_{bo} = Bus tube diameter

n = Number of conductors per phase bundle

24.5 APPENDIX E

EFFECTIVE ELECTRIC AND MAGNETIC FIELD STRENGTHS UNDER DIFFERENT BUSBAR CONFIGURATIONS

24.5.1 Effective Field Strength (E_e) for Tubular Conductors in a Three Phase System (See Chapter 16)

Appendix E comprises tables of values of the calculated surface voltage gradient ($\mathbf{E_e}$ kV/cm) of each phase of a 3 phase busbar system for a variety of system voltages ($\mathbf{V_L}$ kV), bus tube diameters ($\mathbf{d_{bo}}$ mm), phase spacing ($\mathbf{s_p}$ m), and conductor heights above the ground ($\mathbf{h_c}$ m)

Table 24.10: Study Results of Electric Field Strength at 1,8m Above the Ground [E] (kV/m) vs Bus Tube Height above the Ground [h_c] (m)

Attachment Height [h_c] (m)	Electric Field Strength [E] (kV/m)	
	Maximum	Minimum
8	21,609	10,021
10	15,506	8,745
12	11,742	7,313
14	9,231	5,972
16	7,513	4,752
18	6,194	3,689
20	5,198	2,781

Table 24.11: Study Results of Electric Field Strength at 1,8m Above the Ground [E] (kV/m) vs Bus Tube Height above the Ground [h_c] (m) for given Phase Spacings (s_p)

Conductor Height [h_c]	Phase Spacing [s_p] (m)									Public	Substation Yard
	9.5	10	10.5	11	11.5	12	13	14	15		
	Electric Field Strength [E] (kV/m)										
11	10.8	11.0	11.2	11.4	11.5	11.7	11.9	12.1	12.3	5.0	10.0
12	9.4	9.5	9.7	9.9	10.0	10.1	10.4	10.6	10.8	5.0	10.0
13	8.2	8.3	8.5	8.6	8.8	8.9	9.1	9.4	9.5	5.0	10.0
14	7.2	7.4	7.5	7.6	7.8	7.9	8.1	8.3	8.5	5.0	10.0
15	6.4	6.5	6.7	6.8	6.9	7.0	7.3	7.5	7.6	5.0	10.0
16	5.7	5.8	6.0	6.1	6.2	6.3	6.5	6.7	6.9	5.0	10.0
17	5.1	5.2	5.4	5.4	5.6	5.7	5.9	6.1	6.2	5.0	10.0
18	4.6	4.7	4.9	5.0	5.1	5.2	5.4	5.5	5.7	5.0	10.0
19	4.2	4.3	4.4	4.5	4.6	4.7	4.9	5.0	5.2	5.0	10.0
20	3.8	3.9	4.0	4.1	4.2	4.3	4.5	4.6	4.8	5.0	10.0

24.5.2 Effective Magnetic Field Strength (H) for Tubular Conductors in a Three Phase System (See Chapter 18)

Table 24.12: Study Results of Magnetic Field Strength at 1,8m Above the Ground [H] (μT) vs Bus Tube Height above the Ground [h_c] (m) for given Phase Spacings (s_p)

Bus Tube Height [h_c] (m)	Phase Spacing [s_p] (m)					Public	Substation Yard
	3.5m	4m	4.5m	5m	5.5m		
	Magnetic Field Strength [H] (μT)						
Current 3150A							
4.5	243.7	246.2	247.0	246.9	246.4	100.0	500.0
4.8	216.3	219.9	221.6	222.2	222.2	100.0	500.0
5.0	200.4	204.7	207.0	208.0	208.3	100.0	500.0
5.5	167.3	172.9	176.3	178.4	179.5	100.0	500.0
6.0	141.4	147.6	151.9	154.8	156.6	100.0	500.0
7.0	103.9	110.5	115.6	119.4	122.2	100.0	500.0
8.0	78.9	85.1	90.2	94.4	97.6	100.0	500.0
Current 2500A							
4.5	193.4	195.4	196.0	196.0	195.5	100.0	500.0
4.8	171.6	174.5	175.9	176.4	176.3	100.0	500.0
5.0	159.1	162.5	164.3	165.1	165.4	100.0	500.0
5.5	132.8	137.2	139.9	141.6	142.5	100.0	500.0
6.0	112.2	117.2	120.6	122.8	124.3	100.0	500.0
7.0	82.4	87.7	91.7	94.8	97.0	100.0	500.0
8.0	-	-	-	-	77.5	100.0	500.0
Current 1600A							
4.5	123.8	125.0	125.5	125.4	125.1	100.0	500.0
4.8	109.9	111.7	112.6	112.9	112.9	100.0	500.0
5.0	101.8	104.0	105.1	105.7	105.8	100.0	500.0
5.5	85.0	87.8	89.6	90.6	91.2	100.0	500.0
6.0	-	-	-	-	79.5	100.0	500.0

Current 1250A							
4.5	96.7	97.7	98.0	98.0	97.8	100.0	500.0
4.8	-	-	-	-	88.2	100.0	500.0

CEDEGS ELECTRIC FIELD STUDY RESULTS

Table 24.13: System Voltage = 300kV, Tube Outer Diameter = 160mm, 200mm and 250mm

Attachment Height $[h_{ic})]$ (m)	Maximum System Voltage $[U_{max}]$ (kV)	Tubular Conductor Dia. $[d_{oi}]$ (mm)	Phase Spacing $[s_p]$ (m)				
			3.5	4	4.5	5	5.5
			Electric Field [E] (kV/m)				
4.5	300	160	13.451	14.102	14.197	14.709	14.702
4.8			11.809	12.352	12.564	12.980	13.079
5.0			10.875	11.365	11.633	12.002	12.152
5.5			8.964	9.361	9.719	10.008	10.242
6.0			7.500	7.836	8.243	8.482	8.761
7.0			5.441	5.834	6.127	6.385	6.628
8.0			4.186	4.477	4.750	4.995	5.176
9.0			3.296	3.567	3.799	3.990	4.193
10.0			2.681	2.896	3.100	3.290	3.451
4.5		200	14.233	14.904	14.991	15.520	15.504
4.8			12.489	13.048	13.261	13.689	13.786
5.0			11.498	12.002	12.275	12.654	12.805
5.5			9.472	9.879	10.249	10.544	10.785
6.0			7.920	8.265	8.687	8.932	9.221
7.0			5.744	6.150	6.451	6.719	6.969
8.0			4.417	4.716	5.000	5.253	5.439
9.0			3.477	3.757	3.997	4.194	4.405
10.0			2.828	3.050	3.261	3.457	3.623
4.5		250	15.112	15.804	15.881	16.427	16.400
4.8			13.254	13.829	14.041	14.481	14.575
5.0			12.199	12.715	12.992	13.381	13.533
5.5			10.042	10.458	10.840	11.142	11.390
6.0			8.392	8.744	9.182	9.432	9.732
7.0			6.082	6.502	6.812	7.089	7.347
8.0			4.675	4.983	5.278	5.538	5.729
9.0			3.680	3.969	4.216	4.421	4.638
10.0			2.992	3.221	3.440	3.642	3.814

CEDEGS ELECTRIC FIELD STUDY RESULTS

Table 24.14: System Voltage = 420kV, Tube Outer Diameter = 160mm & 200mm & 250mm

Attachment Height $[h_{ic}]$ (m)	Maximum System Voltage $[U_{max}]$ (kV)	Tubular Conductor Dia. $[d_{oi}]$ (mm)	Phase Spacing $[s_p]$ (m)						
			3.5	4	4.5	5	5.5	6.5	7
			Electric Field [E] (kV/m)						
5.5	420	160	12.550	13.105	13.607	14.011	14.338	14.872	15.142
5.7			11.667	12.185	12.719	13.092	13.449	13.984	14.226
6.0			10.499	10.971	11.539	11.875	12.266	12.800	13.010
6.5			8.888	9.416	9.902	10.207	10.617	11.147	11.319
7.0			7.617	8.167	8.578	8.939	9.279	9.801	9.949
8.0			5.861	6.268	6.651	6.993	7.247	7.748	7.952
10.0			3.753	4.045	4.340	4.605	4.831	5.237	5.398
12.0			2.613	2.838	3.057	3.260	3.443	3.770	3.915
14.0			1.925	2.099	2.269	2.427	2.573	2.839	2.961
5.5		200	13.261	13.830	14.349	14.762	15.099	15.647	15.923
5.7			12.325	12.856	13.409	13.790	14.159	14.709	14.956
6.0			11.088	11.571	12.161	12.504	12.909	13.459	13.673
6.5			9.382	9.930	10.430	10.745	11.168	11.715	11.890
7.0			8.014	8.610	9.032	9.406	9.776	10.295	10.445
8.0			6.184	6.603	7.000	7.354	7.614	8.133	8.344
10.0			3.959	4.269	4.566	4.840	5.072	5.492	5.657
12.0			2.756	2.988	3.215	3.425	3.613	3.951	4.100
14.0			2.031	2.211	2.386	2.549	2.700	2.975	3.101

CEDEGS ELECTRIC FIELD STUDY RESULTS

Table 24.15: System Voltage = 420kV, Tube Outer Diameter = 250mm

Attachment Height $[h_{ic}]$ (m)	Maximum System Voltage $[U_{max}]$ (kV)	Tubular Conductor Dia. $[d_{oi}]$ (mm)	Phase Spacing $[s_p]$ (m)						
			3.5	4	4.5	5	5.5	6.5	7
			Electric Field [E] (kV/m)						
5.5	420	250	14.058	14.641	15.176	15.599	15.946	16.507	16.970
5.7			13.063	13.605	14.178	14.568	14.949	15.513	15.766
6.0			11.748	12.241	12.855	13.204	13.624	14.189	14.407
6.5			9.936	10.503	11.019	11.343	11.780	12.343	12.521
7.0			8.515	9.103	9.537	9.925	10.285	10.841	10.993
8.0			6.544	6.976	7.389	7.753	8.020	8.557	8.777
10.0			4.188	4.509	4.816	5.099	5.339	5.773	5.943
12.0			2.916	3.155	3.391	3.607	3.801	4.151	4.305
14.0			2.149	2.335	2.516	2.684	2.840	3.124	3.254

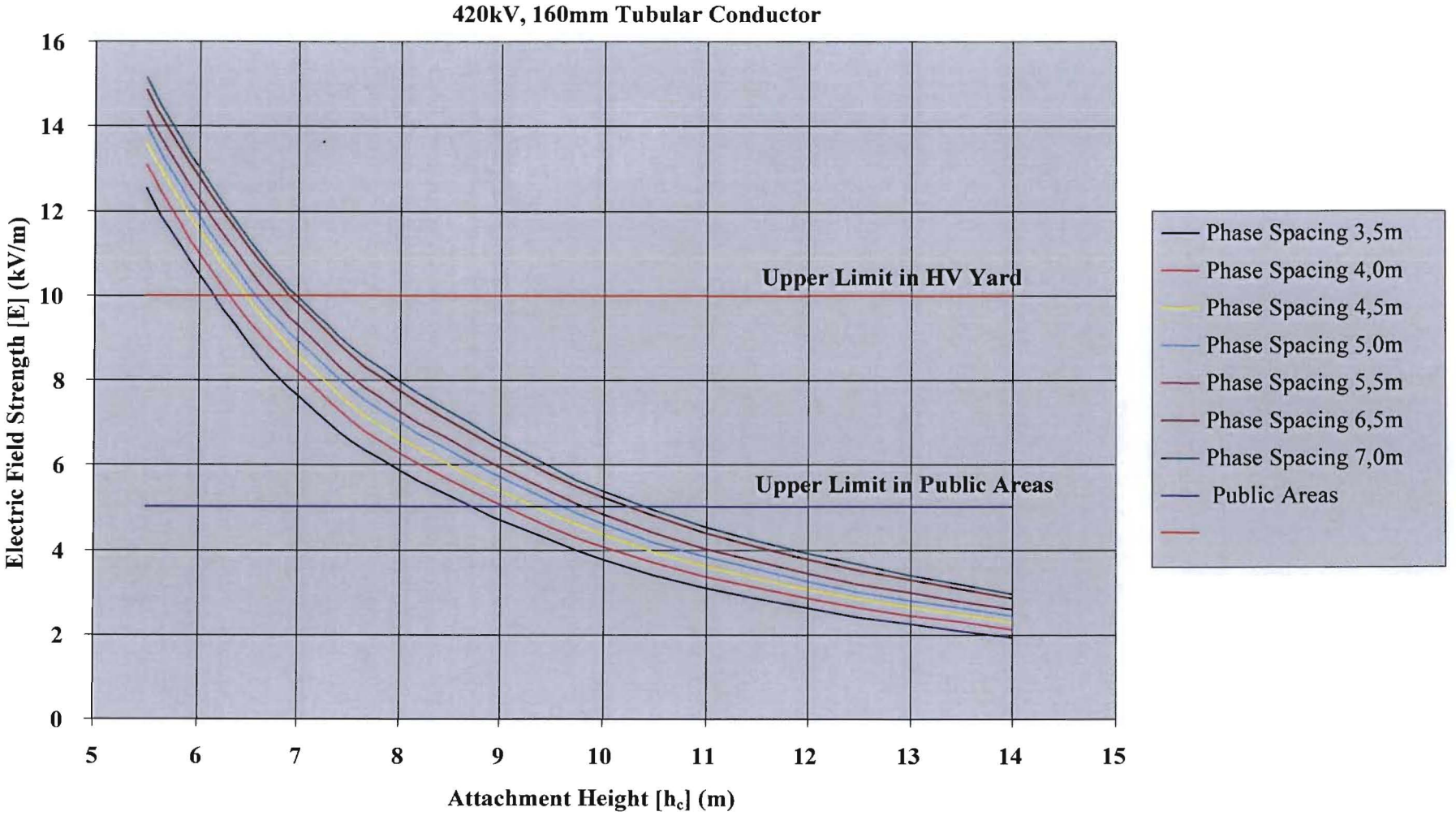

Figure 24.4: Function of Electric Field [E] (kV/m) vs Conductor Height [h_c] (m) for 420kV, 160mm Bus Tube System [Excel Printout from Busbar Programme]

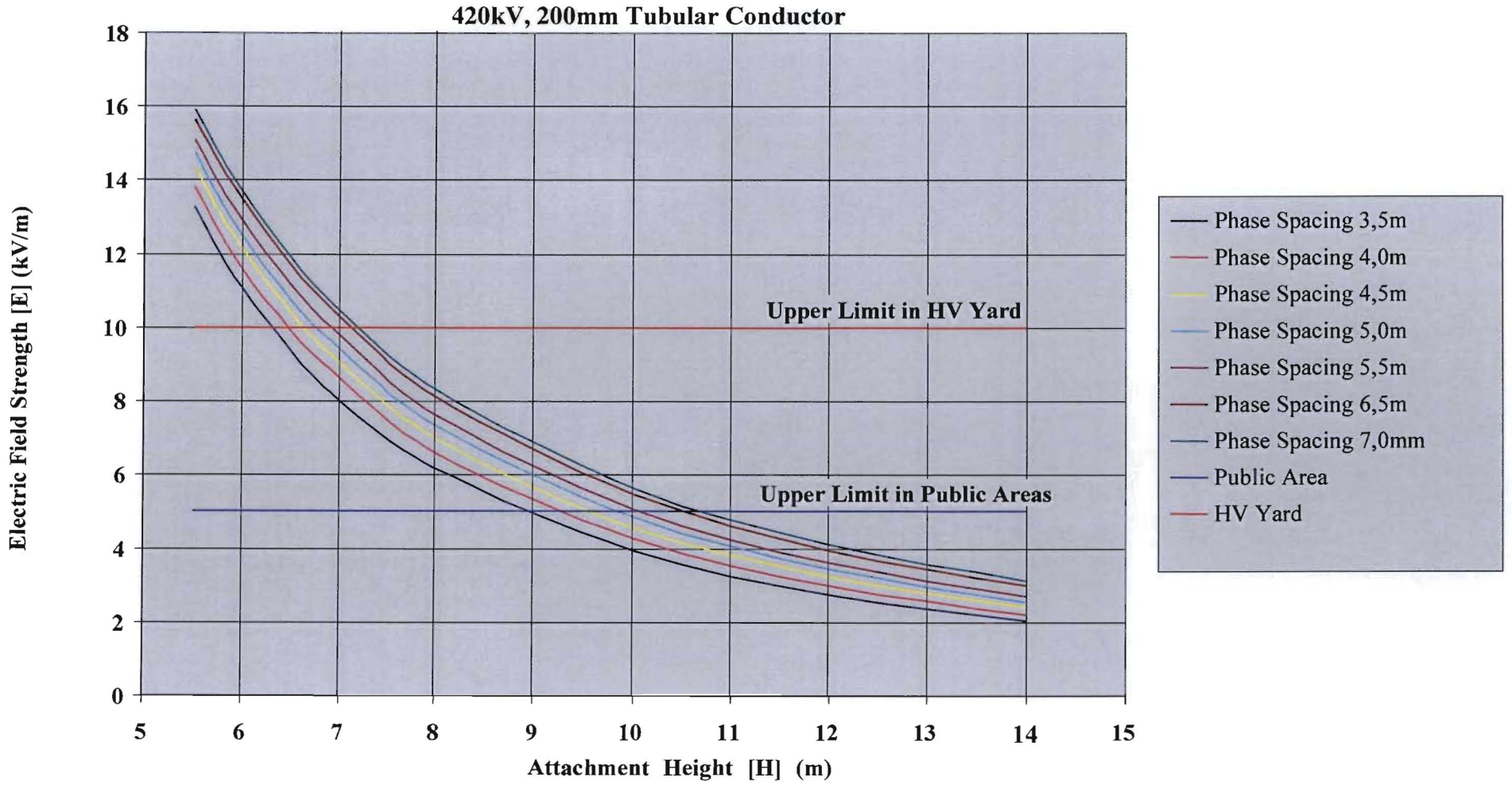

Figure 24.5: Function of Electric Field [E] (kV/m) vs Conductor Height [h_c] (m) for 420kV, 200mm Bus Tube System [Excel Printout from Busbar Programme]

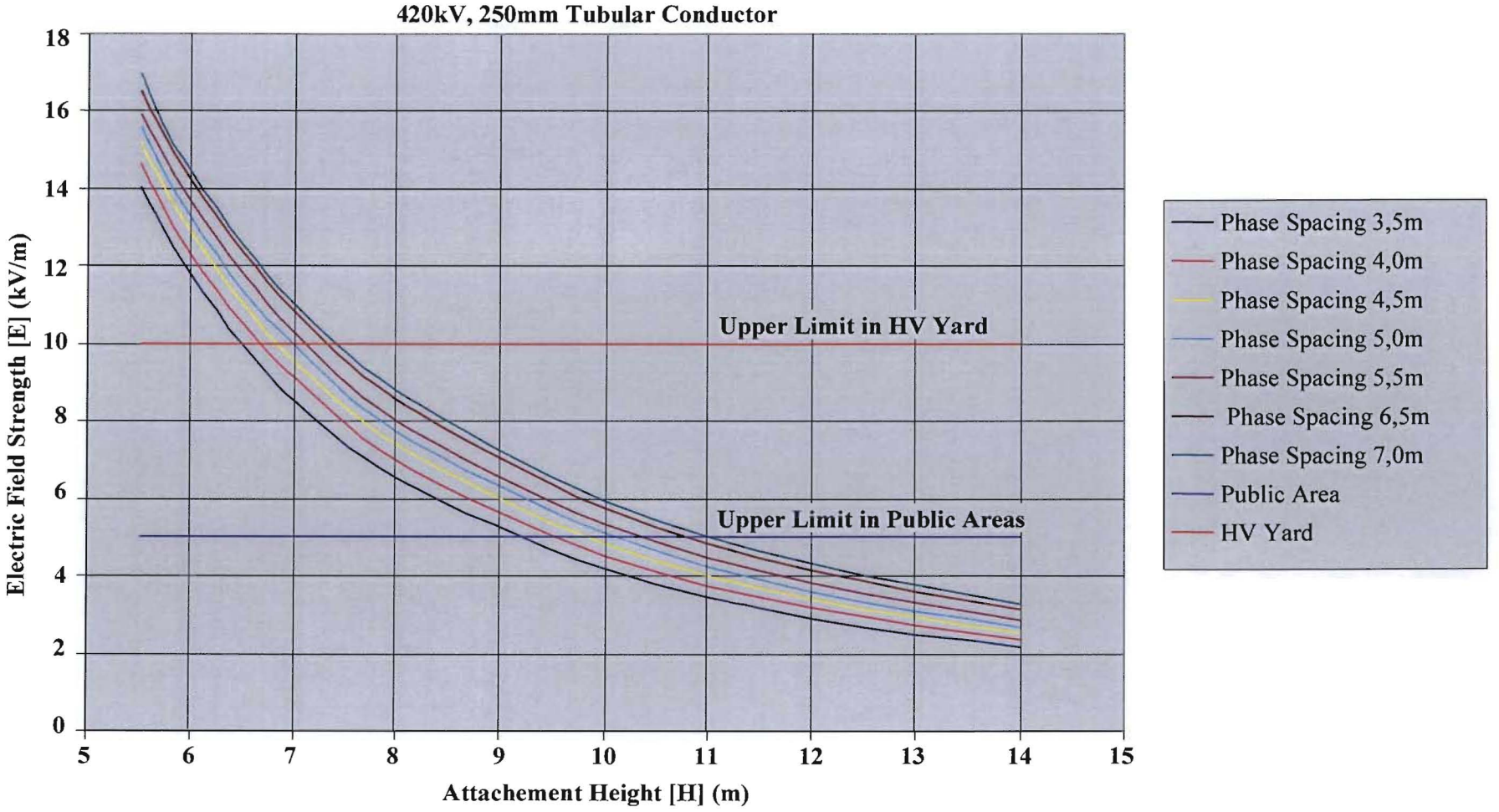

Figure 24.6: Function of Electric Field [E] (kV/m) vs Conductor Height [h_c] (m) for 420kV, 250mm Bus Tube System [Excel Printout from Busbar Programme]

RESULTS FROM CEDEGS ELECTRIC FIELD STUDY

Table 24.16: System Voltage = 800kV, Tube Outer Diameter = 160mm

Attachment Height	Maximum System Voltage	Tubular Conductor Dia.	Phase Spacing [s_p] (m)								
			9.5	10	10.5	11	11.5	12	13	14	15
[h_{ic}] (m)	[U_{max}] kV)	[d_{oi}] (mm)	Electric Field [E] (kV/m)								
10.0	800	160	11.513	11.741	11.896	12.077	12.221	12.363	12.608	12.820	13.004
11.0			9.867	10.051	10.205	10.377	10.493	10.656	10.898	11.108	11.291
12.0			8.541	8.693	8.869	9.008	9.149	9.280	9.516	9.721	9.902
13.0			7.453	7.619	7.770	7.901	8.042	8.150	8.379	8.580	8.757
14.0			6.570	6.724	6.853	6.997	7.116	7.233	7.439	7.627	7.799
15.0			5.835	5.968	6.108	6.232	6.345	6.462	6.662	6.839	6.996
16.0			5.202	5.342	5.467	5.578	5.697	5.798	5.993	6.165	6.318
17.0			4.677	4.800	4.914	5.031	5.133	5.232	5.412	5.580	5.730
18.0			4.218	4.334	4.448	4.551	4.649	4.746	4.918	5.071	5.214
19.0			3.823	3.934	4.036	4.135	4.231	4.318	4.485	4.634	4.767
20.0			3.379	3.579	3.680	3.774	3.860	3.946	4.100	4.245	4.375
25.0			2.275	2.351	2.423	2.492	2.557	2.622	2.742	2.855	2.956
27.0			1.954	2.020	2.085	2.146	2.205	2.262	2.371	2.472	2.564

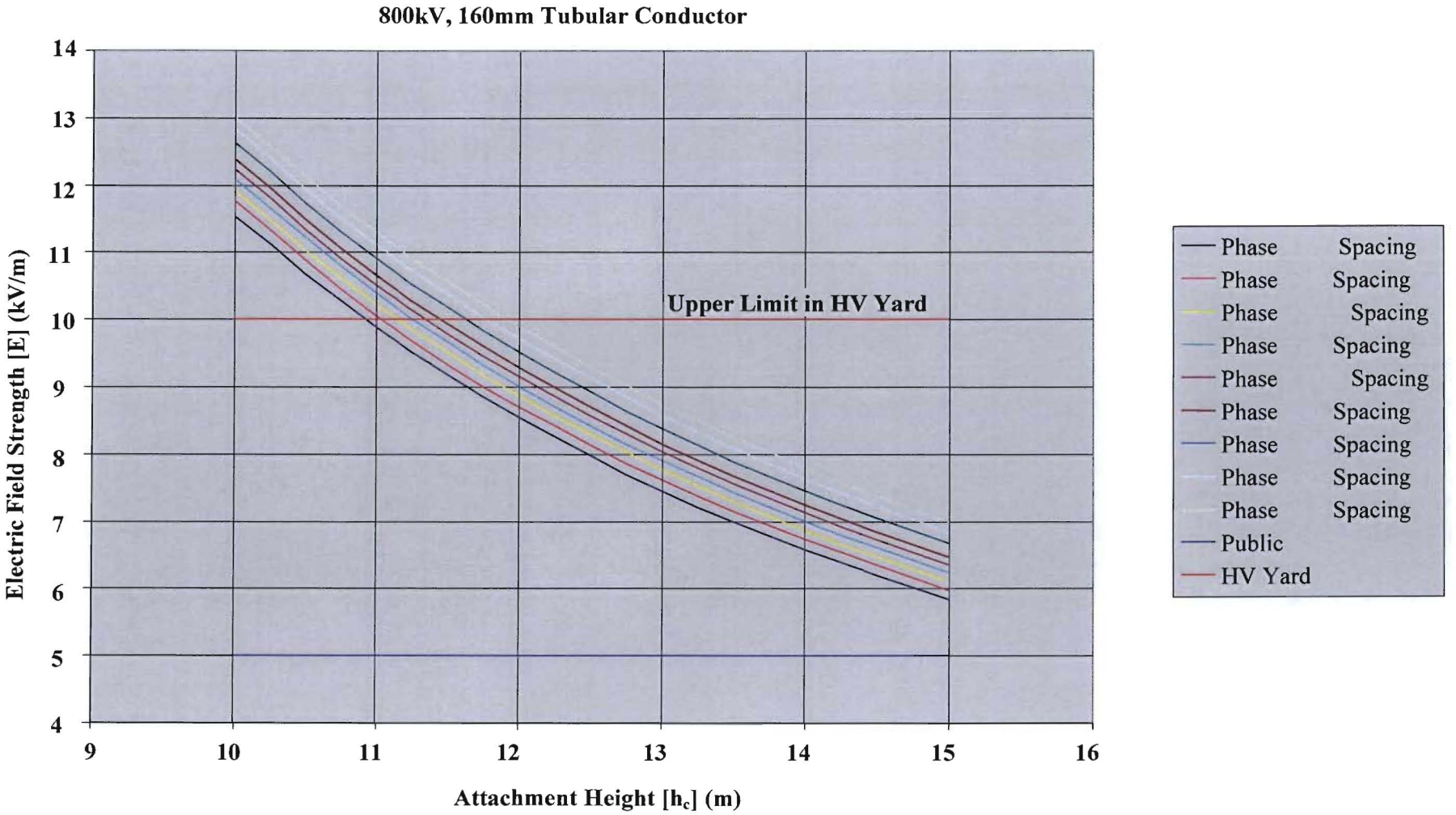

Figure 24.7: Function of Electric Field [E] (kV/m) vs Conductor Height [h_c] (m) for 800kV, 160mm Bus Tube System [Excel Printout from Busbar Programme]

RESULTS FROM CEDEGS ELECTRIC FIELD STUDY

Table 24.17: System Voltage = 800kV, Tube Outer Diameter = 200mm

Attachment Height	Maximum System Voltage	Tubular Conductor Dia.	Phase Spacing [s_p] (m)								
			9.5	10	10.5	11	11.5	12	13	14	15
[h_{ic}](m)	[U_{max}](kV)	[d_{oi}] (mm)	Electric Field [E] (kV/m)								
10.0	800	200	12.047	12.283	12.442	12.630	12.777	12.925	13.177	13.396	13.585
11.0			10.320	10.510	10.669	10.846	10.966	11.135	11.384	11.600	11.789
12.0			8.930	9.086	9.269	9.412	9.558	9.692	9.936	10.148	10.335
13.0			7.789	7.962	8.117	8.252	8.398	8.509	8.746	8.953	9.136
14.0			6.866	7.024	7.157	7.306	7.429	7.550	7.763	7.955	8.133
15.0			6.096	6.233	6.378	6.506	6.623	6.743	6.950	7.132	7.294
16.0			5.434	5.579	5.707	5.824	5.945	6.048	6.250	6.427	6.585
17.0			4.884	5.012	5.130	5.249	5.355	5.457	5.643	5.816	5.970
18.0			4.405	4.525	4.642	4.748	4.850	4.949	5.127	5.285	5.432
19.0			3.992	4.107	4.211	4.314	4.413	4.502	4.675	4.828	4.965
20.0			3.633	3.735	3.840	3.936	4.025	4.114	4.273	4.422	4.556
25.0			2.375	2.453	2.527	2.598	2.666	2.733	2.856	2.972	3.078
27.0			2.040	2.108	2.174	2.238	2.298	2.357	2.469	2.573	2.668

RESULTS FROM CEDEGS ELECTRIC FIELD STUDY

Table 24.18: System Voltage = 800kV, Tube Outer Diameter = 250mm

Attachment Height	Maximum System Voltage	Tubular Conductor Dia.	Phase Spacing [s_p] (m)								
			9.5	10	10.5	11	11.5	12	13	14	15
[h_{ic}](m)	[U_{max}](kV)	[d_{oi}] (mm)	Electric Field [E] (kV/m)								
10.0	800	250	12.632	12.878	13.041	13.236	13.387	13.540	13.801	14.025	14.220
11.0			10.818	11.013	11.178	11.361	11.485	11.659	11.916	12.139	12.333
12.0			9.356	9.516	9.706	9.853	10.005	10.143	10.394	10.614	10.806
13.0			8.158	8.337	8.497	8.637	8.787	8.901	9.145	9.360	9.548
14.0			7.189	7.353	7.491	7.644	7.770	7.896	8.116	8.313	8.497
15.0			6.381	6.522	6.673	6.805	6.926	7.049	7.263	7.451	7.618
16.0			5.688	5.837	5.970	6.090	6.215	6.322	6.529	6.713	6.878
17.0			5.112	5.243	5.365	5.448	5.597	5.703	5.894	6.072	6.232
18.0			4.609	4.733	4.854	4.963	5.068	5.171	5.355	5.518	5.669
19.0			4.177	4.295	4.403	4.509	4.611	4.702	4.881	5.039	5.181
20.0			3.800	3.906	4.014	4.114	4.205	4.297	4.461	4.615	4.753
25.0			2.484	2.564	2.641	2.714	2.784	2.853	2.980	3.100	3.208
27.0			2.133	2.204	2.272	2.337	2.399	2.461	2.576	2.683	2.781

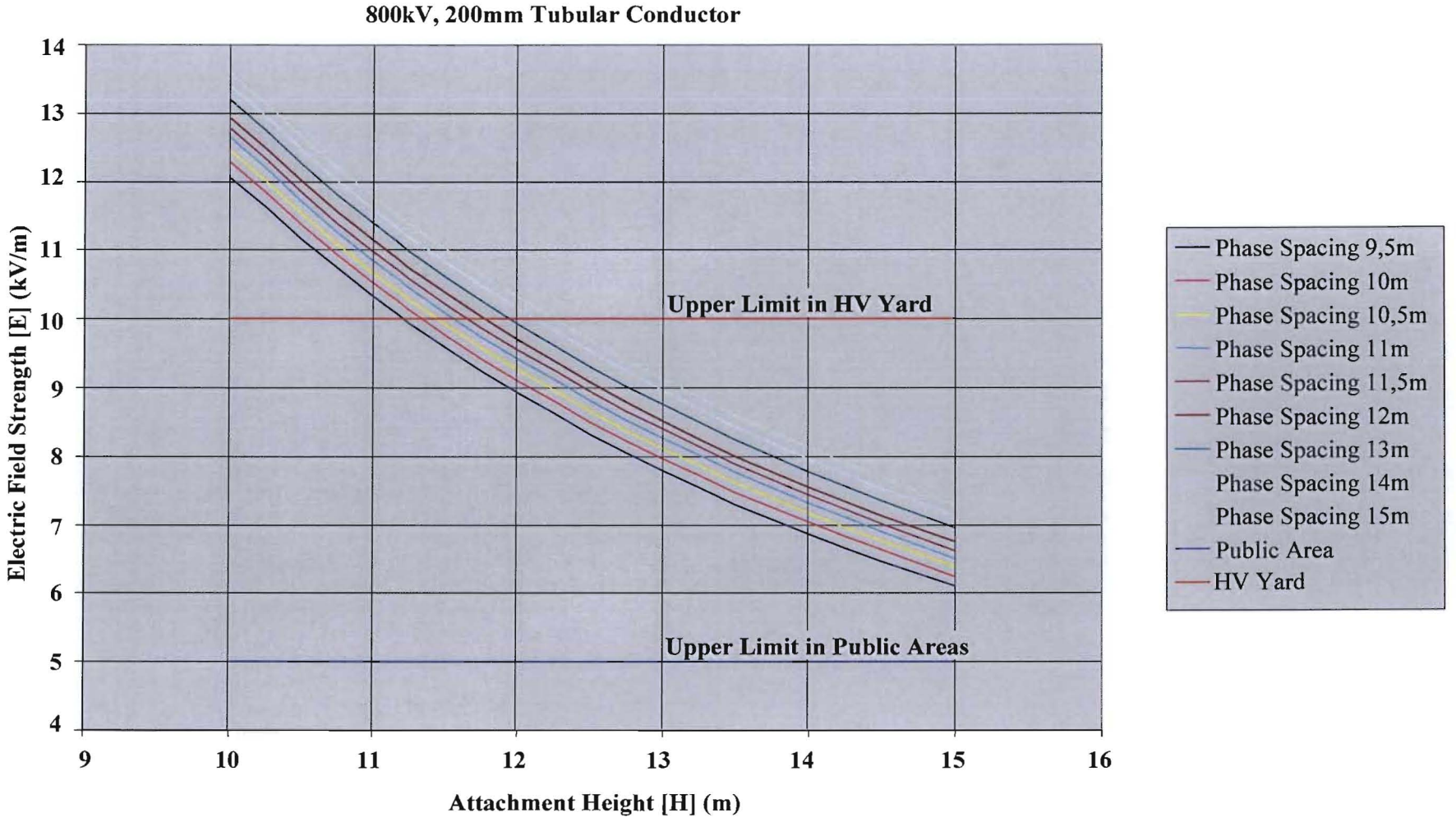

Figure 24.8: Function of Electric Field [E] (kV/m) vs Conductor Height [h_c] (m) for 800kV, 200mm Bus Tube System [Excel Printout from Busbar Programme]

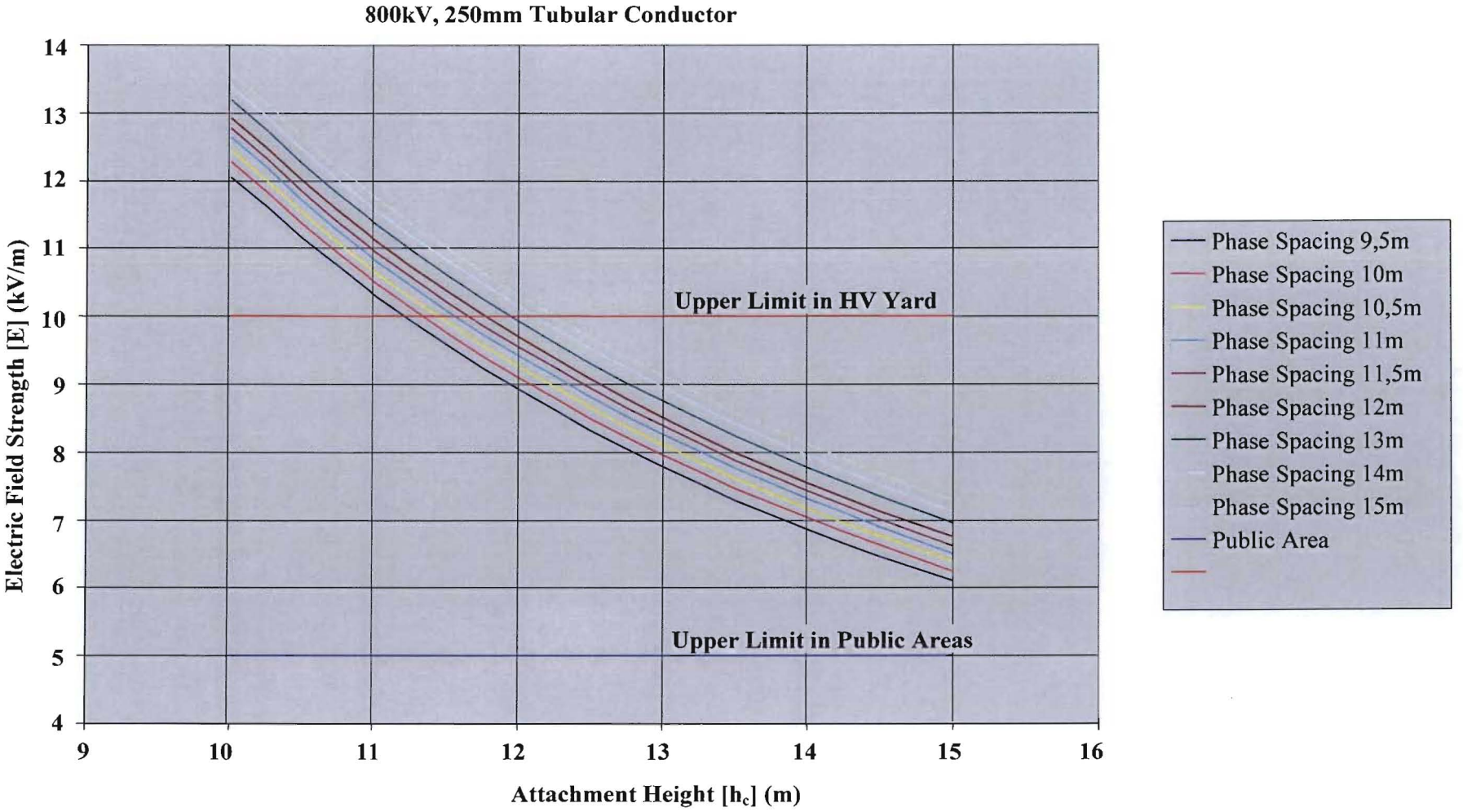

Figure 24.9: Function of Electric Field [E] (kV/m) vs Conductor Height [h_c] (m) for 800kV, 200mm Bus Tube System [Excel Printout from Busbar Programme]

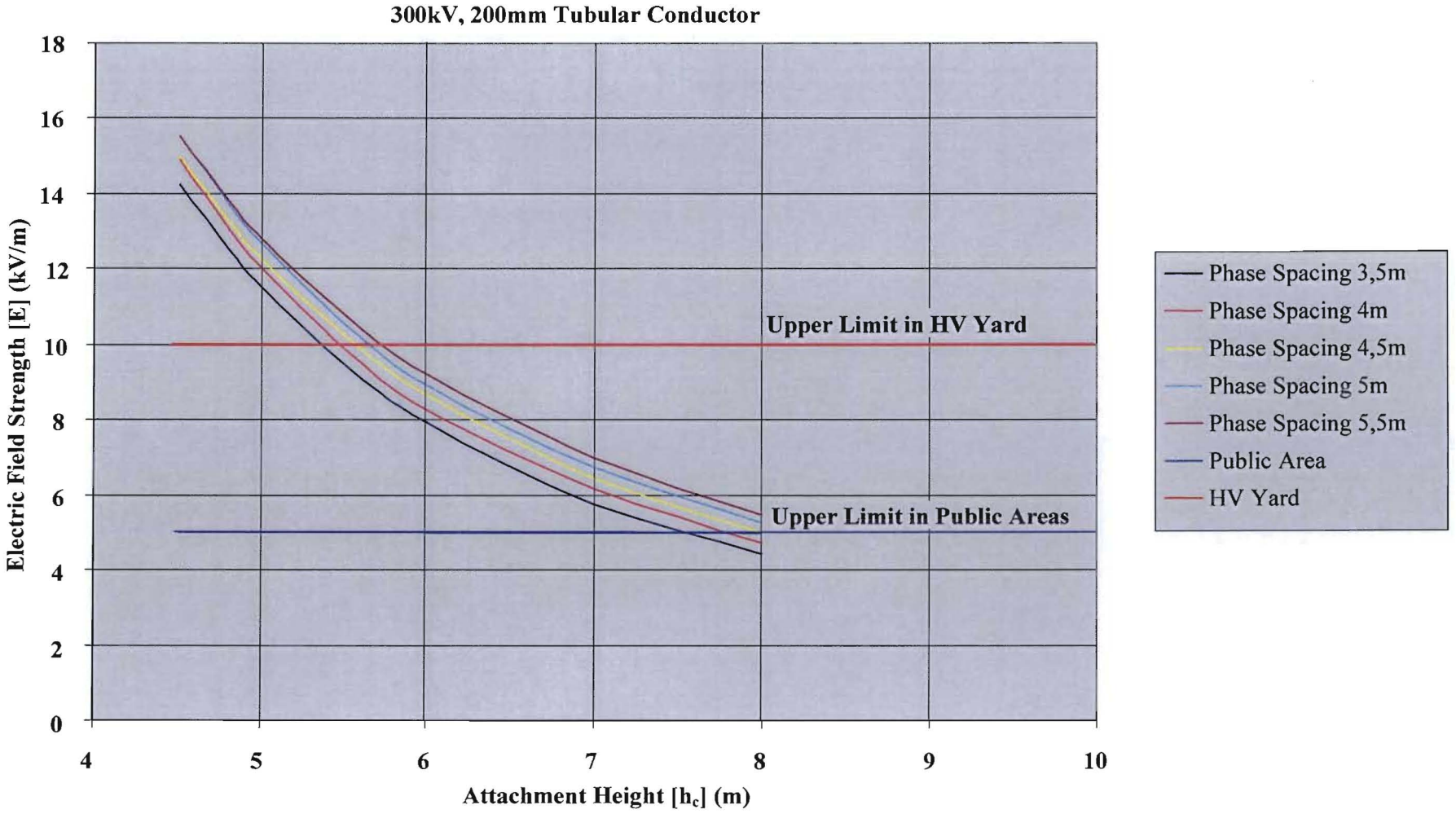

Figure 24.10: Function of Electric Field [E] (kV/m) vs Conductor Height [h_c] (m) for 300kV, 200mm Bus Tube System [Excel Printout from Busbar Programme]

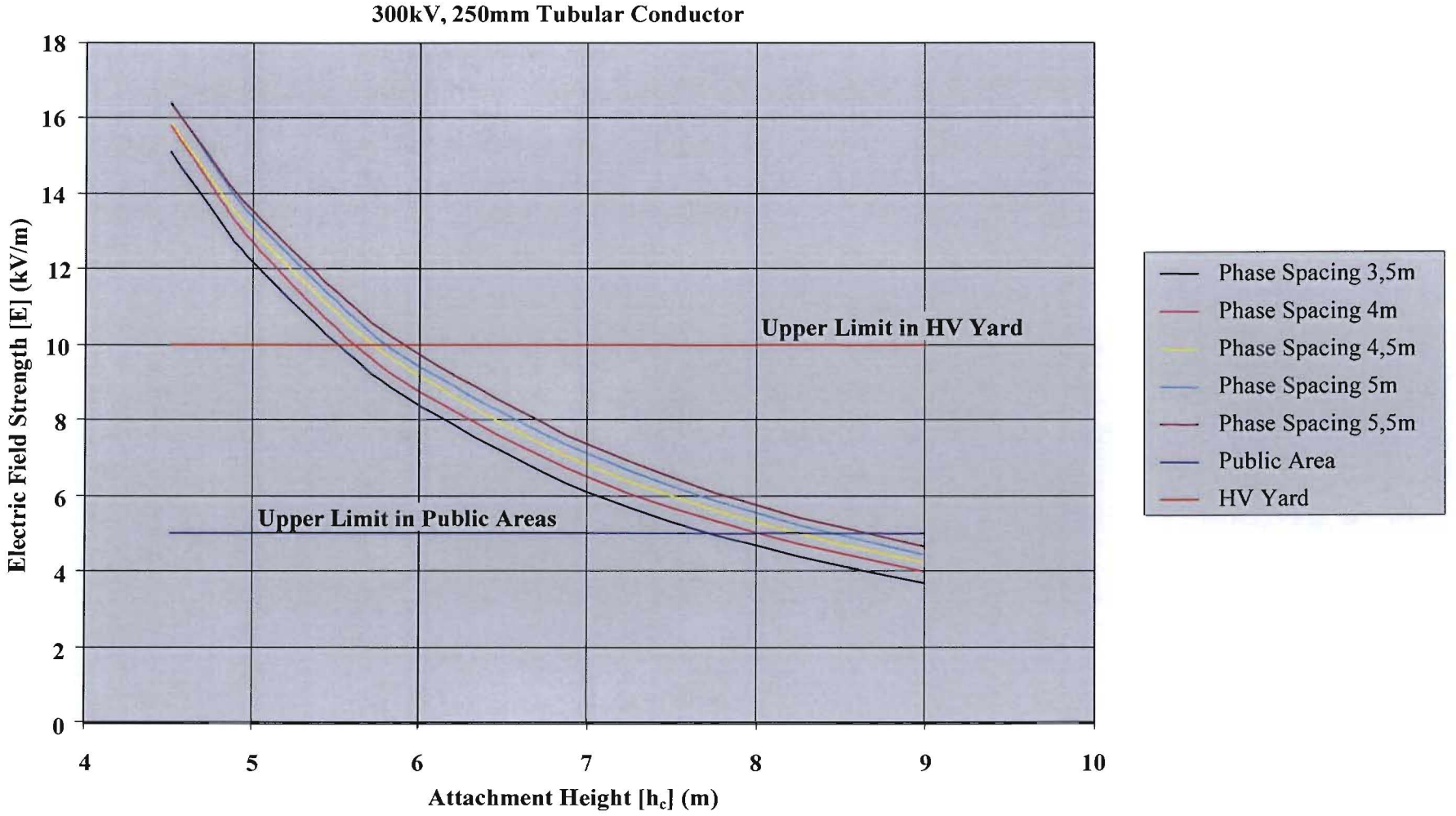

Figure 24.11: Function of Electric Field [E] (kV/m) vs Conductor Height [h_c] (m) for 300kV, 250mm Bus Tube System [Excel Printout from Busbar Programme]

Table 24.19: Natural Logarithms of the Study Values for Electric Field Strength [E] (kV/m) vs Conductor Height [h_c] (m), Phase Spacing [s_p] (m), Bus Tube Diameter [d_{bo}] (mm), and System Voltage [V_L] (kV)

Row No.	$\ln E_i$	1	$\ln(h_{ci})$	$\ln(s_{pi})$	$\ln(d_{oi})$	$\ln(V_i)$	Row No.	$\ln E_i$	1	$\ln(h_{ci})$	$\ln(s_{pi})$	$\ln(d_{oi})$	$\ln(V_i)$
1	2.44	1	2.30	2.25	5.08	6.68	18	1.91	1	2.64	2.30	5.08	6.68
2	2.29	1	2.40	2.25	5.08	6.68	19	1.79	1	2.71	2.30	5.08	6.68
3	2.14	1	2.48	2.25	5.08	6.68	20	1.68	1	2.77	2.30	5.08	6.68
4	2.01	1	2.56	2.25	5.08	6.68	21	1.57	1	2.83	2.30	5.08	6.68
5	1.88	1	2.64	2.25	5.08	6.68	22	1.47	1	2.89	2.30	5.08	6.68
6	1.76	1	2.71	2.25	5.08	6.68	23	1.37	1	2.94	2.30	5.08	6.68
7	1.65	1	2.77	2.25	5.08	6.68	24	1.28	1	3.00	2.30	5.08	6.68
8	1.54	1	2.83	2.25	5.08	6.68	25	0.85	1	3.22	2.30	5.08	6.68
9	1.44	1	2.89	2.25	5.08	6.68	26	0.70	1	3.30	2.30	5.08	6.68
10	1.34	1	2.94	2.25	5.08	6.68	27	2.48	1	2.30	2.35	5.08	6.68
11	1.22	1	3.00	2.25	5.08	6.68	28	2.32	1	2.40	2.35	5.08	6.68
12	0.82	1	3.22	2.25	5.08	6.68	29	2.18	1	2.48	2.35	5.08	6.68
13	0.67	1	3.30	2.25	5.08	6.68	30	2.05	1	2.56	2.35	5.08	6.68
14	2.46	1	2.30	2.30	5.08	6.68	31	1.92	1	2.64	2.35	5.08	6.68
15	2.31	1	2.40	2.30	5.08	6.68	32	1.81	1	2.71	2.35	5.08	6.68
16	2.16	1	2.48	2.30	5.08	6.68	33	1.70	1	2.77	2.35	5.08	6.68
17	2.03	1	2.56	2.30	5.08	6.68	34	1.59	1	2.83	2.35	5.08	6.68

Row No.	lnE_i	1	$ln(h_{ci})$	$ln(s_{pi})$	$ln(d_{oi})$	$ln(V_i)$	Row No.	lnE_i	1	$ln(h_{ci})$	$ln(s_{pi})$	$ln(d_{oi})$	$ln(V_i)$
35	1.49	1	2.89	2.35	5.08	6.68	53	2.50	1	2.30	2.44	5.08	6.68
36	1.40	1	2.94	2.35	5.08	6.68	54	2.35	1	2.40	2.44	5.08	6.68
37	1.30	1	3.00	2.35	5.08	6.68	55	2.21	1	2.48	2.44	5.08	6.68
38	0.90	1	3.22	2.35	5.08	6.68	56	2.08	1	2.56	2.44	5.08	6.68
39	0.75	1	3.30	2.35	5.08	6.68	57	1.96	1	2.64	2.44	5.08	6.68
40	2.49	1	2.30	2.40	5.08	6.68	58	1.85	1	2.71	2.44	5.08	6.68
41	2.34	1	2.40	2.40	5.08	6.68	59	1.74	1	2.77	2.44	5.08	6.68
42	2.20	1	2.48	2.40	5.08	6.68	60	1.64	1	2.83	2.44	5.08	6.68
43	2.07	1	2.56	2.40	5.08	6.68	61	1.54	1	2.89	2.44	5.08	6.68
44	1.95	1	2.64	2.40	5.08	6.68	62	1.44	1	2.94	2.44	5.08	6.68
45	1.83	1	2.71	2.40	5.08	6.68	63	1.35	1	3.00	2.44	5.08	6.68
46	1.72	1	2.77	2.40	5.08	6.68	64	0.94	1	3.22	2.44	5.08	6.68
47	1.62	1	2.83	2.40	5.08	6.68	65	0.79	1	3.30	2.44	5.08	6.68
48	1.52	1	2.89	2.40	5.08	6.68	66	2.51	1	2.30	2.48	5.08	6.68
49	1.42	1	2.94	2.40	5.08	6.68	67	2.37	1	2.40	2.48	5.08	6.68
50	1.33	1	3.00	2.40	5.08	6.68	68	2.23	1	2.48	2.48	5.08	6.68
51	0.91	1	3.22	2.40	5.08	6.68	69	2.10	1	2.56	2.48	5.08	6.68
52	0.76	1	3.30	2.40	5.08	6.68	70	1.98	1	2.64	2.48	5.08	6.68

Row No.	$\ln E_i$	1	$\ln(h_{ci})$	$\ln(s_{pi})$	$\ln(d_{oi})$	$\ln(V_i)$	Row No.	$\ln E_i$	1	$\ln(h_{ci})$	$\ln(s_{pi})$	$\ln(d_{oi})$	$\ln(V_i)$
71	1.87	1	2.71	2.48	5.08	6.68	90	1.01	1	3.22	2.56	5.08	6.68
72	1.76	1	2.77	2.48	5.08	6.68	91	0.86	1	3.30	2.56	5.08	6.68
73	1.65	1	2.83	2.48	5.08	6.68	92	2.55	1	2.30	2.64	5.08	6.68
74	1.56	1	2.89	2.48	5.08	6.68	93	2.41	1	2.40	2.64	5.08	6.68
75	1.46	1	2.94	2.48	5.08	6.68	94	2.27	1	2.48	2.64	5.08	6.68
76	1.37	1	3.00	2.48	5.08	6.68	95	2.15	1	2.56	2.64	5.08	6.68
77	0.96	1	3.22	2.48	5.08	6.68	96	2.03	1	2.64	2.64	5.08	6.68
78	0.82	1	3.30	2.48	5.08	6.68	97	1.92	1	2.71	2.64	5.08	6.68
79	2.53	1	2.30	2.56	5.08	6.68	98	1.61	1	2.77	2.64	5.08	6.68
80	2.39	1	2.40	2.56	5.08	6.68	99	1.61	1	2.83	2.64	5.08	6.68
81	2.25	1	2.48	2.56	5.08	6.68	100	1.61	1	2.89	2.64	5.08	6.68
82	2.13	1	2.56	2.56	5.08	6.68	101	1.61	1	2.94	2.64	5.08	6.68
83	2.01	1	2.64	2.56	5.08	6.68	102	1.45	1	3.00	2.64	5.08	6.68
84	1.90	1	2.71	2.56	5.08	6.68	103	1.05	1	3.22	2.64	5.08	6.68
85	1.79	1	2.77	2.56	5.08	6.68	104	0.91	1	3.30	2.64	5.08	6.68
86	1.69	1	2.83	2.56	5.08	6.68	105	2.57	1	2.30	2.71	5.08	6.68
87	1.59	1	2.89	2.56	5.08	6.68	106	2.42	1	2.40	2.71	5.08	6.68
88	1.50	1	2.94	2.56	5.08	6.68	107	2.29	1	2.48	2.71	5.08	6.68
89	1.41	1	3.00	2.56	5.08	6.68	108	2.17	1	2.56	2.71	5.08	6.68

Row No.	$\ln E_i$	1	$\ln(h_{ci})$	$\ln(s_{pi})$	$\ln(d_{oi})$	$\ln(V_i)$	Row No.	$\ln E_i$	1	$\ln(h_{ci})$	$\ln(s_{pi})$	$\ln(d_{oi})$	$\ln(V_i)$
109	2.05	1	2.64	2.71	5.08	6.68	128	1.29	1	3.00	2.25	5.30	6.68
110	1.95	1	2.71	2.71	5.08	6.68	129	0.86	1	3.22	2.25	5.30	6.68
111	1.82	1	2.77	2.71	5.08	6.68	130	0.71	1	3.30	2.25	5.30	6.68
112	1.72	1	2.83	2.71	5.08	6.68	131	2.51	1	2.30	2.30	5.30	6.68
113	1.62	1	2.89	2.71	5.08	6.68	132	2.35	1	2.40	2.30	5.30	6.68
114	1.53	1	2.94	2.71	5.08	6.68	133	2.21	1	2.48	2.30	5.30	6.68
115	1.48	1	3.00	2.71	5.08	6.68	134	2.07	1	2.56	2.30	5.30	6.68
116	1.08	1	3.22	2.71	5.08	6.68	135	1.95	1	2.64	2.30	5.30	6.68
117	0.94	1	3.30	2.71	5.08	6.68	136	1.83	1	2.71	2.30	5.30	6.68
118	2.49	1	2.30	2.25	5.30	6.68	137	1.72	1	2.77	2.30	5.30	6.68
119	2.33	1	2.40	2.25	5.30	6.68	138	1.61	1	2.83	2.30	5.30	6.68
120	2.19	1	2.48	2.25	5.30	6.68	139	1.51	1	2.89	2.30	5.30	6.68
121	2.05	1	2.56	2.25	5.30	6.68	140	1.41	1	2.94	2.30	5.30	6.68
122	1.93	1	2.64	2.25	5.30	6.68	141	1.32	1	3.00	2.30	5.30	6.68
123	1.81	1	2.71	2.25	5.30	6.68	142	0.90	1	3.22	2.30	5.30	6.68
124	1.69	1	2.77	2.25	5.30	6.68	143	0.75	1	3.30	2.30	5.30	6.68
125	1.59	1	2.83	2.25	5.30	6.68	144	2.52	1	2.30	2.35	5.30	6.68
126	1.48	1	2.89	2.25	5.30	6.68	145	2.37	1	2.40	2.35	5.30	6.68
127	1.38	1	2.94	2.25	5.30	6.68	146	2.23	1	2.48	2.35	5.30	6.68

Row No.	$\ln E_i$	1	$\ln(h_{ci})$	$\ln(s_{pi})$	$\ln(d_{oi})$	$\ln(V_i)$	Row No.	$\ln E_i$	1	$\ln(h_{ci})$	$\ln(s_{pi})$	$\ln(d_{oi})$	$\ln(V_i)$
147	2.09	1	2.56	2.35	5.30	6.68	166	1.46	1	2.94	2.40	5.30	6.68
148	1.97	1	2.64	2.35	5.30	6.68	167	1.37	1	3.00	2.40	5.30	6.68
149	1.85	1	2.71	2.35	5.30	6.68	168	0.95	1	3.22	2.40	5.30	6.68
150	1.74	1	2.77	2.35	5.30	6.68	169	0.81	1	3.30	2.40	5.30	6.68
151	1.64	1	2.83	2.35	5.30	6.68	170	2.55	1	2.30	2.44	5.30	6.68
152	1.54	1	2.89	2.35	5.30	6.68	171	2.39	1	2.40	2.44	5.30	6.68
153	1.44	1	2.94	2.35	5.30	6.68	172	2.26	1	2.48	2.44	5.30	6.68
154	1.35	1	3.00	2.35	5.30	6.68	173	2.13	1	2.56	2.44	5.30	6.68
155	0.93	1	3.22	2.35	5.30	6.68	174	2.01	1	2.64	2.44	5.30	6.68
156	0.78	1	3.30	2.35	5.30	6.68	175	1.89	1	2.71	2.44	5.30	6.68
157	2.54	1	2.30	2.40	5.30	6.68	176	1.78	1	2.77	2.44	5.30	6.68
158	2.38	1	2.40	2.40	5.30	6.68	177	1.68	1	2.83	2.44	5.30	6.68
159	2.24	1	2.48	2.40	5.30	6.68	178	1.58	1	2.89	2.44	5.30	6.68
160	2.11	1	2.56	2.40	5.30	6.68	179	1.48	1	2.94	2.44	5.30	6.68
161	1.99	1	2.64	2.40	5.30	6.68	180	1.39	1	3.00	2.44	5.30	6.68
162	1.87	1	2.71	2.40	5.30	6.68	181	0.98	1	3.22	2.44	5.30	6.68
163	1.76	1	2.77	2.40	5.30	6.68	182	0.83	1	3.30	2.44	5.30	6.68
164	1.66	1	2.83	2.40	5.30	6.68	183	2.56	1	2.30	2.48	5.30	6.68
165	1.56	1	2.89	2.40	5.30	6.68	184	2.41	1	2.40	2.48	5.30	6.68

Row No.	$\ln E_i$	1	$\ln(h_{ci})$	$\ln(s_{pi})$	$\ln(d_{oi})$	$\ln(V_i)$	Row No.	$\ln E_i$	1	$\ln(h_{ci})$	$\ln(s_{pi})$	$\ln(d_{oi})$	$\ln(V_i)$
185	2.27	1	2.48	2.48	5.30	6.68	204	1.63	1	2.89	2.56	5.30	6.68
186	2.14	1	2.56	2.48	5.30	6.68	205	1.54	1	2.94	2.56	5.30	6.68
187	2.02	1	2.64	2.48	5.30	6.68	206	1.45	1	3.00	2.56	5.30	6.68
188	1.91	1	2.71	2.48	5.30	6.68	207	1.05	1	3.22	2.56	5.30	6.68
189	1.80	1	2.77	2.48	5.30	6.68	208	0.90	1	3.30	2.56	5.30	6.68
190	1.70	1	2.83	2.48	5.30	6.68	209	2.59	1	2.30	2.64	5.30	6.68
191	1.60	1	2.89	2.48	5.30	6.68	210	2.45	1	2.40	2.64	5.30	6.68
192	1.50	1	2.94	2.48	5.30	6.68	211	2.32	1	2.48	2.64	5.30	6.68
193	1.41	1	3.00	2.48	5.30	6.68	212	2.19	1	2.56	2.64	5.30	6.68
194	1.01	1	3.22	2.48	5.30	6.68	213	2.07	1	2.64	2.64	5.30	6.68
195	0.86	1	3.30	2.48	5.30	6.68	214	1.96	1	2.71	2.64	5.30	6.68
196	2.58	1	2.30	2.56	5.30	6.68	215	1.86	1	2.77	2.64	5.30	6.68
197	2.43	1	2.40	2.56	5.30	6.68	216	1.76	1	2.83	2.64	5.30	6.68
198	2.30	1	2.48	2.56	5.30	6.68	217	1.66	1	2.89	2.64	5.30	6.68
199	2.17	1	2.56	2.56	5.30	6.68	218	1.57	1	2.94	2.64	5.30	6.68
200	2.05	1	2.64	2.56	5.30	6.68	219	1.49	1	3.00	2.64	5.30	6.68
201	1.94	1	2.71	2.56	5.30	6.68	220	1.09	1	3.22	2.64	5.30	6.68
202	1.83	1	2.77	2.56	5.30	6.68	221	0.95	1	3.30	2.64	5.30	6.68
203	1.73	1	2.83	2.56	5.30	6.68	222	2.61	1	2.30	2.71	5.30	6.68

Row No.	$\ln E_i$	1	$\ln(h_{ci})$	$\ln(s_{pi})$	$\ln(d_{oi})$	$\ln(V_i)$	Row No.	$\ln E_i$	1	$\ln(h_{ci})$	$\ln(s_{pi})$	$\ln(d_{oi})$	$\ln(V_i)$
223	2.47	1	2.40	2.71	5.30	6.68	242	1.63	1	2.83	2.25	5.52	6.68
224	2.34	1	2.48	2.71	5.30	6.68	243	1.53	1	2.89	2.25	5.52	6.68
225	2.21	1	2.56	2.71	5.30	6.68	244	1.43	1	2.94	2.25	5.52	6.68
226	2.10	1	2.64	2.71	5.30	6.68	245	1.34	1	3.00	2.25	5.52	6.68
227	1.99	1	2.71	2.71	5.30	6.68	246	0.91	1	3.22	2.25	5.52	6.68
228	1.88	1	2.77	2.71	5.30	6.68	247	0.76	1	3.30	2.25	5.52	6.68
229	1.79	1	2.83	2.71	5.30	6.68	248	2.56	1	2.30	2.30	5.52	6.68
230	1.69	1	2.89	2.71	5.30	6.68	249	2.40	1	2.40	2.30	5.52	6.68
231	1.60	1	2.94	2.71	5.30	6.68	250	2.25	1	2.48	2.30	5.52	6.68
232	1.52	1	3.00	2.71	5.30	6.68	251	2.12	1	2.56	2.30	5.52	6.68
233	1.12	1	3.22	2.71	5.30	6.68	252	2.00	1	2.64	2.30	5.52	6.68
234	0.98	1	3.30	2.71	5.30	6.68	253	1.88	1	2.71	2.30	5.52	6.68
235	2.54	1	2.30	2.25	5.52	6.68	254	1.76	1	2.77	2.30	5.52	6.68
236	2.38	1	2.40	2.25	5.52	6.68	255	1.66	1	2.83	2.30	5.52	6.68
237	2.24	1	2.48	2.25	5.52	6.68	256	1.55	1	2.89	2.30	5.52	6.68
238	2.10	1	2.56	2.25	5.52	6.68	257	1.46	1	2.94	2.30	5.52	6.68
239	1.97	1	2.64	2.25	5.52	6.68	258	1.36	1	3.00	2.30	5.52	6.68
240	1.85	1	2.71	2.25	5.52	6.68	259	0.94	1	3.22	2.30	5.52	6.68
241	1.74	1	2.77	2.25	5.52	6.68	260	0.79	1	3.30	2.30	5.52	6.68

Row No.	$\ln E_i$	1	$\ln(h_{ci})$	$\ln(s_{pi})$	$\ln(d_{oi})$	$\ln(V_i)$	Row No.	$\ln E_i$	1	$\ln(h_{ci})$	$\ln(s_{pi})$	$\ln(d_{oi})$	$\ln(V_i)$
261	2.57	1	2.30	2.35	5.52	6.68	280	1.81	1	2.77	2.40	5.52	6.68
262	2.41	1	2.40	2.35	5.52	6.68	281	1.70	1	2.83	2.40	5.52	6.68
263	2.27	1	2.48	2.35	5.52	6.68	282	1.60	1	2.89	2.40	5.52	6.68
264	2.14	1	2.56	2.35	5.52	6.68	283	1.51	1	2.94	2.40	5.52	6.68
265	2.01	1	2.64	2.35	5.52	6.68	284	1.41	1	3.00	2.40	5.52	6.68
266	1.90	1	2.71	2.35	5.52	6.68	285	1.00	1	3.22	2.40	5.52	6.68
267	1.79	1	2.77	2.35	5.52	6.68	286	0.85	1	3.30	2.40	5.52	6.68
268	1.68	1	2.83	2.35	5.52	6.68	287	2.59	1	2.30	2.44	5.52	6.68
269	1.58	1	2.89	2.35	5.52	6.68	288	2.44	1	2.40	2.44	5.52	6.68
270	1.48	1	2.94	2.35	5.52	6.68	289	2.30	1	2.48	2.44	5.52	6.68
271	1.39	1	3.00	2.35	5.52	6.68	290	2.17	1	2.56	2.44	5.52	6.68
272	0.97	1	3.22	2.35	5.52	6.68	291	2.05	1	2.64	2.44	5.52	6.68
273	0.82	1	3.30	2.35	5.52	6.68	292	1.94	1	2.71	2.44	5.52	6.68
274	2.58	1	2.30	2.40	5.52	6.68	293	1.83	1	2.77	2.44	5.52	6.68
275	2.43	1	2.40	2.40	5.52	6.68	294	1.72	1	2.83	2.44	5.52	6.68
276	2.29	1	2.48	2.40	5.52	6.68	295	1.62	1	2.89	2.44	5.52	6.68
277	2.16	1	2.56	2.40	5.52	6.68	296	1.53	1	2.94	2.44	5.52	6.68
278	2.03	1	2.64	2.40	5.52	6.68	297	1.44	1	3.00	2.44	5.52	6.68
279	1.92	1	2.71	2.40	5.52	6.68	298	1.02	1	3.22	2.44	5.52	6.68

Row No.	$\ln E_i$	1	$\ln(h_{ci})$	$\ln(s_{pi})$	$\ln(d_{oi})$	$\ln(V_i)$	Row No.	$\ln E_i$	1	$\ln(h_{ci})$	$\ln(s_{pi})$	$\ln(d_{oi})$	$\ln(V_i)$
299	0.88	1	3.30	2.44	5.52	6.68	318	1.98	1	2.71	2.56	5.52	6.68
300	2.61	1	2.30	2.48	5.52	6.68	319	1.88	1	2.77	2.56	5.52	6.68
301	2.46	1	2.40	2.48	5.52	6.68	320	1.77	1	2.83	2.56	5.52	6.68
302	2.32	1	2.48	2.48	5.52	6.68	321	1.68	1	2.89	2.56	5.52	6.68
303	2.19	1	2.56	2.48	5.52	6.68	322	1.59	1	2.94	2.56	5.52	6.68
304	2.07	1	2.64	2.48	5.52	6.68	323	1.50	1	3.00	2.56	5.52	6.68
305	1.95	1	2.71	2.48	5.52	6.68	324	1.09	1	3.22	2.56	5.52	6.68
306	1.84	1	2.77	2.48	5.52	6.68	325	0.95	1	3.30	2.56	5.52	6.68
307	1.74	1	2.83	2.48	5.52	6.68	326	2.64	1	2.30	2.64	5.52	6.68
308	1.64	1	2.89	2.48	5.52	6.68	327	2.50	1	2.40	2.64	5.52	6.68
309	1.55	1	2.94	2.48	5.52	6.68	328	2.36	1	2.48	2.64	5.52	6.68
310	1.46	1	3.00	2.48	5.52	6.68	329	2.24	1	2.56	2.64	5.52	6.68
311	1.05	1	3.22	2.48	5.52	6.68	330	2.12	1	2.64	2.64	5.52	6.68
312	0.90	1	3.30	2.48	5.52	6.68	331	2.01	1	2.71	2.64	5.52	6.68
313	2.62	1	2.30	2.56	5.52	6.68	332	1.90	1	2.77	2.64	5.52	6.68
314	2.48	1	2.40	2.56	5.52	6.68	333	1.80	1	2.83	2.64	5.52	6.68
315	2.34	1	2.48	2.56	5.52	6.68	334	1.71	1	2.89	2.64	5.52	6.68
316	2.21	1	2.56	2.56	5.52	6.68	335	1.62	1	2.94	2.64	5.52	6.68
317	2.09	1	2.64	2.56	5.52	6.68	336	1.53	1	3.00	2.64	5.52	6.68

Row No.	$\ln E_i$	1	$\ln(h_{ci})$	$\ln(s_{pi})$	$\ln(d_{oi})$	$\ln(V_i)$	Row No.	$\ln E_i$	1	$\ln(h_{ci})$	$\ln(s_{pi})$	$\ln(d_{oi})$	$\ln(V_i)$
337	1.13	1	3.22	2.64	5.52	6.68	356	2.03	1	1.95	1.25	5.08	6.04
338	0.99	1	3.30	2.64	5.52	6.68	357	1.77	1	2.08	1.25	5.08	6.04
339	2.65	1	2.30	2.71	5.52	6.68	358	1.34	1	2.30	1.25	5.08	6.04
340	2.51	1	2.40	2.71	5.52	6.68	359	0.96	1	2.48	1.25	5.08	6.04
341	2.38	1	2.48	2.71	5.52	6.68	360	0.64	1	2.64	1.25	5.08	6.04
342	2.26	1	2.56	2.71	5.52	6.68	361	2.57	1	1.70	1.39	5.08	6.04
343	2.14	1	2.64	2.71	5.52	6.68	362	2.50	1	1.74	1.39	5.08	6.04
344	2.03	1	2.71	2.71	5.52	6.68	363	2.40	1	1.79	1.39	5.08	6.04
345	1.93	1	2.77	2.71	5.52	6.68	364	2.24	1	1.87	1.39	5.08	6.04
346	1.83	1	2.83	2.71	5.52	6.68	365	2.10	1	1.95	1.39	5.08	6.04
347	1.74	1	2.89	2.71	5.52	6.68	366	1.84	1	2.08	1.39	5.08	6.04
348	1.64	1	2.94	2.71	5.52	6.68	367	1.39	1	2.30	1.39	5.08	6.04
349	1.56	1	3.00	2.71	5.52	6.68	368	1.03	1	2.48	1.39	5.08	6.04
350	1.17	1	3.22	2.71	5.52	6.68	369	0.74	1	2.64	1.39	5.08	6.04
351	1.02	1	3.30	2.71	5.52	6.68	370	2.61	1	1.70	1.50	5.08	6.04
352	2.53	1	1.70	1.25	5.08	6.04	371	2.54	1	1.74	1.50	5.08	6.04
353	2.46	1	1.74	1.25	5.08	6.04	372	2.44	1	1.79	1.50	5.08	6.04
354	2.35	1	1.79	1.25	5.08	6.04	373	2.29	1	1.87	1.50	5.08	6.04
355	2.19	1	1.87	1.25	5.08	6.04	374	2.15	1	1.95	1.50	5.08	6.04

Row No.	$\ln E_i$	1	$\ln(h_{ci})$	$\ln(s_{pi})$	$\ln(d_{oi})$	$\ln(V_i)$	Row No.	$\ln E_i$	1	$\ln(h_{ci})$	$\ln(s_{pi})$	$\ln(d_{oi})$	$\ln(V_i)$
375	1.90	1	2.08	1.50	5.08	6.04	394	1.57	1	2.30	1.70	5.08	6.04
376	1.46	1	2.30	1.50	5.08	6.04	395	1.22	1	2.48	1.70	5.08	6.04
377	1.13	1	2.48	1.50	5.08	6.04	396	0.96	1	2.64	1.70	5.08	6.04
378	0.83	1	2.64	1.50	5.08	6.04	397	2.70	1	1.70	1.87	5.08	6.04
379	2.64	1	1.70	1.61	5.08	6.04	398	2.64	1	1.74	1.87	5.08	6.04
380	2.57	1	1.74	1.61	5.08	6.04	399	2.55	1	1.79	1.87	5.08	6.04
381	2.48	1	1.79	1.61	5.08	6.04	400	2.41	1	1.87	1.87	5.08	6.04
382	2.32	1	1.87	1.61	5.08	6.04	401	2.28	1	1.95	1.87	5.08	6.04
383	2.19	1	1.95	1.61	5.08	6.04	402	2.04	1	2.08	1.87	5.08	6.04
384	1.95	1	2.08	1.61	5.08	6.04	403	1.65	1	2.30	1.87	5.08	6.04
385	1.53	1	2.30	1.61	5.08	6.04	404	1.34	1	2.48	1.87	5.08	6.04
386	1.19	1	2.48	1.61	5.08	6.04	405	1.03	1	2.64	1.87	5.08	6.04
387	0.88	1	2.64	1.61	5.08	6.04	406	2.71	1	1.70	1.95	5.08	6.04
388	2.66	1	1.70	1.70	5.08	6.04	407	2.65	1	1.74	1.95	5.08	6.04
389	2.60	1	1.74	1.70	5.08	6.04	408	2.56	1	1.79	1.95	5.08	6.04
390	2.51	1	1.79	1.70	5.08	6.04	409	2.42	1	1.87	1.95	5.08	6.04
391	2.36	1	1.87	1.70	5.08	6.04	410	2.29	1	1.95	1.95	5.08	6.04
392	2.23	1	1.95	1.70	5.08	6.04	411	2.08	1	2.08	1.95	5.08	6.04
393	1.97	1	2.08	1.70	5.08	6.04	412	1.69	1	2.30	1.95	5.08	6.04

Row No.	$\ln E_i$	1	$\ln(h_{ci})$	$\ln(s_{pi})$	$\ln(d_{oi})$	$\ln(V_i)$	Row No.	$\ln E_i$	1	$\ln(h_{ci})$	$\ln(s_{pi})$	$\ln(d_{oi})$	$\ln(V_i)$
413	1.36	1	2.48	1.95	5.08	6.04	432	0.79	1	2.64	1.39	5.30	6.04
414	1.09	1	2.64	1.95	5.08	6.04	433	2.66	1	1.70	1.50	5.30	6.04
415	2.58	1	1.70	1.25	5.30	6.04	434	2.60	1	1.74	1.50	5.30	6.04
416	2.51	1	1.74	1.25	5.30	6.04	435	2.50	1	1.79	1.50	5.30	6.04
417	2.41	1	1.79	1.25	5.30	6.04	436	2.34	1	1.87	1.50	5.30	6.04
418	2.24	1	1.87	1.25	5.30	6.04	437	2.20	1	1.95	1.50	5.30	6.04
419	2.08	1	1.95	1.25	5.30	6.04	438	1.95	1	2.08	1.50	5.30	6.04
420	1.82	1	2.08	1.25	5.30	6.04	439	1.52	1	2.30	1.50	5.30	6.04
421	1.38	1	2.30	1.25	5.30	6.04	440	1.17	1	2.48	1.50	5.30	6.04
422	1.01	1	2.48	1.25	5.30	6.04	441	0.87	1	2.64	1.50	5.30	6.04
423	0.71	1	2.64	1.25	5.30	6.04	442	2.69	1	1.70	1.61	5.30	6.04
424	2.63	1	1.70	1.39	5.30	6.04	443	2.62	1	1.74	1.61	5.30	6.04
425	2.55	1	1.74	1.39	5.30	6.04	444	2.53	1	1.79	1.61	5.30	6.04
426	2.45	1	1.79	1.39	5.30	6.04	445	2.37	1	1.87	1.61	5.30	6.04
427	2.30	1	1.87	1.39	5.30	6.04	446	2.24	1	1.95	1.61	5.30	6.04
428	2.15	1	1.95	1.39	5.30	6.04	447	2.00	1	2.08	1.61	5.30	6.04
429	1.89	1	2.08	1.39	5.30	6.04	448	1.58	1	2.30	1.61	5.30	6.04
430	1.45	1	2.30	1.39	5.30	6.04	449	1.23	1	2.48	1.61	5.30	6.04
431	1.09	1	2.48	1.39	5.30	6.04	450	0.94	1	2.64	1.61	5.30	6.04

Row No.	$\ln E_i$	1	$\ln(h_{ci})$	$\ln(s_{pi})$	$\ln(d_{oi})$	$\ln(V_i)$	Row No.	$\ln E_i$	1	$\ln(h_{ci})$	$\ln(s_{pi})$	$\ln(d_{oi})$	$\ln(V_i)$
451	2.71	1	1.70	1.70	5.30	6.04	470	2.71	1	1.74	1.95	5.30	6.04
452	2.65	1	1.74	1.70	5.30	6.04	471	2.62	1	1.79	1.95	5.30	6.04
453	2.56	1	1.79	1.70	5.30	6.04	472	2.48	1	1.87	1.95	5.30	6.04
454	2.41	1	1.87	1.70	5.30	6.04	473	2.35	1	1.95	1.95	5.30	6.04
455	2.28	1	1.95	1.70	5.30	6.04	474	2.12	1	2.08	1.95	5.30	6.04
456	2.03	1	2.08	1.70	5.30	6.04	475	1.73	1	2.30	1.95	5.30	6.04
457	1.62	1	2.30	1.70	5.30	6.04	476	1.41	1	2.48	1.95	5.30	6.04
458	1.28	1	2.48	1.70	5.30	6.04	477	1.13	1	2.64	1.95	5.30	6.04
459	0.99	1	2.64	1.70	5.30	6.04	478	2.64	1	1.70	1.25	5.52	6.04
460	2.70	1	1.70	1.87	5.30	6.04	479	2.57	1	1.74	1.25	5.52	6.04
461	2.64	1	1.74	1.87	5.30	6.04	480	2.46	1	1.79	1.25	5.52	6.04
462	2.55	1	1.79	1.87	5.30	6.04	481	2.30	1	1.87	1.25	5.52	6.04
463	2.41	1	1.87	1.87	5.30	6.04	482	2.14	1	1.95	1.25	5.52	6.04
464	2.28	1	1.95	1.87	5.30	6.04	483	1.88	1	2.08	1.25	5.52	6.04
465	2.05	1	2.08	1.87	5.30	6.04	484	1.43	1	2.30	1.25	5.52	6.04
466	1.66	1	2.30	1.87	5.30	6.04	485	1.07	1	2.48	1.25	5.52	6.04
467	1.33	1	2.48	1.87	5.30	6.04	486	0.77	1	2.64	1.25	5.52	6.04
468	1.04	1	2.64	1.87	5.30	6.04	487	2.68	1	1.70	1.39	5.52	6.04
469	2.77	1	1.70	1.95	5.30	6.04	488	2.61	1	1.74	1.39	5.52	6.04

Row No.	$\ln E_i$	1	$\ln(h_{ci})$	$\ln(s_{pi})$	$\ln(d_{oi})$	$\ln(V_i)$	Row No.	$\ln E_i$	1	$\ln(h_{ci})$	$\ln(s_{pi})$	$\ln(d_{oi})$	$\ln(V_i)$
489	2.50	1	1.79	1.39	5.52	6.04	508	2.43	1	1.87	1.61	5.52	6.04
490	2.35	1	1.87	1.39	5.52	6.04	509	2.30	1	1.95	1.61	5.52	6.04
491	2.21	1	1.95	1.39	5.52	6.04	510	2.05	1	2.08	1.61	5.52	6.04
492	1.94	1	2.08	1.39	5.52	6.04	511	1.63	1	2.30	1.61	5.52	6.04
493	1.51	1	2.30	1.39	5.52	6.04	512	1.28	1	2.48	1.61	5.52	6.04
494	1.15	1	2.48	1.39	5.52	6.04	513	0.99	1	2.64	1.61	5.52	6.04
495	0.85	1	2.64	1.39	5.52	6.04	514	2.77	1	1.70	1.70	5.52	6.04
496	2.72	1	1.70	1.50	5.52	6.04	515	2.70	1	1.74	1.70	5.52	6.04
497	2.65	1	1.74	1.50	5.52	6.04	516	2.61	1	1.79	1.70	5.52	6.04
498	2.55	1	1.79	1.50	5.52	6.04	517	2.47	1	1.87	1.70	5.52	6.04
499	2.40	1	1.87	1.50	5.52	6.04	518	2.33	1	1.95	1.70	5.52	6.04
500	2.26	1	1.95	1.50	5.52	6.04	519	2.08	1	2.08	1.70	5.52	6.04
501	2.00	1	2.08	1.50	5.52	6.04	520	1.68	1	2.30	1.70	5.52	6.04
502	1.57	1	2.30	1.50	5.52	6.04	521	1.34	1	2.48	1.70	5.52	6.04
503	1.22	1	2.48	1.50	5.52	6.04	522	1.04	1	2.64	1.70	5.52	6.04
504	0.92	1	2.64	1.50	5.52	6.04	523	2.80	1	1.70	1.87	5.52	6.04
505	2.75	1	1.70	1.61	5.52	6.04	524	2.74	1	1.74	1.87	5.52	6.04
506	2.68	1	1.74	1.61	5.52	6.04	525	2.65	1	1.79	1.87	5.52	6.04
507	2.58	1	1.79	1.61	5.52	6.04	526	2.51	1	1.87	1.87	5.52	6.04

Row No.	$\ln E_i$	1	$\ln(h_{ci})$	$\ln(s_{pi})$	$\ln(d_{oi})$	$\ln(V_i)$	Row No.	$\ln E_i$	1	$\ln(h_{ci})$	$\ln(s_{pi})$	$\ln(d_{oi})$	$\ln(V_i)$
527	2.38	1	1.95	1.87	5.52	6.04	546	1.69	1	1.95	1.25	5.08	5.70
528	2.15	1	2.08	1.87	5.52	6.04	547	1.43	1	2.08	1.25	5.08	5.70
529	1.75	1	2.30	1.87	5.52	6.04	548	1.19	1	2.20	1.25	5.08	5.70
530	1.42	1	2.48	1.87	5.52	6.04	549	0.99	1	2.30	1.25	5.08	5.70
531	1.14	1	2.64	1.87	5.52	6.04	550	2.65	1	1.50	1.39	5.08	5.70
532	2.83	1	1.70	1.95	5.52	6.04	551	2.51	1	1.57	1.39	5.08	5.70
533	2.76	1	1.74	1.95	5.52	6.04	552	2.43	1	1.61	1.39	5.08	5.70
534	2.67	1	1.79	1.95	5.52	6.04	553	2.24	1	1.70	1.39	5.08	5.70
535	2.53	1	1.87	1.95	5.52	6.04	554	2.06	1	1.79	1.39	5.08	5.70
536	2.40	1	1.95	1.95	5.52	6.04	555	1.76	1	1.95	1.39	5.08	5.70
537	2.17	1	2.08	1.95	5.52	6.04	556	1.50	1	2.08	1.39	5.08	5.70
538	1.78	1	2.30	1.95	5.52	6.04	557	1.27	1	2.20	1.39	5.08	5.70
539	1.46	1	2.48	1.95	5.52	6.04	558	1.06	1	2.30	1.39	5.08	5.70
540	1.18	1	2.64	1.95	5.52	6.04	559	2.65	1	1.50	1.50	5.08	5.70
541	2.60	1	1.50	1.25	5.08	5.70	560	2.53	1	1.57	1.50	5.08	5.70
542	2.47	1	1.57	1.25	5.08	5.70	561	2.45	1	1.61	1.50	5.08	5.70
543	2.39	1	1.61	1.25	5.08	5.70	562	2.27	1	1.70	1.50	5.08	5.70
544	2.19	1	1.70	1.25	5.08	5.70	563	2.11	1	1.79	1.50	5.08	5.70
545	2.01	1	1.79	1.25	5.08	5.70	564	1.81	1	1.95	1.50	5.08	5.70

Row No.	$\ln E_i$	1	$\ln(h_{ci})$	$\ln(s_{pi})$	$\ln(d_{oi})$	$\ln(V_i)$	Row No.	$\ln E_i$	1	$\ln(h_{ci})$	$\ln(s_{pi})$	$\ln(d_{oi})$	$\ln(V_i)$
565	1.56	1	2.08	1.50	5.08	5.70	584	1.43	1	2.20	1.70	5.08	5.70
566	1.33	1	2.20	1.50	5.08	5.70	585	1.24	1	2.30	1.70	5.08	5.70
567	1.13	1	2.30	1.50	5.08	5.70	586	2.66	1	1.50	1.25	5.30	5.70
568	2.69	1	1.50	1.61	5.08	5.70	587	2.52	1	1.57	1.25	5.30	5.70
569	2.56	1	1.57	1.61	5.08	5.70	588	2.44	1	1.61	1.25	5.30	5.70
570	2.49	1	1.61	1.61	5.08	5.70	589	2.25	1	1.70	1.25	5.30	5.70
571	2.30	1	1.70	1.61	5.08	5.70	590	2.07	1	1.79	1.25	5.30	5.70
572	2.14	1	1.79	1.61	5.08	5.70	591	1.75	1	1.95	1.25	5.30	5.70
573	1.85	1	1.95	1.61	5.08	5.70	592	1.49	1	2.08	1.25	5.30	5.70
574	1.61	1	2.08	1.61	5.08	5.70	593	1.25	1	2.20	1.25	5.30	5.70
575	1.38	1	2.20	1.61	5.08	5.70	594	1.04	1	2.30	1.25	5.30	5.70
576	1.19	1	2.30	1.61	5.08	5.70	595	2.70	1	1.50	1.39	5.30	5.70
577	2.69	1	1.50	1.70	5.08	5.70	596	2.57	1	1.57	1.39	5.30	5.70
578	2.57	1	1.57	1.70	5.08	5.70	597	2.49	1	1.61	1.39	5.30	5.70
579	2.50	1	1.61	1.70	5.08	5.70	598	2.29	1	1.70	1.39	5.30	5.70
580	2.33	1	1.70	1.70	5.08	5.70	599	2.11	1	1.79	1.39	5.30	5.70
581	2.17	1	1.79	1.70	5.08	5.70	600	1.82	1	1.95	1.39	5.30	5.70
582	1.89	1	1.95	1.70	5.08	5.70	601	1.55	1	2.08	1.39	5.30	5.70
583	1.64	1	2.08	1.70	5.08	5.70	602	1.32	1	2.20	1.39	5.30	5.70

Row No.	$\ln E_i$	1	$\ln(h_{ci})$	$\ln(s_{pi})$	$\ln(d_{oi})$	$\ln(V_i)$	Row No.	$\ln E_i$	1	$\ln(h_{ci})$	$\ln(s_{pi})$	$\ln(d_{oi})$	$\ln(V_i)$
603	1.12	1	2.30	1.39	5.30	5.70	622	2.74	1	1.50	1.70	5.30	5.70
604	2.71	1	1.50	1.50	5.30	5.70	623	2.62	1	1.57	1.70	5.30	5.70
605	2.58	1	1.57	1.50	5.30	5.70	624	2.55	1	1.61	1.70	5.30	5.70
606	2.51	1	1.61	1.50	5.30	5.70	625	2.38	1	1.70	1.70	5.30	5.70
607	2.33	1	1.70	1.50	5.30	5.70	626	2.22	1	1.79	1.70	5.30	5.70
608	2.16	1	1.79	1.50	5.30	5.70	627	1.94	1	1.95	1.70	5.30	5.70
609	1.86	1	1.95	1.50	5.30	5.70	628	1.69	1	2.08	1.70	5.30	5.70
610	1.61	1	2.08	1.50	5.30	5.70	629	1.48	1	2.20	1.70	5.30	5.70
611	1.39	1	2.20	1.50	5.30	5.70	630	1.29	1	2.30	1.70	5.30	5.70
612	1.18	1	2.30	1.50	5.30	5.70	631	2.72	1	1.50	1.25	5.52	5.70
613	2.74	1	1.50	1.61	5.30	5.70	632	2.58	1	1.57	1.25	5.52	5.70
614	2.62	1	1.57	1.61	5.30	5.70	633	2.50	1	1.61	1.25	5.52	5.70
615	2.54	1	1.61	1.61	5.30	5.70	634	2.31	1	1.70	1.25	5.52	5.70
616	2.36	1	1.70	1.61	5.30	5.70	635	2.13	1	1.79	1.25	5.52	5.70
617	2.19	1	1.79	1.61	5.30	5.70	636	1.81	1	1.95	1.25	5.52	5.70
618	1.90	1	1.95	1.61	5.30	5.70	637	1.54	1	2.08	1.25	5.52	5.70
619	1.66	1	2.08	1.61	5.30	5.70	638	1.30	1	2.20	1.25	5.52	5.70
620	1.43	1	2.20	1.61	5.30	5.70	639	1.10	1	2.30	1.25	5.52	5.70
621	1.24	1	2.30	1.61	5.30	5.70	640	2.76	1	1.50	1.39	5.52	5.70

Row No.	$\ln E_i$	1	$\ln(h_{ci})$	$\ln(s_{pi})$	$\ln(d_{oi})$	$\ln(V_i)$	Row No.	$\ln E_i$	1	$\ln(h_{ci})$	$\ln(s_{pi})$	$\ln(d_{oi})$	$\ln(V_i)$
641	2.63	1	1.57	1.39	5.52	5.70	660	2.59	1	1.61	1.61	5.52	5.70
642	2.54	1	1.61	1.39	5.52	5.70	661	2.41	1	1.70	1.61	5.52	5.70
643	2.35	1	1.70	1.39	5.52	5.70	662	2.24	1	1.79	1.61	5.52	5.70
644	2.17	1	1.79	1.39	5.52	5.70	663	1.96	1	1.95	1.61	5.52	5.70
645	1.87	1	1.95	1.39	5.52	5.70	664	1.71	1	2.08	1.61	5.52	5.70
646	1.61	1	2.08	1.39	5.52	5.70	665	1.49	1	2.20	1.61	5.52	5.70
647	1.38	1	2.20	1.39	5.52	5.70	666	1.29	1	2.30	1.61	5.52	5.70
648	1.17	1	2.30	1.39	5.52	5.70	667	2.80	1	1.50	1.70	5.52	5.70
649	2.77	1	1.50	1.50	5.52	5.70	668	2.68	1	1.57	1.70	5.52	5.70
650	2.64	1	1.57	1.50	5.52	5.70	669	2.61	1	1.61	1.70	5.52	5.70
651	2.56	1	1.61	1.50	5.52	5.70	670	2.43	1	1.70	1.70	5.52	5.70
652	2.38	1	1.70	1.50	5.52	5.70	671	2.28	1	1.79	1.70	5.52	5.70
653	2.22	1	1.79	1.50	5.52	5.70	672	1.99	1	1.95	1.70	5.52	5.70
654	1.92	1	1.95	1.50	5.52	5.70	673	1.75	1	2.08	1.70	5.52	5.70
655	1.66	1	2.08	1.50	5.52	5.70	674	1.53	1	2.20	1.70	5.52	5.70
656	1.44	1	2.20	1.50	5.52	5.70	675	1.34	1	2.30	1.70	5.52	5.70
657	1.24	1	2.30	1.50	5.52	5.70							
658	2.80	1	1.50	1.61	5.52	5.70		$\ln E_{ave}$	N				
659	2.67	1	1.57	1.61	5.52	5.70		1.89	675				

Table 24.20: CDEGS Study Results of Magnetic Flux Density at 1,8m Above the Ground [B] (μT) vs Bus Tube Height above the Ground [h_c = 6,5m to 13m) and System Current [I_m = 3150A, 4000A and 5000A]

Attachment Height	Maximum Phase Current	Phase Spacing (s_p) (m)												
		3.5	4	4.5	5	5.5	9.5	10	10.5	11	12	13	14	15
(h_{ci}) (m)	(I_{max}) (A)	Magnetic Field (B) (μT)												
5.5	800	-	-	-	-	45.6	-	-	-	-	-	-	-	-
5.5	1250	-	-	-	-	71.2	-	-	-	-	-	-	-	-
5.5	1600	85.0	87.8	89.6	90.6	91.2	-	-	-	-	-	-	-	-
5.7		-	-	-	79.1	79.6	-	-	-	-	-	-	-	-
6		-	-	-	-	79.5	-	-	-	-	-	-	-	-
5.5	2500	132.8	137.2	139.9	141.6	142.5	-	-	-	-	-	-	-	-
5.7		124.0	128.6	131.7	133.6	134.7	-	-	-	-	-	-	-	-
6		112.2	117.2	120.6	122.8	124.3	-	-	-	-	-	-	-	-
6.5		95.8	101.0	104.8	107.5	109.4	-	-	-	-	-	-	-	-
7		82.4	87.7	91.7	94.8	97.0	-	-	-	-	-	-	-	-
8		-	-	-	-	77.5	-	-	-	-	-	-	-	-
5.5	3150	167.3	172.9	176.3	178.4	179.5	-	-	-	-	-	-	-	-
5.7		156.2	162.1	165.9	168.3	169.7	-	-	-	-	-	-	-	-
6		141.4	147.6	151.9	154.8	156.6	-	-	-	-	-	-	-	-

RESULTS FROM CEDEGS MAGNETIC FIELD STUDY

Table 24.20: System Voltage = 800kV, 420kV & 300kV

Attachment Height	Maximum Phase Current	Phase Spacing (s_p) (m)												
		3.5	4	4.5	5	5.5	9.5	10	10.5	11	12	13	14	15
(h_{ci}) (m)	(I_{max}) (A)	Magnetic Field (B) (μT)												
6.5	3150	120.7	127.2	132.0	135.5	137.9	-	-	-	-	-	-	-	-
7		103.9	110.5	115.6	119.4	122.2	-	-	-	-	-	-	-	-
8		78.9	85.1	90.2	94.4	97.6	-	-	-	-	-	-	-	-
10		-	-	-	76.0	79.4	-	-	-	-	-	-	-	-
5.5	4000	212.5	219.5	223.9	226.5	227.9	-	-	-	-	-	-	-	-
5.7		198.4	205.8	210.7	213.7	215.6	-	-	-	-	-	-	-	-
6		179.5	187.5	192.9	196.5	198.9	-	-	-	-	-	-	-	-
6.5		153.2	161.6	167.7	172.0	175.1	-	-	-	-	-	-	-	-
7		131.9	140.3	147.0	151.6	155.2	-	-	-	-	-	-	-	-
8		101.6	109.6	116.2	121.4	125.6	-	-	-	-	-	-	-	-
10		-	-	-	-	83.1	-	-	-	-	-	-	-	-
5.5	5000	265.6	274.4	279.9	283.1	284.9	-	-	-	-	-	-	-	-
5.7		248.0	257.3	263.4	267.2	269.4	-	-	-	-	-	-	-	-
6		224.4	234.3	241.1	245.7	248.6	-	-	-	-	-	-	-	-

RESULTS FROM CEDEGS MAGNETIC FIELD STUDY

Table 24.20: System Voltage = 800kV, 420kV & 300kV

Attachment Height	Maximum Phase Current	Phase Spacing (s_p) (m)												
		3.5	4	4.5	5	5.5	9.5	10	10.5	11	12	13	14	15
(h_{ci}) (m)	(I_{max}) (A)	Magnetic Field (B) (μT)												
6.5	5000	191.5	202.0	209.6	215.0	218.8	-	-	-	-	-	-	-	-
7		164.9	175.4	183.5	189.5	194.0	-	-	-	-	-	-	-	-
8		125.2	135.1	143.2	149.8	155.0	-	-	-	-	-	-	-	-
10		77.9	85.8	92.7	98.7	103.9	-	-	-	-	-	-	-	-
10	3150	-	-	-	-	-	78.5	79.1	79.6	80.0	80.5	80.8	80.9	80.9
10	4000	-	-	-	-	-	99.7	100.5	101.1	101.5	102.2	102.6	102.7	102.9
11		-	-	-	-	-	86.7	87.7	88.5	89.2	90.1	90.8	91.2	91.4
12		-	-	-	-	-	-	-	-	-	-	-	-	82.0
10	5000	-	-	-	-	-	124.6	125.6	126.3	126.9	127.8	128.1	128.4	128.4
11		-	-	-	-	-	108.4	109.6	110.6	111.4	112.7	113.5	114.0	114.3
12		-	-	-	-	-	95.0	96.4	97.6	98.6	100.1	101.2	102.0	102.5
13		-	-	-	-	-	83.8	85.3	86.6	87.7	89.5	90.9	91.9	92.6

Table 24.21: Natural Logarithms of the Study Values for Magnetic Flux Density [B] (μT) vs Conductor Height [h_c] (m), Phase Spacing [s_p] (m) and System Current [I_m] (A)

Row No.	$\ln B_i$	1	$\ln(h_{ci})$	$\ln(s_{pi})$	$\ln(I_i)$		Row No.	$\ln B_i$	1	$\ln(h_{ci})$	$\ln(s_{pi})$	$\ln(I_i)$
1	6.0	1	1.5	1.3	8.5		18	4.5	1	2.3	1.4	8.5
2	5.8	1	1.6	1.3	8.5		19	6.0	1	1.5	1.5	8.5
3	5.8	1	1.6	1.3	8.5		20	5.9	1	1.6	1.5	8.5
4	5.6	1	1.7	1.3	8.5		21	5.8	1	1.6	1.5	8.5
5	5.4	1	1.8	1.3	8.5		22	5.6	1	1.7	1.5	8.5
6	5.1	1	1.9	1.3	8.5		23	5.5	1	1.8	1.5	8.5
7	4.8	1	2.1	1.3	8.5		24	5.2	1	1.9	1.5	8.5
8	4.6	1	2.2	1.3	8.5		25	5.0	1	2.1	1.5	8.5
9	4.4	1	2.3	1.3	8.5		26	4.7	1	2.2	1.5	8.5
10	6.0	1	1.5	1.4	8.5		27	4.5	1	2.3	1.5	8.5
11	5.9	1	1.6	1.4	8.5		28	6.0	1	1.5	1.6	8.5
12	5.8	1	1.6	1.4	8.5		29	5.9	1	1.6	1.6	8.5
13	5.6	1	1.7	1.4	8.5		30	5.8	1	1.6	1.6	8.5
14	5.5	1	1.8	1.4	8.5		31	5.6	1	1.7	1.6	8.5
15	5.2	1	1.9	1.4	8.5		32	5.5	1	1.8	1.6	8.5
16	4.9	1	2.1	1.4	8.5		33	5.2	1	1.9	1.6	8.5
17	4.7	1	2.2	1.4	8.5		34	5.0	1	2.1	1.6	8.5

Row No.	$\ln B_i$	1	$\ln(h_{ci})$	$\ln(s_{pi})$	$\ln(I_i)$		Row No.	$\ln B_i$	1	$\ln(h_{ci})$	$\ln(s_{pi})$	$\ln(I_i)$
35	4.8	1	2.2	1.6	8.5		53	4.4	1	2.2	1.3	8.3
36	4.6	1	2.3	1.6	8.5		54	5.7	1	1.5	1.4	8.3
37	6.0	1	1.5	1.7	8.5		55	5.6	1	1.6	1.4	8.3
38	5.9	1	1.6	1.7	8.5		56	5.6	1	1.6	1.4	8.3
39	5.8	1	1.6	1.7	8.5		57	5.4	1	1.7	1.4	8.3
40	5.7	1	1.7	1.7	8.5		58	5.2	1	1.8	1.4	8.3
41	5.5	1	1.8	1.7	8.5		59	4.9	1	1.9	1.4	8.3
42	5.3	1	1.9	1.7	8.5		60	4.7	1	2.1	1.4	8.3
43	5.0	1	2.1	1.7	8.5		61	4.4	1	2.2	1.4	8.3
44	4.8	1	2.2	1.7	8.5		62	5.7	1	1.5	1.5	8.3
45	4.6	1	2.3	1.7	8.5		63	5.6	1	1.6	1.5	8.3
46	5.7	1	1.5	1.3	8.3		64	5.6	1	1.6	1.5	8.3
47	5.6	1	1.6	1.3	8.3		65	5.4	1	1.7	1.5	8.3
48	5.5	1	1.6	1.3	8.3		66	5.3	1	1.8	1.5	8.3
49	5.4	1	1.7	1.3	8.3		67	5.0	1	1.9	1.5	8.3
50	5.2	1	1.8	1.3	8.3		68	4.8	1	2.1	1.5	8.3
51	4.9	1	1.9	1.3	8.3		69	4.5	1	2.2	1.5	8.3
52	4.6	1	2.1	1.3	8.3		70	5.7	1	1.5	1.6	8.3

Row No.	$\ln B_i$	1	$\ln(h_{ci})$	$\ln(s_{pi})$	$\ln(I_i)$		Row No.	$\ln B_i$	1	$\ln(h_{ci})$	$\ln(s_{pi})$	$\ln(I_i)$
71	5.6	1	1.6	1.6	8.3		89	5.1	1	1.7	1.3	8.1
72	5.6	1	1.6	1.6	8.3		90	5.0	1	1.8	1.3	8.1
73	5.4	1	1.7	1.6	8.3		91	4.6	1	1.9	1.3	8.1
74	5.3	1	1.8	1.6	8.3		92	4.4	1	2.1	1.3	8.1
75	5.0	1	1.9	1.6	8.3		93	5.5	1	1.5	1.4	8.1
76	4.8	1	2.1	1.6	8.3		94	5.4	1	1.6	1.4	8.1
77	4.6	1	2.2	1.6	8.3		95	5.3	1	1.6	1.4	8.1
78	5.7	1	1.5	1.7	8.3		96	5.2	1	1.7	1.4	8.1
79	5.6	1	1.6	1.7	8.3		97	5.0	1	1.8	1.4	8.1
80	5.6	1	1.6	1.7	8.3		98	4.7	1	1.9	1.4	8.1
81	5.4	1	1.7	1.7	8.3		99	4.4	1	2.1	1.4	8.1
82	5.3	1	1.8	1.7	8.3		100	5.5	1	1.5	1.5	8.1
83	5.0	1	1.9	1.7	8.3		101	5.4	1	1.6	1.5	8.1
84	4.8	1	2.1	1.7	8.3		102	5.3	1	1.6	1.5	8.1
85	4.6	1	2.2	1.7	8.3		103	5.2	1	1.7	1.5	8.1
86	5.5	1	1.5	1.3	8.1		104	5.0	1	1.8	1.5	8.1
87	5.4	1	1.6	1.3	8.1		105	4.8	1	1.9	1.5	8.1
88	5.3	1	1.6	1.3	8.1		106	4.5	1	2.1	1.5	8.1

Row No.	$\ln B_i$	1	$\ln(h_{ci})$	$\ln(s_{pi})$	$\ln(I_i)$		Row No.	$\ln B_i$	1	$\ln(h_{ci})$	$\ln(s_{pi})$	$\ln(I_i)$
107	5.5	1	1.5	1.6	8.1		125	5.1	1	1.6	1.3	7.8
108	5.4	1	1.6	1.6	8.1		126	4.9	1	1.7	1.3	7.8
109	5.3	1	1.6	1.6	8.1		127	4.7	1	1.8	1.3	7.8
110	5.2	1	1.7	1.6	8.1		128	4.4	1	1.9	1.3	7.8
111	5.0	1	1.8	1.6	8.1		129	5.3	1	1.5	1.4	7.8
112	4.8	1	1.9	1.6	8.1		130	5.2	1	1.6	1.4	7.8
113	4.5	1	2.1	1.6	8.1		131	5.1	1	1.6	1.4	7.8
114	4.4	1	2.2	1.6	8.1		132	4.9	1	1.7	1.4	7.8
115	5.5	1	1.5	1.7	8.1		133	4.8	1	1.8	1.4	7.8
116	5.4	1	1.6	1.7	8.1		134	4.5	1	1.9	1.4	7.8
117	5.3	1	1.6	1.7	8.1		135	5.3	1	1.5	1.5	7.8
118	5.2	1	1.7	1.7	8.1		136	5.2	1	1.6	1.5	7.8
119	5.1	1	1.8	1.7	8.1		137	5.1	1	1.6	1.5	7.8
120	4.8	1	1.9	1.7	8.1		138	4.9	1	1.7	1.5	7.8
121	4.6	1	2.1	1.7	8.1		139	4.8	1	1.8	1.5	7.8
122	4.4	1	2.2	1.7	8.1		140	4.5	1	1.9	1.5	7.8
123	5.3	1	1.5	1.3	7.8		141	5.3	1	1.5	1.6	7.8
124	5.1	1	1.6	1.3	7.8		142	5.2	1	1.6	1.6	7.8

Row No.	$\ln B_i$	1	$\ln(h_{ci})$	$\ln(s_{pi})$	$\ln(I_i)$		Row No.	$\ln B_i$	1	$\ln(h_{ci})$	$\ln(s_{pi})$	$\ln(I_i)$
143	5.1	1	1.6	1.6	7.8		161	4.5	1	1.7	1.4	7.4
144	5.0	1	1.7	1.6	7.8		162	4.8	1	1.5	1.5	7.4
145	4.8	1	1.8	1.6	7.8		163	4.7	1	1.6	1.5	7.4
146	4.6	1	1.9	1.6	7.8		164	4.7	1	1.6	1.5	7.4
147	5.3	1	1.5	1.7	7.8		165	4.5	1	1.7	1.5	7.4
148	5.2	1	1.6	1.7	7.8		166	4.8	1	1.5	1.6	7.4
149	5.1	1	1.6	1.7	7.8		167	4.7	1	1.6	1.6	7.4
150	5.0	1	1.7	1.7	7.8		168	4.7	1	1.6	1.6	7.4
151	4.8	1	1.8	1.7	7.8		169	4.5	1	1.7	1.6	7.4
152	4.6	1	1.9	1.7	7.8		170	4.8	1	1.5	1.7	7.4
153	4.4	1	2.1	1.7	7.8		171	4.7	1	1.6	1.7	7.4
154	4.8	1	1.5	1.3	7.4		172	4.7	1	1.6	1.7	7.4
155	4.7	1	1.6	1.3	7.4		173	4.5	1	1.7	1.7	7.4
156	4.6	1	1.6	1.3	7.4		174	4.4	1	1.8	1.7	7.4
157	4.4	1	1.7	1.3	7.4		175	4.6	1	1.5	1.3	7.1
158	4.8	1	1.5	1.4	7.4		176	4.6	1	1.5	1.4	7.1
159	4.7	1	1.6	1.4	7.4		177	4.6	1	1.5	1.5	7.1
160	4.6	1	1.6	1.4	7.4		178	4.6	1	1.5	1.6	7.1

Row No.	$\ln B_i$	1	$\ln(h_{ci})$	$\ln(s_{pi})$	$\ln(I_i)$		Row No.	$\ln B_i$	1	$\ln(h_{ci})$	$\ln(s_{pi})$	$\ln(I_i)$
179	4.6	1	1.5	1.7	7.1		197	5.5	1	1.8	1.5	8.5
180	4.5	1	1.6	1.7	7.1		198	5.3	1	1.9	1.5	8.5
181	5.6	1	1.7	1.3	8.5		199	5.2	1	1.9	1.5	8.5
182	5.5	1	1.7	1.3	8.5		200	5.0	1	2.1	1.5	8.5
183	5.4	1	1.8	1.3	8.5		201	4.5	1	2.3	1.5	8.5
184	5.3	1	1.9	1.3	8.5		202	5.6	1	1.7	1.6	8.5
185	5.1	1	1.9	1.3	8.5		203	5.6	1	1.7	1.6	8.5
186	4.8	1	2.1	1.3	8.5		204	5.5	1	1.8	1.6	8.5
187	4.4	1	2.3	1.3	8.5		205	5.4	1	1.9	1.6	8.5
188	5.6	1	1.7	1.4	8.5		206	5.2	1	1.9	1.6	8.5
189	5.6	1	1.7	1.4	8.5		207	5.0	1	2.1	1.6	8.5
190	5.5	1	1.8	1.4	8.5		208	4.6	1	2.3	1.6	8.5
191	5.3	1	1.9	1.4	8.5		209	5.7	1	1.7	1.7	8.5
192	5.2	1	1.9	1.4	8.5		210	5.6	1	1.7	1.7	8.5
193	4.9	1	2.1	1.4	8.5		211	5.5	1	1.8	1.7	8.5
194	4.5	1	2.3	1.4	8.5		212	5.4	1	1.9	1.7	8.5
195	5.6	1	1.7	1.5	8.5		213	5.3	1	1.9	1.7	8.5
196	5.6	1	1.7	1.5	8.5		214	5.0	1	2.1	1.7	8.5

Row No.	$\ln B_i$	1	$\ln(h_{ci})$	$\ln(s_{pi})$	$\ln(I_i)$		Row No.	$\ln B_i$	1	$\ln(h_{ci})$	$\ln(s_{pi})$	$\ln(I_i)$
215	4.6	1	2.3	1.7	8.5		233	4.8	1	2.1	1.5	8.3
216	5.4	1	1.7	1.3	8.3		234	5.4	1	1.7	1.6	8.3
217	5.3	1	1.7	1.3	8.3		235	5.4	1	1.7	1.6	8.3
218	5.2	1	1.8	1.3	8.3		236	5.3	1	1.8	1.6	8.3
219	5.0	1	1.9	1.3	8.3		237	5.1	1	1.9	1.6	8.3
220	4.9	1	1.9	1.3	8.3		238	5.0	1	1.9	1.6	8.3
221	4.6	1	2.1	1.3	8.3		239	4.8	1	2.1	1.6	8.3
222	5.4	1	1.7	1.4	8.3		240	5.4	1	1.7	1.7	8.3
223	5.3	1	1.7	1.4	8.3		241	5.4	1	1.7	1.7	8.3
224	5.2	1	1.8	1.4	8.3		242	5.3	1	1.8	1.7	8.3
225	5.1	1	1.9	1.4	8.3		243	5.2	1	1.9	1.7	8.3
226	4.9	1	1.9	1.4	8.3		244	5.0	1	1.9	1.7	8.3
227	4.7	1	2.1	1.4	8.3		245	4.8	1	2.1	1.7	8.3
228	5.4	1	1.7	1.5	8.3		246	4.4	1	2.3	1.7	8.3
229	5.4	1	1.7	1.5	8.3		247	5.1	1	1.7	1.3	8.1
230	5.3	1	1.8	1.5	8.3		248	5.1	1	1.7	1.3	8.1
231	5.1	1	1.9	1.5	8.3		249	5.0	1	1.8	1.3	8.1
232	5.0	1	1.9	1.5	8.3		250	4.8	1	1.9	1.3	8.1

Row No.	$\ln B_i$	1	$\ln(h_{ci})$	$\ln(s_{pi})$	$\ln(I_i)$		Row No.	$\ln B_i$	1	$\ln(h_{ci})$	$\ln(s_{pi})$	$\ln(I_i)$
251	4.6	1	1.9	1.3	8.1		269	4.8	1	1.9	1.6	8.1
252	4.4	1	2.1	1.3	8.1		270	4.5	1	2.1	1.6	8.1
253	5.2	1	1.7	1.4	8.1		271	4.3	1	2.3	1.6	8.1
254	5.1	1	1.7	1.4	8.1		272	5.2	1	1.7	1.7	8.1
255	5.0	1	1.8	1.4	8.1		273	5.1	1	1.7	1.7	8.1
256	4.8	1	1.9	1.4	8.1		274	5.1	1	1.8	1.7	8.1
257	4.7	1	1.9	1.4	8.1		275	4.9	1	1.9	1.7	8.1
258	4.4	1	2.1	1.4	8.1		276	4.8	1	1.9	1.7	8.1
259	5.2	1	1.7	1.5	8.1		277	4.6	1	2.1	1.7	8.1
260	5.1	1	1.7	1.5	8.1		278	4.4	1	2.3	1.7	8.1
261	5.0	1	1.8	1.5	8.1		279	4.9	1	1.7	1.3	7.8
262	4.9	1	1.9	1.5	8.1		280	4.8	1	1.7	1.3	7.8
263	4.8	1	1.9	1.5	8.1		281	4.7	1	1.8	1.3	7.8
264	4.5	1	2.1	1.5	8.1		282	4.6	1	1.9	1.3	7.8
265	5.2	1	1.7	1.6	8.1		283	4.4	1	1.9	1.3	7.8
266	5.1	1	1.7	1.6	8.1		284	4.9	1	1.7	1.4	7.8
267	5.0	1	1.8	1.6	8.1		285	4.9	1	1.7	1.4	7.8
268	4.9	1	1.9	1.6	8.1		286	4.8	1	1.8	1.4	7.8

Row No.	lnB_i	1	$ln(h_{ci})$	$ln(s_{pi})$	$ln(I_i)$		Row No.	lnB_i	1	$ln(h_{ci})$	$ln(s_{pi})$	$ln(I_i)$
287	4.6	1	1.9	1.4	7.8		305	4.4	1	1.7	1.3	7.4
288	4.5	1	1.9	1.4	7.8		306	4.5	1	1.7	1.4	7.4
289	4.9	1	1.7	1.5	7.8		307	4.5	1	1.7	1.5	7.4
290	4.9	1	1.7	1.5	7.8		308	4.5	1	1.7	1.6	7.4
291	4.8	1	1.8	1.5	7.8		309	4.4	1	1.7	1.6	7.4
292	4.7	1	1.9	1.5	7.8		310	4.5	1	1.7	1.7	7.4
293	4.5	1	1.9	1.5	7.8		311	4.4	1	1.7	1.7	7.4
294	5.0	1	1.7	1.6	7.8		312	4.4	1	1.8	1.7	7.4
295	4.9	1	1.7	1.6	7.8		313	4.8	1	2.3	2.3	8.5
296	4.8	1	1.8	1.6	7.8		314	4.7	1	2.4	2.3	8.5
297	4.7	1	1.9	1.6	7.8		315	4.6	1	2.5	2.3	8.5
298	4.6	1	1.9	1.6	7.8		316	4.4	1	2.6	2.3	8.5
299	5.0	1	1.7	1.7	7.8		317	4.8	1	2.3	2.3	8.5
300	4.9	1	1.7	1.7	7.8		318	4.7	1	2.4	2.3	8.5
301	4.8	1	1.8	1.7	7.8		319	4.6	1	2.5	2.3	8.5
302	4.7	1	1.9	1.7	7.8		320	4.4	1	2.6	2.3	8.5
303	4.6	1	1.9	1.7	7.8							
304	4.4	1	2.1	1.7	7.8							

Row No.	lnB_i	1	$ln(h_{ci})$	$ln(s_{pi})$	$ln(I_i)$		Row No.	lnB_i	1	$ln(h_{ci})$	$ln(s_{pi})$	$ln(I_i)$
321	4.8	1	2.3	2.4	8.5							
322	4.7	1	2.4	2.4	8.5							
323	4.6	1	2.5	2.4	8.5		339	4.6	1	2.5	2.6	8.5
324	4.5	1	2.6	2.4	8.5		340	4.5	1	2.6	2.6	8.5
325	4.8	1	2.3	2.4	8.5		341	4.9	1	2.3	2.7	8.5
326	4.7	1	2.4	2.4	8.5		342	4.7	1	2.4	2.7	8.5
327	4.6	1	2.5	2.4	8.5		343	4.6	1	2.5	2.7	8.5
328	4.5	1	2.6	2.4	8.5		344	4.5	1	2.6	2.7	8.5
329	4.9	1	2.3	2.5	8.5		345	4.6	1	2.3	2.3	8.3
330	4.7	1	2.4	2.5	8.5		346	4.5	1	2.4	2.3	8.3
331	4.6	1	2.5	2.5	8.5		347	4.6	1	2.3	2.3	8.3
332	4.5	1	2.6	2.5	8.5		348	4.5	1	2.4	2.3	8.3
333	4.9	1	2.3	2.6	8.5		349	4.6	1	2.3	2.4	8.3
334	4.7	1	2.4	2.6	8.5		350	4.5	1	2.4	2.4	8.3
335	4.6	1	2.5	2.6	8.5		351	4.6	1	2.3	2.4	8.3
336	4.5	1	2.6	2.6	8.5		352	4.5	1	2.4	2.4	8.3
337	4.9	1	2.3	2.6	8.5		353	4.6	1	2.3	2.5	8.3
338	4.7	1	2.4	2.6	8.5		354	4.5	1	2.4	2.5	8.3

Row No.	lnB_i	1	$ln(h_{ci})$	$ln(s_{pi})$	$ln(I_i)$		Row No.	lnB_i	1	$ln(h_{ci})$	$ln(s_{pi})$	$ln(I_i)$
355	4.6	1	2.3	2.6	8.3		365	4.4	1	2.3	2.4	8.1
356	4.5	1	2.4	2.6	8.3		366	4.4	1	2.3	2.5	8.1
357	4.6	1	2.3	2.6	8.3		367	4.4	1	2.3	2.6	8.1
358	4.5	1	2.4	2.6	8.3		368	4.4	1	2.3	2.6	8.1
359	4.6	1	2.3	2.7	8.3		369	4.4	1	2.3	2.7	8.1
360	4.5	1	2.4	2.7	8.3							
361	4.4	1	2.5	2.7	8.3							
362	4.4	1	2.3	2.3	8.1		$Ln(H_{ave})$		N			
363	4.4	1	2.3	2.3	8.1		5.0		369			
364	4.4	1	2.3	2.4	8.1							

24 APPENDIX F

Table 24.22: Sensitivity of Design to Tolerances in Bus Tubing Outer Diameter (d_{bo}) and Tube Wall Thickness (t_w)

Fault Current (kA)	PI Strength - V=132kV, s_p=3m, No ARC, W_b=12m												
	d_{bo}=118.8 t_w=5.6	d_{bo}=118.8 t_w=6	d_{bo}=118.8 t_w=6.4	d_{bo}=120 t_w=5.6	d_{bo}=120 t_w=6	d_{bo}=120 t_w=6.4	d_{bo}=121.2 t_w=5.6	d_{bo}=121.2 t_w=6	d_{bo}=121.2 t_w=6.4	Best Case	Worst Case	% Deviation	% Deviation
12	571.91	570.55	569.20	580.25	578.90	577.55	587.39	586.06	584.71	569.20	587.39	-1.68	1.47
16	796.22	794.34	792.46	806.51	804.64	802.76	815.30	813.44	811.58	792.46	815.30	-1.51	1.33
25	1535.28	1531.64	1528.01	1551.98	1548.37	1544.77	1566.22	1562.64	1559.06	1528.01	1566.22	-1.32	1.15
31.5	2270.83	2265.46	2260.07	2293.92	2288.59	2283.26	2313.55	2308.27	2302.99	2260.07	2313.55	-1.25	1.09
40	-	3479.81	3471.54	3521.71	3513.54	3505.36	3550.31	3542.20	3534.10	0.00	0.00	-	-
50	-	-	-	-	-	-	-	-	-	-	-	-	-
63	-	-	-	-	-	-	-	-	-	-	-	-	-

Table 24.23: Force on Post Insulator (F_{PI}) Subjected to Various Fault Currents for a Range of Wind Speeds (V_w) - Tubular Conductor (120mm x 6mmWT)

Bus Tubing		120mm x 6mmWT		Terrain Category		1
Wind Speed (km/h)	Alloy	AlMgSi0,5F25		2% Proof Stress		195MPa
	Fault Current (kA)					
	12	16	25	31.5	40	50
	Force on Post Insulator (N)					
0	1150	1380	2875	4485	7130	11040
10	1150	1380	2875	4485	7130	11040
20	1150	1380	2875	4485	7130	11040
30	1150	1380	2875	4485	7130	11040
40	1265	1495	2790	4485	7245	11155
50	1265	1495	2790	4485	7245	11155
60	1265	1495	2790	4485	7245	11270
70	1380	1725	3220	4715	7360	11270
80	1380	1725	3220	4830	7475	11385
90	1380	1840	3335	4830	7475	11385
100	1495	1955	3450	4945	7590	11500
110	1610	1955	3450	5060	7705	11615
120	1610	2070	3565	5175	7820	11730
130	1840	2300	3795	5290	7935	11845
140	1840	2300	3910	5520	8085	11960
150	2070	2530	4025	5635	8280	12190
160	2185	2530	4140	5750	8395	12305

Table 24.24: Force on Post Insulator Subjected to Various Fault Currents for a Range of Wind Speeds - Tubular Conductor (200mm x 8mmWT)

Bus Tubing		200mm x 8mmWT		Terrain Category		1
Wind Speed (km/h)	Alloy	AlMgSi0,5F25		2% Proof Stress		195MPa
	Fault Current (kA)					
	12	16	25	31.5	40	50
	Force on Post Insulator (N)					
0	2530	2760	3910	5405	8165	12420
10	2530	2760	3910	5405	8165	12420
20	2530	2760	3910	5405	8165	12420
30	2530	2760	4025	5520	8250	12535
40	2530	2760	4025	5520	8395	12650
50	2645	2875	4140	5750	8510	12765
60	2760	2990	4255	5865	8625	12880
70	2875	3105	4485	5980	8740	12995
80	2875	3220	4600	6210	8970	13225
90	2990	3335	4830	6440	9200	13455
100	3220	3565	5060	6670	9430	13685
110	3450	3795	5290	6900	9775	14030
120	3680	4025	5520	7245	10005	14260
130	3910	4370	5865	7475	10350	14720
140	4255	4600	6210	7820	10695	14950
150	4485	4945	6550	8280	11155	15410
160	4830	5290	7015	8625	11500	15755

Table 24.25: Force on Post Insulator Subjected to Various Fault Currents for a Range of Wind Speeds - Tubular Conductor (250mm x 6mmWT)

Bus Tubing	250mm x 6mmWT			Terrain Category		1
Wind Speed (km/h)	Alloy	AlMgSi0,5F25		2% Proof Stress		195MPa
	Fault Current (kA)					
	12	16	25	31.5	40	50
	Force on Post Insulator (N)					
0	2990	3220	4025	5290	7475	11270
10	2990	3220	4025	5290	7590	11270
20	2990	3220	4025	5290	7590	11385
30	3150	3335	4140	5405	7705	11500
40	3150	3335	4255	5520	7820	11615
50	3220	3450	4370	5635	7935	11845
60	3335	3565	4480	5750	8165	11960
70	3450	3680	4715	5980	8395	12305
80	3565	3795	4945	6210	8625	12650
90	3680	4025	5060	6440	8855	12880
100	3910	4255	5405	6785	9200	13340
110	4140	4485	5750	7130	9545	13685
120	4370	4715	6095	7475	9890	14145
130	4715	5060	6440	7820	10350	14490
140	5060	5520	6900	8280	10810	15180
150	5520	5980	7360	8855	11270	15640
160	5980	6440	7820	9315	11840	

Table 24.26: Dynamic Stress in a Tubular Conductor (250mm x 8mmWT) Subjected to Various Fault Currents for a Range of Safety Factors

Bus Tubing		250mm x 8mmWT		Terrain Category		1
Wind Speed (km/h)	Alloy	AlMgSi0,5F25		2% Proof Stress		195MPa
	Fault Current (kA)					
	12	16	25	31.5	40	50
	Force on Post Insulator (N)					
0	3910	4140	4715	5865	7935	11500
10	3910	4140	4715	5865	7935	11500
20	4025	4140	4830	5865	7935	11500
30	4025	4140	4830	5890	8050	11615
40	4025	4255	4945	5980	8165	11730
50	4140	4255	5060	6210	8280	11845
60	4140	4370	5175	6325	8510	12190
70	4255	4485	5290	6440	8740	12305
80	4370	4600	5520	6785	8970	12535
90	4485	4715	5750	6900	9315	12880
100	4715	4830	5980	7245	9545	13110
110	4830	5175	6210	7590	9890	13750
120	5060	5405	6555	7820	10235	13915
130	5405	5750	7015	8280	10695	14375
140	5750	6095	7360	8740	11155	14835
150	6210	6440	7820	9200	11615	15295
160	6555	6900	8280	9600	12190	15870

Table 24.27: Dynamic Stress in a Tubular Conductor (250mm x 8mmWT) Subjected to Various Fault Currents for a Range of Safety Factors

Bus Tubing	250mm x 8mmWT				Terrain Category		1
Safety Factor SF_{Al}	Fault Current (kA)						
	12	16	25	31.5	40	50	63
	Dynamic Stress in Conductor (MPa)						
1.8	39.5	44.0	61.1	79.7	111.7	160.3	240.7
1.9	41.7	46.5	64.5	84.1	117.9	169.2	254.0
2	43.9	49.2	67.9	88.5	124.1	178.1	267.4
2.1	46.1	51.4	71.3	92.9	130.3	187.0	280.8
2.2	48.3	53.8	74.7	97.4	136.5	195.9	294.1
2.3	50.4	56.3	78.1	101.8	142.7	204.9	-
2.4	52.6	58.7	81.5	106.2	148.9	213.8	-
2.5	54.8	61.2	84.9	110.6	155.1	222.7	-
2.6	57.0	63.6	88.3	115.0	161.4	230.0	-
2.65	58.1	64.8	90.0	117.3	164.5	236.0	-

Table 24.28: Dynamic Stress in a Tubular Conductor (250mm x 8mmWT) Subjected to Various Fault Currents for a Range of Values of Post Insulator Dynamic Factors [ν_F]

Bus Tubing		**250mm x 8mmWT**			**Terrain Category**		**1**
ν_F	**Alloy**	**AlMgSi0,5F25**			**2% Proof Stress**		**195MPa**
	Fault Current (kA)						
	12	**16**	**25**	**31.5**	**40**	**50**	**63**
	Force on Post Insulator (N)						
0.2	4945	5060	5405	5865	6670	7935	10120
0.3	5060	5175	5865	6555	7820	9890	13340
0.4	5060	5405	6210	7245	8970	11730	16445
0.5	5175	5520	6670	7935	10235	13685	-
0.6	5290	5635	7015	8625	11500	15755	-
0.7	5290	5750	7475	9430	12765	-	-
0.8	5405	5865	7935	10235	14030	-	-
0.9	5520	6095	8395	10925	15295	-	-
1	5635	6325	8855	11730	16560	-	-

Table 24.29: Dynamic Stress in a Tubular Conductor (250mm x 8mmWT) Subjected to Various Fault Currents for a Range of Values of Bus Tube Conductor Factors [ν_σ]

Bus Tubing		250mm x 8mmWT			Terrain Category		1
	Alloy	AlMgSi0,5F25			2% Proof Stress		195MPa
	Fault Current (kA)						
	12	16	25	31.5	40	50	63
ν_σ	Dynamic Stress in Conductor (MPa)						
0.2	25.42	28.41	39.24	51.16	71.73	102.95	154.54
0.3	38.13	42.41	58.86	77.65	109.13	154.43	230.00
0.4	50.84	56.81	78.48	103.53	154.50	205.90	-
0.5	63.38	71.02	99.01	129.41	179.33	257.38	-
0.6	76.26	84.83	118.81	155.30	215.20	-	-
0.7	88.97	99.72	137.34	179.04	251.07	-	-
0.8	101.68	115.00	158.42	204.62	286.93	-	-
0.9	115.00	127.83	176.58	230.00	-	-	-
1	126.76	141.58	195.00	255.78	-	-	-

Table 24.30: Dynamic Stress in a Tubular Conductor (250mm x 8mmWT) Subjected to Various Fault Currents for a Range of Values of Dynamic Factor for Auto-Reclosing [ν_r]

Bus Tubing		250mm x 8mmWT			Terrain Category		1	Bus Tubing		250mm x 8mmWT		Terrain Category		1
ν_r	Alloy	AlMgSi0,5F25			2% Proof Stress		195MPa	Alloy		AlMgSi0,5F25		2% Proof Stress		195MPa
	Fault Current (kA)							Fault Current (kA)						
	12	16	25	31.5	40	50	63	12	16	25	31.5	40	50	63
	Force on Post Insulator (N)							Dynamic Stress in Conductor (MPa)						
1	5060	5290	5980	6900	8395	10810	14835	36.68	39.43	49.72	61.05	80.98	111.67	162.92
1.1	5060	5290	6210	7130	8855	11500	16100	40.72	44.10	56.72	70.65	95.00	132.36	195.00
1.2	5175	5405	6325	7360	9315	12190	16905	44.84	48.92	64.18	80.93	110.14	154.82	230.00
1.3	5175	5405	6440	7590	9660	12880	-	49.14	53.87	72.05	92.91	126.41	179.05	266.32
1.4	5175	5520	6555	7820	10120	13570	-	53.30	58.98	80.29	103.54	143.81	205.06	-
1.5	5290	5520	6785	8165	10580	14260	-	57.79	64.24	88.97	115.00	162.34	232.85	-
1.6	5290	5635	6900	8395	10925	15065	-	62.06	69.64	98.08	128.90	182.00	262.41	-
1.7	5290	5635	7015	8740	11385	15755	-	66.55	75.21	107.60	142.62	202.79	293.75	-
1.8	5290	5635	7245	8855	11845	16445	-	71.35	80.92	117.56	157.04	224.72	-	-

Table 24.31: Impact on Dynamic Stress in a Tubular Conductor (250mm x 8mmWT) by Employing Different Safety Factors [SF_{AL}]

Bus Tubing	250mm x 8mmWT			Terrain Category		1	Aluminium Alloys					
Safety Factor	Fault Current (kA)											
	12	16	25	31.5	40	50	63	D50S.TF	D65S.TF	6063T6	6061T6	AlMgSi.0,5F22	AlMgSi.0,5F25
SF_{Al}	Dynamic Stress in Conductor (MPa)							0,2% Proof Stress for Different Alloys					
1.8	39.5	44.0	61.1	79.7	111.7	160.3	240.7	170	240	214	276	160	195
1.9	41.7	46.5	64.5	84.1	117.9	169.2	254.0	170	240	214	276	160	195
2	43.9	49.2	67.9	88.5	124.1	178.1	267.4	170	240	214	276	160	195
2.1	46.1	51.4	71.3	92.9	130.3	187.0	280.8	170	240	214	276	160	195
2.2	48.3	53.8	74.7	97.4	136.5	195.9	294.1	170	240	214	276	160	195
2.3	50.4	56.3	78.1	101.8	142.7	204.9	-	170	240	214	276	160	195
2.4	52.6	58.7	81.5	106.2	148.9	213.8	-	170	240	214	276	160	195
2.5	54.8	61.2	84.9	110.6	155.1	222.7	-	170	240	214	276	160	195
2.6	57.0	63.6	88.3	115.0	161.4	230.0	-	170	240	214	276	160	195
2.65	58.1	64.8	90.0	117.3	164.5	236.0	-	170	240	214	276	160	195